

**PRACTICAL CONSIDERATIONS FOR FULL-
SCALE APPLICATION OF HYBRID
FORWARD OSMOSIS SYSTEM:
ASSESSMENT THROUGH PILOT-SCALE
EXPERIMENTS AND FULL-SCALE
SIMULATIONS**

by

JUNGEUN KIM

A Thesis submitted in fulfilment for the degree of
Doctoral of Philosophy



**School of Civil and Environmental Engineering
Faculty of Engineering and Information Technology
University of Technology Sydney (UTS),
New South Wales, Australia**

April 2018

CERTIFICATE OF AUTHORSHIP/ORIGINALITY

I certify that this thesis has not previously been submitted for a degree nor has it been submitted as part of requirements for a degree except as fully acknowledge within the text.

I also certify that the thesis has been written by me. Any help that I have received in my research work and the preparation of the thesis itself has been acknowledged. In addition, I certify that all information sources and literature used are indicated in the thesis. I also acknowledge that this study was supported by Australian Government Research Training Program.

Signature of Candidate

JUNGEUN KIM

Production Note:

Signature removed prior to publication.

ACKNOWLEDGMENTS

I owe my deepest appreciation and gratitude to my supervisors, Dr. Sherub Phuntsho (principal supervisor) and Prof. Hokyong Shon (alternate/co-supervisor). Without their continuous optimism concerning this work, enthusiasm, encouragement and support, this study would hardly have been completed. I also express my warmest appreciation to Dr. Laura Chekli, Dr. Leonard Tijing, Dr. Gaetan Blandin and A/Prof. Pierre Le Clech who gave insightful comments and suggestions.

Furthermore, I would like to offer my special tanks to Dr. Mohammed Johir. He made enormous contribution to my experimental works. I would also like to thank the following people for their invaluable support, encouragement, and friendship; Tahir Majeed, Soleyman Sahebi, Fouzy Lotfi, Sungil Lim, Yunchul Woo, Youngkwon Choi, Yunju Jo, Van Huy Tran, Syed Muztuza Ali, Ralph Gonzales, Nirenkumar Pathak, Hyojin Yoon, Sohyun Lee, Heajin Park, and Heejeong Lee.

Last but not the least, my heartfelt appreciation goes to all my family members, my father Seokdong Kim, mother Jaeim Woo and younger sister Jihye Kim who have been extraordinarily tolerant and supportive during the entire course of my PhD. I would also extend my gratitude to my husband Myoungjun Park. Without his guidance and persistent help, this thesis would not have been possible.

JOURNAL ARTICLES PUBLISHED OR SUBMITTED**

1. ***Kim, J. E.**; Phuntsho, S.; Ali, S. M.; Choi, J. Y.; Shon, H. K., Forward osmosis membrane modular configurations for osmotic dilution of seawater by forward osmosis and reverse osmosis hybrid system, *Water research* **2018**, *128*, 183-192.
2. ***Kim, J. E.**; Phuntsho, S.; Chekli, L.; Choi, J. Y.; Shon, H. K., Life cycle assessment of hybrid FO-RO/NF system with selected inorganic draw solutes for the treatment of saline impaired water, *Desalination* **2018**, *429*, 96-104.
3. ***Kim, J. E.**; Phuntsho, S.; Chekli, L.; Hong, S.; Ghaffour, N.; Leiknes, T.; Choi, J. Y.; Shon, H. K., Environmental and economic impacts of fertilizer drawn forward osmosis and nanofiltration hybrid system. *Desalination* **2017**, *416*, 76-85.
4. **Kook, S.; **Kim, J.E.**; Kim, S.-J.; Lee, J.; Han, D.; Phuntsho, S.; Shim, W.-G.; Hwang, M.; Shon, H. K.; Kim, I. S., Effect of initial feed and draw flowrates on performance of an 8040 spiral-wound forward osmosis membrane element. *Desalination and Water Treatment* **2017**. In press.
5. **Chekli, L.; **Kim, J. E.**; El Saliby, I.; Kim, Y.; Phuntsho, S.; Li, S.; Ghaffour, N.; Leiknes, T.; Kyong Shon, H., Fertilizer drawn forward osmosis process for sustainable water reuse to grow hydroponic lettuce using commercial nutrient solution. *Separation and Purification Technology* **2017**, *181*, 18-28.
6. ***Kim, J.E.**; Blandin, G.; Phuntsho, S.; Verliefde, A.; Le-Clech, P.; Shon, H., Practical considerations for operability of an 8" spiral wound forward osmosis module: Hydrodynamics, fouling behavior and cleaning strategy. *Desalination* **2017**, *404*, 249-258.
7. **Phuntsho, S.; **Kim, J. E.**; Hong, S.; Ghaffour, N.; Leiknes, T.; Choi, J. Y.; Shon, H. K., A closed-loop forward osmosis-nanofiltration hybrid system: Understanding process implications through full-scale simulation. *Desalination* **2017**, *421*, 169-178.
8. *Chekli, L.; Phuntsho, S.; **Kim, J. E.**; Kim, J.; Choi, J. Y.; Choi, J.-S.; Kim, S.; Kim, J. H.; Hong, S.; Sohn, J., A comprehensive review of hybrid forward osmosis systems: Performance, applications and future prospects. *Journal of Membrane Science* **2016**, *497*, 430-449.
9. **Sahebi, S.; Phuntsho, S.; **Kim, J. E.**; Hong, S.; Shon, H. K., Pressure assisted fertiliser drawn osmosis process to enhance final dilution of the fertiliser draw

solution beyond osmotic equilibrium. *Journal of Membrane Science* **2015**, *481*, 63-72.

10. **Majeed, T.; Phuntsho, S.; Sahebi, S.; **Kim, J. E.**; Yoon, J. K.; Kim, K.; Shon, H. K., Influence of the process parameters on hollow fiber-forward osmosis membrane performances. *Desalination and Water Treatment* **2015**, *54*, (4-5), 817-828.
11. **Majeed, T.; Sahebi, S.; Lotfi, F.; **Kim, J. E.**; Phuntsho, S.; Tijing, L. D.; Shon, H. K., Fertilizer-drawn forward osmosis for irrigation of tomatoes. *Desalination and Water Treatment* **2015**, *53*, (10), 2746-2759.
12. **Kim, J. E.**; Phuntsho, S.; Lotfi, F.; Shon, H. K., Investigation of Pilot-Scale 8040 Fo Membrane Module under Different Operating Conditions for Brackish Water Desalination. *Desalination and Water Treatment* **2015**, *53*, (10), 2782-2791.

BOOK CHAPTERS

1. Phuntsho, S.; **Kim, J. E.**; Majeed, T.; Lotfi, F.; Sahebi, S.; Shon, H. K., "Fertiliser Drawn Forward Osmosis Desalination for Fertigation." In *Forward Osmosis: Fundamentals and Applications*; Edited by Hk Shon Et Al.: American Society of Civil Engineers (ASCE). ISBN: 9780784414071, 2015.
2. Shon, H. K.; Chekli, L.; Phuntsho, S.; **Kim, J. E.**; Cho, J., "Draw Solutes in Forward Osmosis Process." In *Forward Osmosis: Fundamentals and Applications*; Edited by Hk Shon Et Al.: American Society of Civil Engineers (ASCE): ISBN: 9780784414071, 2015.

Publications made during the PhD candidature including articles not entirely related to the Thesis. *Articles related to the Thesis.**

CONFERENCE PAPERS AND PRESENTATIONS

1. **Kim, J. E.;** Ali, S. M.; Phuntsho S.; Choi J. Y.; Shon H. K., Spiral wound forward osmosis membrane module for the osmotic dilution of seawater using wastewater, 8th IWA Specialised Membrane Technology Conference (IWA-MTC 2017), 4-9 September 2017, Oral Presentation.
2. **Kim, J. E.;** Phuntsho S.; Shon H. K., Fertiliser drawn forward osmosis process: Pilot-scale desalination of mine impaired water for fertigation, International Forward Osmosis Summit (IFOS), 2-4 December 2016, *Awarded the Best Poster Presentation*.
3. **Kim, J. E.;** Phuntsho S.; Shon H. K., Fertiliser drawn forward osmosis process: Pilot-scale desalination of mine impaired water for fertigation, International Water Association (IWA), 9-13 October 2016, Poster Presentation.
4. **Kim, J. E.;** Phuntsho S.; Chekli L.; Hong S. K.; Ghaffour N.; Leiknes T.; Shon H. K., Life cycle assessment of fertiliser drawn forward osmosis and nanofiltration hybrid system, The 5th IWA Regional Conference on Membrane Technology (IWA-RMTC 2016), 22-24 August 2016. Oral Presentation.
5. **Kim, J. E.;** Phuntsho S.; Hong S. K.; Ghaffour N.; Leiknes T.; Choi J. Y.; Shon H. K., Environmental and economic assessment of fertilizer drawn forward osmosis and nanofiltration hybrid system for desalination of mine impaired water, Desalination for the Environment: Clean Water and Energy (EDS), 22-26 May 2016. Oral Presentation.
6. **Kim, J. E.;** Phuntsho S.; Shon H. K., Environmental and economic assessment of fertilizer drawn forward osmosis and nanofiltration hybrid system, North American Membrane Society (NAMS), 12-25 May 2016. Oral Presentation.
7. **Kim, J. E.;** Phuntsho S.; Shon H. K., A comparative life cycle assessment of fertilizer drawn forward osmosis and nanofiltration (FO-NF) hybrid system for mine impaired water desalination, International Desalination Workshop (IDW), 18-21 November 2015, *Awarded the Best Poster Presentation*.
8. Phuntsho S.; **Kim J. E.;** Hong S. K.; Chanan A.; Randall D.; Elimelech M.; and Shon H. K., Pilot-scale pressure assisted fertiliser drawn forward osmosis for fertigation, International Conference on Emerging Water Desalination Technologies in Municipal and Industrial Applications, 28-29 August 2015. Oral Presentation.

9. Phuntsho S.; **Kim J. E.**; Shon H. K.; Fertilizer drawn forward osmosis process: Pilot-scale desalination of mine impaired water for fertigation, International Conference on Materials for Advanced Technologies, 26-29 July 2015. Oral Presentation.
10. Phuntsho S.; **Kim J. E.**; Park M. J.; Shon H. K., Pilot-scale fertilizer driven forward osmosis desalination and graphene oxide incorporated thin-film composite forward osmosis membrane, International Conference on Desalination using Membrane Technology, 28 June-03 July 2015. Oral Presentation.
11. **Kim J. E.**, 'Pilot-scale low-energy forward osmosis process for brackish water desalination' Presentation at Faculty of Engineering & IT Showcase, 2013. **Awarded best poster presentation award.**
12. **Kim J. E.**, 'Pilot-scale low-energy forward osmosis process for brackish water desalination' Presentation at Faculty of Engineering & IT Showcase, 2013. **Awarded best oral presentation award (The best innovation prize).**
13. **Kim J. E.**, Sherub Phuntsho, Ho Kyong Shon. 'Pilot-scale nanofiltration system as post-treatment for fertiliser-drawn forward osmosis desalination for direct fertigation' Presentation at International Desalination and workshop (IDW), Jeju, Korea, 28-31 October 2012. **Awarded best oral presentation award.**

Presentations made during the Ph.D. candidature including oral and poster presentations.

LIST OF ABBREVIATIONS

| | |
|----------|-------------------------------------|
| AOP | Advanced oxidation process |
| BWRO | Brackish water reverse osmosis |
| CA | Cellulose acetate |
| CAPEX | Capital expense |
| CC | Membrane cleaning chemicals |
| CNT | Carbon nanotube |
| CP | Concentration polarization |
| CS | Corrugated spacer |
| CTA | Cellulose triacetate |
| DDS | Diluted draw solution |
| DI water | Deionized water |
| DS | Forward osmosis |
| EC | Electrical conductivity |
| EC | Energy |
| ECP | External concentration polarisation |
| ED | Electrodialysis |
| EDTA | Ethylenediaminetetraacetic acid |
| EP | Eutrophication |
| ET | Ecotoxicity |
| FDFO | Fertiliser driven forward osmosis |
| FMR | Fossil fuel and mineral resource |
| FO | Forward osmosis |
| FS | Feed solution |
| GAC | Granular activated carbon |
| GO | Graphene oxide |
| GW | Global warming |
| HF | Hollow fibre |
| HTI | Hydration technology innovations |
| HTI | Human toxicity |
| ICP | Internal concentration polarisation |

| | |
|--------|-----------------------------------|
| IP | Interfacial polymerization |
| LCA | Life cycle assessment |
| LCI | Life cycle inventory |
| LCIA | Life cycle impact assessment |
| LPRO | Low-pressure reverse osmosis |
| MBC | Membrane brine concentrator |
| MBR | Membrane bioreactor |
| MD | Membrane distillation |
| MDC | Microbial desalination cells |
| MED | Multi-effect distillation |
| MF | Microfiltration |
| MNPs | Magnetic nanoparticles |
| MR | Membrane replacement |
| MS | Medium spacer |
| MSF | Multi-stage flash |
| MW | Molecular weight |
| NF | Nanofiltration |
| OD | Osmotic dilution |
| OD | Ozone depletion |
| OMBR | Osmotic membrane bioreactor |
| OPEX | Operational expense |
| PA | Polyamide |
| PAA | Polyacrylic acid |
| PAFO | Pressure-assisted forward osmosis |
| PAO | Pressure-assisted osmosis |
| PAspNa | Poly aspartic acid sodium salt |
| PBI | Polybenzimidazole |
| PES | Polyethersulfone |
| PET | Polyethylene terephthalate |
| PRO | Pressure retarded osmosis |
| PSf | Polysulfone |
| PV | Photovoltaic |
| rGO | Reduced graphene oxide |

| | |
|-------|---|
| RO | Reverse osmosis |
| ROSA | Reverse osmosis system analysis |
| RSF | Reverse solute flux |
| RSS | Red sea salt |
| SEC | Specific energy consumption |
| SOA | Ammonium sulphate or $(\text{NH}_4)_2\text{SO}_4$ |
| SRSF | Specific reverse solute flux |
| SRT | Solids retention time |
| SWFO | Spiral wound forward osmosis |
| SWRO | Seawater reverse osmosis |
| TDS | Total dissolved solids |
| TFC | Thin-film composite |
| TFI | Thin-film inorganic |
| TFN | Thin-film nanocomposite |
| TMA | Trimethylamine |
| TOC | Total organic carbon |
| TREG | Triethyleneglycol |
| TrOCs | Trace organic compounds |
| UF | Ultrafiltration |
| VMD | Vacuum membrane distillation |
| WHO | World health organization |
| WPT | Wastewater treatment plant |
| ZLD | Zero-liquid discharge |

LIST OF SYMBOLS

| | | |
|-----------|---|---|
| A | Pure water permeability coefficient | $\text{Lm}^{-2}\text{h}^{-1}\text{bar}^{-1}$ |
| μ | Dynamic viscosity | |
| B | Salt permeability coefficient | ms^{-1} |
| C | Molar solute concentration | Moles or M |
| C_{D0} | Initial draw solution concentration | Moles or M |
| C_{Db} | Bulk draw solution concentration | Moles or M |
| C_{F0} | Initial feed solution concentration | Moles or M |
| C_{Fb} | Bulk feed solution concentration | Moles or M |
| D | Solute diffusivity | m^2s^{-1} |
| D_D | Diffusion coefficient of the draw solute | m^2/s |
| D_F | Diffusion coefficient of the feed solute | m^2/s |
| d_h | Hydraulic diameter | m |
| D_h | Diffusion coefficient of the feed channel | m^2/s |
| J_s | Salt flux | $\text{gm}^{-2}\text{h}^{-1}$ or $\text{mmolesm}^{-2}\text{h}^{-1}$ |
| J_w | Water flux | $\text{Lm}^{-2}\text{h}^{-1}$ |
| k | Mass transfer coefficient | |
| K | Solute resistivity | sm^{-1} |
| L | Length of channel | m |
| M | Molar concentration of the solution | Moles or M |
| M_w | Molecular weight | Mole/g |
| P | Applied pressure | Bar |
| Q_{D0} | Initial draw flow rate | L/min |
| Q_{F0} | Initial feed flow rate | L/min |
| Q_P | Permeate flow rate | L/min |
| R | Salt rejection | % |
| Re | Reynolds number | |
| RR_{FO} | Forward osmosis feed recovery | % |
| S | Structural parameter | m |
| Sc | Schmidt number | |
| Sh | Sherwood number | |

| | | |
|-------------|-----------------------------------|-----|
| Π | Osmotic pressure | bar |
| $\Delta\Pi$ | Net osmotic pressure | |
| $\Pi_{D,b}$ | Bulk draw osmotic pressure | bar |
| $\Pi_{D,m}$ | Osmotic pressure at support layer | bar |
| $\Pi_{F,b}$ | Bulk feed osmotic pressure | bar |
| $\Pi_{F,m}$ | Osmotic pressure at active layer | bar |
| ρ | Solution density | |

TABLE OF CONTENTS

| | |
|---|-------------|
| CERTIFICATE OF AUTHORSHIP/ORIGINALITY | ii |
| ACKNOWLEDGMENTS..... | iii |
| JOURNAL ARTICLES PUBLISHED OR SUBMITTED** | iv |
| CONFERENCE PAPERS AND PRESENTATIONS..... | vi |
| LIST OF ABBREVIATIONS | viii |
| TABLE OF CONTENTS | xiii |
| LIST OF TABLES | xix |
| LIST OF FIGURES..... | xxii |
| ABSTRACT | xxix |
| CHAPTER 1 | 1 |
| INTRODUCTION..... | 1 |
| 1.1. Introduction | 1 |
| 1.2. Research motivation..... | 5 |
| 1.2.1. Water reuse as a solution for water scarcity problems | 5 |
| 1.2.2. Desalination for safe water supply | 5 |
| 1.3. Need for cost-effective water technologies..... | 6 |
| 1.4. Objectives and the research scope | 6 |
| 1.5. Structure of the study | 7 |
| CHAPTER 2 | 10 |
| LITERATURE REVIEW | 10 |
| 2.1. Introduction | 11 |
| 2.2. Forward osmosis process | 11 |

| | |
|--|-----------|
| 2.2.1. Classification of osmotic agent DS..... | 12 |
| 2.2.2. Development of forward osmosis membranes | 16 |
| 2.3. Sustainability of forward osmosis hybrid systems | 23 |
| 2.3.1. Seawater and brackish water desalination | 26 |
| 2.3.1.1. Hybrid systems for the recovery of DS..... | 26 |
| 2.3.1.2. FO as an advanced desalination pre-treatment process..... | 31 |
| 2.3.2. Hybrid FO systems as an alternative to conventional desalination process | 34 |
| 2.3.3. Wastewater treatment | 41 |
| 2.3.3.1. OMBR-RO hybrid systems | 41 |
| 2.3.3.2. Other hybrid systems for wastewater treatment | 43 |
| 2.3.4. Simultaneous wastewater treatment and seawater desalination | 49 |
| 2.4. Environmental and economic life cycle assessment of hybrid FO systems | 53 |
| CHAPTER 3 | 58 |
| MATERIALS AND METHODS | 58 |
| 3.1. Introduction | 59 |
| 3.2. Experimental procedure and operating conditions | 59 |
| 3.2.1. Chemicals and solutions used | 59 |
| 3.2.1.1. Feed solutions for the forward osmosis process | 59 |
| 3.2.1.2. Feed solutions for the nanofiltration and reverse osmosis processes | 60 |
| 3.2.1.3. Draw solutions for the forward osmosis process | 60 |
| 3.2.2. Membranes and their characteristics..... | 61 |
| 3.2.2.1. Forward osmosis (FO) membranes | 61 |
| 3.2.2.2. Reverse osmosis (RO) and Nanofiltration (NF) membranes..... | 62 |
| 3.2.3. Bench-scale experimental set-up | 65 |
| 3.2.3.1. Bench-scale FO system | 65 |
| 3.2.3.2. Bench-scale NF/RO systems | 67 |
| 3.2.3.3. Pilot-scale FO with NF experimental set-up | 69 |
| 3.3. Analytical methods for the solution samples..... | 71 |
| 3.3.1. Speciation and osmotic pressure of the solutions used | 71 |
| 3.3.2. Determination of the reverse diffusion of draw solutes | 71 |

| | |
|------------------------|-----------|
| CHAPTER 4 | 73 |
|------------------------|-----------|

| | |
|---|-----------|
| HYBRID FORWARD OSMOSIS AND NANOFILTEATION SYSTEM: PILOT-SCALE DESALINATION OF MINE IMPAIRED WATER FOR FERTIGATION..... | 73 |
|---|-----------|

| | |
|---|-----------|
| 4.1. Introduction | 74 |
| 4.2. Materials and Method..... | 74 |
| 4.2.1. Location and source of saline water | 74 |
| 4.2.2. Fertiliser draw solution..... | 77 |
| 4.2.3. Operation of pilot-scale FDFO-NF desalination system | 78 |
| 4.2.4. Water quality monitoring and the test fertigation..... | 80 |
| 4.3. Results and discussion..... | 81 |
| 4.3.1. Process optimisation study | 81 |
| 4.3.2. Long-term operation of the FDFO process | 83 |
| 4.3.3. Operation of the nanofiltration process | 89 |
| 4.3.4. Test fertigation of turf grass and potted tomato plants..... | 92 |
| 4.3.5. Implications of solute fluxes in a closed loop FDFO-NF system | 95 |
| 4.4. Concluding remarks..... | 99 |

| | |
|------------------------|------------|
| CHAPTER 5 | 100 |
|------------------------|------------|

| | |
|--|------------|
| LIFE CYCLE ENVIRONMENTAL AND ECONOMIC IMPACTS OF FORWARD OSMOSIS AND NANOFILTRATION HYBRID SYSTEM | 100 |
|--|------------|

| | |
|--|------------|
| 5.1. Introduction | 101 |
| 5.2. Materials and Methods | 102 |
| 5.2.1. Life cycle assessment of hybrid desalination systems | 102 |
| 5.2.1.1. Life cycle inventory (LCI) analysis | 103 |
| 5.2.1.2. Methodology of life cycle impact assessment..... | 111 |
| 5.2.2. Sensitivity analysis | 112 |
| 5.2.3. Hybrid process design conditions | 116 |
| 5.2.3.1. Conventional RO hybrid desalination processes | 116 |
| 5.2.3.2. FDFO-NF hybrid desalination process | 117 |

| | |
|--|------------|
| 5.3. Results and discussion..... | 119 |
| 5.3.1. Environmental impact assessment of desalination hybrid systems..... | 119 |
| 5.3.2. Economic analysis: Operation expenditure (OPEX) | 122 |
| 5.3.3. Sensitivity analysis of the FDFO-NF hybrid system | 124 |
| 5.4. Concluding remarks..... | 130 |
| | |
| CHAPTER 6 | 132 |
| | |
| ENVIRONMENTAL AND ECONOMIC ASSESSMENT OF HYBRID FO-RO/NF SYSTEM WITH SELECTED INORGANIC DRAW SOLUTES FOR THE TREATMENT OF MINE IMPAIRED WATER | 132 |
| 6.1. Introduction | 133 |
| 6.2. Materials and Methods | 135 |
| 6.2.1. Bench-scale FO experiments | 135 |
| 6.2.2. Full-scale simulation of FO, RO and NF processes | 137 |
| 6.3. Environmental and economic life cycle assessment | 140 |
| 6.3.1. Environmental impact assessment | 140 |
| 6.3.2. Economic life cycle assessment | 145 |
| 6.4. Results and discussion..... | 149 |
| 6.4.1. Draw solute performances..... | 149 |
| 6.4.2. Evaluation of the DS reconcentration in RO and NF processes..... | 150 |
| 6.4.3. Environmental impact assessment of FO hybrid systems | 151 |
| 6.4.3.1. Baseline environmental life cycle assessment..... | 151 |
| 6.4.3.2. Impact of operational adjustment of FO-NF hybrid system..... | 153 |
| 6.4.3.3. Impact of FO brine disposal on environmental potential..... | 154 |
| 6.4.4. CAPEX and OPEX cost evaluation | 157 |
| 6.5. Concluding remarks..... | 161 |
| | |
| CHAPTER 7 | 163 |

| | |
|--|----------------|
| PRACTICAL CONSIDERATIONS FOR OPERABILITY OF SPIRAL WOUND FORWARD OSMOSIS MODULE: HYDRODYNAMICS FOULING BEHAVIOUR AND CLEANING STRATEGY..... | 163 |
| 7.1. Introduction | 164 |
| 7.2. Materials and Methods | 167 |
| 7.2.1. Spiral wound FO membrane module | 167 |
| 7.2.2. Feed and draw solutions | 169 |
| 7.2.3. Pilot-scale system and experimental procedure..... | 169 |
| 7.2.4. Fouling cycles and cleaning experimental procedure | 172 |
| 7.3. Results and discussion..... | 173 |
| 7.3.1. Impact of operating conditions on module hydrodynamics | 173 |
| 7.3.1.1. Impact of feed and draw flow rates on pressure-drop (without permeation) | 173 |
| 7.3.1.2. Impact of feed and draw channel pressurisation on pressure-drop | 176 |
| 7.3.2. Relative contribution of hydraulic pressure to permeation flux | 178 |
| 7.3.3. Fouling behaviour in SW FO modules and impact on hydraulic performance | 180 |
| 7.3.4. Fouling reversibility by osmotic backwash | 184 |
| 7.4. Concluding remarks..... | 186 |
| CHAPTER 8 | 187 |
| FORWARD OSMOSIS MEMBRANE MODULAR CONFIGURATIONS FOR OSMOTIC DILUTION OF SEAWATER BY FORWARD OSMOSIS AND REVERSE OSMOSIS HYBRID SYSTEM | 187 |
| 8.1. Introduction | 188 |
| 8.2. Materials and Methods | 189 |
| 8.2.1. Spiral wound FO membrane element | 189 |
| 8.2.2. Feed and draw solutions | 190 |
| 8.2.3. Pilot-scale experimental procedure | 190 |
| 8.2.4. Determination of pure water permeability and salt rejection | 191 |

| | |
|---|------------|
| 8.3. Results and discussion..... | 193 |
| 8.3.1. Correlation between the operational parameters of an FO module operation..... | 193 |
| 8.3.2. Determination of possible element arrangement options in series..... | 198 |
| 8.3.2.1. Simulating the variations of flow rate and pressure along the FO module | 198 |
| 8.3.2.2. Exploring different FO element arrangement scenarios: sensitivity analysis..... | 202 |
| 8.3.3. Performance simulations of the different modular options..... | 204 |
| 8.3.4. Implications of the configuration options | 208 |
| 8.4. Concluding remarks..... | 211 |
| | |
| CHAPTER 9 | 213 |
| | |
| CONCLUSIONS AND RECOMMENDATIONS | 213 |
| 9.1. Conclusions..... | 214 |
| 9.1.1. Long-term module-scale operation of forward osmosis and nanofiltration hybrid system in the field..... | 214 |
| 9.1.2. Environmental and economic feasibility of the FO hybrid system | 215 |
| 9.1.3. Different types of inorganic draw solutes in the life cycle assessment of the FO hybrid systems | 215 |
| 9.1.4. Spiral wound forward osmosis membrane module operation: hydrodynamics, fouling behavior and cleaning strategy | 217 |
| 9.1.5. FO membrane module configuration options for osmotic dilution of seawater by FO-RO hybrid system | 218 |
| 9.2. Recommendations | 219 |
| | |
| REFERENCES..... | 224 |

LIST OF TABLES

| | |
|---|----|
| Table 2 - 1. Classification of draw solutes and characteristic of the different types of DS | 12 |
| Table 2 - 2. Physiochemical properties and experimental water flux of organic and inorganic based draw solutes tested as DS. Adapted from (Achilli et al. 2010; Akther et al. 2015; Chekli et al. 2012) | 15 |
| Table 2 - 3. Recent advancement of FO membranes. Adapted and modified from Akther et al. (2015)..... | 18 |
| Table 2 - 4. Different spiral wound module tested for pilot-scale FO operation. Adapted from (Blandin, Verliefe, et al. 2016) | 22 |
| Table 2 - 5. A comparison of different configurations of hybrid FO systems | 25 |
| Table 2 - 6. Summary of hybrid FO desalination systems..... | 36 |
| Table 2 - 7. Summary of hybrid FO systems for wastewater treatment | 46 |
| Table 2 - 8. Quantitative comparison of total energy consumption, total capital costs and space footprint for the different configurations and conventional SWRO plant (adapted from (Sim et al. 2013a))..... | 50 |
| Table 3 - 1. List of chemicals used as draw solutes..... | 61 |
| Table 3 - 2. Basic properties of the membranes used in experiments. The material composition is as provided by the manufacturer..... | 63 |
| Table 4 - 1. Characteristics of the saline water from a water treatment plant show for one typical sample (1 st long term operation cycle) together with the standard deviation of twelve collected samples presented in the brackets..... | 77 |
| Table 4 - 2. Characteristics of the feed water and diluted DS before and after the FDFO experiments. The average feed rejection rates (R) for each ion were determined based on the average concentrations of each ion in the initial and final DS. The standard deviation of all the six samples is provided in the brackets). (FS _i : initial feed solution, | |

FS_F: final feed solution, DS_F=final draw solution, *R*: feed rejection rate, SRSF: specific reverse solute flux). The osmotic pressure of the two types of saline feed water presented in Table 1 was calculated using the ROSA software (Version 9.1, Filmtec DOW™ Chemicals, USA). 89

Table 4 - 3. Characteristics of NF permeate using diluted fertiliser DS as the feed. The standard deviation of all the six samples is provided in the brackets. 92

Table 4 - 4. Types of water used for test fertigation of crops. Hunter water was the tap water delivered to the pilot site in the water taker..... 95

Table 5 - 1. Characterisation of mine impaired feed water for all hybrid systems and NF feed and permeate water for the NF process in the FDFO-NF hybrid system. 106

Table 5 - 2. Operational phase of life cycle inventories (LCI) for all hybrid processes. 107

Table 5 - 3. Environmental impact categories used in LCIA (Bengtsson et al. 2010; Fritzmann et al. 2007; Hancock et al. 2012; PRé-Consultants 2008). 111

Table 5 - 4. Parameters included in the sensitivity analysis. 114

Table 5 - 5. Flux modelling adapted in this study for FO full-scale simulation. 115

Table 5 - 6. Input parameters used for FO flux estimation based on the pilot operation data. 116

Table 5 - 7. The hybrid process design conditions used in this study and the process simulation results. 119

Table 6 - 1. Characterization of DSs used for FO and feed solution for RO and NF experiments 136

Table 6 - 2. Input parameters for each draw solution used for FO process simulation. 136

Table 6 - 3. Simulation equations for a continuous close-loop FO-RO and FO-NF hybrid systems (Deshmukh et al. 2015; Phuntsho, Kim, Johir, et al. 2016; Shaffer et al. 2012). 139

| | |
|---|-----|
| Table 6 - 4. Manufacturer specifications of RO and NF membranes used in this study..... | 140 |
| Table 6 - 5. Life cycle inventory data for all unit processes..... | 142 |
| Table 6 - 6. Economic values used in cost analysis for desalination processes (Australian dollar)..... | 146 |
| Table 6 - 7. Typical cost parameters for desalination plant, values of FO hybrid plant were estimated based on the literature, simulation and optimization of currently available desalination plant (100,000 m ³ /day)..... | 148 |
| Table 6 - 8. FO experimental water flux (J_w), RSF (J_s), and SRSF (J_s/J_w) behaviours using 1 M DSs with BGW as FS in the FO process..... | 149 |
| Table 6 - 9. ROSA software simulation results of RO and NF processes using different RO and NF membrane modules (Version 9.1, Filmtech Dow Chemicals, USA)..... | 150 |
| Table 7 - 1. Specifications of two spiral wound forward osmosis membrane modules employed in this study..... | 168 |
| Table 7 - 2. HTI CTA and Toray TFC FO membrane properties (i.e., water and salt (NaCl) permeability coefficients and rejection of the active layer, the structural parameter of the support layer and membrane thickness)..... | 168 |
| Table 7 - 3. Sea Salt of 35 g/L prepared in Milli-Q Water (Blandin et al. 2013)..... | 169 |
| Table 7 - 4. Experimental conditions for module hydrodynamic tests..... | 170 |
| Table 7 - 5. Comparison of specific reverse salt flux (SRSF, J_s/J_w) behaviour in pilot-scale FO and PAO processes using two different SW FO modules: CTA and TFC.... | 180 |
| Table 8 - 1. Input data for the performance simulation of FO and PAO processes. | 189 |
| Table 8 - 2. Six different modular configuration options for sensitivity analysis..... | 204 |

LIST OF FIGURES

| | |
|---|----|
| Figure 1 - 1. Structure of the research..... | 9 |
| Figure 2 - 1. Flow direction in a spiral wound module modified for FO applications. The feed stream flows through the central tube into the inner side of the membrane envelope and the draw stream flows in the space between the rolled envelopes. Figure adapted from (Mehta 1982)..... | 22 |
| Figure 2 - 2. Overview of distribution of applications and integrated systems | 24 |
| Figure 2 - 3. A design of quasi-continuous temperature driven FO desalination with a semi-IPN hydrogel coated onto the outside surface of the FO hollow fiber membranes (adapted from (Cai et al. 2013). Apart from the energy needed to pump the saline water feed through the lumen of the hollow fibers, the periodic temperature modulation within 15 °C (e.g., between 25 and 40 °C) is essentially the only driving force for desalination in this configuration. This temperature difference can be readily obtained using warm air generated from industrial waste heat | 30 |
| Figure 2 - 4. Comparative estimation of energy cost for SWRO and hybrid FO-LPRO | 33 |
| Figure 2 - 5. Schematic of an OD-RO hybrid process plant for simultaneous treatment of wastewater and seawater desalination (DS: Draw solution; FS: Feed solution; RO: Reverse osmosis; WW: Wastewater)..... | 52 |
| Figure 2 - 6. ONE Desal project overview: From lab-scale development and optimization to hybrid FO-RO plant operation | 57 |
| Figure 3 - 1. Schematic diagram of a spiral wound forward osmosis (FO) module showing the direction of water in the module | 64 |
| Figure 3 - 2. Schematic diagram of a 4040 spiral wound reverse osmosis (RO) and nanofiltration (NF) module showing the direction of water in the module | 64 |
| Figure 3 - 3. Feed solutions for the nanofiltration and reverse osmosis processes | 66 |

| | |
|---|----|
| Figure 3 - 4. Bench-scale pressure based membrane processes experimental setup. (a) Schematic drawing of the bench scale NF/RO unit and (b) a photo of bench-scale NF/RO unit..... | 68 |
| Figure 3 - 5. A schematic diagram of (a) FO process, (b) NF process and (c) a photo of pilot-scale FDFO-NF hybrid system installed at University of Technology Sydney (UTS) | 70 |
| Figure 4 - 1. Location of the pilot-scale FDFO-NF desalination testing site at the Centennial Coalmine site under the State of NSW, Australia..... | 76 |
| Figure 4-2. Schematic diagram of the FDFO-NF desalination system used for pilot-scale testing in the field. | 80 |
| Figure 4 - 3. Variations of the performance parameters during the FDFO pilot unit process optimisation process. (a) Water flux and cumulative extracted volume with time, (b) DS concentrations or EC at the inlet/outlet and the dilution factor with time, (c) feed TDS or EC and feed recovery rates with time and (d) water flux under different feed flow rates. Initial DS and FS volumes are 200 L and 5,000 L respectively. | 83 |
| Figure 4 - 4. Performance of the FDFO desalination process on longer run cycles. (a) Variation of water flux with operation time and (b) the variation of water flux with the cumulative volume of water extracted during the batch operation process showing together the baseline fluxes before and after cleaning of the FO membrane and the picture showing algae growth in the feed water tank during the cycle 4 of the operation. Baseline fluxes were conducted using 0.5 M SOA as DS and tap water as FS at a feed crossflow rate of 4.2 m ³ h ⁻¹ | 86 |
| Figure 4 - 5. Performance of the NF process as post-treatment using the diluted fertiliser DS from the FDFO desalination process as NF feed water. Variations of the (a) specific NF permeate flux and (b) NF permeate electrical conductivity with the cumulative increase in the NF feed concentration (diluted fertiliser) during the batch NF operation process..... | 92 |
| Figure 4 - 6. Visual monitoring of the turf grass during the entire period of the test fertigation at the Davos turf farm | 93 |

Figure 4 - 7. Potted tomato plants at the various stages of the growth during test fertigation using four different types of test water 95

Figure 4 - 8. Implications of solutes transfer through the FO and NF membranes assessed based on the (a) expected variations of the draw solute concentrations in the FDFO feed concentrate/brine at different FDFO feed recovery rates where the NH_4^+ and SO_4^{2-} concentrations in the brine was calculated using the relationship [$\text{SRSF} \times \text{RR}/(1-\text{RR})$] (RR is the feed recovery rate) and (b) expected variations of the feed solute (NaCl) concentrations in the concentrated SOA DS under different FO and NF rejection rates. For simulation, NaCl feed rejection of CTA FO membrane at $R_{\text{FO}}=87.6\%$, SRSF of NaCl was assumed at 0.46 g/L (She et al. 2012), for $R_{\text{FO}}=90\%$, SRSF was assumed at 0.327 g/L (Ren et al. 2014) and the NF feed recovery rate was assumed about 84%... 98

Figure 5 - 1. Boundaries of the coal mine impaired water desalination system for all hybrid systems – life cycle inventory (LCI) for environmental and economic impact assessment. 103

Figure 5 - 2. Modelled water flux as a function of experimental water flux. The modelled water flux was calculated using Equation. 3 in Table 5-5. Feed concentration was constant at 1.66 bars (feed water was converted to the concentration of NaCl and calculated the osmotic pressure using OLI software). The draw solution concentration varied. The feed rate was 70 L/min, the draw flow rate was 7 L/min, and temperature was 25°C..... 113

Figure 5 - 3. Schematic diagram of hybrid desalination systems of (a) MF-RO (b) UF-RO and (c) FDFO-NF. N.B. P: Pump and HP: High pressure pump. 118

Figure 5 - 4. Relative contribution analysis of (a) three operational components for each hybrid system and (b) of four hybrid processes for three main components under six impact categories. FDFO-NF with CTA and TFC and an average water flux was around 3 and 10 LMH, respectively. Three operational components refer to membrane materials, electricity, and chemicals. 122

Figure 5 - 5. (a) Cost contribution analysis of three main operational components for four hybrid systems and (b) specific cost contribution analysis of FDFO-NF with CTA

and TFC hybrid systems. MR, EC, and CC refer to the costs of membrane replacement, energy consumption, and cleaning chemicals. 124

Figure 5 - 6. Unit OPEX cost of the FDFO-NF using (a) CTA and (b) TFC FO membrane modules as a function of FO average water fluxes and FO module cost variation (AUD\$200-AUD\$1,500). Plant capacity 100,000 m³/day. The average flux ($J_{ave.}$) of the FDFO-NF (CTA) refers to 3, 6, 8, and 25 LMH and that of the FDFO-NF (TFC) refers to 10, 11, 20, and 25 LMH..... 127

Figure 5 - 7. Sensitivity analysis of FDFO-NF (CTA and TFC) OPEX costs as a function of NF process recovery rates. The FO module cost was assumed to be \$1,250/module in 2016, and the average FO water fluxes were estimated based on the closed-loop mass-balance simulation of the FDFO-NF hybrid system..... 129

Figure 6 - 1. Thermodynamic properties of draw solutions used in this study, calculated using OLI Stream Analyser 3.2 (OLI Systems, Inc., Morris Plains, NJ) (a) Osmotic pressure, (b) viscosity (c) electrical conductivity and (d) diffusivity as a function of molar concentration of the four draw solutions at 25 °C. 137

Figure 6 - 2. A schematic diagram of a closed-loop FO and RO/NF hybrid system operation. *MgSO₄ was excluded for a simulation of the post-treatment processes due to its poor performance in the FO process (see Section 6.4.1)..... 141

Figure 6 - 3. Specific parameters for cost estimation for desalination processes..... 146

Figure 6 - 4. Relative contribution analysis of various components of the FO-RO and FO-NF hybrid systems with DSs to global warming impact (a) without DS replenishment and (b) with DS replenishment in FO hybrid systems. 152

Figure 6 - 5. Initial and optimised (a) energy use and (b) global warming impact for FO-NF hybrid systems with different DSs. Target data: final product concentration of 100 mg/L TDS and brine concentration of 0.6 M NaCl (i.e. seawater osmotic pressure). . 154

Figure 6 - 6. The impact of FO brine disposal on (a) energy and (b) global warming per unit of water produced for each hybrid system with different DSs. FO brine disposal energy was calculated based on the optimised conditions of FO hybrid system: final

| | |
|---|-----|
| product concentration of 100 mg/L TDS and brine concentration of 0.6 M NaCl (i.e. seawater osmotic pressure)..... | 156 |
| Figure 6 - 7. (a) Life cycle cost analysis (\$/m ³ water produced) and (b) impacts of SRSF on the OPEX cost of each hybrid desalination system based on a plant capacity of 100,000 m ³ /d. The SRSF was down to 0.01 g/L. The RO and NF permeates were assumed to be the same for all hybrid systems (≈ 500 mg/L)..... | 159 |
| Figure 6 - 8. Total water cost of the FO-NF90 hybrid system with different DSs (NaCl, MgCl ₂ , and Na ₂ SO ₄) to produce 100,000 m ³ /d. | 161 |
| Figure 7 - 1. Schematic diagram of the pilot-scale FO experimental set up and illustration of 8040 spiral wound FO modules: (a) CS CTA and (b) MS TFC (CS: corrugated feed spacer and MS: medium diamond shape feed spacer). | 170 |
| Figure 7 - 2. Variation of NaCl concentration with NaCl conductivity..... | 172 |
| Figure 7 - 3. Effect of feed and draw cross-flow velocities on pressure build-up in CTA (a and b) and TFC (c and d) modules. Tap water was used as FS and DS. | 175 |
| Figure 7 - 4. Impact of feed inlet pressure on the feed and draw channel pressurisation with (a) CTA and (b) TFC modules. Feed cross-flow velocity was constant at 0.18 m/s for CTA and 0.37 m/s for TFC, while the draw flow cross-flow velocities for CTA and TFC modules were 0.04 and 0.09 m/s, respectively. Tap water was used as FS and DS. | 177 |
| Figure 7 - 5. Comparison of flux behaviour in pilot-scale FO and PAO processes using two different SW FO modules. Experimental conditions: feed flow rate: 0.18 and 0.37 m/s for CTA and TFC, respectively, draw flow rate: 0.04 m/s for CTA and 0.09 m/s for TFC, and applied pressure in PAO: 1, 2 and 2.5 bar, 35 g/L RSS as DS and tap water as FS..... | 179 |
| Figure 7 - 6. Effect of organic foulant in feed solution on FO fouling of CTA (a and b) and TFC (c and d) modules. (a) and (c) water flux (J _w) as a function of permeate volume (L); (b) and (d) permeate volume (L) and recovery rate (R) as a function of operation time. Fouling experiments were conducted using 35 g/L RSS as DS and feed fouling | |

solution prepared by addition of 1.2 g/L RSS, 0.22 g/L CaCl₂, 0.2 g/L alginate, 0.2 g/L humic acid. 182

Figure 7 - 7. Feed inlet pressure change with CTA and TFC modules. Fouling experiments were conducted using 35 g/L RSS as DS and feed fouling solution prepared by addition of 1.2 g/L RSS, 0.22 g/L CaCl₂, 0.2 g/L alginate, 0.2 g/L humic acid..... 183

Figure 7 - 8. (a) Variation of reverse water flux and feed pressure drop with osmotic backwash operation time, (b) effect of osmotic backwash and physical cleaning on the feed inlet pressure recovery and (c) total organic carbon (TOC, mg/L) concentration as a function of the water volume flushed (L). Physical cleaning with maximum feed cross-flow velocity of 0.44 and 0.91 m/s for CTA and TFC, respectively was performed for 5 min using tap water. The TOC of the feed was around 94 mg/L. 185

Figure 8 - 1. Validation of pilot experimental flux and predicted flux for FO TFC membrane module under (a) FO and (b) PAO operations. 193

Figure 8 - 2. (a) Variations of average water flux and feed and draw solution concentrations along the number of elements and (b) variation of feed and draw inlet pressures (this is related to the feed and draw flow rates of the first element) as a function of feed and draw flow rates. This relationship data was obtained from pilot-scale FO operations. FO experimental conditions: 0.6 M NaCl as DS (seawater), 0.02 M NaCl as FS (wastewater), room temperature, and co-current cross-flow condition..... 197

Figure 8 - 3. (a) Variations of the initial flow rates along the DS channel and feed and draw inlet pressures with the number of elements under different (b) feed and (c) draw flow rates. 201

Figure 8 - 4. Schematic of possible modular design options of the FO process with the integration of PAO process. N.B. WW: Wastewater, SW: Seawater..... 203

Figure 8 - 5. Variations of the feed and draw inlet pressures, P_{FS} and P_{DS} (a) in options 1, 2, and 3 and (b) in options 4, 5, and 6, (c) the cumulative permeation flow rate, Q_P , and (d) the final diluted DS concentration, C_{DDS} under different module design options as shown in Figure 8-4. 207

| | |
|--|-----|
| Figure 8 - 6. Evaluation of (a) total membrane area required (m^2) and (b) specific energy consumption (kWh/m^3) of different FO hybrid process options..... | 210 |
| Figure 9 - 1. Diagram of the progress of development of a commercial FO simulation software..... | 222 |
| Figure 9 - 2. Developed Matlab graphical user-friendly interface (GUI) FO simulation software..... | 223 |

ABSTRACT

Forward osmosis (FO) has recently emerged as one of the most promising low energy technologies for desalination and water reclamation. The FO process is based on the principle of natural osmotic process driven by the concentration difference between a concentrated draw solution (DS) and saline water (i.e. feed water, FS) across a semipermeable membrane. In the FO process, fresh water is extracted from the saline water using special osmotic membranes and the concentrated DS becomes diluted. The membrane fouling problem in FO process is less challenging than the reverse osmosis (RO) process mainly as the FO process operates in the absence of high hydraulic pressure, and this is one of the important operational benefits for FO process application in terms of energy. However, the lack of a desirable DS has limited the application of FO desalination for producing drinking water quality. When a normal inorganic salt solution is used as DS, the recovery of draw solutes from the diluted DS require additional subsequent processes that still require energy and this makes FO unattractive compared to the existing RO desalination technology.

The objectives of this study are therefore to investigate the performances of the hybrid FO systems mainly through pilot-scale operations and simulation for different applications, identify its limitations, evaluate its environmental impacts and conduct economic analysis. The Thesis has been presented in nine chapters that include an assessment of the performance of selected draw solutes under a closed-loop system, practical applicability of FO hybrid system through both simulation and module-scale experiments, and development of a simulation software to design FO process for optimum performance. Most of the chapters are in part or in whole already published during the course of this Ph.D. candidature as listed at the beginning of this Thesis.

Considering the challenges of the FO process for potable water desalination, a novel concept of fertilizer drawn forward osmosis (FDFO) has been introduced. In this process, a highly concentrated fertilizer solution is used as the DS to extract water from saline water sources or any impaired water source using a semi-permeable membrane by natural osmosis. The main advantage of the FDFO desalination process is that the final product water or the diluted fertilizer DS, can be used for direct fertigation and thus the separation

of draw solutes is not necessary. However, due to intrinsic process limitations, the diluted fertilizer DS may not meet the water quality standards for direct fertigation especially when feed water sources with high salinity are used. The final diluted DS may require additional dilution before it is suitable for the direct application and the dilution factor can be quite significant depending on the feed water salinity. To reduce the salt concentration of the diluted DS, the nanofiltration (NF) process has been suggested as one of the post-treatment process options to reduce fertilizer nutrient concentrations in the diluted fertilizer DS. The concept of the integrated FDFO desalination process with NF membrane has been evaluated in bench-scale experiments in the earlier studies. However, in this study, this concept has been demonstrated in a larger-scale in the field.

The pilot-scale FDFO and NF system was operated in the field for about six months for the desalination of saline groundwater from the coal mining activities. Although the FO flux can be significantly lowered when high turbidity feed water is used, however; our long-term operation of the FO pilot-scale indicates that simple hydraulic cleaning could effectively restore the water flux without the need for a rigid chemical cleaning. The NF post-treatment process did not experience any noticeable fouling or scaling issues due to the excellent quality of feed water produced by the FDFO process. Test fertigation of the turfgrass and potted tomato growth indicates that FDFO-NF desalination system can produce water quality that meets irrigation standard. However, FO membrane with higher reverse flux selectivity than the cellulose triacetate FO membrane used in this study is needed for scale-up operation of the FDFO desalination process. The reverse diffusion of draw solutes will be one of the biggest challenges of the FDFO process as the nitrogen concentration in the final concentrated brine may not satisfy the effluent discharge standards. Low FO feed rejection may also likely to result in the gradual build-up of feed solutes (such as Na^+ and Cl^-) in fertiliser draw solution during repetitive recycling of the draw solution by the subsequent NF process consequently affecting the final water quality in terms of Na^+ and Cl^- which can be detrimental to the whole process.

Based on the long-term operational data of the FDFO-NF desalination process, environmental and economic impacts of the FDFO-NF hybrid system were conducted and compared with conventional RO hybrid scenarios using microfiltration (MF) or

ultrafiltration (UF) as a pre-treatment process. The results showed that the FDFO-NF hybrid system using thin film composite forward osmosis (TFC) FO membrane has a less environmental impact than the conventional MF or UF based RO hybrid systems due to lower consumption of energy and cleaning chemicals. The energy requirement for the treatment of mine impaired water by the FDFO-NF hybrid system was 1.08 kWh/m³, which is 13.6% less energy than an MF-RO and 21% less than UF-RO hybrid system under similar feed conditions. In a closed-loop system, the FDFO-NF hybrid system using a TFC FO membrane with an optimum NF recovery rate of 84% had the lowest unit operating cost of AUD \$0.41/m³. Given the current relatively high price and low flux performance of the cellulose triacetate (CTA) and TFC FO membranes, the FDFO-NF hybrid system still holds opportunities to lower the operating expenditure further in the future when high performance membranes are available in the market.

In addition, environmental and economic life cycle assessment (LCA) was carried through the simulation of a full-scale closed-loop FO and RO or NF hybrid system for selecting the most suitable DS. Baseline environmental LCA showed that the dominant components for energy use and global warming are the DS recovery processes (i.e., RO or NF processes) and FO membrane materials, respectively. When considering the DS replenishment in the FO process, the contribution of chemical use to the overall global warming impact was significant for all hybrid systems. Furthermore, from an environmental perspective, the FO-NF hybrid system with Na₂SO₄ shows the lowest energy consumption and global warming with additional considerations of final product water quality and FO brine disposal. From an economic perspective too, the FO-NF with Na₂SO₄ showed the lowest total operating cost due to its lower DS loss and relatively low solute cost. In a closed-loop system, FO-NF with NaCl and Na₂SO₄ as DS had the lowest total water cost at optimum NF recovery rates of 90 and 95%, respectively. Overall, draw solute performances and membrane cost in FO and recovery rate in RO/NF play a crucial role in determining the total water cost and environmental impact of FO hybrid systems in a closed-loop operation.

The operation of a large spiral wound forward osmosis (SW FO) module operation is essential to provide a better understanding and practical insight for a full-scale FO

desalination plant. Therefore, two different 8” SW FO modules (i.e. 8040 CTA and TFC FO membrane modules) were investigated for their module-scale operations in terms of hydrodynamics, operating pressure, water and solute fluxes, fouling behavior and cleaning strategy. FO membrane module operation results indicated that, a significantly lower initial DS flow rate is essential in order to lower the pressure drop and also maintain lower pressure within the DS channel as exceeding the DS pressure above the feed pressure would undermine the integrity of the FO membrane. Under FO and pressure assisted osmosis (PAO, up to 2.5 bar) operations, the TFC FO membrane module featured higher water flux and lower reverse salt flux compared to the CTA FO membrane module. The fouling tests with both the FO membrane modules demonstrated that foulant deposition caused feed inlet pressure build-up, indicating that the FO fouling deposition likely occurred in the feed channel rather than on the membrane surface and the location of foulant deposition.

Performance of an FO hybrid system was evaluated for osmotic dilution of seawater using wastewater effluent as a feed source for simultaneous desalination and water reuse based on 8040 FO membrane module-scale experiments and the extrapolated empirical relationship. The main limiting criteria for module operation is to always maintain higher feed pressure than the draw pressure throughout for safe module operation. The study showed that a single membrane housing cannot accommodate more than 4 elements as the draw pressure exceeds the feed pressure. Six different FO modular configurations were proposed and simulated. A two-stage FO configuration with multiple housings (in parallel) in the second stage using same or larger spacer thickness reduces draw pressure build-up as the draw flow rates are reduced to half in the second stage thereby allowing more than 4 elements in the second stage housing. The lower values for feed pressure (pressure drop) and osmotic driving force in the second stage are compensated by operating under the pressure assisted osmosis (PAO) mode which helps enhance permeate flux and maintains positive pressure differences between the feed and draw chamber. The PAO energy penalty is compensated by enhanced permeate throughput, reduced membrane area, and plant footprint. The contribution of FO/PAO to total energy consumption was not significant compared to post RO desalination (90%) indicating that the proposed two-stage FO modular

configuration is one way of making the full-scale FO operation practical for FO-RO hybrid system.

This thesis finally concludes with recommendations to develop high-performance membranes in terms of solute rejections, permeability and improved fouling resistance for its long-term performances. Improving the solute rejections in the form of low specific reverse solute flux is very important in order to eliminate the issue of brine contamination with the draw solutes especially containing fertilizer nutrients which becomes detrimental for brine management and discharge. High feed solute rejection is essential which otherwise would accumulate in the draw solution in a closed-loop FO-RO/NF hybrid system thereby undermining the product water quality. The current design of spiral wound FO membrane module also needs rethinking. There is a need to significantly improve the packing density of the FO membrane element in order to reduce its footprint and the capital cost since its current packing density is only about a third of the RO membrane element. The module also needs to improve its operational robustness as the current module has significant operational challenges in terms of pressure drop. Finally, the thesis recommends developing a simulation software that can be used for the full or module-scale FO process design and system analysis. A brief structural framework on the desing of the software also has been provided.

CHAPTER 1

INTRODUCTION

1.1. Introduction

The world's population is expected to reach about 9.8 billion by 2050 (2017) and hence there is a significant concern on the sustainability of water, food, and energy resources have been raised on this planet. Maintaining sustainable water resources and providing clean water at low energy and cost and maintain adequate food supply to satisfy people all around the world will be a crucial challenge in this century (Ward & Pulido-Velazquez, 2008). In fact, water, energy and food have strong nexus and the scientific solutions to address water, energy and food could therefore play a crucial role in the peace and stability of the world.

The application of membrane technologies for water purification has gained great interest in the last few decades. Among them, reverse osmosis (RO) process is currently the most advanced and versatile membrane based technology for high quality water purification of any saline water and impaired water sources as an alternative resource to augment fresh water or to reduce pressure on fresh water resources (Greenlee et al., 2009). Although RO desalination technology is seen as a promising alternative in providing fresh water supplies to the arid and densely populated regions of the world, it is still seen as an energy intensive process. Seawater RO process is operated at a very high hydraulic pressure (50 to 60 bar) in order to surpass the high osmotic pressure of the seawater and achieve at least about 50% recovery rate (McGinnis & Elimelech, 2007). In addition, RO also suffers from severe membrane fouling which greatly affects its long-term performance and management of concentrated brine. RO processes have to be generally accompanied by extensive pre-treatment processes depending on the feed water quality which adds significantly to the water cost. Because of the high capital and operational costs, RO technologies are unaffordable for many developing economies. Because of the high water cost compared to the fresh water supplies, RO technologies are also economically not viable for large-scale water uses such as for irrigation. A desalination technology that consumes much lower energy and has a low fouling tendency could become a game changer by making the desalination technology more affordable to all the societies in the world and also grow food thereby ensuring both the global water and food security. Low energy technology could also reduce its carbon footprint with lower environmental impact.

Forward osmosis (FO) has recently emerged as a new desalination technology due to the lower energy requirements compared to the conventional desalination technologies such as RO technology. Many efforts have therefore been made to improve the overall FO process efficiency (Choi et al., 2009; McGinnis & Elimelech, 2007). In FO process, natural osmosis (i.e. the absence of hydraulic pressure) is the main driving force and thus water is naturally separated from saline water sources through a semi-permeable membrane due to a concentration gradient between a highly concentrated draw solution (DS) that has high osmotic pressure and a saline water source that has low osmotic pressure (Cath et al., 2006a). This offers several advantages over conventional pressure-driven membrane processes (e.g. RO) such as lower energy consumption and membrane fouling tendency (Cornelissen et al., 2008; Mi & Elimelech, 2010). Recent studies have reported that fouling in the FO process is physically reversible which reduces the need for chemical cleaning frequency (Mi & Elimelech, 2008; Mi & Elimelech, 2010). This ultimately reduces both capital and operation costs of the FO process.

Although FO desalination using a natural osmotic process is more beneficial compared to RO desalination using a high hydraulic pressure, it has some technical drawbacks such as a lack of suitable FO membranes and draw solutes. Many contributions have been made to improve the performance of FO membranes, particularly with thin film composites, carbon nanotube, graphene oxide (GO) and a few other composite membranes (Amini et al., 2013; Arena et al., 2011b; Cath et al., 2006a; Dumée et al., 2013; Han et al., 2012). The research on FO membrane fabrication using different materials have significantly intensified attention on a wider application of the FO process.

In addition, a suitable draw solute is essential for the application of the FO desalination process for potable and non-potable water because its successful application will depend on the selected draw solute. For drinking water applications, the draw solutes in the water need to be recovered/ reconcentrated to produce high quality water (i.e. drinking water standards). In fact, the separation of the draw solute requires additional separation and recovery stages thus consuming additional energy. Therefore, a challenge remains in finding a desirable draw solute for the application of the FO process for drinking water production.

Although FO desalination consumes a much lower rate of energy than conventional desalination processes, it cannot be considered as a stand-alone process mainly due to its

technological limitations mentioned above. Coupling wastewater and seawater streams have therefore emerged as a new approach to develop FO process. FO process is hybridized with seawater RO (SWRO) process and this is referred to as the FO-RO hybrid or osmotic dilution (Altaee et al., 2014b). In the FO-RO hybrid system, an impaired water source (e.g. secondary effluent or tertiary treated effluent) is used as a low salinity feed solution (FS) and water is extracted from to seawater DS by the osmotic pressure difference. The first study on the FO-RO hybrid system reported four major benefits over SWRO desalination including lower energy consumption, reduction of wastewater volume (i.e. wastewater reuse), multi-barrier protection (i.e. high water quality), and increased RO membrane module lifetime (i.e. low membrane fouling) (Cath et al., 2010a). In the FO-RO hybrid configuration, an aspect of the FO process is to reduce the salinity of seawater by osmotic dilution, with the diluted seawater being fed to the subsequent RO desalination process. This results in lower RO feed salinity and thus lower energy consumption and higher water production. Therefore, several hybrid FO systems have been developed for various applications including seawater and brackish water desalination, wastewater treatment, fertigation, and dewatering of RO concentrate. In fact, it has been reported that FO used as a pre-treatment process can be more beneficial in improving the overall efficiency of conventional desalination processes. In particular, when the primary objective is to reduce the energy consumption, FO with the highest possible dilution of seawater by wastewater contributes to the decrease in RO operating pressure (Blandin et al., 2016a). Considering the merit of integrating FO process into the conventional desalination processes, an economic assessment of FO hybrid systems has further demonstrated that it can have positive economics outcomes compared to stand-alone SWRO mainly due to savings in operating costs (Blandin et al., 2015b; Cath et al., 2010a; Valladares Linares et al., 2016).

However, there are some drawbacks and challenges of the FO hybrid system including investment costs for implementing FO process and limited information of a large-scale FO operation data. The first economic assessment conducted by Cath et al. (2009) showed USD 0.43\$/m³ cost savings in regard to the hybrid FO-RO system compared to RO. However, this study considered high energy cost and FO membrane capital costs. Yangali-Quintanilla et al. (2011) further reported that when using FO process as a pre-treatment for RO process, energy consumption for RO process was down to 1.5 kWh/m³ whereas that for stand-alone SWRO was 2.5 to 4 kWh/m³. Although this indicates that

FO can help reduce the operating cost of the RO process, the dilution factor in the FO process should be enough to maintain low operating pressure. Previous studies have pointed out that the key parameter to improve FO economics is FO water fluxes (Blandin et al., 2015b; Deshmukh et al., 2015; Hancock et al., 2012; Zhao et al., 2012c). The recent study revealed that FO processes with lower membrane module cost (USD 30\$/m²) and higher water flux ($\geq 15 \text{ Lm}^{-2}\text{h}^{-1}$) become economically sustainable (Yangali-Quintanilla et al., 2015). Another study confirmed that the current state of commercial FO membrane modules still limits FO-RO hybrid systems' sustainability due to the high capital cost which is significantly dependent on membrane module performance, packing density, and membrane module cost (Blandin et al., 2015b).

Despite significant efforts to develop new FO membranes and modules, only a few membrane modules are commercially available. The most mature module design for a large-scale FO process is spiral wound modules. It was developed by HTI using the cellulose tri acetate FO membrane sheets, varying from 2.5 to 8 inches in diameter. Although most pilot-scale FO studies were carried out using the HTI cellulose triacetate (CTA) module and it was the leader in FO membrane development (Elimelech, 2007; Hancock et al., 2011b; Kim et al., 2014a; Kim et al., 2013a; McGinnis et al., 2012), high investment costs resulting from its poor performance and low packing density limit real application of FO processes. To overcome this limitation, the development of thin-film composite (TFC) membranes which consist of a polyamide (PA) active layer formed by interfacial polymerization on top of a polysulfone substrate has been focused on (Wang et al., 2012). Toray Inc., one of the other membrane suppliers, has developed 8-inch spiral wound TFC membrane modules which have significantly improved performance but their module configurations and optimized conditions are not explicitly described in the open literature as yet. Furthermore, a module-scale FO analysis provided the determination of system-level performance parameters and thus achieved practical insights on the economic feasibility of implementing full-scale FO hybrid systems.

1.2. Research motivation

1.2.1. Water reuse as a solution for water scarcity problems

Sustainable ways of meeting water demand are required to reduce the use of pristine water sources. Since the quality of reclaimed water is compromised, science and technology play a significant role in advancing the water recycling industry. Non-potable water reuse is now widely accepted including landscape irrigation, toilet flushing, vehicle washing and so on. Although the final product water from wastewater treatment is suitable for discharge into the environment, it cannot be accepted for human consumption mainly due to a potential health risk caused by organic micropollutants. To produce high-level water quality, a double or multi-barrier approach can be considered for removal of contaminants. Membrane technologies such as RO and nanofiltration (NF) are therefore expected to play a crucial role in reclaiming water from unconventional water sources.

1.2.2. Desalination for safe water supply

Brackish groundwater and seawater desalination are one of the most promising methods for the augmentation of shrinking water supplies. Membrane desalination processes such as RO and NF are capable of producing a high quality product and removing the majority of contaminants from brackish groundwater and seawater. In Australia, agricultural usage accounts for the highest water consumption of up to 70% of Australia's total water usage (Rutherford & Finlayson, 2011). Desalination is a proven technology that has been used for domestic water supplies and industrial applications (Grafton et al., 2010). However, the energy required for seawater RO desalination has almost reached a plateau and the current cost of desalinated water is still comparatively high. Nevertheless, the increased implementation of desalination technology and increased efficiency results in the decreased cost of desalinated water. In order to further enhance the sustainability of wastewater reclamation and desalination, alternatives must be found to decrease the overall cost and increase the efficiency of the overall process.

1.3. Need for cost-effective water technologies

Forward osmosis has received great attention in recent years because of its low energy consumption compared to the RO process and thus has been investigated in regard to several applications including wastewater treatment and desalination. There is a new approach which involves using seawater or highly concentrated saline water as a DS to extract freshwater from impaired water. The driving force for water extraction in FO is the osmotic gradient between two water streams, such as seawater and impaired water with the absence of hydraulic pressure. This, therefore, results in the low energy cost of the FO process. The diluted seawater is then fed into an RO desalination process that produces high water quality due to high salt rejection. This can provide a new approach for hybridizing the FO process with other conventional desalination processes such as RO and NF.

In the FO-RO hybrid system, seawater DS is being diluted during the FO process and thus the effect of the final concentration of the diluted DS on the energy required for the RO process is significant. This, therefore, indicates that the energy required for a desalination plant can be diminished and thus make it economically favorable. In addition, the concentrated impaired water can be discharged into a wastewater treatment plant for reclamation and used for other beneficial purposes for communities and the environment (e.g. the dilution of the RO brine/concentrate). With the addition of the FO process before the RO process, several issues related to RO membrane modules can be mitigated; fouling potential and chemical cleaning frequency thus lowering the operating cost of the RO process. This study is an initiative in understanding the practical prospects of FO hybrid systems for potable and non-potable reuses.

1.4. Objectives and the research scope

The concept of integrating FO process for various applications including seawater and brackish water desalination and wastewater treatment for potable and non-potable reuses has been widely studied in the recent years. However, there have been only a few studies on the module-scale operation of the FO process and lacks detailed study on the environmental impact and economic assessment of FO-RO/NF hybrid systems. The main objective of this study is, therefore, to advance the concept of FO hybrid systems through

module-scale pilot operations and conduct environmental impact and economic assessment in order to understand their competitiveness over the existing technologies. Specifically, this study, therefore, focused on the following objectives:

- Evaluate the technical feasibility of the FO-NF hybrid system for fertigation purposes through pilot operation in the field operation to understand the long-term performances and its limitations
- Conduct an environmental and economic assessment of FO hybrid systems and compare with the MF/UF-RO hybrid systems
- Understand the performances and its limitations of the full-scale FO process through the operations of pilot-scale FO membrane unit using commercially available spiral wound FO membrane element including their fouling issues
- Develop a simple model to simulate the performance of the FO module with multiple FO membrane elements arranged in series in housing under different volumetric flow rates and the pressure differentials and providing optional design options for a full-scale FO hybrid system

1.5. Structure of the study

This thesis consists of nine chapters with the background, research motivation and objectives of the study included in the Introduction Chapter 1. Chapter 2 provides a comprehensive literature review of the current state of hybrid FO systems.

A detailed description of the materials and methods covering details of the lab and pilot experimental investigations common to all the chapters are presented in Chapter 3, while specific information about experimental methods can be found in their respective chapters.

As shown in Figure 1-1, this thesis is divided into four phases and the results obtained from each study were used to develop a commercial forward osmosis design software.

Chapter 4 evaluates the long-term operation of the pilot-scale FO-NF hybrid system in the field at one of coal mining sites to assess its technical feasibility and limitations to understand its potential for commercial application.

Chapter 5 conducts an environmental and economic life cycle assessment of hybrid FO systems for fertigation and compared with the MF/UF-RO hybrid systems. The main challenges of the FO hybrid systems for commercialization are also discussed.

In addition to hybrid FO systems for non-potable reuse in Chapter 5, more detail on the influence of the selected draw solute on the life cycle assessment of FO hybrid systems under a closed-loop operation is included separately in Chapter 6.

Chapter 7 evaluates the influence of the hydrodynamic parameters in a module-scale FO membrane operational performances and fouling behaviors using different commercial FO membrane modules.

Chapter 8 evaluates the operational performances of the FO membrane module containing multiple FO membrane elements in series considering the operational safety of the FO process. Several module arrangement scenarios were proposed and evaluated for their performances and their economies of FO hybrid systems in terms of capital and operational costs.

Conclusions from this study and recommendations for future studies are presented in Chapter 9.

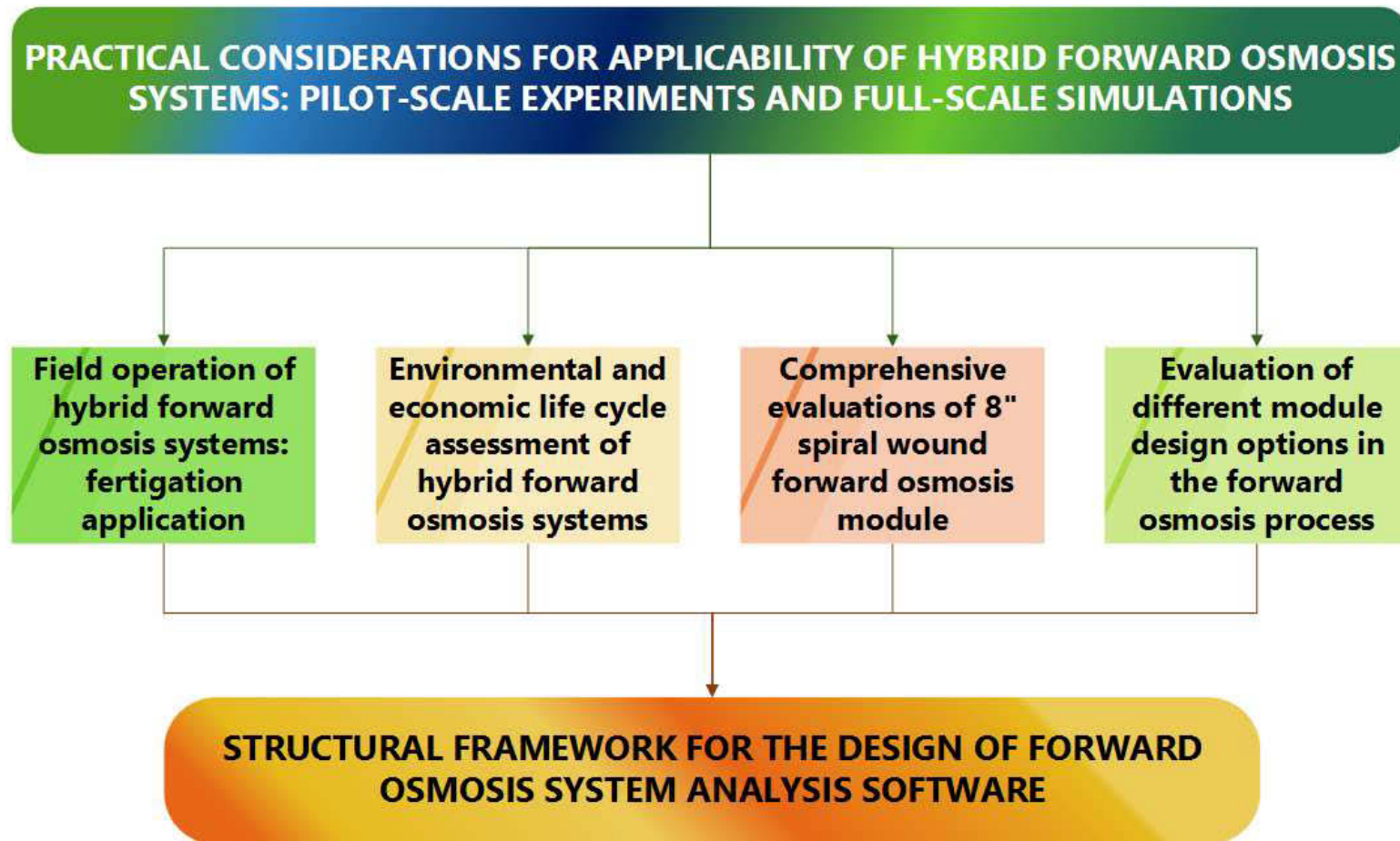


Figure 1 - 1. Structure of the research

CHAPTER 2

LITERATURE REVIEW

This chapter was published as: Chekli, L.; Phuntsho, S.; **Kim, J. E.**; Kim, J.; Choi, J. Y.; Choi, J.-S.; Kim, S.; Kim, J. H.; Hong, S.; Sohn, J., A comprehensive review of hybrid forward osmosis systems: Performance, applications and future prospects. *Journal of Membrane Science* **2016**, *497*, 430-449.

2.1. Introduction

This chapter includes a brief review of the literature, which has formed the basis of this research on the recent development and performance of hybrid forward osmosis systems. It consists of a brief review of forward osmosis (FO) in general, followed by existing hybrid FO systems and their performance in various applications and the economic and environmental aspects of implementing a full-scale FO hybrid system. The review identifies some of the limitations of existing hybrid FO systems and suggests the strategies and prospects for a future research area for its commercial application. FO membranes have been identified as being practically important to the overall efficiency of FO technology because the performance of FO membranes is directly related to both capital and operating cost. Although significant efforts have been made to improve the FO membranes from both researchers and industries, most studies have been conducted using small flat sheet coupons thus information regarding module design is still limited. Since this research covers the practical operation of FO hybrid systems, a brief discussion of module-scale FO operations are also discussed at the end.

This chapter is an extension of the review paper published in *Journal of Membrane Science* (Chekli et al., 2016).

2.2. Forward osmosis process

Forward osmosis (FO) has attracted attention as a promising membrane technology for desalination. The principle of a natural osmosis is to draw the water molecules from a saline feed water to a higher concentrated solution when two solutions are separated by a semi-permeable membrane. The driving force is therefore generated by the osmotic gradient between two solutions of different concentrations. Such natural driving force in the FO process does not require hydraulic pressure and thus the energy requirement is significantly less (Cath et al., 2006a; Chekli et al., 2012; McCutcheon et al., 2005; Phuntsho et al., 2012 a). In addition, the fouling potential in the FO process is significantly lower than conventional hydraulic pressure-driven membrane processes (e.g., RO) due to the absence of the hydraulic pressure (Altaee et al., 2013; Cath et al., 2006a). Membranes used for FO also offer a high rejection rate of a wide range of

contaminants and thus this results in a growing interest in exploiting this osmotic process for various applications, including food and pharmaceutical processing, wastewater treatment, and desalination (Cath et al., 2006a; McCutcheon et al., 2005).

However, FO technology has some major technological barriers limiting its commercial application. The first barrier is the lack of suitable draw solution (DS), which is an osmotic agent and thus easily affects FO performance. The second is the lack of suitable FO membranes. An overview of the recent studies on draw solutes/solution advancement and FO membrane fabrication are discussed in the following sections.

2.2.1. Classification of osmotic agent DS

There are several factors used to select an acceptable DS for FO – high water flux, simple recovery/regeneration, and minimal reverse solution diffusion (Akther et al., 2015; Chekli et al., 2012). Therefore, early FO studies focused on developing draw solutes using various types of draw agents that are categorized into organic-based DS and inorganic-based DS and other compounds including polyelectrolytes, magnetic nanoparticles (MNPs), and poly aspartic acid sodium salt (PAspNa) (Chekli et al., 2012; Gwak et al., 2015; Hau et al., 2014; Ling et al., 2010), as shown in Table. 2.1.

Table 2 - 1. Classification of draw solutes and characteristic of the different types of DS

| DS in FO | Advantages | Disadvantages |
|--|---|--|
| Organic solutes | <ul style="list-style-type: none"> ▪ High osmotic pressure ▪ High water flux ▪ Costly recovery | <ul style="list-style-type: none"> ▪ Reverse diffusion ▪ Limited commercial availability |
| Inorganic solutes | <ul style="list-style-type: none"> ▪ High osmotic pressure ▪ High water flux ▪ Costly recovery | <ul style="list-style-type: none"> ▪ Reverse diffusion |
| Hybrid organic-inorganic nanoparticles | <ul style="list-style-type: none"> ▪ High osmotic pressure ▪ High water flux ▪ Easy regeneration | <ul style="list-style-type: none"> ▪ Aggregation ▪ Hyman and environmental toxicity |

An overview of the organic and inorganic based DS used in FO processes from the previous review is shown in Table 2.2. Although organic DS usually consists of non-electrolytes, they have the potential to create high osmotic pressure due to the exhibition of high solubility. In particular, glucose and fructose have been used as a DS

for seawater desalination (Kravath & Davis, 1975). Ethanol has been also used as DS for FO desalination (McCormick et al., 2008). A concentrated sugar solution such as sucrose has been tested as the DS for the direct osmotic concentration of tomato juice (Petrotos et al., 1998), as shown in Table 2.2.

Inorganic-based compounds as the DS are extensively used today. Recent studies of inorganic DS have been conducted by Achilli et al. (2010) and Tan and Ng (2010). Achilli et al. (2010) developed a protocol for the selection of optimal DS for FO applications. The 14 inorganic draw solutes were tested and their performance in terms of water flux and reverse salt flux was evaluated. Monovalent inorganic salts such as NaCl, NH₄Cl, and KCl have been extensively used due to their high water fluxes. However, they need to be recovered by an additional process such as reverse osmosis (RO), with significant energy consumption. In addition, due to their low hydrated radius, the reverse salt flux from the DS to the FS is a significant issue during the operation. Reverse salt flux from the DS to the FS consequently affects both the cost of replenishing the lost draw solutes and the quality of the discharged feed water. To overcome these issues, multivalent ions such as MgCl₂, CaCl₂, and MgSO₄ have been tested as DS in FO. The results showed that the reverse diffusion of solutes can be reduced when using multivalent ions due to a larger hydrated radius as presented in Table 2.2.

Fertiliser-based draw solutes were also suggested and tested as DS by Phuntsho et al. (2011). In this concept, fertilizer can be diluted by the desalinated water from the feed side (i.e. low salinity water) and thus the diluted fertilizer solution can be directly applied for fertigation without the need for the recovery of the draw solutes. From this aspect, although this fertilizer drawn FO process can provide low energy consumption than other conventional desalination processes (e.g., RO), the final diluted concentration has to be controlled to meet the suitable nutrient concentrations for irrigation. Further approaches such as pre- and post-treatment processes or applying additional pressure to the feed side have been studied as a means of overcoming this problem (Sahebi et al., 2015).

The use of magnetic nanoparticles (MNPs) as DS has gained a great deal of scientific attention due to the feasibility of applications for biocatalysts and drug delivery and its easy recovery. It can be classified into three different types: the polyacrylic acid magnetic nanoparticles (PAA MNPs), the 2-Pyrrolidone magnetic nanoparticles (2-Pyrrol MNPs) and the triethyleneglycol magnetic nanoparticles (TREG MNPs). The main advantages of MNPs are their large molecular size compared to organic and inorganic compounds. In addition, they can produce a very high osmotic pressure of 70 atm which is much higher than the seawater osmosis pressure of 26 atm, thus can be one of the very attractive osmotic agents for desalination applications.

The concerns about the concentrated RO brine from an RO desalination plant become significant as it contains highly concentrated organic and inorganic compounds (Bamaga et al., 2011; Chekli et al., 2012). Therefore, a proper management of the RO concentrate is required to avoid any negative effects on the receiving environment. A recent study conducted by Bamaga et al. (2011) has utilized RO brines as the DS for a hybrid FO and RO system where FO process is used as a pre-treatment process to reduce fouling or scaling propensity in RO process. This study clearly demonstrated the advantages of the use of concentrated RO brines as the DS, including a very high osmotic pressure and thus producing higher water fluxes in FO and the efficiency of the RO process as a recovery process. Therefore, this concept of coupling the FO and RO processes is used to lower the energy required for desalination.

Table 2 - 2. Physiochemical properties and experimental water flux of organic and inorganic based draw solutes tested as DS. Adapted from (Achilli et al., 2010; Akther et al., 2015; Chekli et al., 2012)

| DS Tested | MW | Osmotic pressure at 2 M (atm) | pH at 2 M | Max. solubility (M) | Experimental water flux (Lm ⁻² h ⁻¹) | References | |
|--|--|-------------------------------|-----------|---------------------|---|-------------------------|--|
| Organic-based DS | Ethanol | 46.1 | 43.93 | 7.0 | Miscible | N/A | (McCormick et al., 2008) |
| | Sucrose | 342.3 | 56.81 | 6.2 | 6.1 | 0.35 | (Petrotos et al., 1998) |
| | Glucose | 180.2 | 55.03 | 7.0 | 800.0 | 0.24 | (Kravath & Davis, 1975) |
| | Fructose | 180.2 | 55.02 | 7.0 | 22.4 | 7.5 | (Kravath & Davis, 1975) |
| Inorganic-based DS | CaCl ₂ | 111.0 | 217.6 | 6.29 | 7.4 | 2.64 | (Achilli et al., 2010; Roy et al., 2016) |
| | KBr | 119.0 | 89.7 | 6.92 | 4.5 | 2.84 | (Achilli et al., 2010) |
| | KHCO ₃ | 110.1 | 79.3 | 7.84 | 2 | 2.25 | (Achilli et al., 2010) |
| | K ₂ SO ₄ | 174.2 | 32.4 | 7.33 | 0.6 | 2.52 | (Achilli et al., 2009b; Tan & Ng, 2010) |
| | MgCl ₂ | 95.2 | 256.5 | 5.64 | 4.9 | 2.33 | (Achilli et al., 2009b) |
| | MgSO ₄ | 120.4 | 54.8 | 6.7 | 2.8 | 1.54 | (Achilli et al., 2009b) |
| | NaCl | 58.4 | 100.4 | 6.98 | 5.4 | 2.68 | (Achilli et al., 2009b) |
| | NaHCO ₃ | 84.0 | 46.7 | 7.74 | 1.2 | 2.47 | (Achilli et al., 2009b) |
| | Na ₂ SO ₄ | 142.0 | 95.2 | 7.44 | 1.8 | 2.14 | (Achilli et al., 2009b) |
| | NH ₄ HCO ₃ | 79.1 | 66.4 | 7.69 | 2.9 | 2.04 | (Achilli et al., 2009b) |
| | NH ₄ NO ₃ | 80.0 | 64.9 | 4.87 | 84 | 4.177 | (Phuntsho et al., 2011) |
| | (NH ₄) ₂ SO ₄ | 132.1 | 92.1 | 5.46 | 5.7 | 5.391 | (Phuntsho et al., 2011) |
| | NH ₄ Cl | 53.5 | 87.7 | 4.76 | 7.4 | 5.348 | (Phuntsho et al., 2011) |
| | Ca(NO ₃) ₂ ·4H ₂ O | 164.1 | 108.5 | 4.68 | 7.9 | 5.022 | (Phuntsho et al., 2011) |
| | NaNO ₃ | 84.99 | 81.1 | 5.98 | 10.5 | 5.706 | (Phuntsho et al., 2011) |
| | KCl | 74.6 | 89.3 | 6.8 | 4.6 | 6.337 | (Phuntsho et al., 2011) |
| | NH ₄ H ₂ PO ₄ | 115.03 | 86.3 | 3.93 | 3.7 | 4.349 | (Phuntsho et al., 2011) |
| (NH ₄) ₂ HPO ₄ | 132.06 | 95 | 8.12 | 6.5 | 3.892 | (Phuntsho et al., 2011) | |
| KNO ₃ | 101.10 | 64.9 | 5.99 | 3.3 | 4.429 | (Phuntsho et al., 2011) | |

2.2.2. Development of forward osmosis membranes

One of the major drawbacks of FO process is the lack of suitable FO membranes. However, significant advancements in FO membranes have been made with cellulosic, thin film composite, and chemically modified membranes.

In the early stage of osmotic studies, the conventional RO membranes were used and proved unsuitable for the FO process as it produces low flux even when very high concentration was used. Wang et al. (2007) developed the first of phase inversion membranes using a type of asymmetric polybenzimidazole (PBI) hollow fiber NF membrane via dry-jet phase inversion. The results showed that this membrane could be effectively applied to the FO process due to its high divalent ion rejection and significant water flux. Moreover, the PBI NF hollow fiber membrane was improved to achieve a higher water flux by using p-xylene dichloride for cross-linking (Wang et al., 2009).

The majority of studies have been conducted using cellulose tri acetate (CTA) through phase inversion to develop more suitable semi-permeable membranes, which have high flux, salt rejection, and high mechanical strength to support high hydraulic pressures. Unlike a typical RO membrane, which has a very thin selective layer with a thick porous fabric support layer, a total thickness of cellulose-based FO membranes is only 50 μm due to the absence of the thick support layer. Most of the recent FO studies have used a CTA FO membrane, and these studies show that although CTA FO membranes could be effectively used for FO applications, structural properties of FO membranes need to be improved to minimize concentration polarization effects (Cath et al., 2006a).

Many studies have proposed that the ideal FO membrane should have a dense selective layer with high rejection but minimum thickness and tortuosity, high water flux, and high mechanical strength to withstand fluid flow (Cath et al., 2006a). Several studies have recently utilized polyamide (PA) based thin film composites (TFC) FO membranes with significantly enhanced structural properties such as porosity and thickness. The fabrication methods for the TFC FO membranes are similar to the TFC PA RO membranes. A porous substrate is prepared via phase inversion and then a PA

rejection layer is formed on the top by interfacial polymerization (Song et al., 2011; Wei et al., 2011a; Yip et al., 2010). Both flat sheet and hollow fiber TFC FO membranes have been developed and demonstrated for FO applications as presented in Table 2-3.

In addition to TFC membranes, few chemical modification methods have also been used recently for a novel TFC FO membranes (Emadzadeh et al., 2014). Titanium dioxide (TiO_2) nanocomposite substrate was used to improve the performances of polysulfone (PSf) substrate. It was successfully demonstrated that the addition of an appropriate amount of TiO_2 into PSf substrate could improve the performance of TFC membrane during FO applications due to the decrease in a structural parameter, which results in reduced CP effects. Results from various investigations indicate that other properties such as hydrophilicity and the membrane charge (Widjojo et al., 2011) are significant in making highly efficient membranes. An overview of recent FO membrane fabrications is provided by Akther et al. (2015) and is shown in Table 2.3, including their fabrication methods.

Table 2 - 3. Recent advancement of FO membranes. Adapted and modified from Akther et al. (2015).

| Year | Membranes | Materials | Preparation methods | References |
|------|---|---|---|--------------------------|
| 2005 | Capsule wall | Cellulose acetate (CA) or ethyl cellulose | Dip-coating, phase inversion | (Wang et al., 2007) |
| 2007 | Hollow fiber NF | Polybenzimidazole (PBI) | Dry-jet wet phase inversion | (Wang et al., 2007) |
| 2008 | Flat sheet cellulose acetate | Cellulose acetate | Phase inversion and then annealing at 80–95 °C | (Gerstandt et al., 2008) |
| 2009 | Dual-layer hollow fiber NF | PBI–PES/PVP | Dry-jet wet phase inversion (i.e. coextrusion technology) | (Chou et al., 2010) |
| 2010 | Hollow fibre | PES substrates, polyamide (PA) active layer | Dry-jet wet spinning and interfacial polymerization (IP) | (Yang et al., 2009) |
| 2010 | Hollow fiber NF | Cellulose acetate | Dry-jet wet spinning | (Su et al., 2010) |
| 2010 | Flat sheet double-skinned | Cellulose acetate | Phase inversion, and then annealing at 85 °C | (Wang et al., 2010a) |
| 2010 | Flat sheet TFC | Polysulfone (PSf) support, PA active layer | Phase inversion and IP | (Yip et al., 2010) |
| 2010 | Double dense-layer | Cellulose acetate | Phase inversion | (Zhang et al., 2010) |
| 2011 | Modified RO | PSf support modified by polydopamine | Chemical coating | (Arena et al., 2011a) |
| 2011 | Flat sheet composite | CA cast on a nylon fabric | Phase inversion | (Sairam et al., 2011) |
| 2011 | Flat sheet composite | PAN substrate, multiple PAH/PSS polyelectrolyte Layers | Layer-by-layer assembly | (Saren et al., 2011) |
| 2011 | Positively charged hollow fiber | PAI substrate treated by PEI | Chemical modification | (Setiawan et al., 2011) |
| 2011 | Positively charged flat sheet | PAI substrate treated by PEI | Chemical modification | (Qiu et al., 2012) |
| 2011 | Flat sheet TFC PA | PES/SPSf substrate, PA active layer | Phase inversion and IP | (Wang et al., 2012) |
| 2011 | Flat sheet TFC PA | PES/sulfonated polymer substrate, PA active layer | Phase inversion and IP | (Widjojo et al., 2011) |
| 2011 | Flat sheet TFC PA | PSf support, PA active layer | Phase inversion and IP | (Wei et al., 2011a) |
| 2011 | Nanoporous PES | PES cast on PET fabric | Phase inversion | (Yu et al., 2011) |
| 2011 | Cellulose ester | Cellulose ester | Phase inversion | (Zhang et al., 2011) |
| 2011 | Flat sheet TFC PA | PES nanofiber support, PA active layer | Electro-spinning and IP | (Song et al., 2011) |
| 2011 | Flat sheet TFC PA | PSf nanofiber support, PA active layer | Electro-spinning and IP | (Bui et al., 2011) |
| 2012 | Polymeric nanofiber incorporated TFC PA | Polyethylene terephthalate (PET) nanofibers, PSf microporous support, PA active layer | Electro-spinning, phase separation and IP | (Hoover et al., 2013) |
| 2012 | TFC PA | Super porous CNT non-woven Bucky-paper (BP) support, PA active layer | Plasma treatment of CNT BPs support and IP | (Dumée et al., 2013) |
| 2012 | Dual-layer hollow fiber NF | PES inner support layer and PAI active layer post-treated by PEI | Dry-jet wet spinning, one-step coextrusion, multi-layer polyelectrolyte depositions | (Setiawan et al., 2013) |

| Year | Membranes | Materials | Preparation methods | References |
|-------------|-------------------------------|--|--|--------------------------|
| 2013 | Thin-film inorganic (TFI) | Stainless steel mesh (SSM) substrate, micro-porous silica xerogels active layer | Dip-coating and calcining for 4 h at 500 °C in nitrogen followed by cooling to 25 °C | (You et al., 2013) |
| 2014 | Thin-film nanocomposite (TFN) | PSf-titanium dioxide(TiO ₂) nanocomposite substrate, PA active layer | IP | (Emadzadeh et al., 2014) |
| 2014 | Tri-bore hollow fiber TFC | Matrimid® 5218 polymer substrate, PA active layer | Dry-jet wet spinning and IP | (Luo et al., 2014b) |
| 2015 | Flat sheet TFC PA | Silica-polysulfone mixed matrix substrate, PA active layer | Phase inversion and IP | (Liu & Ng, 2015) |
| 2015 | Flat sheet TFC PA | A novel hydrophilic Cellulose ester membrane support, PA active layer | Phase inversion and IP | (Ong et al., 2015) |
| 2016 | Flat sheet TFC PA | CaCO ₃ nanocomposite substrate, PA active layer | Non-solvent induced phase separation (NIPS) and IP | (kuang et al., 2016) |

Based on information available (Table 2-3), it can be noticed that most of the development has focused on a small size membrane for lab-scale FO tests. Although laboratory-scale modules have been designed for holding pack membranes including flat sheet or tubular/capillary membranes, development of module design for large-scale applications certainly has importance. There are three different module configurations that can be used for larger-scale FO applications including plate and frame, spiral wound, and hollow fiber modules.

Plate and frame: This module configuration is the simplest device for holding flat sheet membranes. Plate and frame modules can be manufactured from lab-scale applications that hold single and small size membrane coupons to full-scale systems that hold more than 1700 membranes (Cath et al., 2006a). There are two main limitations of plate and frame modules for membrane applications. The first one is the lack of adequate membrane support thus leading to operational restrictions (i.e. low hydraulic pressure). In addition, the construction of large plate and frame membrane modules is more complicated, and it has low packing density. This results in a larger system footprint, higher capital costs, and higher operating costs. However, Porifera has recently developed commercially available plate and frame modules under the commercial name of PFO elements. Porifera PFO elements have relatively high packing density, low-pressure drop and effective membrane surface from 1 up to 7 m² per module (Blandin et al., 2016a). Nevertheless, due to the lack of practical information on the performance of this module configuration, further research is required.

Spiral wound: In the early stage of FO studies, FO module design was mainly adapted from existing commercial RO configurations which consisted of only one stream flowing under the direct control of its flow velocity tangential to the membrane. The permeate stream flows very slowly in the channel formed by the two glued membranes and thus affects hydraulics on the permeate side. Therefore, FO modules differ from typical RO modules and consist of four ports (feed and draw inlets and outlets). Figure 2-1 shows flow patterns in a spiral wound module for FO applications. The draw solution flows through the spacers and between the rolled membrane envelopes, in the same way, that a feed stream flows in a spiral-wound element for RO. However, unlike RO elements, the collecting tube is bonded halfway through so that the feed solution

cannot flow to the other side. Instead, an additional glue line at the center of the membrane envelope provides a pathway for the feed to flow inside the envelope. Commercially available spiral wound modules were developed by HTI using the CTA FO membrane with a wide range of module sizes, varying from 2.5 to 8 inches in diameter and a variety of feed spacers. Most FO studies on pilot-scale were performed using spiral wound CTA FO membranes as shown in Table 2-4. In this configuration, however, the impact of hydraulic pressure on the overall process efficiency is one of the major limitations. Although FO is driven by an osmotic driving force, the pressure drop and build-up have influenced the performance (Kim & Park, 2011b). Thus, a minimal amount of hydraulic pressure needs to be applied to transfer water along the module.

Hollow fiber: There are some benefits to use hollow fiber membranes for FO processes. This hollow fiber can be easily packed in bundles directly inside a holding vessel and thus its packing density is relatively high. In addition, these modules allow streams to flow freely on both sides of the membrane without a thick support layer, thus reducing the concentration polarization (CP) effects. Module-scale of hollow fiber membranes was developed by Toyobo and proved that it could be operated at high hydraulic pressure (25 bar) (Blandin et al., 2016a). However, the application of hollow fiber membranes for FO is limited (Cath et al., 2006a; Zhao et al., 2012c) as compared to flat sheet semi-permeable membranes.

It is clear that module configuration is of crucial importance and evaluative testing of FO performance will be essential before the membrane goes to commercialization. More work is thus required to determine the optimum configuration for FO scale-up including effects of flow dynamics (i.e. cross flow velocity) and channel thickness/type on pressure drop and hydraulic pressure.

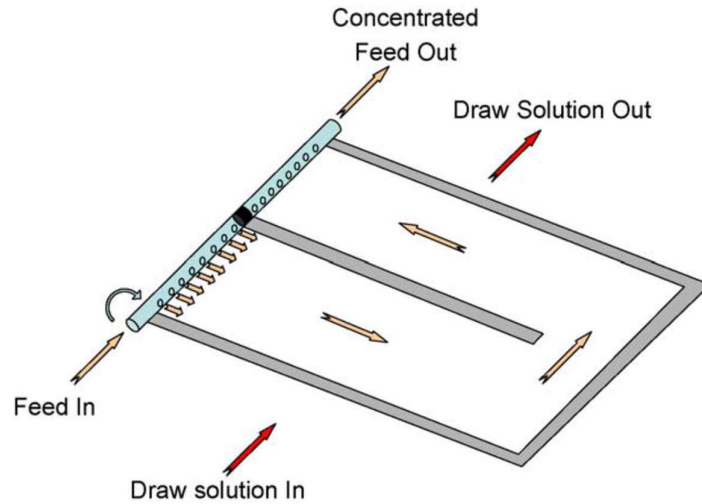


Figure 2 - 1. Flow direction in a spiral wound module modified for FO applications. The feed stream flows through the central tube into the inner side of the membrane envelope and the draw stream flows in the space between the rolled envelopes. Figure adapted from (Mehta, 1982)

Table 2 - 4. Different spiral wound module tested for pilot-scale FO operation. Adapted from (Blandin et al., 2016a)

| Module | Feed spacer | Draw spacer | Effective membrane area (m ²) | Feed inlet pressure (bar) | Draw inlet pressure (bar) | References |
|---------|------------------------|------------------|---|---------------------------|---------------------------|----------------------------|
| 4040 | 2.5 mm RO feed spacer | N/A | 1.58 | N/A | N/A | (Hancock et al., 2011b) |
| 4040-MS | 1.14 mm RO feed spacer | Permeate carrier | 3.2 | 1.22 | 1 | (Kim & Park, 2011b) |
| 8040-MS | 1.14 mm RO feed spacer | Permeate carrier | 11.2 | N/A | 2 | (Kim et al., 2014a) |
| 8040-CS | 2.5 mm RO feed spacer | Permeate carrier | 9 | < 1 | < 0.7 | (Kim et al., 2014a) |
| 4040-MS | 1.14 mm RO feed spacer | N/A | 3.3 | 0.7-1.1 | 0.5 | (Cornelissen et al., 2011) |

*4040: 4-inch diameter, 40-inch length

*8040: 8-inch diameter, 40-inch length

*CS: Corrugated spacer

*MS: Medium spacer

*N/A: Not available

2.3. Sustainability of forward osmosis hybrid systems

Since less energy is required to desalinate seawater due to the use of natural osmotic pressure in the FO process, it has been studied for a range of applications including seawater desalination, wastewater treatment and water purification, food processing and other uses. However, it has been proven that FO is not the ultimate process mainly due to the fact that the separation and recovery of the DS are required. Therefore, in the last few years, several hybrid FO systems have been developed for various applications including seawater and brackish water desalination (60%), wastewater treatment (about 13%) or both (i.e. simultaneous treatment systems), and fertigation as shown in Fig. 2.2. More specifically, Table 2-5 shows a comparison of different configurations of FO hybrid systems. One good application is the combination of FO with membrane distillation (MD) to desalinate water that is often challenging for stand-alone MD. In this hybrid configuration, the use of FO as pre-treatment for MD processes could reduce inorganic scaling and/or organic fouling while the MD process is used to recover the DS using low-grade heat (Xie et al., 2013a). The integration of FO with nanofiltration (NF) has also been recently proposed in the context of fertilizer driven forward osmosis (FDFO) as the final diluted fertilizer DS was not able to apply for direct irrigation (Phuntsho et al., 2013 a). Including these applications, providing a comprehensive and up-to-date review of the recent development and performance of hybrid FO systems is vital. Therefore, the following section will review the existing hybrid FO systems and their performance in different applications.

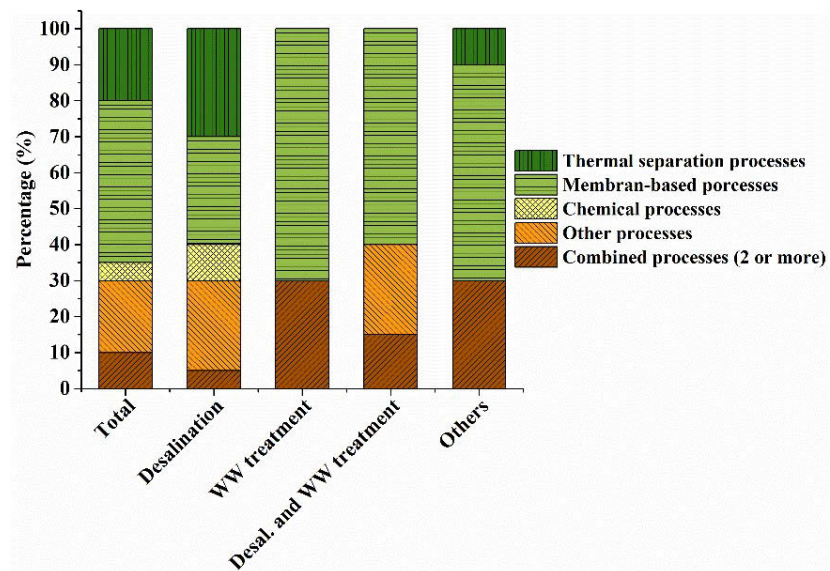


Figure 2 - 2. Overview of distribution of applications and integrated systems

Table 2 - 5. A comparison of different configurations of hybrid FO systems

| Schematic of hybrid FO systems | Details | Examples |
|--------------------------------|---|--|
| | <ul style="list-style-type: none"> ▪ Bench-scale studies to evaluate the performance of a recovery process for a specific/novel draw solution | <ul style="list-style-type: none"> ▪ Ultrafiltration (UF) for the recovery of magnetic nanoparticles (MNPs) |
| | <ul style="list-style-type: none"> ▪ FO is tested as an alternative pre-treatment to conventional separation technologies and integrated in existing processes | <ul style="list-style-type: none"> ▪ Hybrid FO-RO system whereby FO is tested as an advanced desalination pre-treatment process |
| | <ul style="list-style-type: none"> ▪ FO is tested as an alternative process to conventional membrane technologies and integrated in existing processes | <ul style="list-style-type: none"> ▪ FO integrated into membrane bioreactor (MBR) to potentially replace conventional processes such as UF |
| | <ul style="list-style-type: none"> ▪ FO is tested as a post-treatment process to reduce the volume of waste generated by conventional processes | <ul style="list-style-type: none"> ▪ Hybrid RO-FO system whereby FO is used to concentrate RO brine in conventional seawater desalination plant |
| | <ul style="list-style-type: none"> ▪ Stand-alone FO process requires additional post-treatment to meet standard requirements | <ul style="list-style-type: none"> ▪ Hybrid FDFO-NF process to meet the standards for irrigation |

2.3.1. Seawater and brackish water desalination

2.3.1.1. Hybrid systems for the recovery of DS

Initially, the development of hybrid FO desalination processes was mainly designed for the separation of draw solutes. McCutcheon et al. (2005) and McCutcheon et al. (2006a) developed a novel ammonia-carbon dioxide (i.e. NH_4HCO_3) FO process. In the context of this process, water is extracted from seawater (i.e. feed water) and dilutes the NH_4HCO_3 DS. In order to achieve the fresh water from the diluted DS, a heating process such as membrane distillation (MD) was used as a separation method. From the bench-scale FO process demonstration, results showed that this hybrid desalination process can achieve a high water flux of $25 \text{ L/m}^2\text{h}$ and a salt rejection of 95% with CTA FO membrane with a calculated driving force of more than 200 bar. Although an electrical power requirement of FO desalination process was less than 0.25 kWh/m^3 , the thermal DS recovery process was more than 75 kWh/m^3 . This means that this hybrid desalination process is not practical unless sources of waste heat can be available to power the regeneration process. All results of the previous work on ammonia-carbon dioxide FO process has exposed the other critical limitations including the high reverse draw solute flux (Table 2-6) and the presence of trace ammonia in the final product. In fact, it has emphasized the need for high performance membranes and an easily separable DS to overcome such limitations.

Therefore, as discussed in Section 2.2.1, alternative DS which can induce a high osmotic pressure were tested for seawater desalination. For example, the performance of organic compounds, both neutral and charged 2-methylimidazole based compounds as DS in a hybrid FO-MD desalination system was investigated by Yen et al. (2010a). Results showed that a water flux of about 8 LMH was observed across the MD membrane but this type of DS exhibited high reverse solute flux (i.e. up to $80 \text{ g/m}^2\text{h}$). Guo et al. (2014) also investigated a new type of Na^+ - functionalized carbon quantum dots (Na_CQDs) with ultra-small size and rich ionic strength in a hybrid FO-MD desalination process. It was demonstrated that a high osmotic pressure produced by this type of draw solute contributed to high water flux and negligible reverse solute flux. In addition, the fabrication of Na_CQDs is simple and straightforward and thus it is inexpensive draw solute. During the five times repeated FO tests, a high FO water flux

of 29.8 LMH was observed and after few cycles it was slightly dropped and maintained at 28.8 LMH with negligible reverse solute flux. The diluted Na₂CQDs solution from FO was reconcentrated using MD at 45 °C. After the fifth cycle, the water flux was also slightly decreased from 4 to 3.4 LMH. Alnaizy et al. (2013) recently reported that copper sulfate (CuSO₄) can be used as a new draw solute in FO desalination. However, an average water flux of 3.57 LMH was observed using 200,000 ppm copper sulfate DS, showing that it could be more suitable for brackish water desalination (i.e. 3.96 bar) due to its low osmotic pressure of 29.94 bar to extract water from seawater feed (i.e. 32.17 bar) and concentration polarization effects. Moreover, the diluted DS was recovered by a metathesis precipitation reaction of copper sulfate with barium hydroxide. Insoluble barium sulfate (BaSO₄) was separated from copper sulfate DS, and it can be used for commercial applications such as a thickener in oil well drilling fluids for crude oil and natural gas exploration.

Recently, a new class of DS has been proposed as it generates a very high osmotic driving force in FO. Ling and Chung (2011b) successfully demonstrated a hybrid FO magnetic field system using hydrophilic magnetic nanoparticles (MNPs) as draw solutes. In terms of its feasibility, it produced moderate water fluxes up to 18 LMH but lower reverse solute fluxes compared to conventional inorganic compounds such as NaCl and MgCl₂ due to the larger size of MNPs. However, a slight decrease of the water flux was attributed to agglomeration of MNPs under the high strength magnetic field. Ultrasonic treatments were conducted to overcome this issue. It was found that ultrasonication reduced the size of agglomerated magnetic nanoparticles but was not able to completely restore the DS efficiency (Ling & Chung, 2011a). MingáLing (2011) therefore proposed a hybrid system consisting of FO coupled with a low strength magnetic field with a view to reducing the possibility of agglomeration thus a significant increase in efficiency. The performance of this hybrid system was well maintained through 5 cycles of reuse but the result was very poor (less than 2 LMH). The major limitations of the synthesis of MNPs are its complexity and cost. In addition, due to the polydispersity of the MNPs, their recovery by the magnetic field is only partial since the magnetic force of smaller MNPs is not predominant. Therefore, smaller MNPs could pass through the magnetic field and thus remain in the final product water. This requires further treatment to achieve the drinking water guidelines. Ling and

Chung (2012) also investigated electric fields as a recovery method for MNPs. This study demonstrated the use of surface-dissociated nanoparticles as draw solutes in FO processes and their reconcentration via an integrated electric field-nanofiltration (NF) system. In the electric field-NF system, the negatively charged nanoparticles were regenerated at an operating voltage of less than 70 V whereas the NF system (i.e. at an applied pressure of 5 bar) was used to recover the product water and reconcentrate the alkaline solution (i.e. Na^+ and Ca^{2+}). This alkaline solution was utilized to dissolve and separate the nanoparticles prior to being reused in the FO process. Results of this study showed that the water flux as well as the size of the MNPs remained quite stable. Nevertheless, Luo et al. (2014a) claimed that the application of NF to reconcentrate the alkaline solution may not be viable since the rejection of Na^+ and Ca^{2+} cannot be completely removed by the NF membrane. Besides, the alkaline solution feeding the NF process may shorten its lifespan. Finally, the energy evaluation of the integrated electric field and NF system is required.

Ge and Chung (2013) tested a new class of DS consisting of hydroacid complexes to enhance FO process efficiency. It has several interesting characteristics such as expanded configurations, abundant hydrophilic groups and ionic species. An NF process of 10 bar was used to separate the draw solute from the diluted DS after FO operation. As presented in Table 2-6, NF membrane had a rejection rate of up to 90% while the FO process produced a water flux of up to 17.4 LMH with 2 M Fe-CAc as DS and synthetic seawater (i.e. 3.5 wt% NaCl) as feed.

As a number of novel DSs to advance FO technology have been proposed, a variety of innovative DS recovery technologies have been also suggested. Li et al. (2011b) reported that new composite polymer hydrogels were incorporated with light-absorbing carbon particles to enhance their heating and dewatering of the composites. Therefore, the solar dewatering process recovers the pure water and regenerate polymer hydrogels under exposure to sunlight at an irradiation intensity of 1.0 kW/m^2 . Although the use of solar energy to regenerate the hydrogels can significantly reduce the capital and operational costs, the water extracted by the hydrogels when exposed to sunlight comes mainly in the vapor stage. Therefore, the additional process will be required to change vapor into liquid water which will ultimately incur an extra economic impact as a result of the process. In terms of performance, although the polymer hydrogels can produce

a high osmotic pressure of about 2.7 MPa at 27 °C, the water flux at room temperature ranged from 0.55 to 1.1 LMH. This low water flux was mainly due to the poor diffusivity through the membrane support layer resulting in severe internal concentration polarization (ICP) (Li et al., 2011a; Li et al., 2011b). When increasing the temperature to 50 °C, the water flux was improved, but this requires a high hydraulic pressure of 30 bar during the dewatering process. Zeng et al. (2013) further investigated polymer-graphene composite hydrogels as a draw agent to enhance water flux in FO. Composite hydrogels with small amounts of graphene oxide significantly enhanced the water flux in the FO process due to greater swelling degrees and better shape adaptability. Hydrogels with 1.2 wt% graphene oxide showed the highest performance but water flux remained significantly lower than that produced by conventional DS as shown in Table 2-6.

Cai et al. (2013) explored thermally responsive hydrogels having a semi-interpenetrating network (semi-IPN) structure for a new concept of temperature driven FO desalination of brackish water. They observed the water fluxes ranging from 0.12 to 0.18 LMH after a 5 h operation. Moreover, the study has also found that increasing the contact area between FO membrane and hydrogels can improve the performance of the FO process due to significantly faster water absorption. From this result, the authors suggested the use of hollow fiber (HF) FO membranes where semi-IPN hydrogels can be coated onto the outside surface on the membrane (i.e. shell side) for quasi-continuous FO desalination as shown in Figure 2-3. For a practical application, future work is required, including the development of an ideal hydrogel drawing agent and FO membranes.

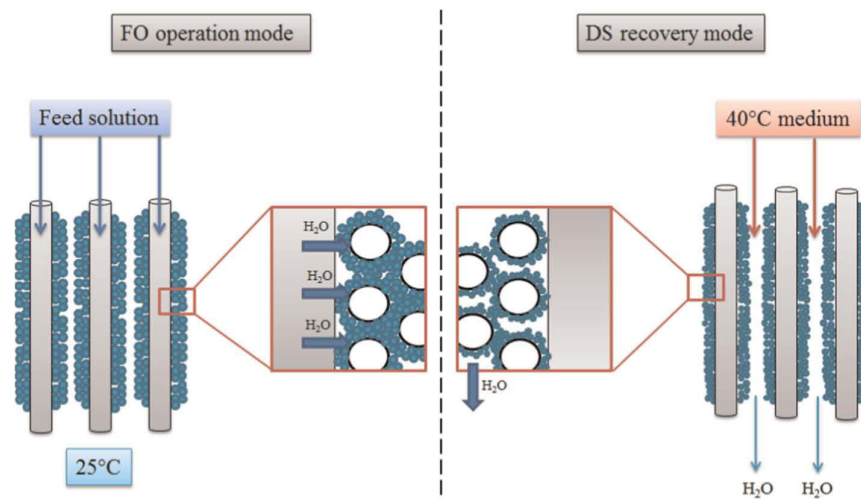


Figure 2 - 3. A design of quasi-continuous temperature driven FO desalination with a semi-IPN hydrogel coated onto the outside surface of the FO hollow fiber membranes (adapted from (Cai et al., 2013)). Apart from the energy needed to pump the saline water feed through the lumen of the hollow fibers, the periodic temperature modulation within 15 °C (e.g., between 25 and 40 °C) is essentially the only driving force for desalination in this configuration. This temperature difference can be readily obtained using warm air generated from the industrial waste heat

Razmjou et al. (2013b) tested the effect of hydrogels particle size ranged from 2 μm up to 1000 μm) on the FO performance as well as the efficiency of both gas pressure and heating stimuli on the release of water from swollen hydrogels. The results showed that small hydrogels particle size (i.e. 2-25 μm) was more beneficial in increasing the initial swelling rate mainly due to the higher surface contact between the membrane and the smaller hydrogel particles, meaning that better particle to particle contact areas and particle-membrane contact results in higher performance of the FO process. In addition, it was found that gas pressure stimulus (i.e. 600 kPa gas pressure) was more effective for dewatering large particles whereas temperature stimulus (i.e. 60 °C) was more effective with small particles. Results also indicated that the amount of water recovered by gas pressure was significantly higher than that using the external hydraulic pressure of 30 bar which is more appropriate if applied at a practical scale. They further conducted research on the effect of incorporating MNPs into the hydrogel network and using magnetic heating as an alternative stimulus to recover the water from the swollen hydrogels (Razmjou et al., 2013a). It was demonstrated that faster and more effective deswelling can be obtained by incorporating magnetic heating as the temperature stimuli since the temperature variation was not significant throughout the hydrogel

network. The dewatering process through magnetic heating was highly influenced by the MNP's loading and the intensity of the magnetic field. Although the liquid water recovery through magnetic heating was still low (i.e. 53%), it had a much higher recovery than other conventional heating methods (i.e. 7%). One other practical drawback with hydrogels could be in the modular design where hydrogels DS can be fed to the membranes. The DS chamber thickness may have to be much larger to accommodate hydrogels in the process thereby increasing the process footprint.

Hartanto et al. (2015) more recently synthesized sub-micron size hydrogels (i.e. 200–300 nm) via surfactant-free emulsion polymerization due to the low water flux and dewatering ability of conventional macroscale hydrogels. Their study demonstrated that new co-polymer microgels for cost-effective FO desalination processes performed significantly better than macroscale hydrogels with water flux observed up to 23.8 LMH and 20 LMH after 3 cycles and liquid water recovery of 72.4 %, showing their potential as the next generation of DS for FO desalination.

2.3.1.2. FO as an advanced desalination pre-treatment process

Hybrid FO-RO systems

Due to high removal efficiency of suspended solids, microorganisms, and a wide range of dissolved solids and organics, FO has been recommended as a pre-treatment option for low-pressure RO (LPRO) for the recovery of glucose in the first hybrid FO-RO system proposed by Yaeli (1992). It was observed pre-treatment using FO could decrease the fouling propensity of feed water in the subsequent RO process. The diluted glucose DS from the FO process was treated by an RO process where an LPRO membrane separated potable water from the glucose solution. However, it was found that the recovery of draw solutes was difficult as a result of the relatively low osmotic efficiency of glucose which also created high ICP effects due to its large molecular size and thus high diffusion coefficient.

The performance of FO coupled with LPRO for the desalination of the red seawater was assessed by Yangali-Quintanilla et al. (2011). The results showed that the energy consumption associated with the hybrid FO-LPRO ranged from 1.3 to 1.5 kWh/m³, which is much lower than the standard high-pressure stand-alone seawater RO (SWRO)

process (i.e. 2.5 – 4 kWh/m³). Therefore, this hybrid system can be considered as an economically feasible technology. The specific energy consumption between RO and FO-LPRO is shown in Figure. 2-4.

More recently, FO-RO and RO seawater desalination processes were compared (Altaee et al., 2014b). RO process was utilized for the draw solute regeneration due to its high efficiency and applicability for a variety of ionic solution treatments. This study proved the benefit of using FO process as pre-treatment process including high removal efficiency of dissolved solids and ultimately high quality of the final product water produced from the subsequent RO process. A recent review article on the performance of FO membranes in rejecting total organic compounds (TrOCs) pointed out that the hybrid FO-RO system demonstrates significantly high TrOCs rejection of 99% due to dual barrier membrane processes (Coday et al., 2014). Similarly, the study conducted by Shaffer et al. (2012) showed that the integrated FO and RO process can be more effective in removing boron as compared to the conventional two-pass RO process. However, when operating the process in a closed-loop system, the accumulation of boron diffused through the FO membrane may become significant (Xie et al., 2013a). This will affect the quality of the final product water and thus require additional methods to improve water quality. In this regard, adsorption by granular activated carbon (GAC), UV₂₅₄ light oxidation (Xie et al., 2013a) and ion exchange (Shaffer et al., 2012) have been suggested to reduce accumulated contaminants.

Pressure assisted forward osmosis (PAFO) whereby a moderate hydraulic pressure is applied in the feed side of the FO process can contribute to savings in the subsequent process due to enhanced water flux in the FO process caused by a synergistic effect of hydraulic and osmotic pressure. In fact, the enhancement of the water flux from PAFO will result in further dilution of the DS beyond osmotic equilibrium thus reducing the total energy cost in RO. In addition, as mentioned earlier, the fouling and scaling propensity in the RO process will be reduced due to a high rejection rate in the FO process. In this regard, Blandin et al. (2015b) assessed the economic sustainability of FO-RO hybrid process for seawater desalination with integrating PAFO. The results showed that the PAFO-RO hybrid system can be more beneficial than the FO-RO hybrid system mainly due to additional savings in total capital cost, in particular

membrane installation cost. In the context of PAFO, although it requires more energy than FO, this can be counteracted with capital and operational costs for increasing the DS concentration. Under such circumstances, the future success of FO desalination significantly depends on the development of novel FO membranes, combining higher water flux, lower fouling propensity, and higher fouling reversibility which could enable FO becoming an advanced pre-treatment process.

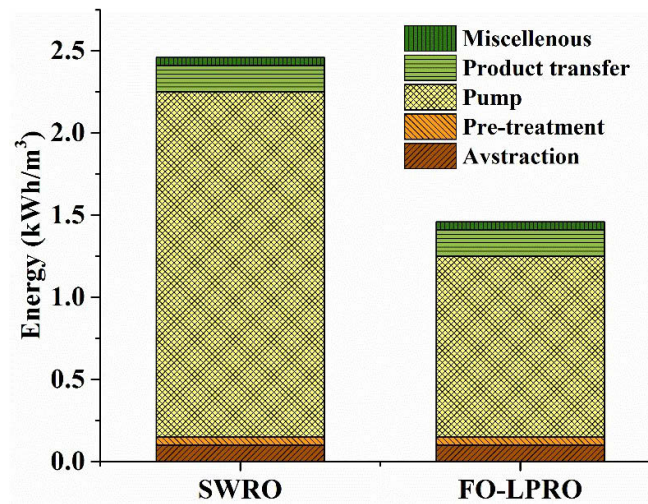


Figure 2 - 4. Comparative estimation of energy cost for SWRO and hybrid FO-LPRO

Hybrid FO-MSF/MED system

Multi-stage flash (MSF) and multi-effect distillation (MED) are conventional desalination technologies which are commonly employed in the Middle Eastern countries where feed waters generally have high salinity, high temperature and high levels of impurities. It is necessary to mitigate the fouling potential of the feed water by reducing the natural organic matter as well as the suspended solids. In most cases, however, pre-treatment processes are not designed to remove dissolved solids which are responsible for scaling, a major issue for thermal processes (Shaffer et al., 2015a). The major issues in both MSF and MED processes are deposition and accumulation of scale materials on the surface of heat exchangers. Thus, this results in decreasing the heat transfer efficiency, minimizing the operating temperatures and overall system recovery (Van der Bruggen & Vandecasteele, 2002). Although NF has been proposed as a pre-treatment due to its high rejection rate of divalent ions (Mabrouk, 2013), the

use of the NF process resulted in high operating costs as well as high fouling tendency because it is a pressure-driven membrane process (Altaee & Zaragoza, 2014b).

Therefore, FO has been recently investigated as an alternative pre-treatment to reduce a potential fouling and scaling risk to the subsequent processes. Altaee et al. (Altaee et al., 2013; Altaee et al., 2014a; Altaee & Zaragoza, 2014b) suggested modelling on hybrid FO-MSF and FO-MED systems for seawater desalination; simulation showed that FO used as a pre-treatment significantly reduced the concentrations of multivalent ions in the feed water which reduces the scaling effect on the heat exchangers, enabling these thermal processes to work at higher temperatures and result in higher water recovery rates.

2.3.2. Hybrid FO systems as an alternative to conventional desalination process

The use of hybrid FO-NF systems for desalination was evaluated by Tan and Ng (2010). In this application, the process was claimed as an alternative process to the conventional desalination process (i.e. stand-alone RO process). The removal efficiency of the NF membrane was significant for all tested DS, up to 97.9% for Na_2SO_4 . Water fluxes of about 10 LMH were obtained by both FO and NF processes as shown in Table 2-7. Results indicated that a single-pass NF was not sufficient to produce high-quality product water which satisfied the TDS requirements for drinking water defined by WHO. However, after the second-pass NF, a suitable TDS concentration of the final product water was achieved only when using MgSO_4 and Na_2SO_4 as DS. Similarly, Zhao et al. (2012a) tested the performance of the hybrid FO-NF system for the desalination of brackish water. Results showed that this hybrid system has many advantages over the conventional stand-alone RO process such as higher product water quality due to salt rejection of about 97.7% and thus TDS concentration down to 10 mg/L, higher flux recovery after physical cleaning, and less fouling and scaling risk, leading to less flux decline and finally a lower operating pressure of less than 10 bar.

Electrodialysis (ED) has been commercialized for the past three decades for small and medium-scale plants for desalinating brackish water (Charcosset, 2009). In the process,

salt ions in the feed water are transported across ion-exchange membranes under the influence of an applied electric potential, thus removing salt ions and some charged organic compounds (Charcosset, 2009). Although ED does not require high energy consumption like a pressure-driven membrane process and has low fouling and scaling tendency, the operational costs including electrodes and ion exchange membranes remain high and ED membranes have a short lifespan when exposed to a strong electrical field. Therefore, the ED process is not techno-economic feasible technology for desalination of high saline water (Xu & Huang, 2008).

To date, a hybrid membrane system combining ED and FO driven by renewable energy (i.e. solar energy) has been suggested by Zhang et al. (2013). The use of photovoltaic (PV) cells with ED has been proposed for many years for use in areas where solar energy is readily abundant in order to reduce the carbon footprint of the process (Charcosset, 2009). The hybrid FO-ED system was utilized for brackish water and wastewater treatment and high quality permeate water can be achieved with the water production cost of around 3.3-4.9 euros/m³, (based on 300 days of production per year and assuming a daily water production of 130 L) for a small size portable system as shown in Table 2-6.

Table 2 - 6. Summary of hybrid FO desalination systems

| Hybrid system | Draw solution | Membrane type(s) for FO process | FO performance | Remarks | References |
|---------------------|---|---|---|--|---|
| FO-Heating (~60 °C) | NH ₄ HCO ₃ | Commercial flat sheet RO and cellulose triacetate (CTA) FO membranes (lab-scale studies) and polyamide (PA) thin-film composite (TFC) FO membrane (pilot-scale study) | Water flux: 7.2 LMH; Reverse salt flux: 18.2 g/m ² h at 2.8 MPa (lab-scale studies). Water flux: 2.6 LMH, system recovery of 66% and more than 99% total dissolved solids (TDS) removal (Pilot-scale study) | Energy efficient process (i.e. specific energy consumption of the hybrid system is significantly lower than other thermal distillation methods) with high water recovery rate but water quality does not meet the WHO standard for ammonia | (McCutcheon et al., 2006a; McCutcheon et al., 2005; McGinnis & Elimelech, 2007) |
| FO-MD | 2-Methylimidazole-based compounds | Commercial CTA flat sheet FO membrane | Water flux: 0.1–20 LMH (2.0 MDS and DI water as feed). Reverse salt flux: 5–80 g/m ² h | A water flux of about 8 LMH was achieved across the MD membrane. ICP effects were higher when using the 2-methylimidazole-based compound with divalent charge. High reverse salt flux and cost of synthesis remains high. | (Yen et al., 2010b) |
| FO-MD | Na ⁺ -functionalized carbon quantum dots (Na-CQDs) | Commercial TFC FO membrane | Water flux: about 3.5 LMH after the fifth cycle. Almost negligible reverse draw solute permeation. | Better performance compared to NaCl. Inexpensive, chemically inert and biocompatible. | (Guo et al., 2014) |
| FO-Magnetic field | Thermosensitive MNPs | Commercial flat sheet CTA FO membrane | Water flux: <2 LMH. Performance of MNPs remains stable after 5 cycles. | Separation of MNPs under lower strength magnetic field which significantly decreased their agglomeration. Costly and complex synthesis. No information on permeate water quality. | (MingáLing, 2011) |
| | Functionalised MNPs | | Water flux: 10–17 LMH (PRO mode) and 7–9 LMH (FO mode) with PAA-MNPs at | Straightforward and energy efficient process, high water recovery rate | (Ge et al., 2010; Ling et al., 2010) |

| Hybrid system | Draw solution | Membrane type(s) for FO process | FO performance | Remarks | References |
|----------------------|--|---------------------------------------|--|--|----------------------|
| FO-UF | Modified magnetic nanoparticles (PAA-MNPs) | Commercial CTA flat sheet FO membrane | different sizes 3.6–21 nm and DI water as feed water. 9 LMH (FO mode) and 13 LMH (PRO mode) with 0.065 M PEG-(COOH) ₂ MNPs and DI as feed water. The water flux dropped to 10.3 LMH (PRO mode) after 9 cycles. Water flux (PRO mode): Up to 17 LMH with 0.08 mol/L PAA-MNPs and DI water as feed | but slightly drop of water flux due to agglomeration of the MNPs MNPs remained active even after 5 cycles of UF recovery without any alteration. This hybrid system requires lower energy consumption compared to RO and NF. However, the smaller MNPs pass through the UF membrane and therefore synthesis of MNPs suspension with narrower size distribution is required. | (Ling & Chung, 2012) |
| FO-Electric field-NF | Polyelectrolytes (e.g. PAA-Na) | Commercial CTA flat sheet FO membrane | Water flux (PRO mode): 6 LMH with 0.72 g/mL PAA-Na as DS and seawater as feed. | High water recovery rate. Various molecular weights (MW) and expanded polymer structure allowing DS regeneration via low-pressure UF process. High rejection rate (>99%) for PAA with MW of 1800 Da. However, poor salt rejection for DS with low MW. | (Zhao et al., 2014) |

| Hybrid system | Draw solution | Membrane type(s) for FO process | FO performance | Remarks | References |
|--|--|--|---|--|---------------------|
| FO-NF | Hydroxyl acids of citric acid (CAc) (Fe–CAc; Co–CAc and Co2-CAc) | CA, TFC on polyethersulfone supports (TFC–PES) and polybenzimidazole and PES dual layer (PBI–PES) hollow fibre membranes | Water flux: Up to 17.4 LMH with 2.0 M Fe–CAc as DS and synthetic seawater (i.e. 3.5 wt% NaCl) as feed. 90% rejection rate for Fe–CAc by NF membrane. | Low operating pressure (i.e. 10 bar), low reverse draw solute and high rejection rate (i.e. more than 90%) | (Ge & Chung, 2013) |
| FO-Stimuli to heating combined with hydraulic pressure | Hydrogels | Commercial flat sheet CTA FO membrane | Water flux: 0.30–0.96 LMH with 2000 ppm NaCl as feed. Very low water recovery rates (i.e. less than 5%). | Environmental-friendly and relatively energy efficient process but low liquid water recovery rate. Unsuitable for applications that require continuous FO process | (Li et al., 2011b) |
| FO-Stimuli to heating | Semi-interpenetrating network (IPN) – hydrogels | Commercial flat sheet CTA FO membrane | Water flux: Ranging from 0.12 to 0.18 LMH after 5 h operation which is 1.5–3 times higher than conventional hydrogels. Better performance can be achieved by increasing membrane/hydrogel contact area. | At 40 °C, the semi-IPN hydrogels quickly released nearly 100% of the water absorbed during the FO drawing process. Drawing and dewatering cycles are highly reversible. However, very low water flux (i.e. less than 0.5 LMH). | (Zeng et al., 2013) |
| FO-Stimuli response to sunlight | Composite hydrogels reduced graphene oxide | Commercial flat sheet CTA FO membrane | Water flux: Up to 3.1 LMH with 2000 ppm NaCl as feed. Water recovery up to 44.3% at 1.0 kW/m ² with 1 h exposure time. | Environmental-friendly and relatively energy efficient process but low liquid water recovery rate and low water flux. | (Zeng et al., 2013) |
| | Composite hydrogels light-carbon particles | Commercial flat sheet CTA FO membrane | Water flux: Up to 1.32 LMH with 2000 ppm NaCl as feed. Up to 100% water recovery rate when solar light is used with 1 h exposure time at a solar irradiation of 1.0 kW/m ² . | | (Li et al., 2011b) |

| Hybrid system | Draw solution | Membrane type(s) for FO process | FO performance | Remarks | References |
|---|--|--|--|---|------------------------------------|
| FO-Stimuli response to gas pressure | Hydrogels | Commercial flat sheet CTA FO membrane | Water flux: Up to 1.5 LMH with 2000 ppm NaCl as feed. Gas pressure stimuli worked better for large particles whereas temperature stimuli are more effective with small particles | | (Razmjou et al., 2013b) |
| FO-Stimuli response to magnetic heating | Magnetic hydrogels | Commercial flat sheet CTA FO membrane | Water flux: Up to 1.5 LMH with 2000 ppm NaCl as feed. 53% Liquid water recovery via magnetic heating compared to only 7% under convection heating. | | (Razmjou et al., 2013a) |
| FO-Stimuli to heating | Functionalised thermo-responsive microgels | Commercial flat sheet CTA FO membrane | Water flux: Up to 20 LMH after 3 cycles (decrease of 13% compared to initial flux). | A high water flux up to 23.8 LMH and high water recovery ability of 72.4% were achieved. | (Hartanto et al., 2015) |
| FO-RO | Glucose | Not reported | Not reported | Limited water recovery due to the low osmotic efficiency of glucose which also created high ICP effect due to its large molecular weight. | (Yaeli, 1992) |
| FO-LPRO | Red seawater | Commercial CTA flat sheet FO membrane | After 10 days of continuous FO operation, 28% of flux decline was observed (initial water flux of 5 LMH) but membrane cleaning (hydraulically cleaned) allowed 98.8 % water flux recovery. | Energy cost of this hybrid system is only 50% (~1.5 kWh/m ³) of that used for high pressure SWRO desalination | (Yangali-Quintanilla et al., 2011) |
| FO-MSF/MED | Concentrated Brine | No experimental results – modelling studies only | Simulation results showed that FO demonstrates good performance for the removal of divalent ions from feed solution which mitigates the scaling on the surface of heat | Concentrated Brine | (Altaee & Zaragoza, 2014a) |

| Hybrid system | Draw solution | Membrane type(s) for FO process | FO performance | Remarks | References |
|---------------|---|---------------------------------------|--|--|----------------------|
| FO-NF | Various DS tested both inorganic and organic salts | Commercial flat sheet CTA FO membrane | exchangers. FO-MED system is less energy intensive and has greater recovery rate compared to FO-MSF Water flux: 10 LMH for both FO and NF processes. Salt rejection by FO membrane up to 99.4% for all DS tested. | Water flux of about 10 LMH was observed for both FO and NF processes. High salt rejection (i.e. up to 97.9% for NF process) and good quality product water (i.e. meeting the drinking water TDS standard). | (Tan & Ng, 2010) |
| FO-NF | Divalent salts (MgCl ₂ , Na ₂ SO ₄) | Commercial CTA flat sheet FO membrane | Water flux: 8–12 LMH (FO and PRO mode tested). Higher fluxes were obtained with PRO mode but flux decline was more pronounced (most probably related to membrane fouling). Salt rejection of the diluted DS: 97.7%. | Lower operating pressure, less flux decline due to membrane fouling, higher flux recovery after cleaning, higher quality of product water compared to standalone RO process. | (Zhao et al., 2012b) |
| FO-ED | NaCl | Commercial CTA flat sheet FO membrane | Water flux: Up to 3.5 LMH (simulation not experimental) with 1 M NaCl as DS and brackish water or wastewater as feed and assuming 130 L/day product water. | Energy efficient process when ED powered by solar energy. High quality produced water meeting potable water standards but high capital cost and unsuitable to desalinate high saline water | (Zhang et al., 2013) |

2.3.3. Wastewater treatment

2.3.3.1. OMBR-RO hybrid systems

Since the FO process is characterized by low fouling risk due to the absence of applied hydraulic pressure, many efforts for its potential application to wastewater treatment have recently been conducted. Membrane bioreactor (MBR) equipped with low-pressure hollow fiber microfiltration (MF) or UF membranes is becoming the favorable wastewater treatment technology for non-potable reuse applications. This is mainly due to their poor rejection performance compared to conventional treatment technologies which are attributed to higher and more consistent effluent quality (Arévalo et al., 2009). Besides, the energy requirement of MBRs is higher than conventional wastewater treatments, due to the use of pressure and membrane fouling with both MF/UF membranes and RO membranes damaged by the presence of natural organic matter and biofouling (Cornelissen et al., 2008). To avoid these limitations, many studies investigated an innovative osmotic membrane bioreactor (OMBR), in which FO membranes can be used as an alternative to MF/UF membranes. In this OMBR process, an ideal multi-barrier protection can be utilized for indirect or direct potable reuse applications (Achilli et al., 2009b; Alturki et al., 2012; Cornelissen et al., 2008). In fact, the major advantages of using FO membranes into MBRs instead of conventional low-pressure membrane processes are their lower power consumption (driving force refers to the osmotic gradient between the feed and draw solutions), their low membrane fouling tendency, and higher removal efficiency of macromolecules, ions, and TrOCs from the wastewater (Alturki et al., 2013; Hancock & Cath, 2009; Hancock et al., 2011b; Hancock et al., 2013). OMBRs utilizes a submerged FO membrane in a bioreactor containing activated sludge and continuously fed with wastewater (i.e. feed water). Thus, water is moved from the feed side across a semi-permeable FO membrane, and a high salinity DS is diluted. The diluted DS is then reconcentrated in the following process such as RO, this configuration has been also studied by Achilli et al. (2009b) and Bowden et al. (2012b).

However, several studies have reported that one of the major limitations of this hybrid system is the accumulation of dissolved solutes in the feed stream due to a high rejection rate of the FO membrane (Achilli et al., 2009b; Zhang et al., 2012). In

addition, accumulation of draw solutes in the bioreactor occurs due to the reverse diffusing of draw solutes to the bioreactor through the FO membrane. These contribute to the reduction of the osmotic driving force across the FO membrane and thus lower the water flux as well as affecting the microbial conditions inside the bioreactor at elevated solute dissolved concentration (Ye et al., 2009). Some recent studies have proposed salt accumulation models in osmotic membrane bioreactors and the results showed that salt accumulation is significantly affected by the solids retention time (SRT) to maintain salt concentration at a steady state. Although a reduction in the salt concentration in the bioreactor can be attributed by a short SRT, this will also limit the biological nitrogen removal and reduce the water recovery (Ersu et al., 2010).

An alternative hybrid system where either MF or UF membranes are integrated in parallel to the FO membrane into the bioreactor was proposed by (Wang et al., 2014) and (Holloway et al., 2015b). In this hybrid system, the MF/UF membrane continuously removes the dissolved constituents from the reactor. The recovery of beneficial nutrients from the reactor such as nitrogen and phosphorus is possible since they are rejected by the FO membrane. The addition of the MF membrane inside the bioreactor showed increasing total organic carbon (TOC) and $\text{NH}_3\text{-N}$ removals by the activated sludge process as a result of decreasing salt concentration inside the bioreactor diverted by the MF process, thereby helping improve the microbial activity (Wang et al., 2014). Results from the long-term operation of UF-OMBR-RO hybrid system showed that over the first 3 weeks a water flux varied from 3.8 to 5.7 LMH and then stabilized to 4.8 LMH for more than 80 days when the UF membrane operation started. It is most interesting to note here that membrane cleaning during the 124 days of operation in this system configuration was unnecessary. The stable flux was attributed to the UF system drawing the dissolved constituents from the bioreactor which significantly reduced FO membrane fouling compared to conventional OMBR. In fact, the average removal of total nitrogen, total phosphorous and chemical oxygen demand from the bioreactor was greater than 82%, 99%, and 96% respectively. The high phosphorus from the UF permeate at a concentration of higher than 50 mg/L can then be potentially extracted for beneficial non-potable reuse applications. At the same time, the high quality of the RO permeate met the drinking water standard making the product water suitable for potable reuse application. Therefore, the benefits offered by

the simultaneous recovery of nutrients and production of drinking water by this hybrid system could offset the increase of capital and operational costs associated with this additional UF process.

The only issues associated with these two hybrid systems are: (1) the effluent quality from UF or MF membranes, especially the TOC concentration, might exceed the wastewater treatment plant effluent standards and (2) the fouling reduction methods for MF/UF and FO membranes may be different and applying them in the same bioreactor may prove to be complicated (Park et al., 2015). One of the alternatives to using MF or UF membranes to mitigate the membrane fouling issue may be to adopt a separate sludge concentrator to increase the sludge retention time without accumulating salts inside the bioreactor (Park et al., 2015).

An additional driving force to the osmotic pressure such as in the PAFO process in which the reverse salt flux is lowered compared to the FO process is likely to solve the issue related to the detrimental salt accumulation inside the bioreactor. This may be a better and more cost-effective alternative than the hybrid UF-MF-OMBR systems. However, it has to be pointed out that the PAFO process cannot operate in a submerged-type configuration since the additional hydraulic pressure cannot be applied to the feed solution inside the bioreactor.

2.3.3.2. Other hybrid systems for wastewater treatment

A novel cellulose acetate (CA) hollow fiber (HF) FO membrane for wastewater treatment was demonstrated by Su et al. (2012). In this study, the FO process was coupled with NF for the DS reconcentration. Results showed that the NF membrane performed well in terms of DS removal efficiency, with up to 99.6% removal and minimal reverse draw solute being observed in the FO process due to the high molecular weight of the DS (i.e. sucrose). When using synthetic wastewater as FS, water fluxes in the FO process ranged from 6.5–9.9 LMH (Table 2-6). Later, the same group (Su et al., 2013) synthesized a novel polymer (i.e. CA propionate or CAP) to prepare dual-layer HF FO membrane for wastewater treatment. In this study, MD was incorporated as DS recovery process instead of NF, since the MD system would be more economical, especially if waste or low-quality heat is available near the treatment

plant. Results showed that when using CAP-based HF membranes in the FO process, much higher water fluxes and lower reverse salt fluxes were observed compared to CA-based membranes due to its reduced salt diffusivity and salt partition coefficient. The FO and MD processes delivered similar water fluxes (i.e. 12.6 LMH and 13.0 LMH for FO and MD process respectively) when synthetic wastewater was used as FS.

As discussed in the previous section, although PAA-Na solution was developed and proven to have high water flux and minimal reverse flux, its high viscosity limited its applications at ambient conditions with the hybrid FO-UF system (Ge et al., 2012). To overcome this issue, MD was employed as an alternative DS reconcentration process instead of UF since it can operate at a higher temperature of up to 80 °C (Ge et al., 2012). Water fluxes of up to 40 LMH in the FO process were achieved with low reverse fluxes as shown in Table 2-6. Experiments conducted on the FO-MD hybrid system showed that the optimum performance was achieved when the water transfer rates of FO and MD were similar. Finally, they demonstrated that this hybrid FO–MD system integrating polyelectrolytes as DS was suitable (i.e. overall process was stable and repeatable) for dye wastewater treatment. Other successful wastewater treatment applications that have been explored for the hybrid FO–MD system include direct sewer mining (Xie et al., 2013a), water recovery from oily wastewater (Zhang et al., 2014) and water reclamation from shale gas drilling flow-back fluid (Li et al., 2014).

Several studies have investigated the potential of the FO process to remove trace pollutants such as pharmaceuticals and personal care products (D'Haese et al., 2013; Hancock et al., 2011b; Jin et al., 2012; Linares et al., 2011; Xie et al., 2012) and results from these studies confirmed the good performance of the FO process for the rejection of these contaminants. However, none of these studies addressed the issue of FO concentrate disposal and management since feed concentrate following the FO process contains a relatively high level of these compounds. Liu et al. (2015b) recently proposed to integrate electrochemical oxidation into the FO process in order to simultaneously reject trace pharmaceuticals from the feed wastewater and reduce their concentration in the final feed concentrate. Results from this study demonstrated that this hybrid system can reject the trace antibiotics from the feed wastewater (i.e. rejection rate of 98%) as well as reduce their concentration in the final concentrate (i.e. 99% removal) at the same time.

The coagulation or destabilization process is currently the most widely used and economical approach water treatment since it does not require hydraulic or thermal energy (Matilainen et al., 2010). The coagulation relies on the interaction of oppositely charged suspended and dissolved colloids giving rise to a natural destabilization effect and the formation of micro-particles which subsequently form larger and heavier structures called flocs. These flocs can then be easily removed via a simple sedimentation process. The most commonly employed coagulants for water and wastewater treatment are aluminum sulfate ($\text{Al}_2(\text{SO}_4)_3$), ferric chloride (FeCl_3), poly-aluminum chloride (PACl) and polyferric sulfate (PFS) (DeWolfe, 2003). In 1972, Frank (Frank, 1972) showed that $\text{Al}_2(\text{SO}_4)_3$ can be used as DS to desalinate seawater since it can produce a high osmotic pressure. However, the proposed separation method (i.e. precipitation followed by centrifugation) was not economically practical. Since $\text{Al}_2(\text{SO}_4)_3$ is positively charged, it can thus be destabilized in the presence of negatively charged colloids. Therefore, Liu et al. (Liu et al., 2011) recently proposed the use of negatively charged magnetic nanoparticles (i.e. core-shell Fe_3O_4 nanoparticles coated with silicon dioxide – $\text{Fe}_3\text{O}_4@\text{SiO}_2$) to destabilize $\text{Al}_2(\text{SO}_4)_3$. In this study, the FO process is used to concentrate wastewater using $\text{Al}_2(\text{SO}_4)_3$ as the DS. After the FO process, the diluted DS is destabilized by the negatively charged magnetic nanoparticles which can then be recovered by applying an external permanent magnetic field without using energy input. However, there is currently no information on the actual process performance and moreover, the overall regeneration process seems complicated since it involves the use of CaSO_4 and H_2SO_4 which can potentially deteriorate the final water product even at trace levels. Besides, the synthesis of $\text{Fe}_3\text{O}_4@\text{SiO}_2$ is not an easy process which would likely increase the overall cost of the process.

Table 2 - 7. Summary of hybrid FO systems for wastewater treatment

| Hybrid process | Draw solution | Membrane type(s) for FO process | FO performance | Remarks | References |
|----------------|-----------------|---------------------------------------|--|--|--|
| OMBR-RO | Inorganic salts | Commercial CTA flat sheet FO membrane | Water flux: 5.5 LMH (MgSO ₄) to 10.9 LMH (KCl) at 2.8 MPa. Reverse draw solute: 1.2 g/m ² h (MgSO ₄) to 22.0 g/m ² h (KBr) at 2.8 MPa. | Higher water flux compared to that obtained with organic salts but lower salt rejection. | (Achilli et al., 2010) |
| | Organic salts | Commercial CTA flat sheet FO membrane | Water flux: 8.3-9.4 LMH at 2.8 MPa. Reverse draw solute: 1.1-6.0 g/m ² h at 2.8 MPa. | High salt rejection (about 99%) but energy intensive and relatively high replenishment cost compared to inorganic salts. The novel hybrid system performed well in terms of nutrient recovery and salt rejection and membrane fouling was significantly reduced compared to conventional OMBR. A stable flux of 4.8 LMH was achieved over the duration of the investigation (i.e. 120 days) without a single membrane cleaning. This was attributed to the UF system drawing salts from the bioreactor which reduced FO membrane fouling. | (Bowden et al., 2012a) |
| UF-OMBR-RO | RO concentrate | Commercial CTA flat sheet FO membrane | Water flux: Ranging from 5.7 to 3.8 LMH over the first 3 weeks of operation and then average flux of 4.8 LMH once the UF membrane operation started with 26 g/L NaCl as DS and activated sludge as feed. | | (Holloway et al., 2015b; Park et al., 2015; Wang et al., 2014) |
| FO-NF | Sucrose | Double skinned CA HF FO membrane | Water flux: 6.5-9.9 LMH with 0.5 M sucrose as DS and wastewater (i.e. 200- | High salt rejection (i.e. 99.6%) due to sucrose high molecular weight. | (Su et al., 2012) |

| Hybrid process | Draw solution | Membrane type(s) for FO process | FO performance | Remarks | References |
|----------------|---------------------------|---------------------------------------|---|---|----------------------|
| FO–MD | MgCl ₂ | CAP HF FO membrane | 2000 mg/L mixed metal ions) as feed. Minimal reverse draw solute. Water flux: 13–13.7 LMH with 0.5 M MgCl ₂ and synthetic wastewater (i.e. heavy metal ions) as feed. Minimal reverse draw solute. | Great potential for this newly developed CAP HF FO membrane for the application in wastewater reclamation. | (Su et al., 2013) |
| FO–MD | Polyelectrolytes (PAA–Na) | CA HF membrane | Water flux: Up to 40 LMH (at 80 °C with 0.6 g/mL DS and acid orange 8 as feed). Reverse salt flux: Up to 0.14 g/m ² h. | No DS leakage to product water after MD process. Most efficient performance when the water transfer rate of FO matched that of MD. Suitable (i.e. process stable and repeatable) for dye wastewater treatment. Water flux of 8 LMH was achieved. Recovery rate of 80%. Trace organic compounds (TrOCs) can migrate across FO membrane and accumulate in the draw solution but when system is coupled with GAC and UV, it can remove more than 99.5% of TrOCs. Low-cost energy can be used as heat source. | (Ge et al., 2012) |
| FO–MD | NaCl | Commercial CTA flat sheet FO membrane | Water flux: 8 LMH with 1.5 M NaCl as DS and sewage as feed. | Water flux of more than 14 LMH was achieved for FO after 30 h of operation. | (Xie et al., 2013a) |
| FO–MD | NaCl | CTA TFC HF FO membrane | Water flux: About 25 LMH with 2.0 M NaCl as DS and oily | Water flux of more than 14 LMH was achieved for FO after 30 h of operation. | (Zhang et al., 2014) |

| Hybrid process | Draw solution | Membrane type(s) for FO process | FO performance | Remarks | References |
|---|---------------------------------|---------------------------------------|---|--|---------------------|
| FO-MD | NaCl, KCl and MgCl ₂ | Commercial CTA flat sheet FO membrane | <p>wastewater (i.e. 4000 ppm petroleum) as feed; Up to 40 LMH at 60 °C and DI water as feed. Reverse salt flux: Up to 7.3 g/m² h (DI water as feed).</p> <p>Water flux: Up to 23 LMH with 3.0 M KCl as DS at 25 °C and pre-treated shale-gas drilling flow-back fluid as feed. Acceptable reverse salt flux.</p> | <p>Stable water flux of 6 LMH for MD process. Recovery rate of more than 90%. Fouling was found to increase with petroleum concentration. Acetic acid concentration increased in draw solution which decreased its osmotic pressure. KCl was identified as a suitable DS for this application offering high water flux and tolerable reverse salt flux. Water recovery up to 90% was achieved by this hybrid system with high quality product water (i.e. drinking water standard)</p> <p>Integration of electrochemical oxidation into FO process can improve the rejection of trace antibiotics from the feed wastewater (i.e. rejection rate of 98%) as well as reduce their concentration in the final concentrate (i.e. 99% removal).</p> | (Li et al., 2014) |
| Electrochemical oxidation integrated FO process | NaCl | Commercial CTA flat sheet FO membrane | <p>Water flux: Up to 14 LMH with 2.0 M NaCl DS and synthetic wastewater (containing antibiotics) as feed.</p> | <p>Integration of electrochemical oxidation into FO process can improve the rejection of trace antibiotics from the feed wastewater (i.e. rejection rate of 98%) as well as reduce their concentration in the final concentrate (i.e. 99% removal).</p> | (Liu et al., 2015a) |

2.3.4. Simultaneous wastewater treatment and seawater desalination

One efficient way to moderate the energy requirement during RO desalination is via the dilution of the highly saline feed stream since it will reduce the osmotic pressure that needs to be overcome to produce RO permeate (Glueckstern & Priel, 1998). The relatively low salinity of most impaired and reclaimed waters makes them good candidates for such dilution purposes (Lew et al., 2005). However, direct dilution/combination of both streams may contaminate and alter the chemistry of the feed stream in the desalination process, likely aggravating membrane fouling and subsequently lowering product water quality. Therefore, pre-treatment of impaired water before desalination with diluted saline water becomes a necessity.

Recently, researchers started to explore and assess the treatment performance and economics of the FO-RO hybrid process for simultaneous treatment of impaired/reclaimed water and seawater for reuse (Cath & Childress; Cath et al., 2009; Cath et al., 2010b; Hancock et al., 2012; Sim et al., 2013a). In the first FO process, the impaired water is used as feed solution and pre-treated seawater is used as DS which is subsequently diluted and transferred to RO to produce clean potable water. The concentrated impaired water from the first FO unit can be then transferred to the second FO process where concentrated brine from the RO process is used as DS. The osmotically diluted RO brine can be either recycled back to the RO process or discharged to the environment because its environmental impact has been mitigated (Achilli et al., 2009a). The concentrated impaired water can be further dewatered to recover nutrients for use as fertilizer or returned to the wastewater treatment plant for retreatment. This hybrid FO-RO process was estimated to achieve favorable economic returns during operation, with up to 63% recovery (i.e. by FO-RO and assuming SWRO plant operates at 50% water recovery rate) from the impaired water stream. Beyond 63% recovery, the capital costs associated with increasing required membrane area for osmosis could counter-balance the saving from reduced energy consumption of the SWRO process (Cath et al., 2010b). This is because the osmotic pressure of the seawater limits the water flux the FO membrane can generate using wastewater effluent as feed. An example schematic of this hybrid process plant (FO-RO-FO configuration) with simultaneous treatment of seawater and wastewater is shown in Figure 2-5.

Alternative configurations have been recently suggested (Sim et al., 2013a) in which either the two FO processes are replaced by PRO or only the second FO process is replaced by pressure retarded osmosis (PRO) to achieve higher overall water recovery (i.e. up to 80%) and reduced energy consumption (i.e. up to 23%). The FO-PRO configuration was preferred to the PRO-PRO variation since, for the latter, the increase in capital cost (i.e. + 11%) and space footprint (i.e. + 112%) (compared to conventional SWRO plant) outweighs the benefits of reduced energy consumption as shown in Table 2-8. Finally, the economic feasibility of a hybrid PRO-RO system was also assessed for the simultaneous treatment of seawater and wastewater (Kim et al., 2015b). Results showed that inorganic fouling within the support layer of the PRO membrane was a major limitation of this system and caused substantial flux decline. Anti-scaling pre-treatment was tested and proved to be very effective in improving the water flux by inhibiting calcium phosphate scaling. The authors also suggested that future research should focus on the development of high fouling resistant PRO membrane to support the practical application of the PRO-RO system.

Table 2 - 8. Quantitative comparison of total energy consumption, total capital costs and space footprint for the different configurations and conventional SWRO plant (adapted from (Sim et al., 2013a))

| Configuration | Conventional SWRO | FO-PRO | PRO-PRO |
|---|--------------------------|---------------|----------------|
| Specific energy consumption (kWh/m ³) | 1.35 | 1.07 | 1.04 |
| Energy recovery from PRO (kWh/m ³) | N.A. | 0.09 | 0.23 |
| Total capital cost (US\$/m ³) | 0.096 | 0.0874 | 0.1066 |
| Space footprint (8" spiral wound elements) | 5405 | 10380 | 11460 |

In all the hybrid FO-RO configurations discussed above, FO operates in the OD mode and therefore does not require closed-loop DS reconcentration. Instead, the process can operate with both the feed and draw solution in a once-through flow configuration (Cath et al., 2006b) offering the true benefits of FO as a low energy process as it eliminates the energy costs associated with the DS reconcentration process and reduces the operational complexities (Hancock & Cath, 2009). This hybrid process can achieve several benefits related to energy consumption and product water quality: (i) seawater is being diluted before RO desalination, which reduces the energy cost of desalting the seawater; (ii) pre-treatment of impaired water reduces the fouling propensity of water in the RO stage; (iii) provides multi-barrier protection of product water since

contaminants present in the impaired water are prohibited from entering the product water through two established barriers, the FO membrane and then RO membrane units and finally (iv) an opportunity for safe reuse of impaired water can be realized.

The hybrid FO-RO system is still at its early stage of development and many challenges are yet to be overcome before achieving commercial potential. In fact, due to the small difference in osmotic pressure between the wastewater feed and the seawater draw solutions, the produced water flux is quite low and therefore, to increase the process water recovery, a large membrane area will be required thereby increasing the process footprint and capital cost (Hancock et al., 2012). The negative social perception of the reuse of impaired water for drinking water production is another challenge which may impede the successful commercialization of this promising hybrid system (Hoover et al., 2011).

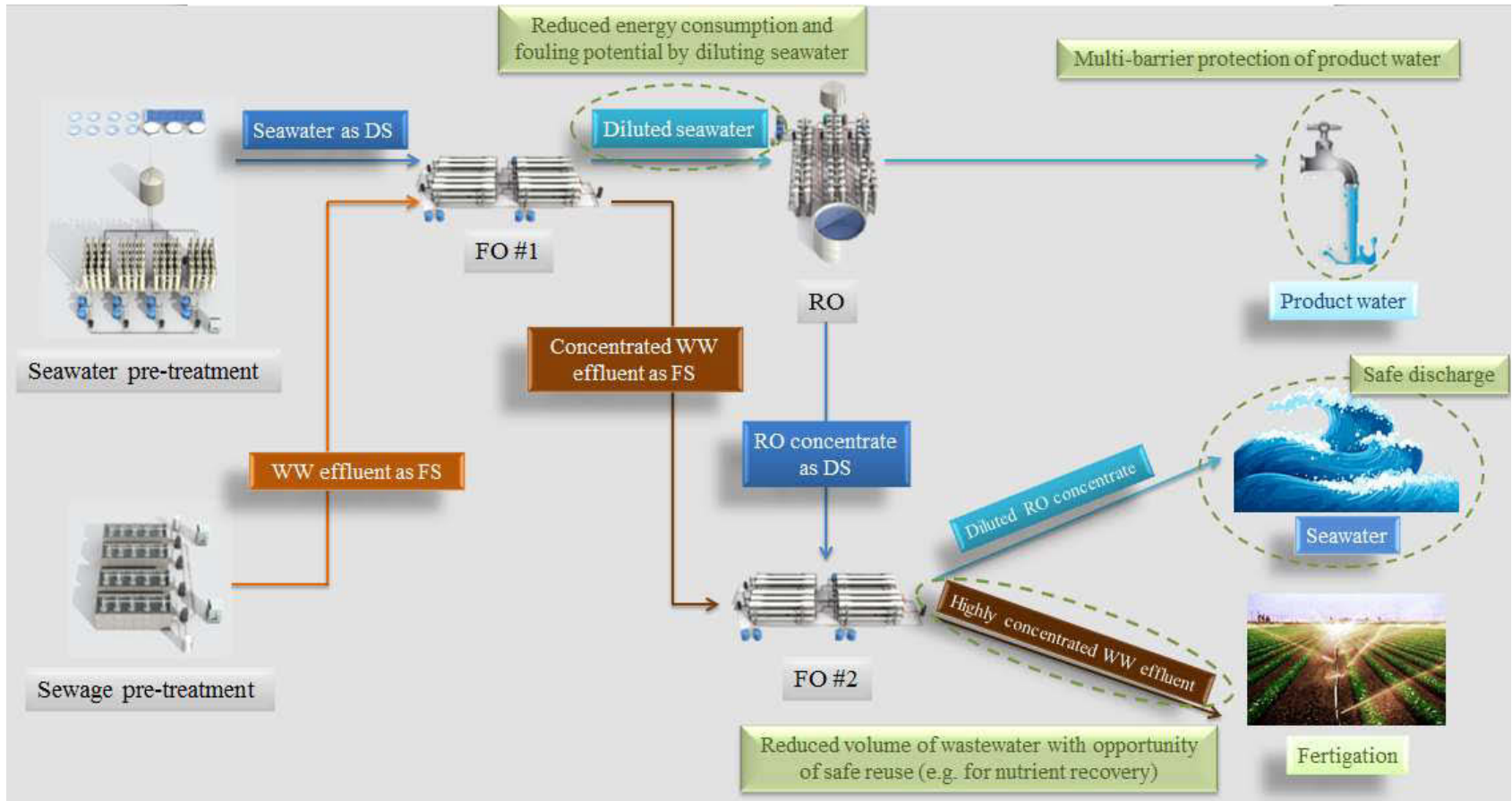


Figure 2 - 5. Schematic of an OD-RO hybrid process plant for simultaneous treatment of wastewater and seawater desalination (DS: Draw solution; FS: Feed solution; RO: Reverse osmosis; WW: Wastewater)

2.4. Environmental and economic life cycle assessment of hybrid FO systems

Life cycle assessment (LCA) is a methodology for implementing the assessment of the environmental impacts associated with the development of consumable products for humans (Organization, 1997). In recent years studies have been conducted that explored the application of LCA methodology to evaluate the environmental impact of water treatment technologies (Biswas, 2009; Muñoz et al., 2008; Raluy et al., 2005a; Raluy et al., 2005b; Raluy et al., 2005c). The main research objectives of these studies were to evaluate the impacts of construction and operations phases of SWRO desalination plants. Each study developed a life cycle inventory (LCI) to explain various reference flows such as construction/building materials, chemicals required for operation (cleaning, primarily anti-scaling and disinfection chemicals) and materials used for membrane fabrication. One of the main results drawn from these studies is that the single greatest contributor to negative environmental impacts refers to energy consumption during the operation phase of SWRO plants, accounting for greater than 85% of the environmental impact (Raluy et al., 2005b).

Additional energy savings may be achieved by integrating FO in RO desalination schemes. Osmotically driven forward osmosis processes have shown very high rejection of contaminants common to wastewater and a low fouling propensity. Consequently, the FO membrane has been incorporated as a pre-treatment process in regard to the conventional desalination technologies as discussed in the previous section. This is attributed to lowering the operating pressure applied in the RO process, meaning that it can use brackish water RO membranes (BWRO) instead of SWRO membranes (i.e., close to 70 MPa) (Phuntsho et al., 2016b; Valladares Linares et al., 2016) thus lowering the negative environmental impacts of the operational phase of the RO facility. Gomez and Cath (2011) reported a cost modelling of an FO-RO hybrid system for seawater desalination and wastewater reuse in Texas. Results indicated that the application of an FO-RO system is not cost effective when compared to the conventional wastewater treatment plant which includes an RO membrane unit followed by an advanced oxidation process (AOP) (ultraviolet (UV) light) for disinfection. However, a critical aspect in the economics of the FO-RO hybrid system was shown as the cost of the FO membrane. If the cost of FO membrane modules can

be as reasonable as RO membrane modules (i.e. comparable to production costs of RO modules with the same packing density), it is expected that FO hybrid system may become economically viable in the future (Gomez & Cath, 2011).

It is important to investigate the environmental and economic impacts of established and novel processes for seawater desalination and wastewater reclamation. Hancock et al. (2012) conducted a comparative life cycle assessment to determine the comparative environmental impacts of coupled seawater desalination and water reclamation using an osmotically driven membrane process (i.e. FO-RO) and established membrane desalination technologies (i.e. SWRO). Higher water permeation of FO membranes and FO packing density could improve the FO technology and thus reduce the environmental impact of the hybrid FO-RO system by 25% compared to SWRO process. A recent study by Coday et al. (2015) did compare the environmental and economic impacts of osmosis and osmotic dilution for desalination and treatment of oil gas exploration wastewater to manage water issues in the oil and gas industry. This includes an FO hybrid system and deep well injection. Results showed that the environmental impacts of FO can be competitive with deep well injection. Additionally, an FO hybrid system can be more economically beneficial due to the much lower cost of water management (up to 60%), compared to conventional deep well disposal.

Although a life cycle cost analysis includes the cost of an asset, or its part throughout its flow in the life cycle, it is ultimately influenced by performance requirements. It includes capital and operational expenditure (CAPEX and OPEX), specifically; CAPEX refers to land, engineering, unit purchase, transportation, installation, etc. while OPEX refers to labor, maintenance and spare parts replacement, energy, and chemicals. The desalinated product water cost depends on both CAPEX and OPEX costs. The differences in water cost estimation, in literature, can be attributed to factors such as differences in (1) fuel or electricity cost, (2) raw material and transportation costs, (3) feed water properties (e.g. salinity and turbidity), (4) land cost, (5) subsidies and (6) cost calculation models or methods (Mezher et al., 2011). More accurate and practical life cycle cost assessment was conducted by Valladares Linares et al. (2016). In their study, a module-scale approach was used to evaluate the performance of the

FO membrane. In addition, a wide range of literature including global trends, real data from desalination/wastewater treatment markets and industrial reports, and commercially available materials were incorporated. A comparative life cost of existing wastewater treatment technologies and proposed seawater desalination and wastewater recovery inducing SWRO, MBR-RO-AOP, and FO-LPRO hybrid systems was considered. In terms of the total water cost per cubic meter of water produced, the hybrid FO-LPRO desalination system showed around 16% lower cost than SWRO. However, the FO-LPRO system has a 21% higher CAPEX and a 56% lower OPEX due to FO module costs (i.e. total membrane area) and savings in energy consumption and cleaning processes, respectively. Sensitivity analysis results, therefore, indicated that FO membrane flux and FO module cost are the main parameters of making the FO-LPRO hybrid system economically viable.

Techno-economic and environmental assessment is necessary for evaluating the practical viability of FO hybrid systems for seawater desalination and wastewater recovery as compared to other conventional water management strategies. The apparent benefit of FO over conventional pre-treatment processes relies on its lower fouling propensity and higher fouling reversibility, making it the ideal candidate for treating challenging feed waters. However, to achieve the commercial potential for the FO hybrid process, the future research should focus on the development of novel membranes with improved fouling resistance as a means of increasing its long-term performance. Modification of membranes with antimicrobial nanomaterials (e.g. carbon nanotubes, graphene or graphene oxide, etc.) has already shown promising biofouling resistance.

2.5. Forward osmosis plant design innovation

There are still several challenges that need to be overcome before successful industrial application of this technology is achieved. In fact, in a recent review focusing on the energy efficiency of the FO process, it was demonstrated that the hybrid FO-RO process consumes more electric energy than RO alone and therefore the term “low energy process” often attributed to FO may only be appropriate in few applications where FO presents apparent advantages over conventional separation processes

(Shaffer et al., 2015b). Osmotic dilution (OD) is one good example and is receiving increasing attention for its energy reduction potential (Hoover et al., 2011). In fact, in the OD approach, the diluted DS is the targeted product. Therefore, no additional process is needed for DS recovery, eliminating one of the major issues impeding the commercialization of the full-scale FO process: lowering the energy cost of the DS recovery process. Recently, OD has been proposed for the simultaneous treatment of wastewater (i.e. feed solution) and seawater (i.e. draw solution) (Boo et al., 2013; Cath et al., 2010b; Hancock et al., 2013) and integrated in a conventional seawater desalination plant (i.e. coupled with seawater RO). Another recent study investigated the feasibility of dual-stage FO/PRO for the osmotic dilution of shale gas wastewater (Altaee & Hilal, 2014). These early lab-scale and pilot-scale studies showed that the hybrid OD-RO system would be very promising for full-scale practical implementation. Aiming this objective, the FO-RO hybrid Desalination Research Center (FOHC, Kookmin University, Korea) has recently initiated an ambitious 5-year project “ONE Desal” (osmosis-based, no fouling, energy-efficient desalination), bringing together academic and industrials with the aim of constructing and operating the first FO-RO hybrid process plant with a capacity of 1,000 m³/day and an energy consumption target of 2.5 kWh/m³ (i.e. 35% less than conventional SWRO) for the simultaneous treatment of impaired water and seawater. This USD \$28 million budget desalination project includes 3 core projects (Figure 2-8) which aim at (i) developing and optimizing the hybrid FO-RO system at lab-scale and pilot-scale, (ii) developing efficient and low-cost pre-treatment technologies and finally (iii) designing and operating the first FO-RO hybrid process plant.

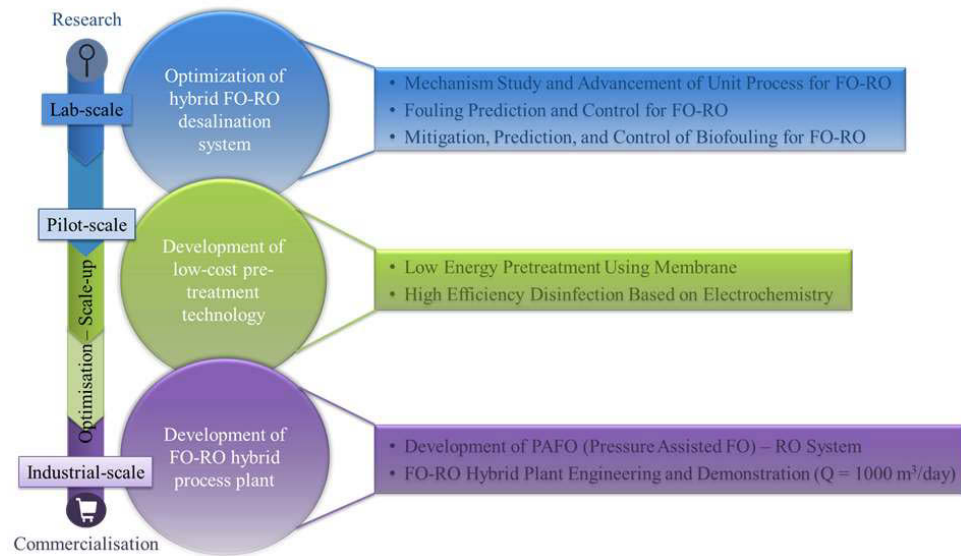


Figure 2 - 6. ONE Desal project overview: From lab-scale development and optimization to hybrid FO-RO plant operation

CHAPTER 3

MATERIALS AND METHODS

3.1. Introduction

In this thesis, a series of theoretical, bench and pilot-scale experimental investigations were conducted. The experimental investigation works are divided into two parts; lab- and pilot-scale of forward osmosis (FO), reverse osmosis (RO) and nanofiltration (NF). Technical feasibility of FO in osmotic dilution and wastewater treatment was tested through long-term field FO operation. Additionally, simple lab-scale FO experiments were carried out using the most common draw solutes selected for this study and concurrently, the post-treatment process (i.e. RO and NF) to reconcentrate the draw solutes for reuse was considered. A life cycle assessment of a hybrid FO-RO/NF system was then conducted using a specific analysis software, which is called Simapro.

With the aid of experimental and life cycle assessment results, more specific pilot-scale experiments were conducted using a module-scale FO membrane in the pilot-scale FO process, and the results obtained from the module-scale FO membrane tests were used for the simulation study. More specifically, practical considerations for operability of the FO module including fouling behavior, water flux enhancement when applying additional pressure and FO membrane module design arrangement options for a full-scale FO hybrid system, making it techno-economic favorable, were evaluated. Finally, the overall structure of the development of software to design a full-scale FO process was established using Microsoft Excel software.

This chapter describes in detail the general experimental methods for the bench-scale experiments conducted within the scope of this study, including the specifications of feed and draw solutions used for the experiments. More specific experimental details can be found in their respective chapters.

3.2. Experimental procedure and operating conditions

3.2.1. Chemicals and solutions used

3.2.1.1. Feed solutions for the forward osmosis process

The type of feed solutions used for this study depended on the study specified in each chapter. For the case of a bench-scale investigation, deionized water or DI (Milli-Q,

Millipore with electrical conductivity (EC) 4.0 $\mu\text{S}/\text{cm}$ and TOC 4 ppb) was used as the FS, especially when the study related to the comparative performances of different draw solution (DS). For the case of a baseline test for the pilot-scale FO process, tap water was used as the FS due to the scale of the experiment (i.e. more than 1,000L).

The FS also consisted of mine impaired groundwater with total dissolved solids (TDS) of 2,500 and 5,600 mg/L, collected from the coal mine site located at Newstan Colliery (Centennial Coal Pty. Ltd), State of New South Wales (NSW), Australia. However, in Chapter 8, the simulated wastewater with TDS of 1,500 mg/L of NaCl solution was used to simulate the actual wastewater effluent found in the Central Park Wastewater Treatment Plant (WPT) located at Sydney, NSW, Australia.

In the pilot-scale FO fouling experiment, the FS was prepared by mixing the following chemicals with tap water: 1.2 g/L red sea salt (RSS), 0.22 g/L CaCl_2 (Ajax Finechem Pty Ltd., Tarend point, Australia), 0.2 g/L humic acid sodium salt (Aldrich, Milwaukee, WIS) and 0.2 g/L alginic acid sodium salt (Sigma Aldrich Co., St Louis, MO).

3.2.1.2. Feed solutions for the nanofiltration and reverse osmosis processes

Nanofiltration (NF) was used a post-treatment process to reduce the final nutrient concentration in the diluted fertilizer DS for direct irrigation as discussed in Chapter 4. Both NF and RO have been considered as a post-treatment process to reconcentration/recover draw solutes from the diluted inorganic based draw solutions discussed in Chapter 6. The specific compositions of the diluted draw solutions can be found in the respective chapters.

3.2.1.3. Draw solutions for the forward osmosis process

As shown in Table 3-1, one specific fertilizer, ammonium sulphate or SOA or $(\text{NH}_4)_2\text{SO}_4$, was used as the DS and its molecular weight (MW) SOA is 132.1 g. This fertilizer was selected based on our previous investigations and it was reagent grade

(Phuntsho et al., 2011; Phuntsho et al., 2012c). In addition, four different types of inorganic based draw solutes such as NaCl, MgCl₂, Na₂SO₄, and MgSO₄ were also used in the experiments in Chapter 5 for the aim of conducting comparative studies. All the draw solutions used for the bench-scale experiments were prepared by dissolving the salts in DI water while that for the pilot-scale experiments were prepared by dissolving the salt in tap water. Except for the field operation of the pilot-scale FO process conducted, all the solutions were prepared at room temperature.

Table 3 - 1. List of chemicals used as draw solutes

| Chemicals | Molecular weight (g) | Remarks |
|---|----------------------|--------------------------|
| (NH ₄) ₂ SO ₄ | 132.1 | Fertiliser reagent grade |
| NaCl | 58.44 | Reagent grade |
| MgCl ₂ | 95.21 | |
| Na ₂ SO ₄ | 142.04 | |
| MgSO ₄ | 120.37 | |
| Simulated Seawater | 0.6 M NaCl | Industrial grade |

3.2.2. Membranes and their characteristics

3.2.2.1. Forward osmosis (FO) membranes

Two different types of FO membranes were available; cellulose triacetate (CTA) was supplied by Hydration Technology Innovations (HTI), LLC, Albany, USA while polyamide thin film composite (TFC) was supplied by Toray Industries (Korea). CTA FO membranes were used only for the pilot-scale FO experiment in this study (Chapter 4) while all other benches and pilot FO experiments were conducted using small and module scale TFC membranes unless stated otherwise.

The pure water permeability (A , Lm²h⁻¹bar⁻¹) and the salt rejection (R , %) for both FO membranes were determined at various applied pressures using a bench-scale RO unit. The A and R values for FO membranes used in this study are therefore summarised in Table 3-2. The results show that the TFC FO membrane had an A value of 5.54±0.14 Lm²h⁻¹bar⁻¹ while the CTA FO membrane had an A value of 1.02±0.03 Lm²h⁻¹bar⁻¹. In addition, the salt rejection of the FO membrane was observed to be 93% for CTA and 87% for TFC as shown in Table 3-2.

Two different types of spiral wound FO membrane modules were also used in pilot-scale FO study. Both spiral wound (SW) membrane modules were 8040 modules made up of several flat-sheet CTA and TFC FO membranes (8040 CTA and TFC FO membrane modules). The number 8040 refers to the module diameter of 8 inches and the module length of 40 inches. A different number of membrane leaves are rolled into a spiral wound configuration and the feed channel spacer is glued to the membrane sheets as shown in Figure 3-1. The diluted DS is collected in the permeate tube. The FO element is loaded inside a polyvinyl chloride (PVC) housing.

3.2.2.2. Reverse osmosis (RO) and Nanofiltration (NF) membranes

A small flat sheet thin film composite (TFC) polyamide (PA) RO and NF (NF 90 and NF 270) were used in the RO process to demonstrate the capability of the draw solute recovery in Chapter 5. The SWRO membrane was selected and the pure water permeability of the RO membrane was $2.07 \pm 0.10 \text{ Lm}^{-2}\text{h}^{-1}\text{bar}^{-1}$ and the NaCl rejection was 99.5%. Two different types of NF membrane were used. The pure water permeability coefficient of the NF 90 was $6.5 \pm 0.20 \text{ Lm}^{-2}\text{h}^{-1}\text{bar}^{-1}$ and the rejection was 85% while that of the NF 270 was $11.2 \pm 0.10 \text{ Lm}^{-2}\text{h}^{-1}\text{bar}^{-1}$ and the rejection was 50% (Table 3-2).

For the pilot-scale NF process (Chapter 4), the NF membrane module consisted of a thin film composite (TFC) polyamide (PA) of pilot NE 4040-90 membrane (NE90) module provided by Woongjin Chemicals, Korea (as shown in Figure 3-2).

Table 3 - 2. Basic properties of the membranes used in experiments. The material composition is as provided by the manufacturer.

| Properties | CTA FO | TFC FO | SW RO | NF90 | NF270 |
|---------------------------------|-------------------------|------------------|--------------------------|--------------------------|--------------------------|
| Manufacturer | HTI | Toray, Korea | Woogjin Chemicals, Korea | Woogjin Chemicals, Korea | Woogjin Chemicals, Korea |
| Pure water permeability | 1.02±0.03 | 5.54±0.14 | 2.07±0.10 | 6.5±0.20 | 11.2±0.10 |
| Rejection (5g/L NaCl at 10 bar) | 93% | 87% | 99.5% | 85% | 50% |
| Material of selective layer | Cellulose triacetate | Polyamide | Polyamide | Polyamide | Polyamide |
| Support layer | Polyester mesh embedded | TFC poly sulfone | TFC poly sulfone | TFC poly sulfone | TFC poly sulfone |

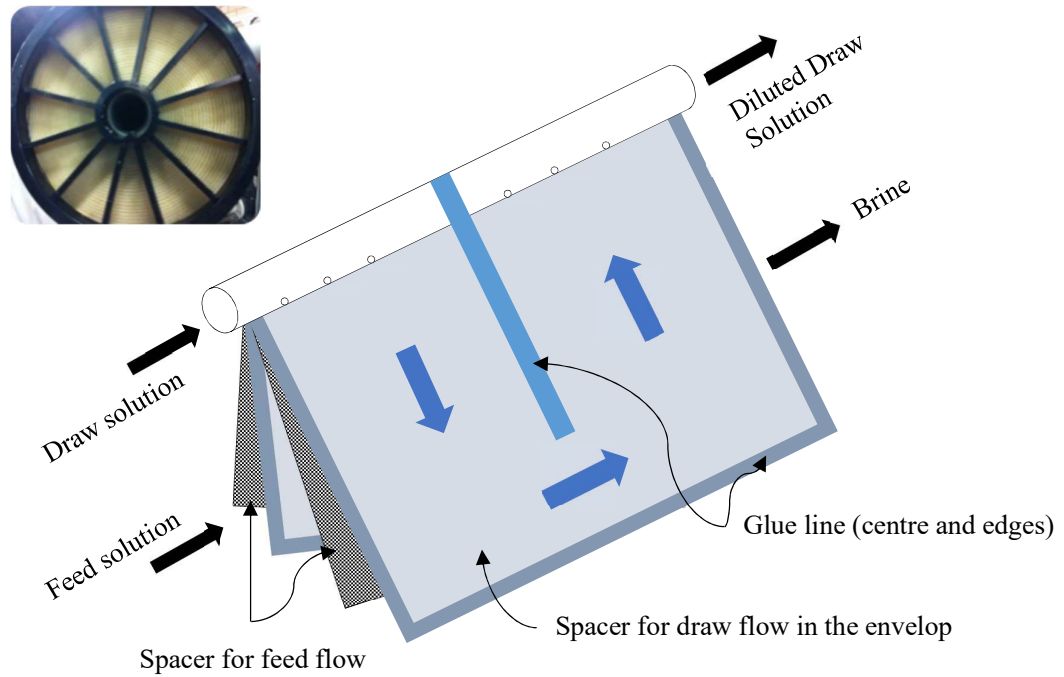


Figure 3 - 1. Schematic diagram of a spiral wound forward osmosis (FO) module showing the direction of water in the module

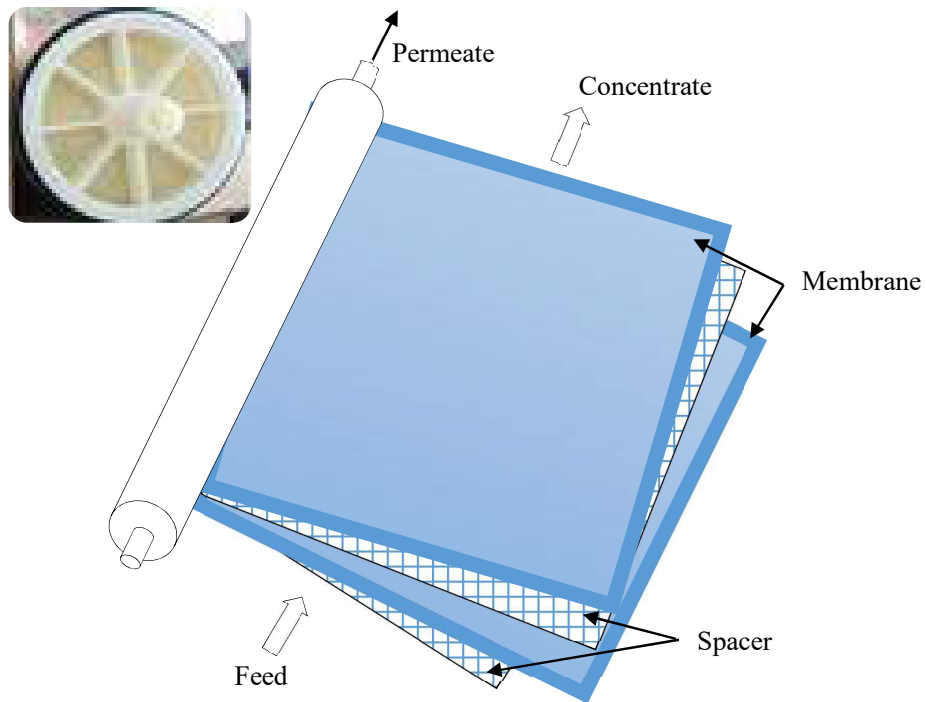


Figure 3 - 2. Schematic diagram of a 4040 spiral wound reverse osmosis (RO) and nanofiltration (NF) module showing the direction of water in the module

3.2.3. Bench-scale experimental set-up

3.2.3.1. Bench-scale FO system

As shown in Figure 3-3, the bench-scale FO unit consists of an FO cell with channel dimensions of 7.7 cm length x 2.6 cm width x 0.3 cm depth and an effective membrane area of $2.002 \times 10^{-3} \text{ m}^2$. Each feed and draw flow channel was controlled independently by a variable speed peristaltic pump (Cole Palmer model 75211-15, 50-5000 RPM and 0.07 HP, Thermo Fisher Scientific, USA), and the operation mode was counter-current flow directions. The volumetric flowrate for the experiments was 400 mL/min. The temperature of all solutions was maintained at $25 \pm 1^\circ\text{C}$ using a temperature water bath controlled by a heater/chiller unless stated otherwise. The water flux across the membrane in the FO process was measured by the change in the weight of the DS tank. The weight change was recorded continuously by connecting a digital mass scale to a data acquisition computer for online data logging at three-minute intervals. The water flux J_w (in $\text{Lm}^{-2}\text{h}^{-1}$) was calculated using the following relationship:

$$J_w = \frac{\text{Change in DS tank volume (L)}}{\text{Time (t)} \times \text{Membrane area (m}^2\text{)}} \quad (3-1)$$

The initial volume of the feed and solution was 2L for all the bench-scale FO experiments unless stated otherwise. The experiments were conducted in a batch mode.

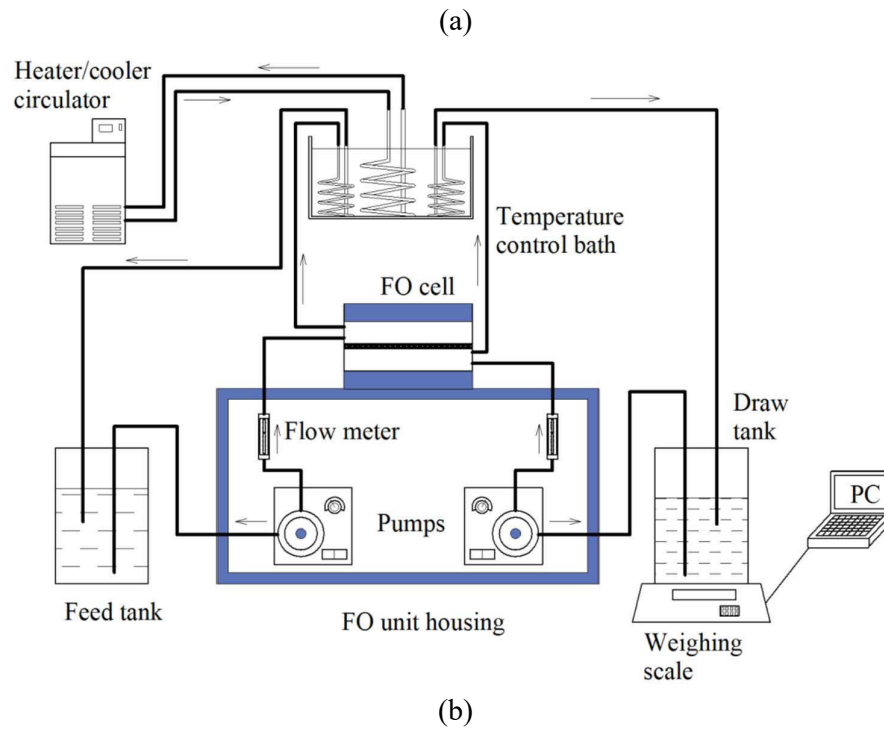


Figure 3 - 3. Feed solutions for the nanofiltration and reverse osmosis processes

3.2.3.2. Bench-scale NF/RO systems

The NF and RO experiments were conducted using a bench-scale crossflow RO membrane cell. The pure water permeability and rejection properties of all the membranes were tested in the same unit. A schematic diagram and a photo of the experimental setup is shown in Figure 3-4. The membrane effective area was $2.002 \times 10^{-3} \text{ m}^2$, similar to the FO cell described in Section 3.2.3.1. The crossflow rates were maintained at 400 mL/min and the initial volume of the FS was 5.0 L. Both the permeate and retentate were recycled back to the feed tank. All experiments were conducted at room temperature ($25 \pm 0.5 \text{ }^\circ\text{C}$). Fresh NF and RO membranes were compacted for 1 hr at 40 bar prior to each experiment. During the measurement of the permeate flux, permeate water volume of 100 mL was collected and the time of collection was measured concurrently. Therefore, the water flux J_w (in $\text{Lm}^{-2}\text{h}^{-1}$) in the NF/RO process was calculated using the following relationship:

$$J_w = \frac{\text{Volume of permeate water collected (L)}}{\text{Time (t)} \times \text{Membrane area (m}^2\text{)}} \quad (3-2)$$

The salt rejection (R, %) of the NF/RO membranes in the NF/RO operation was determined by measuring the electrical conductivity (EC, $\mu\text{S/cm}$) of the feed and the permeate. The relationship is shown as follows:

$$R (\%) = \left(1 - \frac{C_p}{C_0}\right) \times 100 \quad (3-3)$$

where C_p and C_0 are the permeate and initial feed concentrations, respectively. The measured electrical conductivity for both solutions was converted to the molar concentration. It has to be noted here when real salt water or wastewater was used as the FS, the rejection of individual ions was determined by analyzing the collected samples using inductively coupled plasma–mass spectrometry or ICP-MS (Perkin Elmer Elan DRC-e).

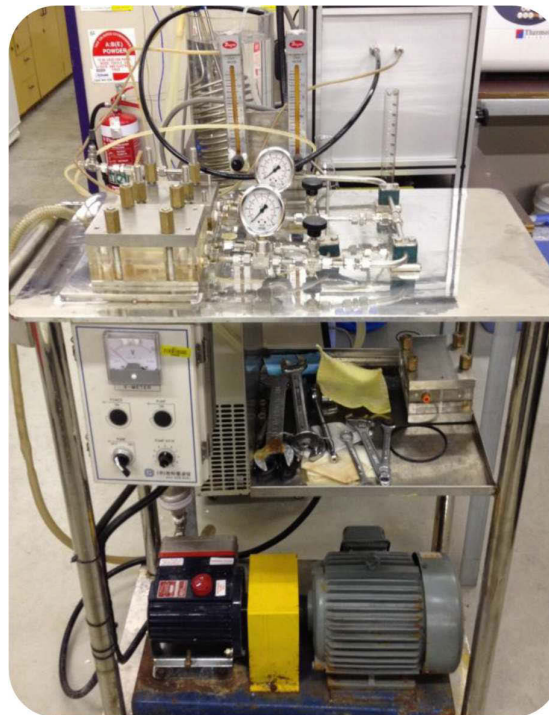
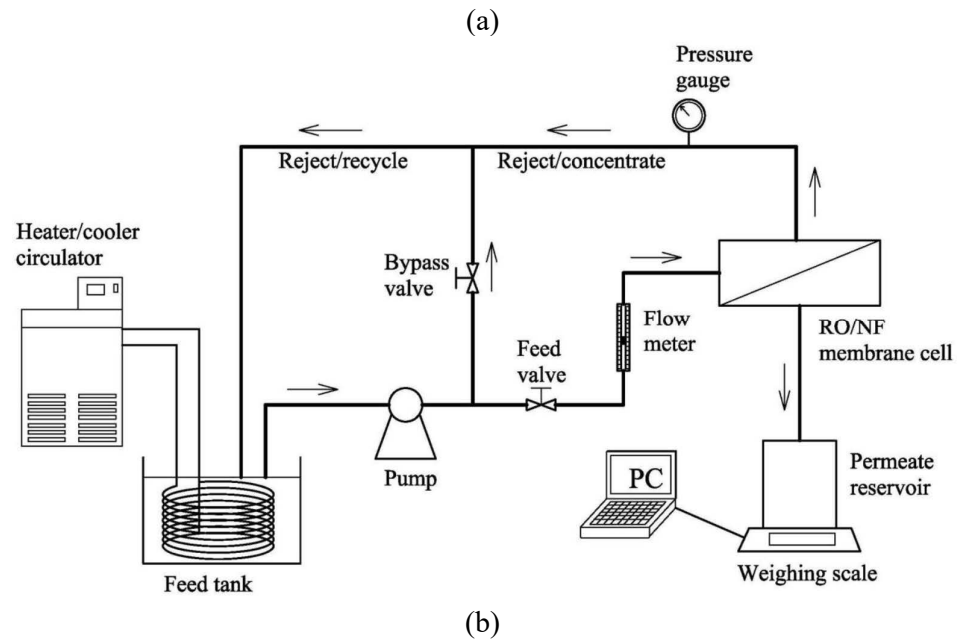
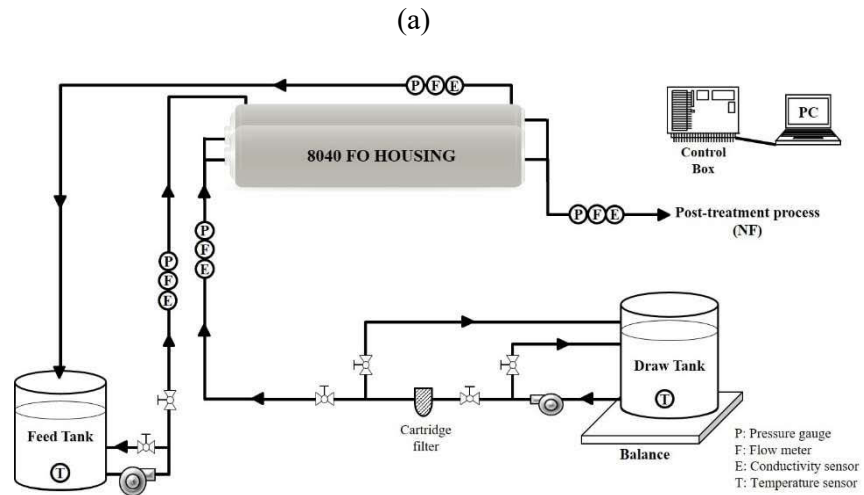


Figure 3 - 4. Bench-scale pressure based membrane processes experimental setup. (a) Schematic drawing of the bench scale NF/RO unit and (b) a photo of bench-scale NF/RO unit

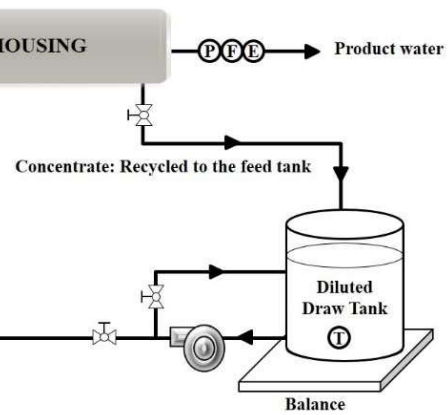
3.2.3.3. Pilot-scale FO with NF experimental set-up

In the FO process, two spiral wound FO membrane modules, which have been described in Section 3.2.2, were loaded in a membrane housing. The schematic diagram of the pilot-scale of the FO and NF hybrid process is shown in Figure 3-5 (a). The water flux across the membrane in the FO process was measured by the change in the weight of the DS tank. The weight change was recorded continuously by connecting a digital mass scale to a data acquisition computer. The temperature of both feed and draw solutions was collected automatically using the temperature sensors. The electrical conductivity of the feed and draw solutions was observed in the FO process. The initial volume of the feed solution was 5,000 L for the FO test conducted in the field and 1,000 L for the FO test conducted at the laboratory at UTS while that of the draw solution was 100 L. The volume of the DS tank for the field test was 5,000 L and that for the laboratory test was 1,000 L. The draw solution was diluted by the addition of fresh water extracted from the FS during the operation of the FO process and thus this was treated in the NF process. The experiments were conducted in a batch mode. The feed solution became concentrated and was recirculated to the pre-treated FS tank. Water flux was calculated using the Eq. (3-1).

Figure 3-5 (b) shows the pilot-scale NF unit in which NF was used as a post-treatment process. The NF process consists of a 4040 membrane module connected to the high pressure pump. The effective membrane area is 7.9 m² and the feed flow rate varies from 0.5 to 1.5 m³/h. The feed pressure can be applied up to 40 bar and the operation pressure was 25 bar. In addition, pure water permeability was tested with different applied pressure (10, 15, 20, and 25 bar). The pilot-scale NF process was evaluated as an option for an FO process to achieve a suitable nutrient concentration in the final product water. The concentrated feed water and the permeate water were recirculated and reused during the pilot-scale NF operation. The permeate water flux J_w (Lm⁻² h⁻¹) was calculated using the Eq. (3-2). The salt rejection of the pressure driven NF membrane was calculated by measuring the electrical conductivity of the feed and permeate (mS/cm) and used the Eq. (3-3).



(b)



(c)



Figure 3 - 5. A schematic diagram of (a) FO process, (b) NF process and (c) a photo of pilot-scale FDFO-NF hybrid system installed at University of Technology Sydney (UTS)

3.3. Analytical methods for the solution samples

3.3.1. Speciation and osmotic pressure of the solutions used

Solution properties, particularly osmotic pressure, dynamic viscosity, density and diffusion coefficient were calculated using the software, Stream Analyzer 9.5 (OLI systems Inc., Morris Plains, NJ, US). This software provides the properties of solutions using a thermodynamic modelling based on published experimental data (McCutcheon et al., 2006).

3.3.2. Determination of the reverse diffusion of draw solutes

The polymeric membrane is not a perfect membrane because it cannot completely reject the solutes, and the solute can therefore transfer from one side to the other side of the membrane (Hancock and Cath, 2009; Phillip et al., 2010; Hancock et al., 2011). The performance of the FO process was also evaluated in terms of reverse solute flux (RSF). The term ‘RSF’ has been commonly used because the diffusion of draw solutes occurs in reverse direction to the water flux, simultaneously. Evaluating the RSF in the FO process is important because it indicates the loss of draw solutes and increases replenishment costs (i.e. operational cost) (Hancock and Cath, 2009). The solute flux of an individual solute (J_s) through any semipermeable membrane is subjected by concentration difference between the two solutions and is commonly described using Fick’s law (Mallevalle et al., 1996).

From our previous investigation, it was found that reverse solute concentration at the feed side was significantly lower than the draw solution concentration used initially. For the dilute solution, the molar concentrations indicated a very good correlation with the electrical conductivity (EC) for all the selected draw solutions, and RSF was therefore monitored using EC as an indicator. When a single compound was used, the RSF was monitored by recording the EC of the DI feed online using a multimeter (CP-500L, ISTEK) with separate probes attached and connected to a computer for data logging. When real impaired water was used as the FS, the RSF was measured by collecting and analyzing the feed water samples at the end of each experiment. Samples were analyzed using inductively coupled plasma–mass spectrometry or ICP-MS

(Perkin Elmer Elan DRC-e at Southern Cross University, Australia). The reverse diffusion of draw solutes towards the feed is measured in terms of RSF and specific reverse solute flux (SRSF). The RSF J_s (in $\text{mmol m}^{-2}\text{h}^{-1}$) was measured using the following relationship:

$$J_s = \frac{(\text{Initial feed volume} - \Delta V) \times C_s \times 1000}{M_w \left(\frac{\text{mol}}{\text{kg}} \right) \times \text{Membrane Area (m}^2) \times \text{Time (h)}} \quad (3-4)$$

where ΔV is the total volume of water that flows to the DS from the FS during a certain operation time (h) of the FO process and C_s is the concentration of the draw solutes in the FS tank at the end of the experiment. The RSF in Eq. (3-4) is therefore a measure of the rate of draw solute lost through reverse diffusion or permeation per unit area of membrane per unit time. Specific reverse solute flux (SRSF), which is a ratio of RSF ($\text{gm}^{-2}\text{h}^{-1}$) to water flux ($\text{Lm}^{-2}\text{h}^{-1}$), has been used to indicate the amount of draw solutes lost by reverse diffusion per unit volume of water extracted from the FS (Hancock and Cath, 2009; Phillip et al., 2010) as follows:

$$SRSF = \frac{J_s (\text{gm}^{-2}\text{h}^{-1})}{J_w (\text{Lm}^{-2}\text{h}^{-1})} \quad (3-5)$$

3.3.3. Total organic carbon (TOC)

The total organic carbon of samples of the feed side collected during the backwashing (Chapter 6) was measured using a TOC analyzer (SGE Anatoc TOC II Analyser).

3.3.4. Ion chromatography

Water quality can be analyzed using ion chromatography. Cations such as Ca^{2+} , Na^+ and NH_4^+ , and anions such as NO_2^- , NO_3^- , PO_4^{3-} , Cl^- and SO_4^{2-} , in the feed, diluted draw fertiliser solutions and NF permeates, were measured in accordance to the APHA Standard Methods, using a Perkin Elmer Elan DRC-e Inductively Coupled Plasma Mass Spectrometer.

CHAPTER 4

HYBRID FORWARD OSMOSIS AND NANOFILTRATION SYSTEM: PILOT-SCALE DESALINATION OF MINE IMPAIRED WATER FOR FERTIGATION

This chapter was published as: Phuntsho, S.; **Kim, J. E.**; Hong, S.; Ghaffour, N.; Leiknes, T.; Choi, J. Y.; Shon, H. K., A closed-loop forward osmosis-nanofiltration hybrid system: Understanding process implications through full-scale simulation. *Desalination* **2017**, *421*,169-178.

4.1. Introduction

In this chapter, the concept of fertiliser driven forward osmosis (FDFO) desalination, in which salt water is converted into nutrient rich water for irrigation using a fertiliser solution as DS, this FO process intends to avoid the issue of DS separation and recovery system (Moody & Kessler, 1976; Phuntsho et al., 2011; Phuntsho et al., 2012b). Fertiliser is required for the growth of crops/plants and the diluted fertilizer DS can thus be directly used for irrigation (referred to as fertigation). The diluted fertilizer concentration however must meet the nutrition standards for direct fertigation and this has been found challenging. The final fertilizer concentrations of the diluted DS are limited by the total dissolved solids (TDS) or osmotic pressure of the feed water based on the principle of osmotic equilibrium between the DS and the FS (Phuntsho et al., 2014a). Some of the options to reduce fertilizer concentrations include direct dilution by mixing with the existing fresh water sources, using blended fertilizer DS to reduce the concentration of individual nutrient and using nanofiltration (NF) as post-treatment process to remove the excess fertilizer concentrations (Phuntsho et al., 2013 a).

The FDFO process has so far mostly studied, mostly through lab-scale experiments except for a recent process optimization study using 8040 FO membrane module (Kim et al., 2014b; Kim & Park, 2011a). This chapter therefore reports a six-month field study of the hybrid FDFO-NF process at a pilot-scale level for the desalination of saline water produced during coal mining activities.

This chapter is an extension of the research article published by the author in Journal of Membrane Science (Phuntsho et al., 2016b).

4.2. Materials and Method

4.2.1. Location and source of saline water

The FDFO-NF pilot desalination system was operated at Newstan Colliery (Centennial Coal Pty. Ltd), State of New South Wales (NSW), Australia (Figure 4-1). The saline water used for the pilot-scale FDFO-NF study was obtained directly from a newly built water treatment plant (WTP) (15 ML/day capacity) which treats the mine ground water. The

WTP process consists of a screen mesh, coagulation/flocculation process followed by a lamella clarifier and multi-media filter, before finally being discharged to the LT Creek.

A typical characteristic of the treated coalmine water from the WTP are presented in Table 1. Water samples from the WTP were collected at the start (12 samples for all short and long-term experiments) and end (six samples for only long-term experiments) of each test operational cycle. The composition of the water samples analyzed as per the APHA standards (APHA, 2005) is presented in Table 4-1. The TDS of the saline ground water, measured as 1,277 (± 45) mg/L is around electrical conductivity (EC) 2.37 (± 0.07) mS/cm. This is acceptable for irrigation water as much higher salinity has been used for some plants, e.g. strawberry tree (3-4 mS/cm), cherry plum (4-8 mS/cm) and brush cherry (>8 mS/cm) (Phocaidis, 2007). Although already at a lower salinity, the FDFO operation was able to produce a diluted DS with lower fertiliser concentrations, however, using a low salinity feed water does not justify using two different processes (i.e. FDFO and NF) and hence the pilot-scale FDFO-NF system was tested in the field with a higher salinity water sources. The normal saline water was therefore first concentrated using an FO process with 1.5 M MgSO_4 as DS with 50% total recovery rate to raise the saline feed water to about EC 5.4 (± 0.5) mS/cm or TDS 2,491 (± 85) mg/L) for pilot testing. The characteristics of the concentrated feed used for the FDFO process is presented in Table 4-1 along with the normal saline water from the WTP.



Figure 4 - 1. Location of the pilot-scale FDFO-NF desalination testing site at the Centennial Coalmine site under the State of NSW, Australia (Newstan Colliery, Miller Rd, Fassifern NSW 2283).

Table 4 - 1. Characteristics of the saline water from a water treatment plant show for one typical sample (1st long-term operation cycle) together with the standard deviation of twelve collected samples presented in the brackets.

| Composition | Normal saline water from the WTP | Feed water used for the FDFO operations |
|--|---|--|
| pH | 7.50(±0.26) | 7.8(±0.30) |
| EC (mS/cm) | 2.37(±0.07) | 5.4(±0.50) |
| TDS (mg/L) | 1,277(±45) | 2,491(±85) |
| Dissolved organic carbon | 1.2(±0.2) | 2.1(±0.53) |
| Turbidity (NTU) | 0.85(±0.15) | 1.0(±0.15) |
| Orthophosphate (mg/L P) | <0.006 | <0.009 |
| Nitrate (mg/L N) | <0.005 | <0.005 |
| Nitrite (mg/L N) | N/D | N/D |
| Ammonia (mg/L N) | 12.3(±1.7) | 12.0(±4.0) |
| Sodium (mg/L) | 470(±18.4) | 812(±67) |
| Potassium (mg/L) | 4.0(±0.3) | 7.0(±1.1) |
| Calcium (mg/L) | 30.1(±1.9) | 48.0(±3.8) |
| Magnesium (mg/L) | 9.0(±0.82) | 22.0(±2.1) |
| SAR | 19.5(±4.0) | 24.5(±3.4) |
| Chloride (mg/L) | 510(±154) | 983(±26) |
| Sulphate (mg/L SO ₄ ²⁻) | 241(±42) | 607(±27) |
| Aluminium (mg/L) | <0.2 | 0.023 |
| Arsenic (mg/L) | <0.002 | 0.001 |
| Cadmium (mg/L) | <0.001 | 0.000 |
| Chromium (mg/L) | 0.002 | 0.000 |
| Copper (mg/L) | 0.001 | 0.043 |
| Iron (mg/L) | 0.069 | 0.014 |
| Manganese (mg/L) | 0.002 | 0.010 |
| Nickel (mg/L) | 0.008 | 0.022 |
| Lead (mg/L) | <0.001 | 0.001 |
| Zinc (mg/L) | 0.035 | 0.189 |

4.2.2. Fertiliser draw solution

In this pilot-scale study, sulphate of ammonia (SOA) or (NH₄)₂SO₄ was selected as the fertilizer DS for two main reasons. Firstly, SOA being a divalent compound, its rejection by the NF membrane is much higher than a monovalent DS (Phuntsho et al., 2013 a) while its performances under the FO process is comparable with other DS based on previous studies (Phuntsho et al., 2011; Phuntsho et al., 2012c).

The fertilizer DS was prepared by dissolving a technical grade (NH₄)₂SO₄ (supplied in 25 kg bag from Chem-Supply, Australia) in tap water at ambient temperature using a variable

speed mixer until all the salts were completely dissolved. The SOA solution appeared slightly murky in colour indicating the presence of impurities. In order to prevent membrane fouling on the support layer side of the FO membrane, the concentrated DS was first pre-filtered using a microfiltration (MF of 0.45 μm pore size) before use. Four different SOA DS concentrations were used in this study: 0.5 M for baseline flux and 0.95 M, 1.89 M and 2.84 M for FDFO performance testing. All long-term FDFO operations were conducted using an SOA DS concentration of 1.89 M (i.e. 2 bags SOA for 200 L DS). The resulting osmotic pressure as a function of SOA concentration are presented elsewhere (Phuntsho et al., 2011; Phuntsho et al., 2012b). The SOA generates an osmotic pressure of 23.6, 43.9, 87.0 and 131.5 atm at 0.5 M, 0.95 M, 1.89 M and 2.84 M, respectively calculated using the thermodynamic modelling software OLI Stream Analyser (Version 9.1 OLI System Inc. Morris Plains, NJ).

4.2.3. Operation of pilot-scale FDFO-NF desalination system

A schematic layout of the pilot-scale FDFO-NF system is presented in Figure 4-2 (or Figure 3.2.3.3). The pilot system was made up of the FO process containing spiral wound 8040 cellulose triacetate (CTA) FO membrane modules (each module containing 1 element) connected in parallel with a total membrane area of 20.2 m^2 (Hydration Technology Innovations, Albany, OR). The NF process consisted of one 4040 spiral wound polyamide thin film composite (TFC) NF membrane module with a membrane area of 7.9 m^2 (NE90 CSM membranes, Woongjin Chemicals, now Toray Chemicals, Korea). The system was not fully optimized in terms of its capacity, consequently, each process had to be operated as a batch process and not as a continuous process. Both the diluted DS and feed concentrate from their respective outlets were therefore recycled back to their respective tanks during the batch operation mode. The volumes of the DS in the DS tank therefore gradually increased while its concentration, and hence the driving force, gradually decreased with operation time. The feed concentrate from the FO module outlet was also recycled back to the FS tank. The volume of the FS tank, however was maintained the same (5,000 L) by filling the FS tank with incoming normal saline water from the WTP using a float valve installed at the inlet of the FS tank. In this way, the concentration of the FS also increased slightly with operation time. The long-term batch operation of the FDFO process continued on till the DS tank (5,000 L) was full with the

diluted DS, taking about 7 days. During the process optimization study, however, each batch of the FDFO process was operated for about 6 hr duration.

The final diluted fertilizer DS, after the FDFO batch process, was then processed by the NF membrane, (operated in the batch mode) at a constant operating pressure of 25 bar. The reject/concentrate from the NF was recycled back to the NF feed tank while the NF permeate was stored in a separate tank. In this mode of operation, the fertilizer solution in the NF feed tank (earlier diluted DS tank) increased with the NF operation time.

Flow meters, pressure gauges and EC meters were installed at both the inlet and outlet points of the FDFO and NF processes, with all devices connected to a PC for online data acquisition. EC was used as a surrogate for the FS or DS concentrations at the module inlet/outlet points. The pilot system was not built with a full SCADA system for remote monitoring and control, however, the FO process was operated continuously for several days with visual monitoring was conducted through live video feed. The NF was only operated during the daytime. The water flux for the FDFO process was calculated based on the flow meter reading between the DS outlet and inlet while for the NF process, the flux for the NF process was obtained directly from the NF permeate flow meter readings. All the pilot plant operations were conducted at ambient temperature, without any external control on the environment, between March and August 2014. Although the ambient air temperature varied considerably with the average daily minimum and maximum temperatures of 15.8°C and 26.5°C (March), 13.0°C and 24.0°C (April), 9.0°C and 22.6°C (May), 7.7°C and 19.5°C (June), 4.2°C and 18.8°C (July) and 6.1°C and 18.3°C (August), respectively, (BOM, 2015) of the DS and FS tanks temperatures remained fairly constant (23 - 24°C). This is probably due to heating from the pumps. A fresh SOA DS was used for each operational cycle.

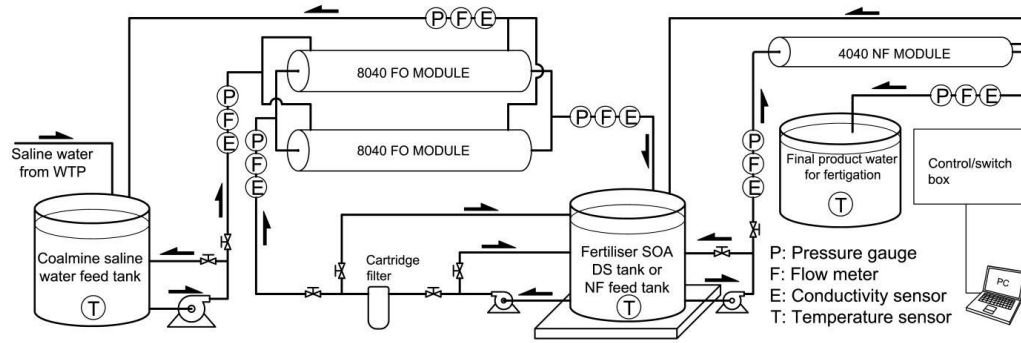


Figure 4-2. Schematic diagram of the FDFO-NF desalination system used for pilot-scale testing in the field.

4.2.4. Water quality monitoring and the test fertigation

Water quality was analyzed according to the APHA standards (APHA, 2005). A Perkin Elmer Elan DRC-e Inductively Coupled Plasma Mass Spectrometer was used for element analysis, similar to our earlier studies (Phuntsho et al., 2013 a; Phuntsho et al., 2013a). Water quality was also assessed in terms of sodium absorption ratio (SAR) values, measuring the relative concentrations of Na^+ to Ca^{2+} and Mg^{2+} ions in the water (Phocaides, 2007). The calculation of SAR values are described elsewhere (ANZ-ECC & ARMCANZ, 2000; Phocaides, 2007). Irrigation water with high SAR values is known to cause sodicity (or sodium toxicity) and loss of soil structure thereby contributing to soil degrading and poor yield of the crops (Phocaides, 2007). Test fertigation was conducted on the turf farm located about 5 km from the pilot plant. Test fertigation was performed on a test bed measuring about 20 m x 10 m and fertigation was applied two to three times every week coinciding with the normal farm irrigation. The growth of turf grass (Buffalo species) in the adjacent field irrigated using their ordinary storm water was used as a control. The test bed was used as it is, without any modification to the normal grass in the farm.

Test fertigation was also performed on the potted tomato plants (Roma species) grown right near the pilot site. The tomato plants were obtained from one of the local plant nursery warehouses in Sydney. A total of 36 tomato plants were used for test fertigation and the plants were divided into 4 different experimental groups and irrigated using the different types of water for comparisons such as tap water, final product water from the

FDFO-NF desalination process and blended water. The growth and health of the plants were monitored throughout the test fertigation.

4.3. Results and discussion

4.3.1. Process optimization study

For the FDFO process optimization, only two major operating parameters were considered: initial DS concentrations and the feed flow rates. Data in Figure 4-3 show the variations of the water flux, cumulative volume of water extracted (ΣV), DS and FS conductivity with operation time during (i.e. batch mode operation where both the DS and FS were recycled back to their respective tanks). The gradual decrease in the water flux with operation time (shown in Figure 4-3 (a)) is because of the increase in the cumulative volume of the water extracted (ΣV) which in turn dilutes the DS in the DS tank thereby gradually losing the driving force with time. The initial water fluxes with 0.95 M, 1.89 M and 2.84 M SOA DS concentrations were 5.9, 7.5 and 8.8 $\text{Lm}^{-2}\text{h}^{-1}$, respectively. These water fluxes are slightly non-linear with the DS concentrations consistent with many previous lab-scale studies because of the enhanced dilutive internal concentration polarisation (ICP) effects when operated at higher water fluxes (Garcia-Castello et al., 2009; Kim & Park, 2011a; Lay et al., 2012; Phuntsho et al., 2013a).

Figure 4-3 (b) shows the EC variations of the DS at the inlet and the outlet of the FO module with operating time. The DS concentration difference (driving force) between the inlet and outlet is much higher at the beginning, indicating the higher DS dilution factor (i.e. ratio of DS concentrations at the inlet to the outlet) achieved within the module during the initial stages of operation. However, the DS dilution factor at the module outlet decreases gradually with operation time due to cumulative loss of the driving force (cumulative DS dilution in the batch process) and hence the water flux with time. Although the DS dilution factor at the module outlet increases at higher inlet DS concentration, this corresponds to higher diluted DS concentration level at the outlet, as evident from the EC of the diluted DS between 1.89 M and 2.85 M. This indicates that when higher DS concentrations are used, it may require more membrane area (or membrane elements) in series to reach the desirable DS dilution (up to osmotic equilibrium concentration) within a single stage FO process (Phuntsho et al., 2014a).

Figure 4-3 (c) shows the variations of the FS EC at the inlet/outlet and the feed recovery rates with operation time for the FO module. The feed recovery rates of a single 8040 FO module were 4.2% at 2.84 M SOA DS concentration, reducing to 2.6% at 0.95 M SOA DS concentration. The feed recovery rate also decreased with time due to the loss of driving force and hence the water flux. The feed recovery rates are comparatively lower than the rated feed recovery rates of a single 8040 RO element (BW30-440i, membrane area of 41 m², recovery rates of 15% at an applied pressure of 15 bar) using a feed water of 2,000 mg/L NaCl (DOW, 2014). Feed recovery rates for the FO module could be increased by using higher initial DS concentration (driving force), however, this also results in higher concentration level of the diluted DS that comes out of the module (ref Figure 4-3 (b) as discussed earlier, which is not desirable. Several factors might contribute towards the lower feed recovery rates of the CTA 8040 FO element. One of the reasons could be due to the comparatively higher cross flow rate differences between the FS (6.0 m³h⁻¹) and FS (0.6 m³h⁻¹) as recommended by the manufacturer for the module operation to maintain a suitable pressure differential between the inlet and out of the module. The other reason could be due to the low packing density of the CTA 8040 FO element (10.1 m²) compared to RO membranes of similar size (41 m², Filmtec DOW™ Chemicals) and lower permeability, and hence lower water flux of the CTA FO membrane compared to TFC RO membrane.

The influence of feed flow rates on the performance of the FDFO process is presented in Figure 4-3(d) at different flow rates of 3.0, 4.2 and 6.0 m³h⁻¹. It is evident from these results that, no significant increase in the water flux was observed when the FDFO pilot-scale unit was operated at higher feed flow rates. This is possibly due to the very low feed recovery rates (2.6-4.2%) at which the FO modules were operated. Therefore, all the subsequent long-term experiments were conducted at a feed flow rate of 4.2 m³h⁻¹ as it provided a reasonable pressure differential between the different inlets and outlets of the module, as recommended by the manufacturer.

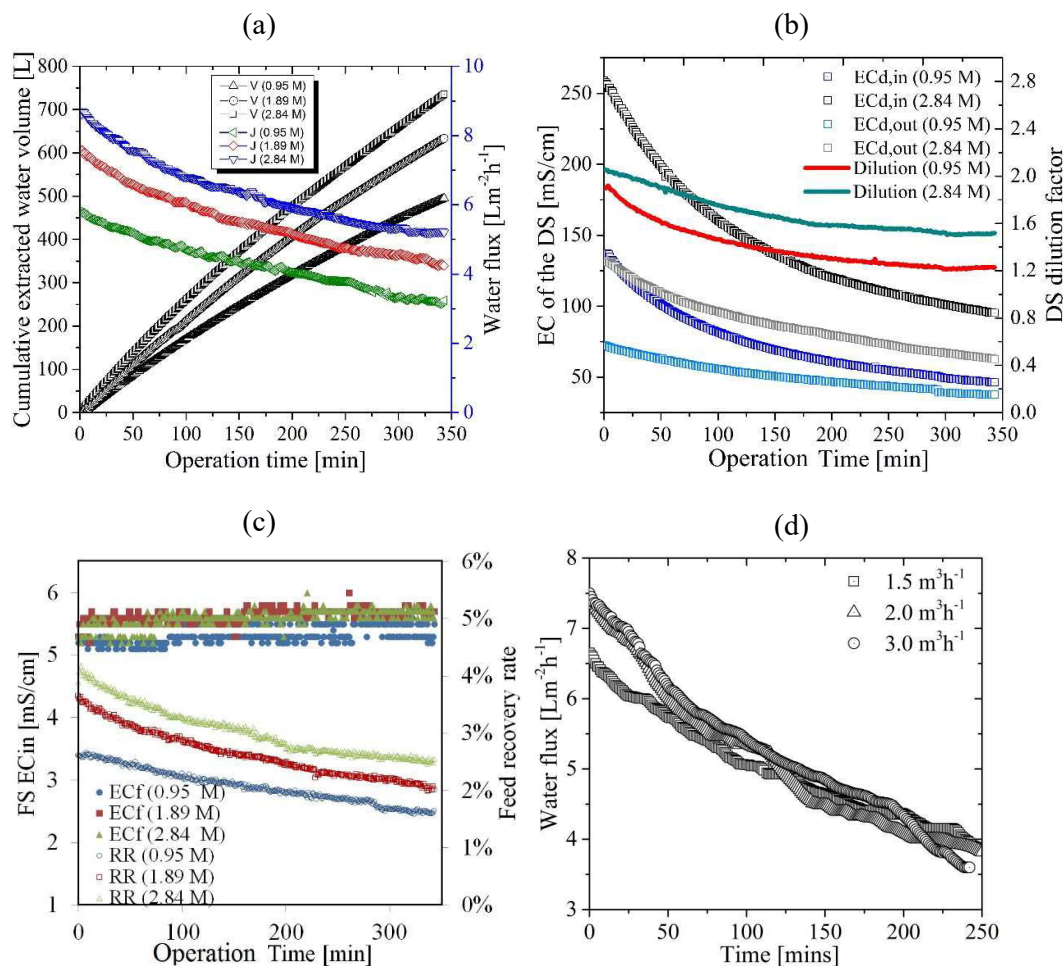


Figure 4 - 3. Variations of the performance parameters during the FDFO pilot unit process optimization process. (a) Water flux and cumulative extracted volume with time, (b) DS concentrations or EC at the inlet/outlet and the dilution factor with time, (c) feed TDS or EC and feed recovery rates with time and (d) water flux under different feed flow rates. Initial DS and FS volumes are 200 L and 5,000 L respectively.

4.3.2. Long-term operation of the FDFO process

Based on the results in Figure 4-3, 1.89 M was selected for all the subsequent long-term operation of the pilot-plant system. Each batch of long-term FDFO operation initially started with 200 L of 1.89 M SOA as DS and at a constant volume (5,000 L) of saline feed water. At the end when the DS tank was full to 5,000 L, its final SOA DS concentration reached to around 0.075 M (4.0 atm), which is closer to the final FS TDS of 4,000 mg/L (3.0 atm). The minimum initial DS volume of 200 L was necessary to accommodate the DS within the dead volume of the pipes, fittings and pump. For the long-term performance, the pilot-scale FDFO process was operated for a total of six

cycles under a batch mode until the 5,000 L DS tank was fully filled, results presented in Figure 4-4.

The variations in water flux with operation time appear quite similar for all the six cycles, indicating a consistent performance of the FDFO process under each batch trial. A closer observation between each batch cycle in Figure 4-4 (a), however, shows that the water flux in the fourth cycle is significantly lower than water fluxes in the other cycles (i.e. the sharper flux decline). Figure 4-4 (b) presents the water flux as a function of cumulative volume, representing water flux under similar DS concentrations (driving force) with the change of the cumulative volume. The baseline water flux presented as a subset plot within Figure 4-4 (b) and conducted using 0.5 M SOA as DS and tap water as FS immediately after Cycle 4 (before cleaning) is much lower than the original baseline water flux, indicating that the CTA FO membrane was indeed fouled during the 4th cycle of operation. The reduction in the water flux observed in the 4th cycle was unexpected since the feed water used for the FDFO process had a similar turbidity of around 1.3 NTU (data not presented). However, it was observed that the turbidity of the feed water in the feed tank at the end of the 4th cycle had significantly increased from the initial 1.3 NTU to 6.5 NTU (data not presented). Significant algae growth inside the feed tank was observed, which is assumed to have been the main contributing factor for this sharp flux decline. The continuous recycling of feed water along with the reverse diffusion of ammonia nitrogen towards the feed tank from the SOA DS is assumed to have enhanced algal growth in the feed tank. Opening of the tank and exposure to the sun might also have promoted algae to grow in the tank. Algal growth is evident from the pictures of the water samples taken out from the tank, shown within Figure 4-4 (b). Since there was no cartridge pre-filter between the feed water tank and the FO membrane module, the algae particles could have contributed to the FO membrane flux decline. Although algae presence was evident in this cycle, flux decline due to biofouling cannot be ruled out entirely as the FDFO process had run for about 4 cycles without any cleaning. It is also therefore possible that biofouling may partly contribute towards the flux decline given the presence of dissolved organic matter in the FDFO feed of about 2.1 (± 0.53) mg/L (refer Table 4-1).

Before the subsequent cycles of FDFO operations, the FO membranes were subjected to hydraulic cleaning using clean tap water at feed flow rates of 6.0 m³h⁻¹ for about 60

minutes and the baseline flux was then determined again. The baseline fluxes presented within Figure 4-4 (b) indicate that hydraulic cleaning was almost able to fully recover the water flux and hence no chemical cleaning was required before the next cycle of operation. Even at the end of the 6th cycle, the water flux and also the baseline flux was still comparable to the earlier cycles, indicating that the FO membrane performed quite well without any significant fouling or scaling issues during the long-term operations. For the subsequent batches (cycles 5 and 6), the feed water in the tank containing algae was filtered by MF before the next cycle of long-term operation. In order to prevent the regrowth of algae in the feed tank, the feed tank was completely closed and housed inside the shed.

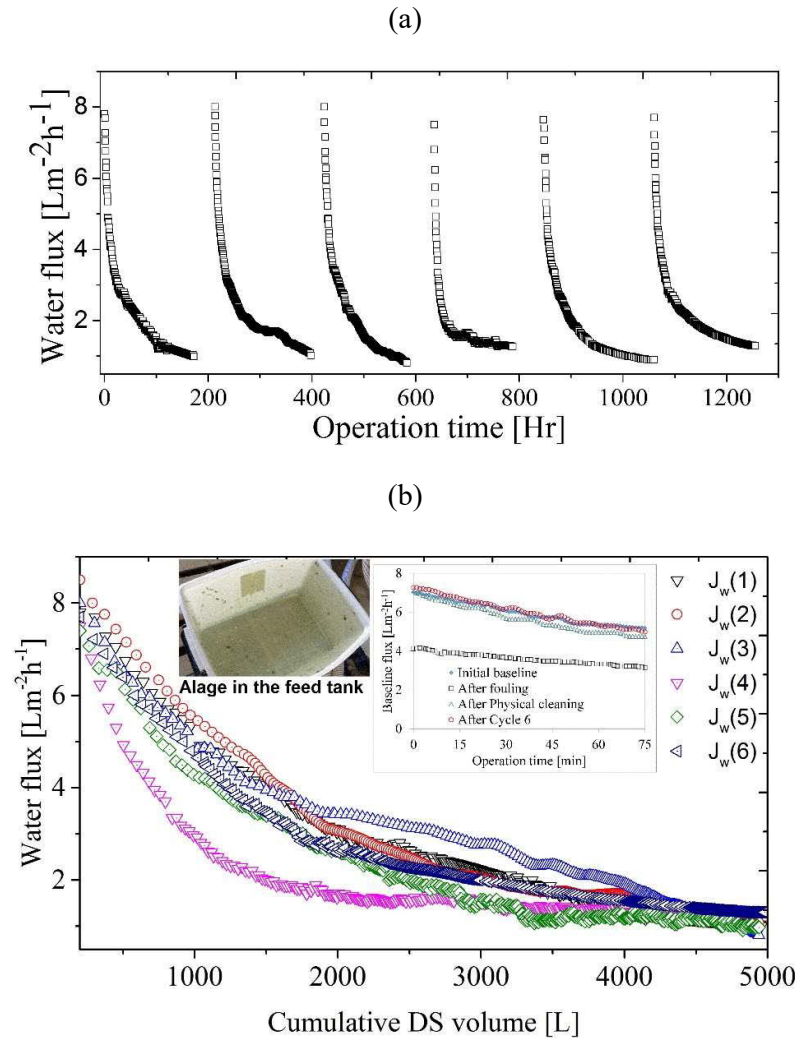


Figure 4 - 4. Performance of the FDFO desalination process on longer run cycles. (a) Variation of water flux with operation time and (b) the variation of water flux with the cumulative volume of water extracted during the batch operation process showing together the baseline fluxes before and after cleaning of the FO membrane and the picture showing algae growth in the feed water tank during the cycle 4 of the operation. Baseline fluxes were conducted using 0.5 M SOA as DS and tap water as FS at a feed crossflow rate of $4.2 \text{ m}^3\text{h}^{-1}$.

Table 4-2 shows the typical composition of the final diluted SOA fertilizer DS (cycle 1) along with their respective initial and final FS compositions. The final diluted fertilizer DS with an EC of $13.49 (\pm 1.5) \text{ mS/cm}$ or a TDS of $7,604 (\pm 845) \text{ mg/L}$ and NH_4^+ of $1,897 (\pm 143) \text{ mg/L}$ is too high for direct fertigation to the plants (Papadopoulos, 1999). Fertigation with high salinity water could decrease the biomass production of the plants due to lowering of plant water potentials and also cause specific ion toxicities and ion imbalances (Munns, 2002). Assuming a TN of 200 mg/L (Papadopoulos, 1999; Phuntsho

et al., 2012c) for certain plants as the maximum concentration limit, this diluted fertilizer DS would require additional dilution by a factor of about 10 which is a significant volume of additional fertigation water required. The excess fertilizer draw solutes would therefore require reduction or dilution before use. The NF process as therefore used as post-treatment for further reducing (or diluting) the fertilizer concentration.

The osmotic pressure of the final diluted fertilizer DS (estimated using ROSA) was 3.7 (± 0.41) bar against the initial feed osmotic pressure of 1.52 (0.05) bar. The osmotic pressure of the final diluted DS is expected to be higher than the initial feed osmotic pressure used in this study since the FDFO process was operated in a batch mode in which the TDS or the osmotic pressure of the feed continued to increase with time from 1.52 (± 0.05) bar (initially) to 2.85 (± 0.14) bar by the end of each batch operation. The osmotic pressure of the final diluted DS is still higher than the osmotic pressure of the final FS, indicating that the diluted DS concentration has not yet reached osmotic equilibrium with the feed osmotic pressure, and hence further dilution could have been possible if the FDFO process had been operated further. This osmotic pressure of the final diluted DS is 10-30% higher than the osmotic pressure of the final feed concentrate.

From Table 2, it is clear that the CTA FO membrane used in this study led to the significant transfer of ions across the membrane in both directions. Rejection of the individual feed ions was observed to be only between 80 and 98%, except for Na at 72%, indicating that the rest of the feed ions have diffused through the membrane towards the DS. This low rejection of the CTA FO membrane, especially monovalent ions such as Na^+ and Cl^- , could be a cause of concern, as these unwanted feed solutes are expected to eventually accumulate in the DS during the NF post-treatment process after repetitive cycles of recycling and reuse operations. A detailed discussion on this implication is included under Section 3.4.

Table 4-2 also presents the specific reverse solute flux (SRSF) of the SOA DS in terms of NH_4^+ and SO_4^{2-} concentrations. Although the term reverse solute flux or RSF (in $\text{gm}^{-2}\text{h}^{-1}$) is also commonly used to measure the rate of reverse diffusion (Wang et al., 2010a; Wang et al., 2015a; Wei et al., 2011c) of draw solutes in this study, SRSF has been used as this parameter relates to the quantitative measurement of the reverse diffusion of draw solutes towards the FS per unit volume of water extracted in the FO process (Hancock et

al., 2011a; Phillip et al., 2010; Phuntsho et al., 2013a). The RSF increases with the increase in the DS concentration, however, it has been observed that the SRSF (or the ratio of RSF ($\text{gm}^{-2}\text{h}^{-1}$) to the water flux ($\text{Lm}^{-2}\text{h}^{-1}$) is fairly constant for a particular draw solute (Phillip et al., 2010) and hence SRSF is used as one of the performance parameters in this study instead of RSF. The SRSF of the SOA DS was $105 (\pm 76)$ mg/L for NH_4^+ and $401 (\pm 85)$ mg/L for SO_4^{2-} as shown in Table 4-2. These SRSF values are slightly lower than the SRSF usually observed during lab-scale experiments in our earlier study (Phuntsho et al., 2012c). These results indicate that some amount of fertilizer DS could be lost towards the FS and cannot be recovered. Mass balance analysis of the NH_4^+ and SO_4^{2-} in the feed tank indicates that about 504 g of NH_4^+ and 1,925 g of SO_4^{2-} (total DS of 2,429 g) are lost by reverse diffusion towards the feed, which translates to 3.7% and 5.3% (total DS loss of 4.9%) of their initial mass in the fertiliser DS, respectively, during each cycle of batch operation. This also shows that, for every mole of SO_4^{2-} that reverse diffuse through the FO membrane, about 1.4 moles of NH_4 reverse diffuse instead of expected 2 moles of NH_4 based on their molar ratios in the $(\text{NH}_4)_2\text{SO}_4$ DS solution. To maintain ion balance on the DS side, ions such as Na^+ or Cl^- may cross the FO membrane towards the DS as indicated by the presence of Na^+ or Cl^- in the DS. This therefore likely enhances the feed solute flux through the membrane resulting in slightly lower rejection rates of Na^+ (72%) or Cl^- (81%) compared to the reported rejection of between 94-99% (McCutcheon et al., 2006b; Ren & McCutcheon, 2014).

The SAR values of the diluted DS in Table 2 increased to $42.0 (\pm 5.5)$ compared to $24.5 (\pm 3.4)$ in the initial feed water due to the high rejection of Ca^{2+} and Mg^{2+} ions compared to Na^+ ions by the FO membrane. The recommended SAR value is less than 6 although SAR values greater than 5 are considered as at the risk of adverse structural impacts associated with sodicity (Phocaidis, 2007). Hence, based on the SAR values from Table 4-2, it is clear that, the diluted fertilizer DS is not suitable for irrigation.

Table 4 - 2. Characteristics of the feed water and diluted DS before and after the FDFO experiments. The average feed rejection rates (R) for each ion were determined based on the average concentrations of each ion in the initial and final DS. The standard deviation of all the six samples is provided in the brackets). (FS_i: initial feed solution, FS_F: final feed solution, DS_F=final draw solution, R: feed rejection rate, SRSF: specific reverse solute flux). The osmotic pressure of the two types of saline feed water presented in Table 1 was calculated using the ROSA software (Version 9.1, Filmtec DOW™ Chemicals, USA).

| Parameters | FS _i | FS _F | DS _F | R (%) | SRSF (mg/L) |
|---|-----------------|-----------------|-----------------|------------|-------------|
| pH | 7.8(±0.30) | 8.0(±0.20) | 7.7(±0.06) | | |
| EC (mS/cm) | 5.4(±0.50) | 7.5(±0.8) | 13.49(±1.5) | | |
| Turbidity (NTU) | 1.00(±0.15) | 1.9(±0.2) | 0.25(±0.05) | | |
| NH ₄ (mg/L N) | 12(±4.0) | 113(±14) | 1897(±143) | | 105(±76) |
| Na (mg/L) | 812(±67) | 1425(±202) | 231(±40) | 72%(±3.5%) | |
| K (mg/L) | 7.0(±1.1) | 19(±7) | 1.2(±0.3) | 83%(±3.6%) | |
| Ca (mg/L) | 48.0(±3.8) | 58(±19) | 1.5(±0.5) | 97%(±1.0%) | |
| Mg (mg/L) | 22.0(±2.1) | 31(±3) | 0.5(±0.3) | 98%(±1.3%) | |
| Cl (mg/L) | 983(±26) | 1897(±595) | 185(±8.7) | 81%(±0.7%) | |
| SO ₄ (mg/L SO ₄ ²⁻) | 607(±27) | 992(±167) | 5288(±233) | | 401(±85) |
| SAR | 24.5 (±3.4) | 37.8 | 42.0(±5.5) | | |
| TDS (mg/L) | 2491(±85) | 4535(±220) | 7604(±845) | | |
| Osmotic pressure (bar) | 1.52(±0.05) | 2.85(±0.14) | 3.70(±0.41) | | |

4.3.3. Operation of the nanofiltration process

With a single 4040 NF element in the module, the maximum recovery rate for the NF module was only 20-25% when operated at a constant transmembrane pressure of 25 bar. Hence, the NF process was operated in a batch mode where the NF concentrate was recycled back to the NF feed tank. In this way, the concentration of the NF feed tank containing fertilizer solution increased constantly with time. Variations of the water flux and the permeate EC has therefore been plotted as a function of the feed concentration or EC at the module inlet instead of operation time.

Figure 4-5 shows the variations of the performance parameters such as specific permeate water flux, NF permeate EC and NF rejection rate as a function of the cumulative EC of the diluted fertilizer DS or the NF feed. The initial NF feed EC was 13.49 (±1.5) mS/cm as per the composition presented in Table 4-2. The lowest desirable final diluted DS concentration from the FDFO process should have an osmotic pressure of 1.52 atm, equal to the osmotic pressure of the initial saline feed water at the inlet. This equivalent

concentration for the DS has been estimated to be $\sim 7,000$ mg/L of SOA (EC of 11.9 mS/cm). Since the maximum volume of the DS tank was 5,000 L and the feed water TDS also slightly increased with time during the operation, the minimum final diluted DS concentration was 7,604 (± 845) mg/L with an osmotic pressure of 3.7 (± 0.41) bar, which is higher than the desired concentration. Hence, it must be understood here that the feed water for the NF post-treatment has an osmotic pressure twice as high as the saline feed water and will increase the energy requirement for the NF process post-treatment.

For each cycle, NF was operated until such time that the water flux was so low at 25 bar to be accurately measured by the permeate flow meter and this happened when the final diluted fertiliser DS or NF feed reached an EC of around 39-42 mS/cm, translating to a total or overall NF feed recovery rate of around 65-70%. The results in Figure 4-5(a) show that the water fluxes for the NF process did not vary significantly, even after six cycles of batch operations, indicating that the NF process performed quite consistently without having any membrane scaling and fouling. This is because the diluted fertilizer DS used as the NF feed is a high quality water, similar to RO treated water, except for the presence of SOA fertilizer solutes. The use of high quality FO treated feed water with very low or no fouling potential could be one of the major advantages since NF is the most energy intensive process in the FDFO-NF desalination system. Any organics and colloids or scaling ions such as Ca^{2+} and Mg^{2+} present in the saline feed water are expected to be almost fully removed during the FO process, as indicated by the water characteristics of the final diluted DS in Table 4-2. It is worth noting here that, during the entire NF operation, the membrane was never cleaned, indicating that cleaning costs of the NF process will also be significantly lower when used as post-treatment process in FDFO desalination.

Figure 4-5 (b) shows the variations of the permeate EC and NF rejection rate with the bulk cumulative EC of the NF feed water. The permeate EC is important as it is directly related to the quality of the product water for fertigation. The permeate EC increases with the increase in the bulk EC of the diluted fertilizer DS in the NF feed tank since the NF was operated in a batch mode, however, the NF rejection rate did not change significantly even at higher NF feed concentration with rejection rates above 96%. There was no significant difference or trend observed in the permeate EC between each NF cycle, Figure 4-5 (b), which is also supported by the similar fertilizer rejection rate of the NF

membrane after several cycles of operations. A typical composition of the NF permeate along with the STD are presented in Table 4-3 and this, in fact, represents a typical quality of the fertigation water produced from the FDFO-NF desalination system. The average EC of the final product water from the FDFO-NF system was about 810 (± 30) $\mu\text{S}/\text{cm}$, which is suitable for irrigation purpose. Table 4-3 provides the detail composition of the final product water from the FDFO-NF desalination system. The average $\text{NH}_4\text{-N}$ concentrations were observed to be 75 (± 15) mg/L , which is lower than the acceptable upper limit of 200 mg/L (Phocaides, 2007; Phuntsho et al., 2012c). The average SO_4^{2-} concentration observed was 165 (± 44) mg/L , which is also and deemed suitable for irrigation. SO_4^{2-} has no reported adverse impact on the soil or plants except for its contribution towards the salinity content, although too high concentration could reduce nitrate, phosphorous and molybdenum absorptivity of the plants (Ayers & Westcot, 1985).

In fact, all other ion concentrations were much lower than the maximum allowable limit for fertigation. Although a higher level of the essential ions such as Ca^{2+} and Mg^{2+} would be preferred, their concentrations dipped below 1.0 g/L (because of the high rejection of these divalent cations by the NF membrane). The low Na^+ concentrations in the final product water (average SAR value 4.0 (± 0.57)) was still lower and within the acceptable values of less than 6 for irrigation (Phocaides, 2007). Given the low permeate EC (Table 4-3) with the NE90 module it appears that even NF membranes as with lower rejection (such as NE70) could also be potentially used as post-treatment in the process, thereby reducing the energy costs as NF70 is expected to have much higher water flux than NE90 given its slightly larger pore size and higher water permeability.

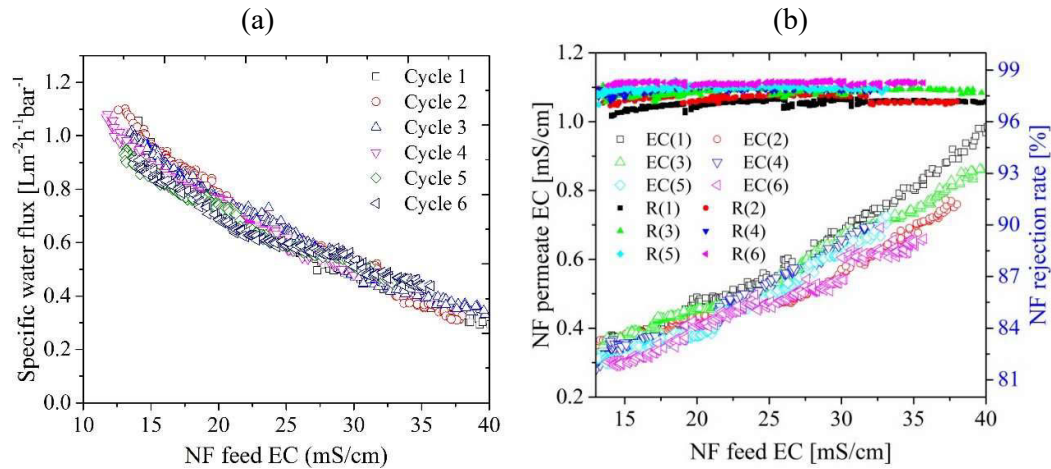


Figure 4 - 5. Performance of the NF process as post-treatment using the diluted fertilizer DS from the FDFO desalination process as NF feed water. Variations of the (a) specific NF permeate flux and (b) NF permeate electrical conductivity with the cumulative increase in the NF feed concentration (diluted fertilizer) during the batch NF operation process.

Table 4 - 3. Characteristics of NF permeate using diluted fertilizer DS as the feed. The standard deviation of all the six samples is provided in the brackets.

| Parameters | Initial NF Feed (DS_F) | P(aver) | NF Con. | R_{NF} (%) |
|------------------|----------------------------|-------------|--------------|--------------|
| pH | 7.7(0.06) | 8.15(0.15) | 8.1(0.17) | |
| EC (mS/cm) | 13.49(1.5) | 0.81(0.03) | 42.9(3.23) | 94.0%(0.2%) |
| Turbidity (NTU) | 0.25(0.05) | 0.1(0.1) | 0.8(0.1) | |
| Ammonia (mg/L N) | 1897(143) | 75(15) | 6,140(562) | 96.0%(0.8%) |
| Sodium (mg/L) | 231(40) | 10(1.1) | 752(63) | 95.7%(3.5%) |
| Potassium (mg/L) | 1.2(0.3) | 0.2(0.1) | 8.5(0.9) | 83.3%(6.9%) |
| Calcium (mg/L) | 1.5(0.5) | 0.15(0.05) | 5.0(1.4) | 90.0%(3.0%) |
| Magnesium (mg/L) | 0.5(0.3) | 0.2(0.07) | 2.0(0.9) | 60.0%(8.4%) |
| Chloride (mg/L) | 185(8.7) | 15(2.1) | 540.0(52.0) | 91.9%(1.0%) |
| SO_4^{2-} | 5288(233) | 165(44) | 17250(2019) | 96.9%(0.8%) |
| TDS | 7604 (845) | ~266 (10.5) | ~24700(8000) | 96.5%(1.5%) |
| SAR | 42.0(5.5) | 4.0(0.57) | 72.4(6.2) | |

4.3.4. Test fertigation of turf grass and potted tomato plants

The final FDFO-NF product water was tested for the fertigation of turf grass and the potted tomato plants. These test fertigation started in April 2014 using the product water from the first batch of the long-term operational cycle. A turf grass area of about 20 m x 10 m was allocated for the test fertigation. The fertigation water was delivered in the 1000 L synthetic tanks to the farm and irrigation was performed using a sprinkler and pump

connected to the tank. Test fertigation was conducted two to three times a week coinciding with the regular irrigation schedule of the turf grass. The quality of the grass was visually monitored by taking photographs of the grass in the test bed and the normal or control land.

The test fertigation was conducted for about four months. Visual comparison of the turf grass in the test bed with the control in Figure 4-6 showed no apparent difference in the health of the grass in terms of colour of the grass and the height of the grass. This indicates that the final product water from the FDFO-NF desalination system is suitable for fertigation of turf grass. A slight change in the grass colour from green during the initial stages of the irrigation to slightly yellowish green during the final stages of irrigation was observed as shown in Figure 4-6 but this was evident for grasses on both the test bed and the control bed. Since this change in colour appeared on the grasses on both the beds, the plant stress must have been caused due to the temperature stress from the cold winter season of June and July that coincided with the test fertigation. The chlorophyll concentration in the plant leaves may change as a response to altered plant physiological functions due to plant stress due to low temperature (Trenholm et al., 2000).

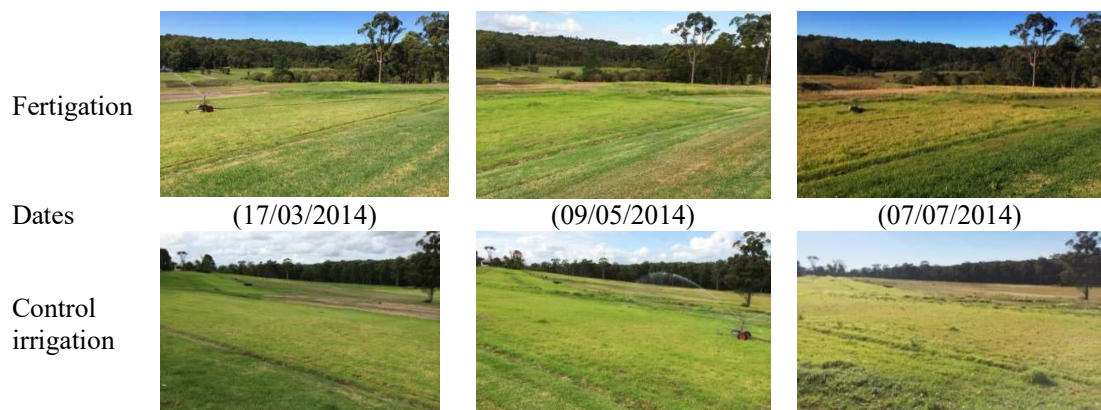


Figure 4 - 6. Visual monitoring of the turf grass during the entire period of the test fertigation at the Davos turf farm

For the test fertigation of the potted tomato plants, the potted plants were divided into four different water types of fertigation water and their compositions described in Table 4-4. The various stages of the growth of potted tomato plants during fertigation are presented in Figure 4-7. The tomato plant saplings (species named Roma and 36 plants in total) were obtained from one of the local plant nurseries at Sydney. The saplings were

then immediately transferred to larger pots as shown in Figure 4-7 containing potting mix (EasyWetta Garden Mulch, Bunnings Warehouse, Australia). Before the test irrigation started, the saplings were allowed to grow for certain days and the saplings were watered using Hunter tap water. Since the water for irrigation in this study did not contain all the essential elements required for the tomato plants, all the plants were therefore initially fed with commercially formulated mixed fertiliser grade (NPK 15.3 : 2.4 : 5.9) for tomato plants (Osmocote® Vegetable, Tomato, Herb & Garden Beds by Scotts Australia) as per the dose recommended by the manufacturer. Once the saplings were grown to a certain height, all the plants were then divided into 4 different groups (8 plants each) and then transferred to a much larger pot. Several plastic sticks were arranged to provide physical support to the plants. Irrigation was conducted two to three times a week except during the rainy weather. The plants were left outside exposed to the environment and no artificial environment was created for the growth of the plants. Each group of the plant was irrigated using the type of water for irrigation presented in Table 4-4.

Given the lack of expertise on the plant physiology, the monitoring of the plant was therefore limited to the physical appearance and also the final quantity of the fruits yielded. There was no significant difference observed between the four groups of plants in terms of the plant size and colour of the tomato fruits at the end of the test period. The only problem encountered was the testing period coincided with the cold winter season (May to July 2014) where the average day's minimum temperature varied from 3.8-14.5°C (May), 4.2-14.1°C (June), -1.5-10.7°C (July) and 0.3-12.7°C (August) (BOM, 2015) and hence the normal yield of the plant seems to have been affected by the cold winter climate. This was also evident from the stresses on the leaves and fruits which were falling off the plants before they could fully ripe irrespective of the types of water used for irrigation.

At the end, the number of fruits yielded by the plants was averaged and the results are presented in Table 4-4. The total tomato yields were 1.4, 1.3, 1.6 and 2.0 kg for tomato plants irrigated using water Types 1, 2, 3 and 4, respectively. There was no significant difference in the yield per plants observed between the four sets of plants irrigated using four different types of water. These results therefore indicate that, the product water from the FDFO-NF is suitable for fertigation of tomato plants. Blending of the FDFO-NF product water with the saline water in suitable proportions could help not only reduce the volume of water needed for desalination but at the same time provide additional nutrients

such as Ca and Mg which might have been rejected during the FO process thereby lowering the SAR values.

Table 4 - 4. Types of water used for test fertigation of crops. Hunter water was the tap water delivered to the pilot site in the water taker

| Code | Composition | Total yield of the plants |
|--------|--|---------------------------|
| Type 1 | Hunter tap water | 1.4 kg |
| Type 2 | NF permeate | 1.3 kg |
| Type 3 | NF permeate diluted 1:1 using tap water | 1.6 kg |
| Type 4 | NF permeate mixed with saline water in 80:20 | 2.0 kg |



Figure 4 - 7. Potted tomato plants at the various stages of the growth during test fertigation using four different types of test water

4.3.5. Implications of solute fluxes in a closed loop FDFO-NF system

Each long-term cycle for the FDFO desalination was operated at a total overall feed recovery rate of about 49% (4,800 L of water permeated from the FS towards the 5,000 L DS tank with the final concentrate volume of 5,000 L). For this overall feed recovery rate, the FDFO concentrate resulted in an NH_4^+ of 105 (± 76) mg/L and SO_4^{2-} of 401 (± 85) mg/L, which is expected to increase at higher recovery rates. Mass balance analysis of the feed and the reverse draw solutes indicate that the concentration of the lost draw solutes in the FO feed brine in a full-scale continuous FDFO operation would increase exponentially as $[\overline{\text{SRSF}} \times \overline{\text{RR}} / (1 - \overline{\text{RR}})]$ with the feed recovery rates ($\overline{\text{RR}}$) as presented in Figure 4-8 (a). This is because, as feed recovery rate increases, brine flow rate decreases but contain the same mass of the draw solutes that reverse diffuse through the membrane and this mass depends on the permeate flow rate and the SRSF. Therefore, a higher feed recovery rate in the FDFO process would likely mean higher concentrations of NH_4^+ and SO_4^{2-} draw solutes in the feed concentrate/brine, which could be a cause of concern not

only from the economic point of view but also for the environmental discharge of the concentrate containing $\text{NH}_4\text{-N}$ nutrient.

According to NSW EPA regulation, the allowable limit for the environmental discharge of TN from a sewage treatment plant is 10 mg/L (NSW-EPA, 2009) and hence, the FDFO concentrate/brine in this study (113 mg/L at 49% feed recovery rate) does not meet the water quality standard for environmental discharge to the creek. The presence of nitrogen in the feed concentrate will therefore be one of the major issues for concentrate management in the FDFO desalination process. The permissible environmental discharge limit for SO_4^{2-} at the coal mine site is 232 mg/L (Howat, 2013) and hence SO_4^{2-} too does not meet the environmental discharge standard. These results indicate that the CTA FO membrane used in this study is not suitable for the FDFO desalination and hence a better performing and high rejecting FO membrane may be essential for the actual FDFO desalination plants.

It is also important to understand the characteristics of the NF concentrate which is to be recycled back to the FDFO process for further reuse as the concentrated DS. The diluted DS (Table 4-2) contains other feed elements such as Na^+ (231±40 mg/L) and Cl^- (185±8.7 mg/L) and based on these results the FO membrane rejection rates were 95.7% (±3.5%) for Na and 92% (±1%) for Cl (average of 94% for Na and Cl added). Although the feed NaCl concentrations in the diluted DS (Tables 4-2 and 4-3) does not appear significant however, as these feed solutes are rejected by the NF membrane, their concentration increases in the NF concentrate to 752 (±63) mg/L for Na^+ and 540 (±52) mg/L for Cl^- in the batch process. As this NF concentrate containing Na^+/Cl^- concentration is recycled back and reused in the FDFO process infinite times, this could eventually build up Na^+ or Cl^- concentrations in the concentrated fertilizer DS.

Figure 4-8 (b) presents the expected increase in the feed Na and Cl concentrations with time in the concentrated DS under a full-scale continuous and closed loop FDFO-NF operation based on rejection rates of the FO membrane (Table 4-2) and NF membrane (Table 4-3). Simulation was performed assuming a plant capacity of 2,200 $\text{m}^3\text{day}^{-1}$, initial SOA DS concentrations of 60 g/L, SRSF of $\text{Na}+\text{Cl}=0.46$ g/L based on other study (She et al., 2012) and compared under three different combined scenarios of FO and NF membrane Na and Cl rejection rates. Based on a simple mass balance calculation within

the closed loop FDFO-NF system, Na and Cl accumulation can be calculated by the following relationship:

$$\text{Accumulation Rate (in g/s)} = \frac{C_{F,in} (1 - R_{FO})(1 + R_{NF} - RR_{NF}) Q_p}{2 - RR_{NF}} \quad (4-1)$$

where $C_{F,in}$ is the feed salt concentration (Na and Cl), R_{FO} is the feed salt rejection by FO membrane, R_{NF} is the feed salt rejection by NF membrane (in the diluted DS), RR_{NF} is the feed (diluted DS) recovery rate of the NF process, and Q_p is the plant capacity.

Based on the above mass balance relationship and for the above assumed plant capacity, the feed salt (Na and Cl) would accumulate at 16.35 gs^{-1} . It is clear from Figure 4-6(b) that after about 20 hours of continuous FDFO-NF operations, the Na and Cl concentration would reach about 68 g/L, which is more than 50% of the total solutes present in the concentrated DS. This will consequently increase the Na/Cl concentrations in the NF permeate (4.08 g/L Na+Cl at 94% NF rejection rate) undermining the irrigation water quality. These simulations took into consideration the NaCl bleeding from the closed system through NF permeate and the re-reverse diffusion of NaCl through the FO membrane towards the feed water. Hence, the accumulation of feed salt within the closed FDFO-NF system could be one of the significant challenges of recycling and reusing the fertilizer DS if a similar CTA FO membrane is used for full-scale FDFO-NF application. This problem, however, could be minimized by using high salt rejecting FO membranes such as polyamide based thin film composite FO membranes for the FDFO process to limit the passage or permeation of Na^+ and Cl^- to the diluted DS.

Figure 4-8 (b) also however shows that, using thin film composite TFC FO membrane (HTI) with comparable NaCl rejection (91.5%) but with lower SRSF (0.279 g/L) (Ren & McCutcheon, 2014) can slow down the NaCl salt build-up. The alternate approach is to use lower rejection NF membranes as presented for NF rejection (80%) that can enhance NaCl bleeding from the closed system thereby slowing down the salt build-up. However, NF permeate must also meet the fertigation standard in terms of salinity and the fertilizer concentration when such NF membranes are used. Theoretically, the salt build-up could be avoided only if the bleeding of NaCl from the system through NF permeation and re-reverse diffusion through the FO membrane is equal to permeation from the FO process.

These findings complement the study by Benavides et al. (2014) that the reverse flux selectivity or the ratio of the forward water flux to the reverse draw solute flux, is a key parameter in the design of FO systems.

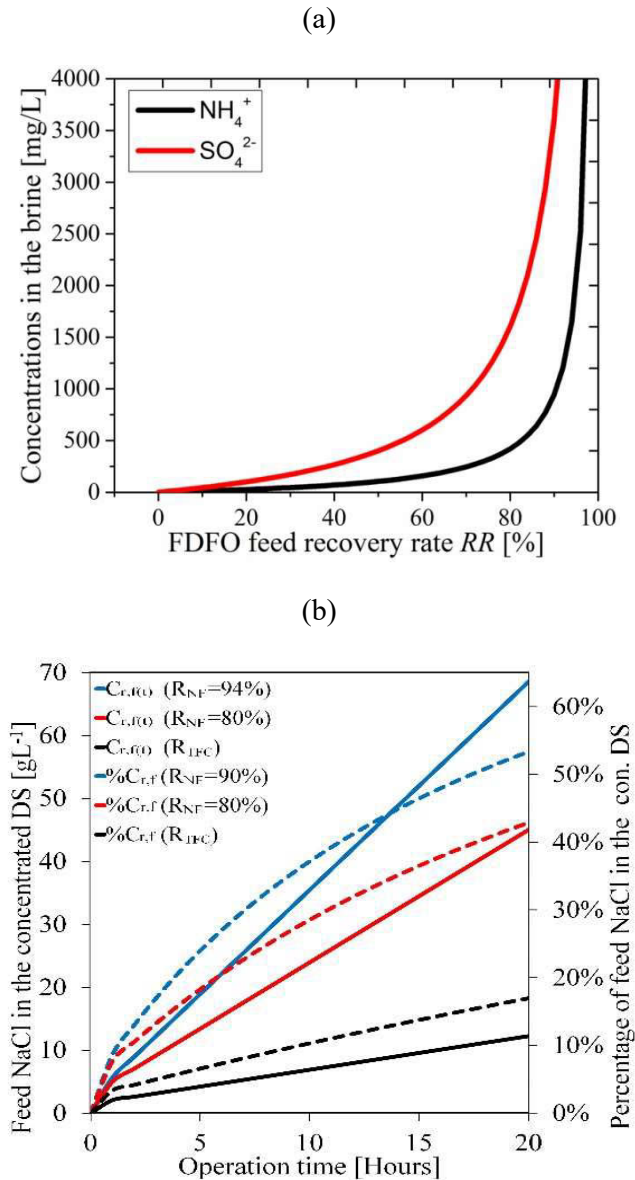


Figure 4 - 8. Implications of solutes transfer through the FO and NF membranes assessed based on the (a) expected variations of the draw solute concentrations in the FDFO feed concentrate/brine at different FDFO feed recovery rates where the NH_4^+ and SO_4^{2-} concentrations in the brine was calculated using the relationship $[\overline{SRSF} \times \overline{RR}/(1-\overline{RR})]$ (RR is the feed recovery rate) and (b) expected variations of the feed solute (NaCl) concentrations in the concentrated SOA DS under different FO and NF rejection rates. For simulation, NaCl feed rejection of CTA FO membrane at $R_{FO}=87.6\%$, SRSF of NaCl was assumed at 0.46 g/L (She et al., 2012), for $R_{FO}=90\%$, SRSF was assumed at 0.327 g/L (Ren & McCutcheon, 2014) and the NF feed recovery rate was assumed about 84% .

4.4. Concluding remarks

The following conclusions have been drawn from this particular study:

- The feed water quality could affect membrane fouling and the performance of the FDFO process, however, this study observed that hydraulic cleaning was adequate to almost fully recover the water flux under the conditions tested.
- Although the NF process could still consume energy, it is expected to perform efficiently without being significantly affected by membrane fouling or scaling issues as it receives an excellent feed water quality treated by the FDFO process.
- Using NF membrane with lower rejection and higher permeability could potentially save NF energy consumption while still meeting the water quality for fertigation.
- Test fertigation conducted on the turf grass and tomato plants using the final product water indicate that, the FDFO-NF desalination system can produce water quality suitable for the fertigation of crops.
- The high SRSF of NH_4^+ and SO_4^{2-} using CTA-FO membrane have failed to meet the standard for feed brine discharge which further increased at higher feed recovery rates, making brine management one of the biggest challenges of the FDFO system.
- Low feed rejection of the CTA FO membrane also could result in the build-up of feed salts such as Na^+ and Cl^- in the DS during repetitive recycling and reuse, eventually affecting the final water quality unless adequate bleeding from the closed FDFO-NF system occurs through NF permeate and also through re-reverse diffusion from the recycled and reused DS.
- This study demonstrates the significance of the need to have FO membranes with higher membrane reverse flux selectivity (e.g. polyamide based thin film composite membranes) for the FDFO-NF desalination technology to become a commercial reality.

CHAPTER 5

LIFE CYCLE ENVIRONMENTAL AND ECONOMIC IMPACTS OF FORWARD OSMOSIS AND NANOFILTRATION HYBRID SYSTEM

This chapter was published as: **Kim, J. E.**; Phuntsho, S.; Chekli, L.; Hong, S.; Ghaffour, N.; Leiknes, T.; Choi, J. Y.; Shon, H. K., Environmental and economic impacts of fertilizer drawn forward osmosis and nanofiltration hybrid system. *Desalination* **2017**, *416*, 76-85.

5.1. Introduction

Among several recent innovations in desalination technologies, forward osmosis (FO) has emerged as a promising candidate for various applications, including irrigation (Subramani et al., 2011). Fertilizer drawn forward osmosis (FDFO), which uses fertilizers as its draw solution (DS), has shown potentially lower additional energy consumption and the diluted DS, containing fertilizer nutrients, can be used as non-potable water for the irrigation of crops (Phuntsho et al., 2011). The pilot study was therefore carried out using a 1,000-4,000 L/d capacity fertilizer drawn forward osmosis and nanofiltration (FDFO-NF) desalination system at Centennial Coal's Newstan colliery in Fassifern, New South Wales for six months as described in Chapter 4. The pilot-scale FDFO-NF process was composed of two spiral wound FO membrane modules and one spiral wound NF membrane module. Flow rates, pressures, and electrical conductivity meters were installed at both the inlet and outlet of the membrane module. All the sensors were connected to a computer and thus collecting the data automatically. The study reported in Chapter 4 revealed that the technology was robust with the potential to produce nutrient rich irrigation water to support the surrounding farming industry. However, FDFO-NF hybrid desalination is a new technology and, therefore environmental and economic life cycle assessment (LCA) is essential to understand its comparative advantages with existing desalination technologies such as reverse osmosis (RO) hybrid systems.

The main scope of this work was, therefore, to conduct an environmental and economic LCA that compares the FDFO-NF hybrid system with two conventional RO hybrid systems in the desalination of mine impaired saline groundwater. It has to be acknowledged that for the economic life cycle assessment of the FDFO-NF hybrid process only operating expenditure (OPEX) was considered due to the system boundary limitation of the current LCA study. Conventional RO hybrid systems use microfiltration (MF) and ultrafiltration (UF) as a pre-treatment process and are termed here as MF-RO and UF-RO hybrid systems, respectively. To authors' knowledge, this work is the first to undertake a detailed environmental and economic analysis of the FDFO-NF hybrid process for irrigation through reuse of coal mine impaired water. This chapter is an extension of the research article published by the author in *Desalination* (Kim et al., 2017c).

5.2. Materials and Methods

The LCA framework used for this study is described elsewhere (Arvanitoyannis, 2008; Coday et al., 2015; Hancock et al., 2012). A standard LCA generally consists of four stages; goal and scope definitions, life cycle inventory analysis (LCI), life cycle impact assessment, and interpretation. The first three stages are briefly described in this section. The last stage, interpretation, is discussed in Section 5.3.

Three hybrid desalination systems were chosen for comparison: MF-RO, UF-RO, and FDFO-NF. FDFO-NF is further divided into two groups, namely FDFO-NF (CTA) which uses cellulose triacetate (CTA) membrane and FDFO-NF (TFC) which uses a thin film composite (TFC) membrane for the forward osmosis process. Figure 5-1 shows the system boundaries under which the LCA was carried out for the desalination of coal mine impaired water. It has to be acknowledged that the data obtained in our previous pilot-scale FDFO-NF hybrid system study was used as the basis for this LCA study. Nevertheless, there were some challenges to incorporate all the operating data for this LCA study. In fact, the main objective of the previous study was to prove technical feasibility of the FDFO-NF process including cleaning strategies for the desalination of saline water produced during coal mining activities. Therefore, the life cycle analysis of all the hybrid system was conducted by assuming and adopting full-scale operating conditions from the previous LCA studies (Biswas, 2009; Coday et al., 2015; Hancock et al., 2012; Shahabi et al., 2015; Valladares Linares et al., 2016). The details will be discussed in Section 5.2.3.

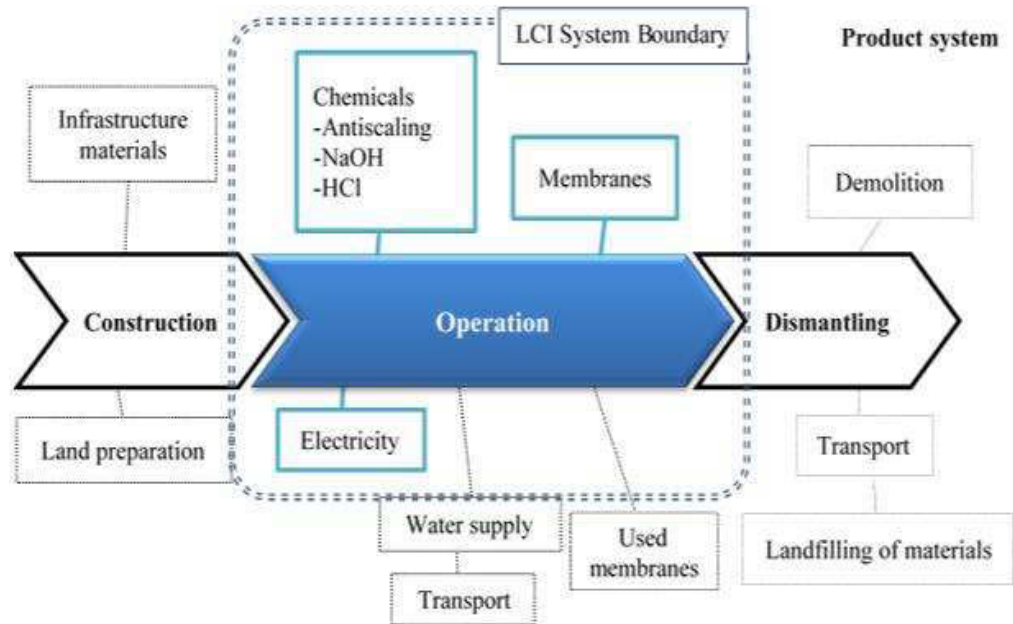


Figure 5 - 1. Boundaries of the coal mine impaired water desalination system for all hybrid systems – life cycle inventory (LCI) for environmental and economic impact assessment.

5.2.1.1. Life cycle inventory (LCI) analysis

To collect the primary data for each hybrid system, an inventory analysis was carried out using the Ecoinvent LCA database version 3.0 and the Australian LCA database, Simapro version 8.1 (Frischknecht et al., 2005; Grant et al., 2001; PRé-Consultants, 2008). Simapro LCA is one of the most widely used software tools. It includes impact assessment methods and several representative databases such as the Australian LCA database. Several common considerations for LCA for all hybrid systems are summarized as follows:

- In cases where no specific database for the production of materials and their quantities could be found in the Australian LCA database, information from the closest found database, Eco-invent, was used for the LCI.
- The types of materials used for MF, UF, NF and RO membranes applicable to this study and the total weight of materials for each membrane module were adopted from published literature (Bonton et al., 2012; Hancock et al., 2012; Tarnacki et al., 2012).
- One of the most challenging parts of the operation phase is simplifying the membrane manufacturing procedure, including the consumption and production of the specific

resources. All process data related to this procedure, including the covering membrane, spacer, membrane housing, collection tube, and glue, were available in previous studies (Coday et al., 2015; Hancock et al., 2012; Valladares Linares et al., 2016).

- The electricity production model is based on the Australian mix electricity data in the Simapro Australian LCI database. It consists of approximately 70% coal, 14% natural gas with remaining 16% derived from several sources, including renewable energy sources (Shahabi et al., 2015). The cost of electricity was calculated at AUD \$0.29/kWh in New South Wales, Australia (AEMC, 2013).
- The LCA in the chemical phase is based on previous studies which include the most commonly used cleaning chemicals and scale inhibitors for each membrane process (UF, MF, RO, FO and NF). However the chemical transport component has been excluded, since transportation conditions are the same in all cases (Zhou et al., 2014).
- It has to be noted that the feed water quality influences the fouling propensity. In this study, as shown in Table 5-1, the concentration of the feed water was assumed to be 2,491 mg/L total dissolved solids (\approx 2,500 mg/L TDS). Based on this feed water quality, the frequency of chemical cleaning for RO hybrid systems for this study was adopted from (Coday et al., 2015; Moch et al., 2008).
- Economic and environmental impacts of brine disposal may lead to different LCA results. However, as mentioned earlier, we conducted the pilot-scale FDFO-NF study at one of the coal mine site in Australia (Chapter 4). Since there is an available wastewater treatment plant (WTP) to treat mine impaired water, FO and RO brines as well as chemical cleaning wastewater can be directly transported to the WTP. For this reason, the current study did not consider the impacts of the brine and/or waste disposal on the LCA results.
- The issues on forward and reverse salt flux and thus accumulation of ammonia and feed water constituents in the feed and draw solutions, respectively, could have significant environmental and economic impacts. However, such issues were not considered in the current study as the scope of this study was first to evaluate comparative advantages of the FDFO-NF system, but the results obtained through the current study will be used as the basis for future comprehensive analyses.

- The construction and decommissioning phases of the plant were not accounted for this study due to its long life span, and given that similar conditions apply to all the three hybrid systems (Zhou et al., 2014).
- The water quality for all hybrid systems was assumed based on the characterization of feed, diluted fertilizer, and final product water as shown in Table 5-1, which was around 2,500 mg/L TDS, 7,600 mg/L TDS, and less than 1,000 mg/L TDS (irrigation purpose), respectively.
- Plant capacity in the LCA was set for the production of 100,000 m³ of reusable water, and this figure was used for all hybrid systems. All materials and energy inputs were determined and normalized based on the functional unit (Hancock et al., 2012). Operational phase of life cycle inventories for all hybrid processes is therefore shown in Table 5-2.
- The LCA study was conducted by focusing on the operational phases (i.e. chemical, membrane and energy consumption). The unit operating expenditure (OPEX, AUD \$/m³) was calculated on an annual basis (Coday et al., 2015).
- Due to the system boundary limitation of the current study, the capital expenditure (CAPEX) was excluded from the current LCA study.
- Membrane costs were based on the market price for 8040 RO modules at AUD \$1,250 and 8040 NF modules at AUD \$1,160, respectively (Bigbrandwater, 2016). The cost of the FO module was assumed to be same as the RO module since it was recently demonstrated that cost of FO modules could be reduced in the future (Holloway et al., 2016).

Table 5 - 1. Characterisation of mine impaired feed water for all hybrid systems and NF feed and permeate water for the NF process in the FDFO-NF hybrid system.

| Parameters | Unit | Saline feed water ² (Average) | Diluted DS ³ (Average) | Final product water (Average) |
|----------------------------------|------------------------------------|---|--------------------------------------|----------------------------------|
| pH | - | 7.8 | 7.7 | 8.15 |
| Conductivity (EC) | mS/cm | 5.40 | 13.5 | 0.81 |
| Total Dissolved Solids (TDS) | mg/L | 2,491 | 7,604 | ~266 |
| Turbidity | NTU | 1.0 | 0.25 | 0.1 |
| Orthophosphate | mg/L P | <0.009 | N/D | N/D |
| Nitrate | mg/L N | <0.005 | N/D | N/D |
| Nitrite | mg/L N | N/D | N/D | N/D |
| Ammonia | mg/L N | 12.0 | 1,897 | 75 |
| Sodium | mg/L | 812.0 | 231 | 10 |
| Potassium | mg/L | 7.0 | 1.2 | 0.2 |
| Calcium | mg/L | 48.0 | 1.5 | 0.15 |
| Magnesium | mg/L | 22.0 | 0.5 | 0.2 |
| Chloride | mg/L | 983.0 | 185 | 15 |
| Sulphate | mg/L SO ₄ ²⁻ | 607.0 | 5288.0 | 165 |
| SAR | - | 24.5 | 42.0 | 4.0 |
| Osmotic pressure ¹ | bar | 1.66 | 3.64 | - |

¹ ROSA software

² It was assumed that the feed water concentration for all hybrid system is similar to the feed water used for the FDFO process in a previous study (Chapter 4).

³ Diluted draw solution (DDS) in the FDFO process was treated by the NF process to meet a suitable water quality for direct irrigation. The average SAR value 4.0 was still lower and within the acceptable values of less than 6 for irrigation (Chapter 4).

Table 5 - 2. Operational phase of life cycle inventories (LCI) for all hybrid processes.

| Unit process | Value | Unit | Design assumptions | Methods |
|----------------------------------|---|-------------------|--|---|
| Chemical use for cleaning | | | | |
| RO and NF | Sodium hypochlorite (NaOCl): 1.22E-4 | kg/m ³ | ▪ Design dosage rate: 200 mg/L | Literature (Moch et al., 2008; Pickering & Wiesner, 1993; Shahabi et al., 2015) |
| | Hydrochloric acid (HCl): 1.59E-03 | kg/m ³ | ▪ Cleaning chemicals | Literature 6 weeks (= 9/year) (Coday et al., 2015; Corral & Yenal, 1932) |
| | Caustic soda (NaOH) :5.26E-04 | kg/m ³ | | |
| | Sodium tri-phosphate (Na ₅ P ₃ O ₁₀) :3.31E-05 | kg/m ³ | ▪ Anti-scalent dosage rate: 2 mg/L | Literature (Corral & Yenal, 1932; Shahabi et al., 2015) |
| MF and UF | Hydrochloric acid (HCl): 4.98E-05 | kg/m ³ | | Literature (Moch et al., 2008; Pickering & Wiesner, 1993; Shahabi et al., 2015) |
| | Caustic soda (NaOH): 1.64E-05 | kg/m ³ | | |
| Membrane materials | | | | |
| MF | 3.42E-02 | kg/m ³ | ▪ Polypropylene (PP): production of MF fibre | |
| | 3.79E-02 | kg/m ³ | ▪ Polyurethane (PU): potting of the module. | |
| | 2.52E-06 | kg/m ³ | ▪ Polyvinylchloride (PVC): membrane housing | |
| UF | 3.59E-02 | kg/m ³ | ▪ Polypropylene (PP): production of UF fibre. | |
| | 3.98E-02 | kg/m ³ | ▪ Polyurethane (PU) is used for potting of the module. | |

| Unit process | Value | Unit | Design assumptions | Methods |
|--------------|-------------------|---|---|---|
| RO | 2.65E-06 | kg/m ³ | <ul style="list-style-type: none"> ▪ Polyvinylchloride (PVC): membrane housing | Literature (Hancock et al., 2012) + Assumptions |
| | 1.24E-03 | kg/m ³ | <ul style="list-style-type: none"> ▪ Polyamide (PA): production of RO fibre | |
| | 1.71E-06 | kg/m ³ | <ul style="list-style-type: none"> ▪ Epoxy resin (Glue): gluing the membrane sheet. | |
| | 3.47E-03 | kg/m ³ | <ul style="list-style-type: none"> ▪ Polyethylene (PE): membrane channel spacer material. | |
| | 3.32E-04 | kg/m ³ | <ul style="list-style-type: none"> ▪ Polyvinylchloride (PVC) is central collection tube. | |
| CTA FO | 3.70E-03 | kg/m ³ | <ul style="list-style-type: none"> ▪ Fibre glass plastic (FRP): membrane housing. | Literature (Hancock et al., 2012) + Assumptions |
| | 5.83E-04 | kg/m ³ | <ul style="list-style-type: none"> ▪ Cellulose acetate: membrane active layer. | |
| | 3.01E-03 | kg/m ³ | <ul style="list-style-type: none"> ▪ Polyester (PET): production of FO fibre (support layer). | |
| | 4.57E-02 | kg/m ³ | <ul style="list-style-type: none"> ▪ Epoxy resin: gluing the membrane sheet. | |
| | 6.60E-04 | kg/m ³ | <ul style="list-style-type: none"> ▪ Suspension polymerised polyvinylchloride (PVC): sealant tape of the module. | |
| | 2.16E-03 | kg/m ³ | <ul style="list-style-type: none"> ▪ Polypropylene (PP): filament tape of the module. | |
| 1.75E-02 | kg/m ³ | <ul style="list-style-type: none"> ▪ Polyethylene (PE): membrane feed channel spacer material. | | |

| Unit process | Value | Unit | Design assumptions | Methods |
|--------------|----------|-------------------|---|---------|
| | 1.09E-02 | kg/m ³ | <ul style="list-style-type: none"> ▪ Polyester (PET): membrane draw channel spacer material. ▪ ABS: centre core flow adapters and anti-telescoping device. ▪ Polyvinylchloride (PVC): central collection tube. ▪ Polyvinylchloride (PVC): membrane housing. | |
| | 3.62E-03 | kg/m ³ | | |
| | 6.14E-03 | kg/m ³ | | |
| | 2.90E-02 | kg/m ³ | | |
| TFC FO | 7.54E-04 | kg/m ³ | <ul style="list-style-type: none"> ▪ Polyamide (PA): membrane active layer. ▪ Polysulfone: membrane support layer. ▪ Epoxy resin: gluing the membrane sheet. ▪ Suspension polymerised polyvinylchloride (PVC): sealant tape of the module. ▪ Polypropylene (PP): filament tape of the module. ▪ Polyethylene (PE): membrane feed channel spacer material. ▪ Polyester (PET): membrane draw channel spacer material. ▪ ABS: centre core flow adapters and anti-telescoping device. | |
| | 3.77E-03 | kg/m ³ | | |
| | 1.37E-02 | kg/m ³ | | |
| | 1.45E-04 | kg/m ³ | | |
| | 5.94E-05 | kg/m ³ | | |
| | 5.24E-03 | kg/m ³ | | |
| | 3.26E-03 | kg/m ³ | | |
| | 7.96E-04 | kg/m ³ | | |

| Unit process | Value | Unit | Design assumptions | Methods |
|--------------|----------|-------------------|--|---------|
| | 1.35E-03 | kg/m ³ | <ul style="list-style-type: none"> ▪ Polyvinylchloride (PVC): central collection tube. | |
| | 6.37E-03 | kg/m ³ | <ul style="list-style-type: none"> ▪ Polyvinylchloride (PVC): membrane housing. | |
| NF | 3.18E-05 | kg/m ³ | <ul style="list-style-type: none"> ▪ Polyamide (PA): production of NF fibre. | |
| | 7.96E-06 | kg/m ³ | <ul style="list-style-type: none"> ▪ Polysulfone: membrane support layer. | |
| | 5.23E-05 | kg/m ³ | <ul style="list-style-type: none"> ▪ Epoxy resin: gluing the membrane sheet. | |
| | 1.62E-04 | kg/m ³ | <ul style="list-style-type: none"> ▪ Polyethylene (PE): membrane channel spacer material. | |
| | 4.63E-05 | kg/m ³ | <ul style="list-style-type: none"> ▪ PVC (polyvinylchloride): central collection tube. | |
| | 3.21E-03 | kg/m ³ | <ul style="list-style-type: none"> ▪ Fibre glass plastic (FRP): membrane housing. | |

5.2.1.2. Methodology of life cycle impact assessment

Life cycle impact assessment (LCIA) is the third stage of the LCA. It aims at comparing the individual indicators calculated from the inventory analysis to contribute to the evaluation of the overall potential impacts of the system (Pryshlakivsky & Searcy, 2013).

In this study, the environmental impact assessment was performed using the Australian indicator set v.3.01. This set includes six relevant impact assessment categories, as shown in Table 5-3. They are global warming (GW), fossil fuel and mineral resource (FMR), eutrophication (EP), human toxicity (HT), ozone depletion (OD), and ecotoxicity (ET). Each category was assessed for the three most important operational components (Figure 5-1): membranes, electricity, and chemicals.

In addition, the economic assessment considered the annual OPEX cost for three components: membrane replacement (MR), energy (EC), and membrane cleaning chemicals (CC). The operating costs for personnel were omitted on the assumption that they would be similar in all the cases. The OPEX data for the conventional RO and NF processes were calculated from secondary data (input data) from the literature (Liyanaarachchi et al., 2016; Moch et al., 2008) and were adopted to estimate the total OPEX costs.

Table 5 - 3. Environmental impact categories used in LCIA (Bengtsson & Howard, 2010; Fritzmann et al., 2007; Hancock et al., 2012; PRé-Consultants, 2008).

| Impact category | Description |
|--|--|
| Global warming (GW) | Effect of greenhouse gases on climate change based on the Intergovernmental Panel on Climate Change |
| Eutrophication (EP) | Effect of excessive levels of macronutrients in the environment caused by emissions of nutrients to air, water, and soil |
| Ozone depletion (OD) | Ozone depletion potential of different gases in terms of chlorinated fluorocarbon 11 equivalent |
| Fossil fuel and mineral resource (FMR) | Effect of extraction of minerals and fossil fuels as a mass of antimony equivalent |
| Eco-toxicity (ET) | Resulting from emissions of toxic substances to air, water, and soil. |
| Human toxicity (HT) | Effect of chemical substance on human health |

The reliability of LCA results is highly dependent on the chosen database due to a large number of input parameters. For instance, manufacturing membrane modules require resources to produce membranes, spacers, housing, collection tubes and adhesives, and this information can vary significantly. These parameters affect the robustness of the environmental and economic LCA outcomes. For this reason, the input and output amounts for the FDFO-NF hybrid system within the life cycle inventory were evaluated and compared using a sensitivity analysis that focused on the FO membrane module average water flux ($\text{Lm}^{-2}\text{h}^{-1}$, LMH) and the FO module cost variations. For the sensitivity analysis with different module average fluxes, the experimental flux data was adopted from the field study of the FDFO-NF process to demonstrate how performances of currently available FO membranes affect the LCA results and were then compared with other conditions including the newly developed FO membranes.

One of the most important parameters in the FDFO-NF hybrid system, especially in a closed-loop system, is the NF recovery rate because it relates to both NF energy consumption and the FO membrane replacement cost (i.e. FO process performance in terms of the average water flux). Performing NF at higher recovery rates increases the inlet DS concentration (osmotic driving force) and hence reduces the membrane area required; however, it also increases the operating cost (i.e. NF energy cost). Therefore, to make the FDFO-NF hybrid system cost-effective, an optimum NF recovery rate is pivotal. Therefore, the sensitivity analysis on the NF process was also conducted at varying NF recovery rates in the closed-loop FDFO-NF hybrid system. The parameters used in the sensitivity analysis are summarized in Table 5-4. All equations are described in Table 5-5, and the input data are presented in Table 5-6.

A sensitivity analysis was performed to provide a more realistic economic and environmental life cycle analysis on the FDFO-NF hybrid desalination process compared to other desalination hybrid systems. To validate the model equations used in this study, water flux was measured from feed water with an osmotic pressure of 1.66 bar and ammonium sulphate draw solution concentrations of 1, 2, and 3 M. As shown in Figure 5-2, the experimental and modelled results show good agreement with the governing Equation.3 in Table 5-5.

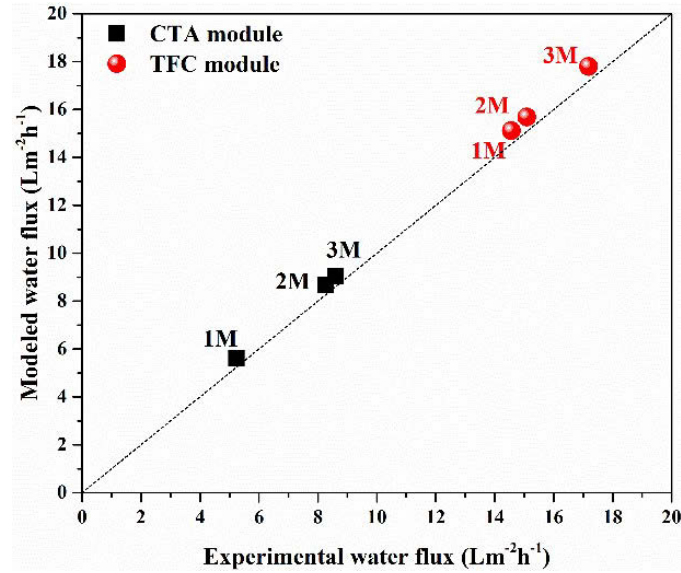


Figure 5 - 2. Modelled water flux as a function of experimental water flux. The modelled water flux was calculated using Equation. 3 in Table 5-5. Feed concentration was constant at 1.66 bars (feed water was converted to the concentration of NaCl and calculated the osmotic pressure using OLI software). The draw solution concentration varied. The feed rate was 70 L/min, the draw flow rate was 7 L/min, and temperature was 25°C.

Table 5 - 4. Parameters included in the sensitivity analysis.

| Parameters varied for the sensitivity analysis | Description of the change of parameter |
|--|--|
| 1. Variation of the module average water flux (J_w) | |
| <ul style="list-style-type: none"> ▪ Experimental data – Long-term pilot operation of the FDFO process (Phuntsho et al., 2016b) | <ul style="list-style-type: none"> ▪ $J_{w, CTA-1}$: 3 LMH ▪ $J_{w, TFC-1}$: 10 LMH |
| <ul style="list-style-type: none"> ▪ Module-scale simulation using currently available FO flux modelling (Deshmukh et al., 2015; Zaviska & Zou, 2014)^{a,b} | <ul style="list-style-type: none"> ▪ $J_{w, CTA-2}$: 8 LMH ▪ $J_{w, TFC-2}$: 20 LMH |
| <ul style="list-style-type: none"> ▪ FO flux data adapted from literature | <ul style="list-style-type: none"> ▪ $J_{w, CTA-3}$: 5.7 LMH (Coday et al., 2015) ▪ $J_{w, TFC-3}$: 11 LMH (Deshmukh et al., 2015) |
| <ul style="list-style-type: none"> ▪ Newly developed FO membranes (Sim et al., 2013b) | <ul style="list-style-type: none"> ▪ $J_{w, CTA-4}$: 25 LMH ▪ $J_{w, TFC-4}$: 25 LMH |
| 2. FO module cost | |
| <ul style="list-style-type: none"> ▪ Assumption of FO module cost | <ul style="list-style-type: none"> ▪ AUD \$200-1,500/module |
| 3. Post-treatment process | |
| <ul style="list-style-type: none"> ▪ NF process recovery rate | <ul style="list-style-type: none"> ▪ At all fixed conditions, only the NF recovery rate varied from 50% to 97% under a continuous closed-loop FDFO-NF hybrid system using a simple mass-balance relation. |

^a The parameter values used for FDFO process simulation using both FO membrane modules (CTA and TFC) are shown in Table 5-6.

^b Validation of experimental water flux and predicted water flux is shown in Figure 5-2, Tables 5-5 and 5-6.

Table 5 - 5. Flux modelling adapted in this study for FO full-scale simulation.

| Model | Model equations |
|--|--|
| A module-scale model governed by solution-diffusion (Deshmukh et al., 2015; Phuntsho et al., 2014b; Tiraferri et al., 2013): | Eq.1 Water recovery, $RR_{FO} = \frac{Q_p}{Q_{F0}}$ |
| | Eq.2 Solute permeability coefficient, $B = \gamma A^3$ (Constant value, $\gamma = 0.0133L^{-2}m^4h^2bar^{-3}$) |
| | Eq.3 Water flux, $J_w = \frac{A \left[\pi_{D,b} \exp\left(-\frac{J_w S}{D}\right) - \pi_{F,b} \exp\left(\frac{J_w}{k_F}\right) \right]}{1 + \frac{B}{J_w} \left[\exp\left(\frac{J_w}{k_F}\right) - \exp\left(-\frac{J_w S}{D}\right) \right]}$ |
| | Eq.4 Mass transfer coefficient, $k_F = \frac{Sh D_F}{D_h}$ |
| | Eq.5 Structural parameter, $S = K_D D = \frac{t_s \cdot \tau}{\varepsilon}$ |
| | Eq.6 Resistance to solute diffusion in the membrane support $K_D = \left(\frac{1}{J_w}\right) \ln \frac{B + A \pi_{D,b}}{B + J_w + A \pi_{F,m}}$ |
| | Eq.7 Solute flux, $J_s = \frac{B \left[C_{D,b} \exp\left(-\frac{J_w S}{D}\right) - C_{F,b} \exp\left(\frac{J_w}{k_F}\right) \right]}{1 + \frac{B}{J_w} \left[\exp\left(\frac{J_w}{k_F}\right) - \exp\left(-\frac{J_w S}{D}\right) \right]}$ |

Q_P = water permeation across the membrane, L/min

Q_{F0} and Q_{D0} = initial feed and draw flow rates, respectively, L/min

C_{F0} and C_{D0} = inlet feed and draw concentrations, respectively, M

C_{Fb} and C_{Db} = bulk feed and draw concentrations, respectively, M

A = membrane water permeability coefficient, $Lm^{-2}h^{-1}bar^{-1}$

$\pi_{F,b}$ and $\pi_{D,b}$ = bulk feed and draw osmotic pressure, respectively, bar

$\pi_{F,m}$ and $\pi_{D,m}$ =

feed and draw osmotic pressure on the active layer and the support layer, respectively, bar

Sherwood number, $Sh = 1.85 \left(Re Sc \frac{d_h}{L} \right)^{0.33}$, Laminar flow

Sherwood number, $Sh = 0.04 Re^{0.75} Sc^{0.33}$, Turbulent flow

Schmidt number, $Sc = \frac{\mu}{\rho D_F}$

μ = dynamic viscosity

ρ = solution density

D_D = diffusion coefficient of the draw solute, m^2/s

D_F = diffusion coefficient of the feed solute, m^2/s

D_h = hydraulic diameter of the feed channel, m

Table 5 - 6. Input parameters used for FO flux estimation based on the pilot operation data.

| Parameters | Unit | Values |
|---|--|-------------|
| Membrane material | | CTA / TFC |
| Pure water permeability, A | $\text{Lm}^{-2}\text{h}^{-1}\text{bar}^{-1}$ | 1.02 / 2.02 |
| Salt permeability, B | $\text{Lm}^{-2}\text{h}^{-1}$ | 0.46 / 0.67 |
| Effective membrane module area | m^2 | 11.2 / 15.3 |
| FS, mine impaired water concentration (\approx NaCl) | M | 0.06 |
| DS, $(\text{NH}_2)_4\text{SO}_4$ or SOA | M | 1.89 |

5.2.3.1. Conventional RO hybrid desalination processes

Figure 5-3 shows the schematic layout for the MF-RO and UF-RO hybrid systems. The input data is presented in Table 5-7. The RO process was assumed to achieve 75% water recovery in both MF-RO and UF-RO given the relatively low TDS of the brackish feed water (TDS 1,000 ~ 10,000 mg/L) (Masters, 1991). It is worth noting here that, the performance simulation of the MF-RO and UF-RO hybrid systems was conducted to treat a feed water with TDS of 2,491 mg/L with an osmotic pressure of 1.66 bar (see Table 5-1). Due to this relatively low feed water concentration, it can be expected that the energy consumption of the MF-RO and UF-RO systems would be much lower than the conventional seawater treatment processes (i.e. 35,000 mg/L TDS). In addition, the specific data inventory of the operation stage for MF-RO and UF-RO were simulated using the membrane manufacturer specifications and ROSA software (Version 9.1, Filmtech Dow Chemicals, USA). The energy consumption and system design of the unit processes for each hybrid system were calculated from the known principles of hydraulic flow (Hancock et al., 2012; Shaffer et al., 2012; Watson et al., 2003). The specific energy consumption (SEC in kWh/m^3) for each hybrid system was estimated from the feed pumping energy for all processes (MF, UF, and RO), backwashing for MF and UF and chemical cleaning processes for RO and NF, as presented in Table 5-7.

5.2.3.2. FDFO-NF hybrid desalination process

Figure 5-3 and Table 5-7 show the process layout diagram and the details of the hybrid FDFO-NF process. The FDFO-NF hybrid desalination process is fully described in Kim et al. (2013a). The 8040 FO membrane module average water flux data in Table 5-7 was derived from the long-term operating performance of the FDFO-NF hybrid system is described in Chapter 4, where two main advantages of the FDFO-NF hybrid process were observed. Flux decline caused by membrane fouling can be fully recovered simply by hydraulic or physical cleaning. This indicates that the FDFO process requires significantly low or no chemical cleaning, unlike other pressure-based membrane processes. Due to the high water quality obtained from the FDFO process (FO acts as pre-treatment to NF), chemical cleaning in the NF process can be significantly lowered in comparison to the RO process in MF-RO and UF-RO hybrid systems. It has to be understood here that the concentration of the diluted DS in the FDFO plays a significant role in NF energy consumption. The diluted fertilizer DS concentration before NF post-treatment was 7,600 mg/L with an osmotic pressure of 3.64 bar (see Table 5-1). Such concentration refers to brackish ground water quality as mentioned above. The operating conditions for the NF post-treatment would be similar to a low-pressure RO post-treatment process for treating relatively low concentrated brackish groundwater (Valladares Linares et al., 2016).

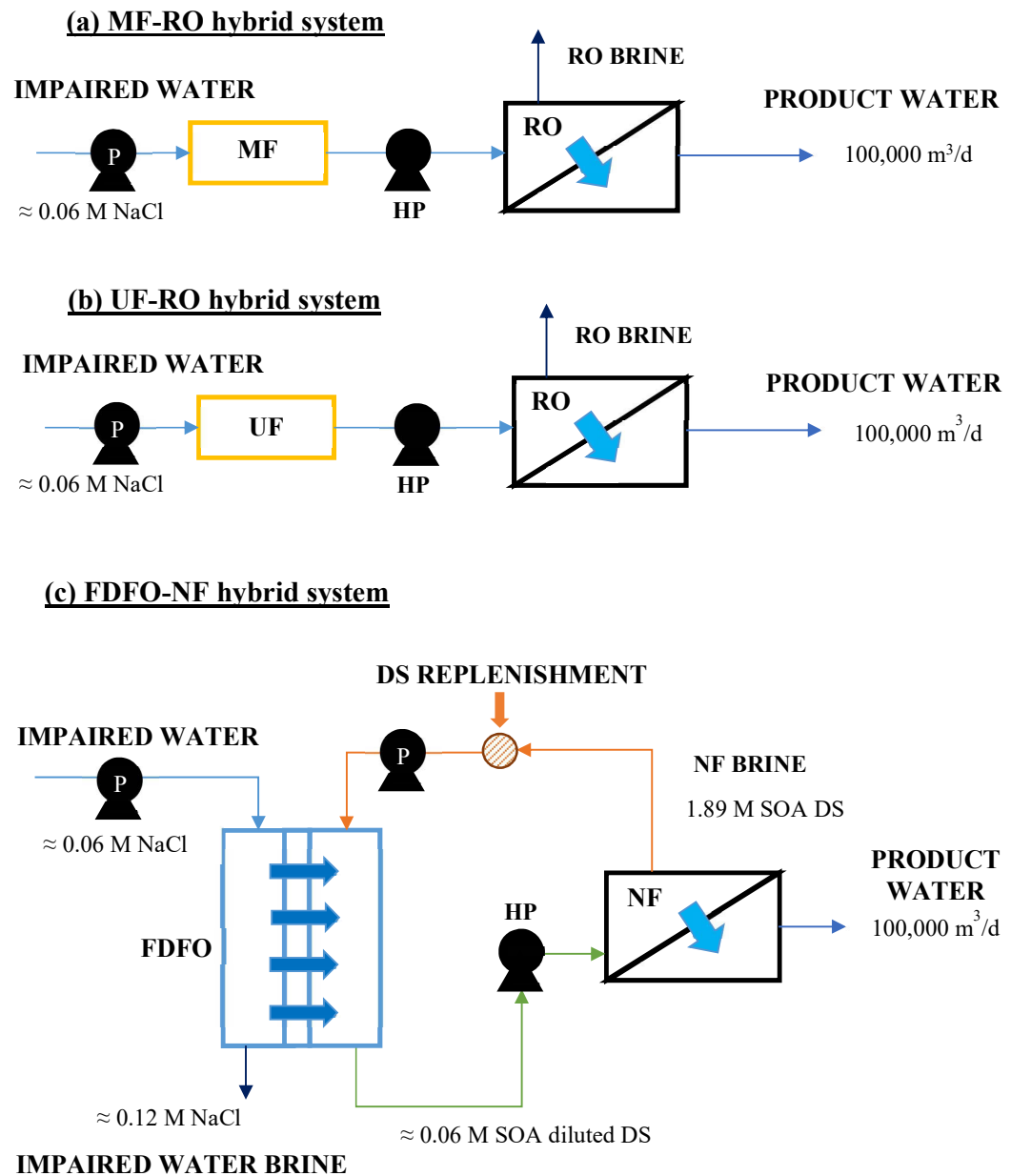


Figure 5 - 3. Schematic diagram of hybrid desalination systems of (a) MF-RO (b) UF-RO and (c) FDFO-NF. N.B. P: Pump and HP: High pressure pump.

Table 5 - 7. The hybrid process design conditions used in this study and the process simulation results.

| Design conditions | Units | MF-RO | UF-RO | FDFO-NF |
|---|---------------------|--------------|--------------|----------------|
| Microfiltration (MF) | | | | |
| Feed flow rate | m ³ /day | 140,000 | | |
| Recovery | % | 95 | | |
| Ultrafiltration (UF) | | | | |
| Feed flow rate | m ³ /day | | 148,000 | |
| Recovery (Hancock et al., 2012) | % | | 90 | |
| Reverse osmosis (RO) | | | | |
| Feed flow rate | m ³ /day | 133,000 | | |
| Recovery (Wilf, 2004) | % | 75 | | |
| Product flow rate | m ³ /day | 100,000 | | |
| ^a Specific energy consumption (Shaffer et al., 2012) | kWh/m ³ | 1.25 | 1.36 | |
| Fertilizer drawn forward osmosis (FDFO) | | | | |
| Feed water: mine impaired water \approx 0.06 M NaCl | | | | |
| Draw solution: 1.89 M Ammonium sulphate (Phuntsho et al., 2016b) | | | | |
| FS flow rate | m ³ /day | | | 220,000 |
| DS flow rate | m ³ /day | | | 43,000 |
| Recovery (Zaviska & Zou, 2014) | % | | | 46 |
| Average flux ($J_{w,CTA}$) [*] | LMH | | | 3 |
| Average flux ($J_{w,TFC}$) [*] | LMH | | | 10 |
| Permeate flow | m ³ /day | | | 100,000 |
| Nano-filtration (NF) | | | | |
| ^b Final diluted fertilizer DS: 0.06 M Ammonium sulphate (Phuntsho et al., 2016b) | | | | |
| Diluted DS flow rate (NF feed) | m ³ /day | | | 143,000 |
| Recovery (Altae & Zaragoza, 2014b) | % | | | 70 |
| Product flow rate | m ³ /day | | | 100,000 |
| ^a Specific energy consumption (Altae & Zaragoza, 2014b; Shaffer et al., 2012) | kWh/m ³ | | | 1.08 |

5.3. Results and discussion

Identifying the most significant issues for each hybrid system is one of the main goals of an LCA interpretation phase. Figure 5-4 presents the relative contribution analysis of the three hybrid systems for each of the six selected environmental impact categories obtained from the simulation input data presented in Table 5-7 (baseline input data). These results clearly show that electricity is one of the key factors in environmental impact for MF-RO and UF-RO hybrid systems. In fact, electricity consumption accounts for more than 70% of the total impact in all categories, except for ozone depletion (OD)

where the contribution was about 30%, as shown in Figure 5-4 (a). Membranes account for less than 30%, except in the OD category which is higher than 70%, and chemicals account for less than 5% of the total impact in the MF-RO and UF-RO hybrid systems. Figure 5-4 (a) shows that, for the FDFO-NF hybrid system, both the membrane materials and the energy consumption play a major contribution to the environmental impact. It is worth noting that the contribution of the TFC FO membrane materials was significantly lower than the CTA membrane because its higher water flux requires less membrane modules. Membranes constituted 40-90% of the impact for the FDFO-NF (CTA) hybrid system in all six categories, with a maximum of 90% for OD. This is mainly due to the amount of raw materials needed to manufacture the membrane modules, including their chemical production (Hancock et al., 2012). The contribution of membranes decreased to 20-85% when TFC FO membranes were used, which indicates that a significant reduction in both environmental and economic impacts could be achieved by improving the performance of the FO membranes. Energy still accounts for more than 50% of the impact in most categories (except OD and human toxicity, HT), although this is much lower than the energy component of the RO hybrid systems.

Figure 5-4 (b) compares the relative contributions of the four hybrid systems in the six environmental impact categories of the three main assessment areas: membranes, electricity, and chemicals. These results clearly show that the FDFO-NF hybrid system has a lower relative contribution to environmental impact in all six impact categories for energy and chemical consumption than the RO hybrid for irrigation purposes. However, Figure 5-4 (b) also shows that the environmental impacts of the FDFO-NF membranes are significantly higher because the low water flux of FO membranes signifies that more membrane modules are required to achieve the same water production. Using a TFC FO membrane with improved water flux can reduce the environmental impacts of the membrane of about 20% and 40% to all impact categories compared to a CTA FO membrane.

It has to be noted that assumptions regarding the chemical cleaning process slightly differ from the previous studies (Hancock et al., 2012; Tarnacki et al., 2012). In fact, chemical cleaning agents such as NaOH, HCl and NaOCl as well as anti-scalant ($\text{Na}_5\text{P}_3\text{O}_{10}$) were assumed to be necessary for all membrane processes in the MF-RO and UF-RO hybrid systems. However, it was assumed (i.e. based on the results obtained in our long-term

pilot-scale study) that the FDFO-NF system does not require chemical cleaning. Recent studies further demonstrated that physical cleaning was very efficient and easy to apply for practical FO operation (Kim et al., 2017a; Lotfi et al., 2017). Nevertheless, it is known that effective cleaning strategies for FO process should be determined by its applications because this affects the techno-economic assessment of the FO process. Since the FDFO-NF hybrid system in this study has a low fouling potential and fouling reversibility, the lower chemical cleaning frequency significantly reduces its environmental impact. In fact, the environmental impact does not include discharge of cleaning chemicals to the environment and hence the advantage of the FDFO-NF system may be even more significant. Conservative life cycle assessment of FO hybrid systems including chemical cleaning for the FO process could be one of the important areas of future studies for full-scale FO implementation. Additionally, NaOH and HCl were assumed to be necessary for the NF process, but at a much lower cleaning frequency than in normal operations (Phuntsho et al., 2016b). Besides, the physical conditions for the cleaning process were assumed to be fixed, and the effects of cleaning time and cross-flow velocity on the cleaning efficiency were assumed to not be significant (Ang et al., 2006).

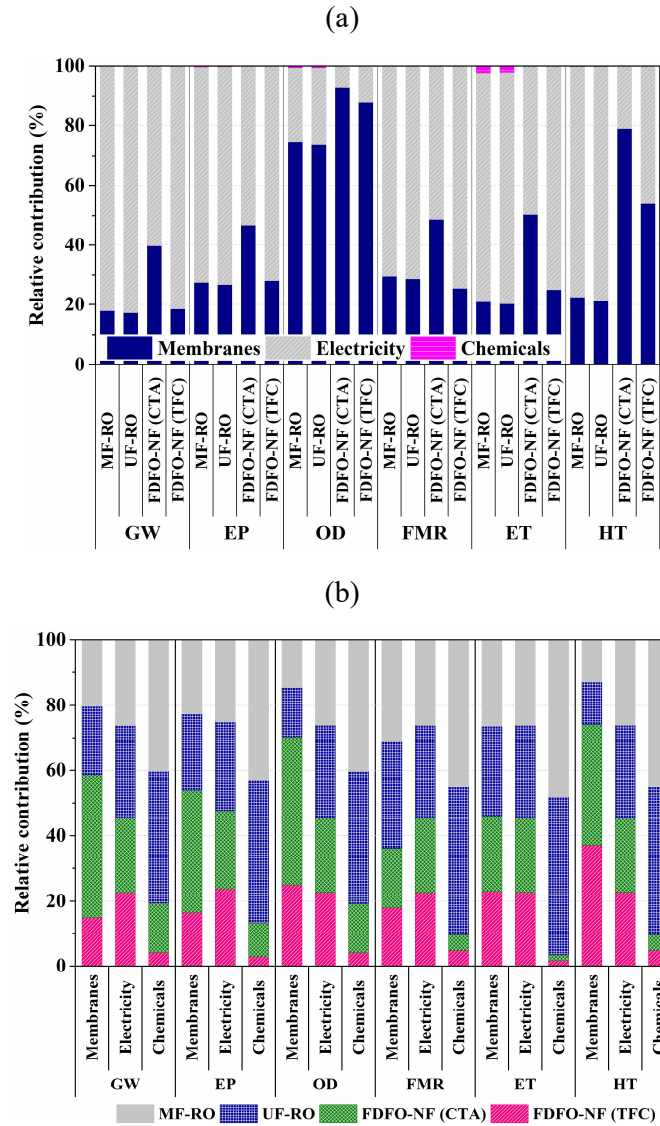


Figure 5 - 4. Relative contribution analysis of (a) three operational components for each hybrid system and (b) of four hybrid processes for three main components under six impact categories. FDFO-NF with CTA and TFC and an average water flux was around 3 and 10 LMH, respectively. Three operational components refer to membrane materials, electricity, and chemicals.

The results presented in Figure 5-5 show the total OPEX cost along with its major cost components for each hybrid system. Figure 5-5 (a) shows that the total OPEX cost per unit volume of product water was the highest for the FDFO-NF (CTA) hybrid system with AUD \$0.81/m³, compared to the MF-RO and UF-RO hybrid systems with AUD \$0.49/m³ and AUD \$0.54/m³, respectively. Based on these results, the FDFO-NF (CTA) desalination system does not appear to be an economically viable alternative for

desalination compared to the existing RO hybrid technologies. However, the lowest total OPEX cost was obtained with the FDFO-NF (TFC) hybrid system at AUD \$0.46/m³, indicating that the FDFO-NF hybrid system can be economically competitive if FO membranes with much higher water flux performances are used. This study, therefore, shows that using current TFC FO membranes, the unit OPEX cost of the product water from the FDFO-NF hybrid system is 5.3% lower than the conventional MF-RO hybrid system and 14.3% lower than UF-RO hybrid system.

Figure 5-5 (a) clearly shows the advantages of the FDFO-NF hybrid system in terms of energy consumption. Table 5-7 shows that the total energy consumption of the FDFO-NF hybrid was 1.08 kWh/m³, which is 13.6% lower than that of MF-RO (1.25 kWh/m³) and 21% lower than that of the UF-RO (1.36 kWh/m³) hybrid system. Energy forms the major cost component of the RO hybrid systems, relatively contributing up to 83.1% of the total OPEX cost compared to FDFO-NF (CTA) and FDFO-NF (TFC) which is only about 40.5% and 71.8%, respectively. It may be noted that this energy consumption does take into account the quality of irrigation water produced from each hybrid system as mentioned earlier (less than 1,000 mg/L based on the product water obtained during the field test of the FDFO-NF hybrid process in Chapter 4).

Figure 5-5 (b) shows a detailed cost analysis for the FDFO-NF hybrid systems to highlight the contribution of each process (FO and NF) separately. These results clearly show that the FO contribution of the energy consumption to the total OPEX cost is not significant (3.4% for CTA and 6.0% for TFC). However, FO membrane replacement costs contribute significantly to the OPEX cost with 55.1% for CTA and 21.4% for TFC. This indicates that the opportunity exists for the FDFO-NF hybrid system to further reduce OPEX costs by reducing the membrane replacement cost and the NF energy consumption. Previous studies (Blandin et al., 2015b; Hancock et al., 2012) have also pointed out that the overall environmental and economic impacts of FO membrane modules can be significantly reduced by improving the performance of FO membranes. The energy consumed by the NF process could also be reduced by operating the process at optimum recovery rates due to its flexibility on recovery rates (Altaee & Zaragoza, 2014b). The sensitivity analysis of the NF recovery rate will be discussed in the following section.

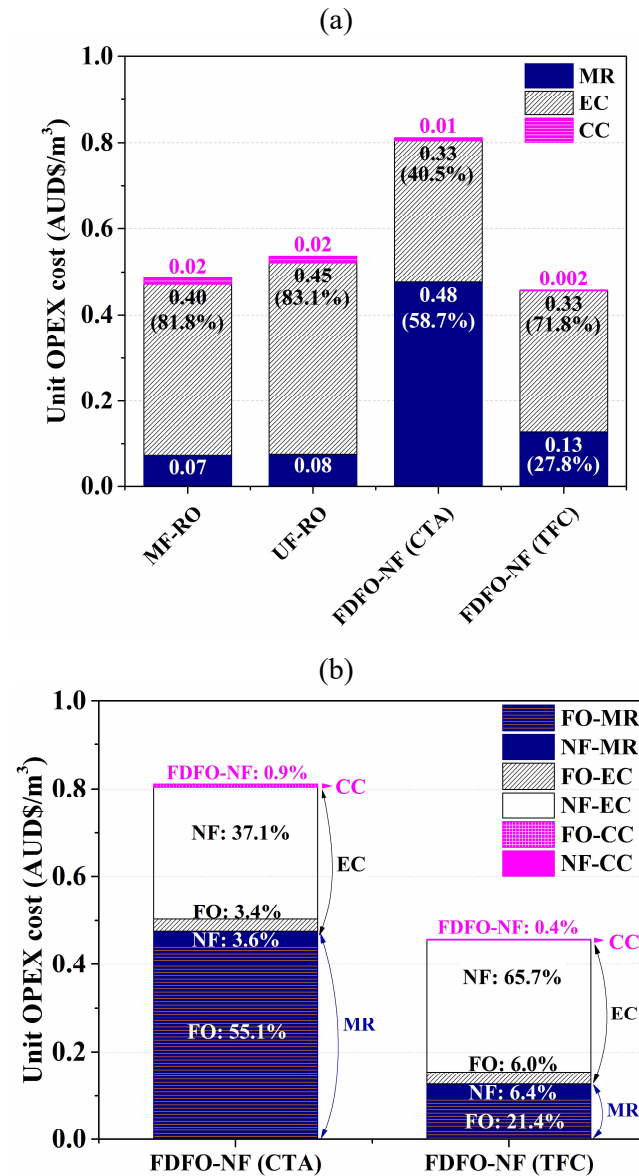


Figure 5 - 5. (a) Cost contribution analysis of three main operational components for four hybrid systems and (b) specific cost contribution analysis of FDFO-NF with CTA and TFC hybrid systems. MR, EC, and CC refer to the costs of membrane replacement, energy consumption, and cleaning chemicals.

Electricity and the cost of replacing membranes are the two major contributing factors to the OPEX cost of the FDFO-NF hybrid system (see Figure 5-5). A sensitivity analysis was undertaken to assess those components and identify opportunities to further reduce the OPEX costs. The key parameters are the cost of the module, the average water flux of the FO membrane, and the recovery rate of the NF process. All the analyses assumed a plant capacity of 100,000 m³/day.

Logically, the two obvious ways to reduce membrane replacement costs are to reduce the cost of the membrane module or reduce the number of modules required. Cheaper modules may result from improvements in mass production, but the development of a market can take time. Reducing the number of modules can only come through drastic improvements in the average water flux of the whole FO membrane system, which contains several FO membrane modules connected in series. As the DS becomes more and more diluted along its length, water flux ultimately decreases. Hence, the average water flux is a significant parameter in estimating the number of membrane modules required, subsequently, their total replacement cost. Figure 5-6 shows a sensitivity analysis of changes in module cost and average water flux. As expected, when the cost of a module decreases and the average water flux increases, the overall OPEX cost decreases for both FDFO-NF hybrid systems. However, membrane replacement costs are much higher in the FDFO-NF system, so the CTA and TFC membranes are discussed separately below.

Figure 5-6 (a) shows the variations in the OPEX cost of the FDFO-NF (CTA) hybrid system with different 8040 CTA FO membrane costs and average water flux levels. At the cost of AUD \$1,250 per module with an average water flux of 3 LMH, the unit OPEX cost of irrigation water is AUD \$0.81/m³. At this price, FDFO-NF (CTA) is not economically viable compared to existing MF-RO and UF-RO hybrid systems. However, when the average water flux exceeds 8 LMH, the membrane replacement cost is significantly reduced, and the OPEX cost per unit decreases below AUD \$0.53/m³, which becomes cost-effective. Achieving such a significant improvement in water flux may be a major challenge for CTA FO membranes, as they are generally reported to have lower water permeability than TFC FO membranes (Yip et al., 2010).

Lowering the cost of the CTA FO membrane module may be another way of reducing the OPEX cost of this system. At the same average water flux of 3 LMH, the FDFO-NF (CTA) hybrid system only becomes cost competitive when the cost of the CTA FO membrane module falls by at least 60% to AUD \$500 per module. This would only be likely if the CTA FO market share significantly improves in the future (Valladares Linares et al., 2016).

As presented earlier in Section 5.3.2, FDFO-NF (TFC) is already cost effective compared to the MF-RO and UF-RO hybrid systems. Figure 5-6 (b) shows how the change in the cost of TFC FO membranes and average water flux affect the unit OPEX cost of irrigation water in the FDFO-NF (TFC) hybrid system. Unlike for the CTA FO membrane, variations in these parameters do not seem to have a significant impact. For example, improving the water flux from 10 LMH to a threshold flux of 30 LMH (Blandin et al., 2015b) is not likely to significantly reduce the OPEX cost of the FDFO-NF (TFC) hybrid system, where membrane replacement only account for 21.4% of the OPEX compared to 55.1% in for the FDFO-NF (CTA) hybrid system (Figure 5-5 (b)). However, there is a potential to improve the module water flux, and this could play a more significant role in further lowering the environmental impact of the FDFO-NF (TFC) hybrid system. Recent publications have reported the fabrication of TFC FO membranes with a water flux at magnitudes 3 to 6 times higher than the CTA FO membrane (Duong & Chung, 2014; Han et al., 2012; Han et al., 2016; Tiraferri et al., 2011; Yip et al., 2010). Therefore, it is clear that opportunities to further improve the membrane and its performance exist, and this could make the FDFO-NF hybrid system more cost-effective than MF-RO or UF-RO hybrid systems.

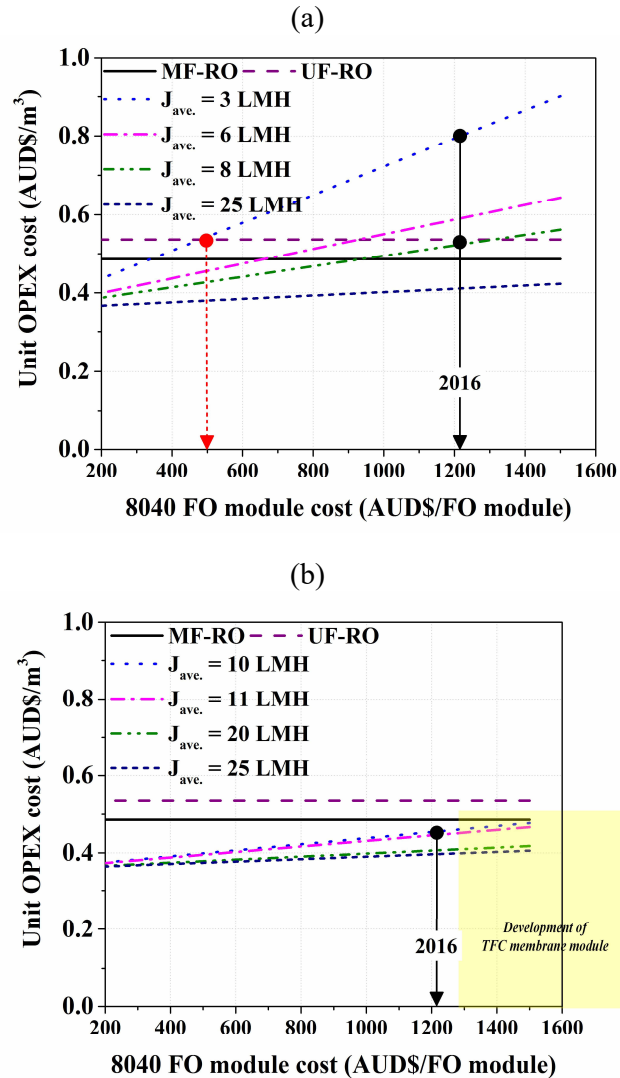


Figure 5 - 6. Unit OPEX cost of the FDFO-NF using (a) CTA and (b) TFC FO membrane modules as a function of FO average water fluxes and FO module cost variation (AUD\$200-AUD\$1,500). Plant capacity 100,000 m³/day. The average flux ($J_{ave.}$) of the FDFO-NF (CTA) refers to 3, 6, 8, and 25 LMH and that of the FDFO-NF (TFC) refers to 10, 11, 20, and 25 LMH.

In a continuous closed-loop FDFO-NF hybrid system (see Figure 5-3), the NF process is critical because it plays a significant role in both NF energy and FO membrane replacement costs. Performing the NF process at a lower recovery rate decreases the driving force in the FO process (lower osmotic pressure of the DS) and increases FO membrane area requirement, but it also lowers energy consumption. Although the module average water flux can be increased by increasing the inlet DS concentration (i.e. increasing the NF recovery rate), the concentration cannot be increased beyond the NF process's optimum recovery rate because the resulting increase in energy consumption

will increase the OPEX cost of the final water. As a result, the determination of the optimum NF feed recovery rate must take into account the membrane replacement cost and the energy consumption.

Figure 5-7 presents a comparison between the unit OPEX cost of water for the FDFO-NF, MF-RO, and UF-RO hybrid systems, given variations in the NF recovery rate. A simulation was carried out assuming SOA fertilizer as DS, NaCl as FS (refer Figure 5-3), NaCl and SOA rejection rates of FO and NF membranes of 90% based on our recent study (Phuntsho et al., 2017a). The NF recovery rate was varied from 50% to 97%. The OPEX cost of the FDFO process decreased rapidly with an increase in the NF recovery rates for both the CTA and TFC FO membranes and gradually increased above an 80% NF recovery rates. When NF is performed at a higher NF feed recovery rate, it produces a proportionately higher concentration of the recycled DS, which in turn increases the driving force of the FDFO process. This ultimately decreases the membrane area required and hence the unit OPEX cost of FO membrane replacement is reduced. However, operating the NF process at a higher recovery requires higher applied pressure which increases the energy cost of the NF process although the NF membrane replacement cost may slightly decrease.

Considering the combined OPEX costs of the FDFO and NF processes, the optimum NF feed recovery rate for the FDFO-NF (CTA) hybrid system was observed to be about 89% with a unit OPEX cost of water of AUD \$0.57/m³. The optimum NF feed recovery rate of the FDFO-NF (TFC) hybrid system, however, ranged between 75% and 91% with a unit OPEX cost of water at about AUD \$0.40/m³. Even at the optimum NF feed recovery rate, the FDFO-NF (CTA) hybrid system remained less cost-effective than conventional RO hybrid systems. Conversely, the FDFO-NF (TFC) hybrid system was found to be more cost-effective than the RO hybrid systems over a wide range of NF feed recovery rates (75-91%). Increasing NF feed recovery rates above the optimum rate increases energy costs, and lowering it below the optimum rate significantly increases membrane replacement costs. For example, if NF in the FDFO-NF (CTA) hybrid system is performed at a lower feed recovery rate of 75%, the unit OPEX cost of water increases to AUD \$1.20/m³ from AUD \$0.58/m³ at the optimum rate of 89%. Likewise, the unit OPEX of the FDFO-NF (TFC) system increases to AUD \$0.49/m³ (at 75% NF recovery rate) from AUD \$0.41/m³ at the optimum recovery rate (at 84% NF recovery rate). At

this unit OPEX costs, the FDFO-NF hybrid system is not cost competitive compared to the conventional RO hybrid systems and the unit OPEX cost of water only increases if the NF process is performed above than the optimum recovery rates. This sensitivity analysis, therefore, shows that potential exists for making the FDFO-NF hybrid system more cost-effective compared to conventional RO hybrid systems for the desalination of saline water. It has to be noted here that capital costs for a high-pressure RO hybrid system could be higher than those for a lower pressure FDFO-NF hybrid system due to the costs for high-pressure pumps, piping, valves, and fittings. This part would be considered as potential cost savings for the FDFO-NF hybrid system.

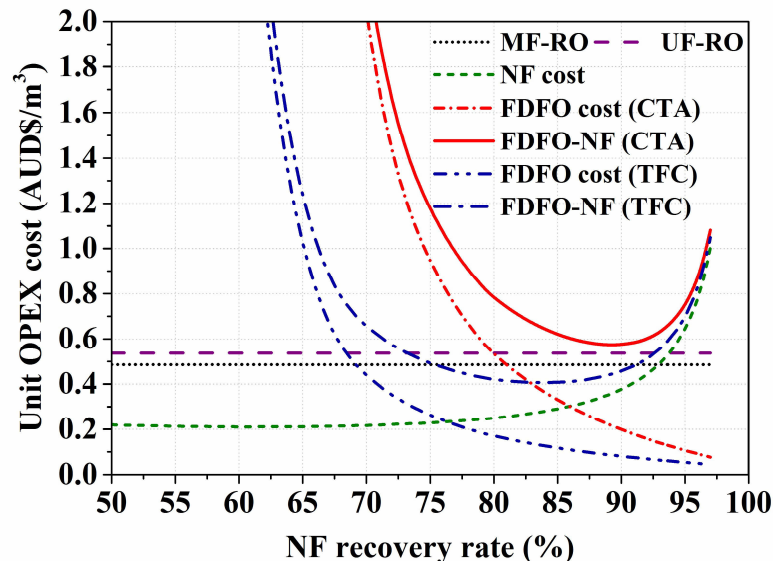


Figure 5 - 7. Sensitivity analysis of FDFO-NF (CTA and TFC) OPEX costs as a function of NF process recovery rates. The FO module cost was assumed to be \$1,250/module in 2016, and the average FO water fluxes were estimated based on the closed-loop mass-balance simulation of the FDFO-NF hybrid system.

5.4. Concluding remarks

This chapter outlined the results of a comparative environmental life cycle assessment and economic analysis for desalination of mine impaired saline water for irrigation purpose. The FDFO-NF hybrid system was compared to conventional MF-RO and UF-RO hybrid systems with the following conclusions drawn:

- Environmental LCA results showed that, compared to conventional RO hybrid systems, the FDFO-NF hybrid system using TFC FO membrane had the lowest overall environmental impact in both energy consumption and use of chemical cleaners.
- The FDFO-NF hybrid system consumes less energy than the RO hybrid system in irrigation water production. The total energy consumption of the FDFO-NF hybrid system was estimated at 1.08 kWh/m³, which is 13.6% lower than the MF-RO system and 21% lower than the UF-RO hybrid system.
- The unit OPEX cost of producing FDFO-NF water using a TFC FO membrane was estimated at AUD \$0.46/m³, which is cost effective when compared to the MF-RO hybrid system at AUD \$0.49/m³ and the UF-RO hybrid system at AUD \$0.54/m³. However, when using a CTA FO membrane, the FDFO-NF hybrid system had a per unit OPEX water cost of AUD \$0.81/m³ which is not cost effective. The energy was found to be the highest cost component of the RO hybrid systems, whereas membrane replacement costs are the highest in the FDFO-NF hybrid systems.
- FDFO-NF with TFC membranes showed the lowest relative environmental impact compared to all other hybrid systems.
- The sensitivity analysis indicated that the FDFO-NF hybrid system using an 8040 CTA FO membrane module is only cost competitive when its module average water flux reaches 8 LMH or, alternatively, if the cost of the CTA FO membrane could be reduced by about 60%.

- The optimum feed recovery rate of the NF process using a TFC FO membrane was 75-92%, which resulted in the lowest unit OPEX water at AUD \$0.41/m³ at 84%. At the optimum NF recovery rate of 89%, the unit cost of water using a CTA FO membrane was AUD \$0.57/m³ which is still not cost competitive compared to conventional RO hybrid systems.
- Results of this chapter clearly show that there is some positive potential of the FDFO-NF for the practical application if incorporating higher reverse flux selectivity FO membrane (i.e. TFC FO) and lowering the FO membrane module cost for the FO process. However, FO membrane studies at modular level are still limited and thus its detailed study including fouling behaviors and effective cleaning strategies needs to be further conducted.
- Based on this study, further chapters focus on the impact of draw solute recovery on environmental and economic life cycle assessment of FO hybrid systems (Chapter 6) and module arrangements and pressure behaviour at modular level of the FO process (Chapters 7 and 8) in order to improve and obtain more accurate, reliable and realistic economic assessment of the FO hybrid systems.

CHAPTER 6

ENVIRONMENTAL AND ECONOMIC ASSESSMENT OF HYBRID FO-RO/NF SYSTEM WITH SELECTED INORGANIC DRAW SOLUTES FOR THE TREATMENT OF MINE IMPAIRED WATER

This chapter was published as: **Kim, J. E.**; Phuntsho, S.; Chekli, L.; Choi, J. Y.; Shon, H. K., Life cycle assessment of hybrid FO-RO/NF system with selected inorganic draw solutes for the treatment of saline impaired water, *Desalination* **2018**, 429, 96-104.

6.1. Introduction

In forward osmosis (FO), selecting the most suitable draw solute is a top priority because its performance and reconcentration are ultimately related to net benefits in terms of total capital and operating costs of an FO process (Chekli et al., 2012). DS for FO applications has to meet main criteria: high solubility, high osmotic pressure, low viscosity, environmental-friendly and cost-effective recovery/reconcentration process (Bai et al., 2011; Chekli et al., 2012; Cornelissen et al., 2011; Hancock & Cath, 2009).

One of the biggest challenges in FO is the loss of draw solutes through reverse salt diffusion (RSF, J_s) across a semi-permeable FO membrane (Bowden et al., 2012a; Cath et al., 2006a; Ge et al., 2013). The RSF causes salt accumulation in the feed stream and produces an environmental issue due to stringent regulations regarding nutrient concentrations for discharging to the environment or injection wells (Blandin et al., 2016a; Holloway et al., 2015a; Phuntsho et al., 2017b). It is important that the selection of the most suitable draw solution for FO applications should be conducted based on the specific FO application (i.e. purpose) and membrane types. Achilli et al. (2010) developed a protocol for the selection of the most suitable DS using different inorganic-based DSs for FO applications using a desktop screening process and laboratory and modelling analyses. However, this study did not include an environmental and economic assessment of DSs. In addition, none of the studies carried out a direct comparison of overall environmental and economic impacts of hybrid FO systems with different DSs to select the most appropriate DS for mine wastewater treatment application.

There are several studies on the environmental and economic life cycle assessment of an FO hybrid system compared to other conventional water treatment technologies. Valladares Linares et al. (2016) investigated the life cycle cost for a hybrid FO and low-pressure reverse osmosis (LPRO) system for seawater desalination and wastewater recovery. This study reported a detailed economic analysis on capital and operational expenses (CAPEX and OPEX) for the hybrid FO-LPRO process and compared it with seawater RO (SWRO) desalination process and a membrane bioreactor-RO-advanced oxidation process (AOP) for wastewater treatment and reuse. Results showed that the

most important variables affecting the economic feasibility of the FO-LPRO system were the FO process due to a large FO membrane area required and FO module cost.

Holloway et al. (2016) further studied two potable reuse technologies: microfiltration/RO/ultraviolet AOP treatment and a hybrid ultrafiltration osmotic membrane bioreactor (UFO-MBR) using an LCA tool and methodology. Results from the LCA showed that overall environmental impact and energy consumption of UFO-MBR treatment were related to a large membrane area in FO and high power consumption in RO. However, by considering the use of RO energy recovery device and higher water permeability FO membranes, results led to the overall reduction of energy use and environmental impacts of the UFO-MBR treatment.

There is compelling empirical evidence that environmental and economic impacts of FO hybrid systems can be reduced by using FO membranes with higher water flux. However, as mentioned earlier, given the system configuration and its application, the environmental and economic impact of FO hybrid system with selected DSs should be conducted to ensure that each stage of the process has no or few impacts on the environment and overall process cost to support a full-scale FO hybrid system implementation. The main objective of the current study was to compare the environmental and economic impacts of FO hybrid systems with different DSs. Different DS recovery processes (i.e. RO and NF) were also considered to compare environmental and economic impacts of the closed-loop FO-RO and FO-NF hybrid systems using energy consumption (kWh/m³) and global warming (GW) impact in carbon dioxide equivalents (kg, CO₂-eq) as indicators. The effect of FO brine disposal and DS replenishment cost was also evaluated. The economic analysis results were finally compared with a conventional SWRO hybrid system. Through these environmental and economic evaluations, the most appropriate draw solute was therefore selected for mine impaired wastewater treatment. However, the current study did not include the effect of pre-treatment for mine impaired wastewater and fouling on the performances in the FO process of the different FO hybrid systems. Therefore, the plant lifetime was assumed based on the literature (Wittholz et al., 2008) and membrane replacement time was assumed based on our previous long-term operation of FO and NF membrane modules (Phuntsho et al., 2016b).

This chapter is an extension of a research article published by the author in Desalination (Kim et al., 2018).

6.2. Materials and methods

6.2.1. Bench-scale FO experiments

Four different draw solutes, NaCl, MgCl₂, Na₂SO₄ and MgSO₄ (Certified ACS-grade), were selected through a desktop screening process based on water flux and RSF results. Mine brackish groundwater (BGW) was employed as feed solution (FS) with total dissolved solids (TDS) of 5,568 mg/L and osmotic pressure of 3.96 bar. The other compositions of the FS are presented in our previous study (Phuntsho et al., 2016b). In FO experiments, each DS was prepared at 1 M concentration which corresponds to different osmotic pressure as presented in Table 6-1 obtained from OLI Stream Analyser 3.2 (OLI Systems, Inc., Morris Plains, NJ). In order to fairly confirm the performances of the DS recovery processes (i.e. RO and NF), the osmotic pressure of NaCl and Na₂SO₄ (i.e. monovalent and divalent ions). Besides it was assumed that MgCl₂ and MgSO₄ have the same molar concentration with NaCl and Na₂SO₄ as their osmotic pressure was around two times higher (MgCl₂) and lower (MgSO₄). It was therefore expected to have further savings in operational costs in terms of FO membrane cost and DS replenishment cost. Fig. S1 of the Supplementary Information (SI) presents the osmotic pressure, viscosity, electrical conductivity (EC) and diffusivity as a function of the concentration of the draw solutes.

A flat sheet TFC FO membrane manufactured by Toray Chemical Korea (TCK) Inc. was used for all experiments. The pure water permeability coefficient (A) and salt rejection (R) were determined under RO mode using DI water and 2 g/L sodium chloride as feed, respectively. The pressure was varied from 4 to 10 bar. The A and R values were 5.53 Lm⁻²h⁻¹bar⁻¹ and 95%. All the input parameters used for FO process simulation including water and salt fluxes (J_w and J_s), rejection (R), salt permeability (B), diffusivity (D) and structural parameter (S) values for each solution are separately shown in Table 6-2.

The effective membrane area of an acrylic FO cell was 20.02 cm² (7.7 cm in length, 2.6 cm in width, and 0.3 cm in depth). The dense active layer of the FO membrane was facing with the feed solution (AL-FS mode), and all the experiments were conducted under counter-current flow mode due to better flux stability with a lower fouling tendency (Tang et al., 2010). All FO experiments were carried out at a constant temperature of 25°C with a flow rate of 400 mL/min for 10 hrs operation time.

The performance of each DS was evaluated for water flux (J_w) and RSF (J_s). J_w was determined by measuring the change in mass of the DS tank (placed on a digital scale connected to a computer) for the duration of each experiment. The first 30 min of data was disregarded in the flux calculation to account for transport equilibration. Two different methods were used to measure RSF of draw solutes. When DI water was used as FS, the EC in the FS tank was measured at the beginning and end of each experiment. When BGW was used as FS, ion compositions in the collected samples at the beginning and end of each experiment were measured using a Perkin Elmer Elan DRC-e Inductively Coupled Plasma Mass Spectrometer.

Table 6 - 1. Characterization of DSs used for FO and feed solution for RO and NF experiments

| Chemicals | Osmotic pressure $\pi@1M$ (bar) | Hydrated diameter, 10 ⁻¹² m (Achilli et al., 2010) |
|---------------------------------|------------------------------------|--|
| NaCl | 46.77 | Cl ⁻ : 300 |
| MgCl ₂ | 92.55 | SO ₄ ²⁻ : 400 |
| Na ₂ SO ₄ | 46.01 | Na ⁺ : 450 |
| MgSO ₄ | 23.31 | Mg ²⁺ : 800 |

Table 6 - 2. Input parameters for each draw solution used for FO process simulation.

| DSs (1 M) | J_w (Lm ⁻² h ⁻¹ bar ⁻¹) | J_s (Lm ⁻² h ⁻¹) | R (%) | B (Lm ⁻² h ⁻¹) | D (m ² /s) | K (s/m) | S (μ m) |
|---------------------------------|--|--|----------|--|--------------------------|------------|-----------------|
| NaCl | 21.16 | 7.55 | 95.1 | 0.76 | 1.41E-09 | 4.21E+05 | 430 |
| MgCl ₂ | 15.23 | 2.34 | 96.8 | 0.86 | 9.36E-10 | 8.21E+05 | 618 |
| Na ₂ SO ₄ | 12.56 | 0.79 | 98.6 | 0.19 | 8.72E-10 | 8.48E+05 | 569 |
| MgSO ₄ | 8.13 | 0.42 | 98.6 | 0.27 | 5.19E-10 | 1.19E+06 | 461 |

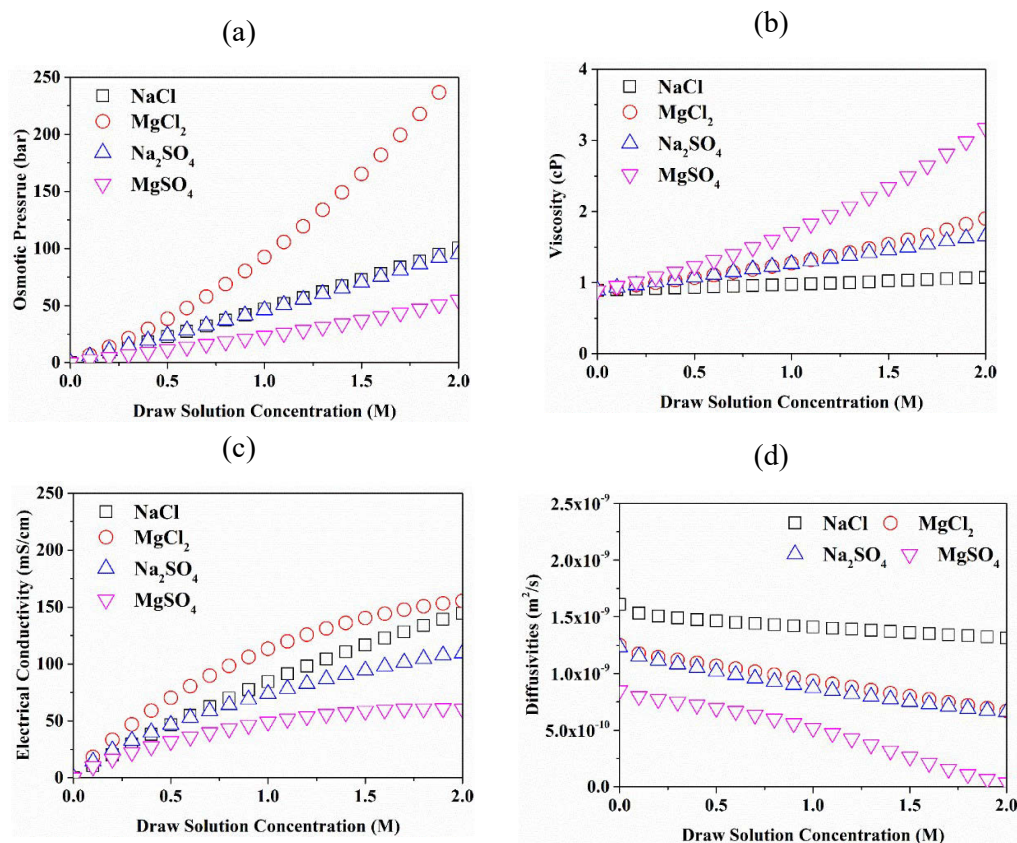


Figure 6 - 1. Thermodynamic properties of draw solutions used in this study, calculated using OLI Stream Analyser 3.2 (OLI Systems, Inc., Morris Plains, NJ) (a) Osmotic pressure, (b) viscosity (c) electrical conductivity and (d) diffusivity as a function of molar concentration of the four draw solutions at 25 °C.

6.2.2. Full-scale simulation of FO, RO and NF processes

A full-scale simulation of FO process was conducted based on a simple mass balance relationship (Liyanarachchi et al., 2016; Phuntsho et al., 2017b) and a module-scale approach (Deshmukh et al., 2015) under a closed-loop FO hybrid system since there is no commercial FO simulation software available. An 8” spiral wound TFC FO membrane module with a total membrane area of 15.3 m² (Toray Industries, Korea) was used. Mass balance equations to calculate the key solution concentrations, flow rates, water flux and salt flux are described in Table 6-3.

The Reverse Osmosis System Analysis (ROSA, Dow Filmtec, Midland, MI) software was used to simulate the performance of full-scale RO and NF processes. An 8” spiral wound polyamide RO and NF membrane modules were utilized in the RO and NF

processes (i.e. DS recovery process). Membrane module details are presented in Table 6-4. The RO and NF system design parameters including a number of stages, pressure vessels, and membrane modules were incorporated into ROSA as input parameters to meet a fixed RO and NF permeate flow rate of 100,000 m³/day. Using the OLI Stream Analyser 3.2, the final diluted DS concentrations were assumed to be equal to the osmotic pressure of BGW FS based on the principle of osmotic equilibrium. It has to be noted that only three DSs (NaCl, MgCl₂, and Na₂SO₄) were used to conduct a full-scale simulation of RO and NF processes. This will be discussed in Section 6.3.1.

Table 6 - 3. Simulation equations for a continuous close-loop FO-RO and FO-NF hybrid systems (Deshmukh et al., 2015; Phuntsho et al., 2016b; Shaffer et al., 2012).

| Modelling results | Units | Calculation |
|--|-------------|---|
| Required FO membrane area, A_{FOmem} | m^2 | $A_{FOmem} = (RR_{FO}Q_F)/J_w$ $J_w = \frac{A \left[\pi_{D,b} \exp\left(-\frac{J_w S}{D}\right) - \pi_{F,b} \exp\left(\frac{J_w}{k_F}\right) \right]}{1 + \frac{B}{J_w} \left[\exp\left(\frac{J_w}{k_F}\right) - \exp\left(-\frac{J_w S}{D}\right) \right]}$ |
| Required RO and NF membrane area, A_{ROmem} and A_{NFmem} | m^2 | $A_{RO/NFmem} = Q_p/J_w$ $J_w = A(\Delta P_{RO/NF} - \Delta\pi)$ |
| Specific energy consumption of RO and NF process | kWh/m^3 | $SEC_{RO/NF} = W_{pump}/Q_p$ $W_{pump} = (\Delta P_{RO/NF} Q_{p1})/\eta_{pump}$ |
| Initial DS flow rate at the FO inlet, $Q_{D,in}$ | m^3/day | $Q_{D,in} = Q_p \left(\frac{1}{RR_{RO/NF}} - 1 \right)$ |
| Diluted DS flow rate at the FO outlet, $Q_{Diluted DS}$ | m^3/day | $Q_{Diluted DS} = Q_{D,in} + Q_p$ |
| Mass balance for the draw solutes | | $C_{D,in}Q_{D,in} = C_{D,out}(Q_{D,in} + Q_p) + SRSF_D Q_p$ |
| Draw solution concentration in the recycled DS (RO and NF brine), $C_{D,r}$ | | $C_{D,r}Q_{D,in} = C_{D,out}(Q_{D,in} + Q_p) + C_{D,p}Q_p$ |
| Final diluted DS concentration (the feed to the post-treatment process), $C_{D,out}$ | mg/L | $C_{D,out} = (1 - RR_{RO/NF})C_{D,in} - RR_{RO/NF}SRSF_D$ |
| Draw solute concentration in RO and NF permeate, $C_{D,p}$ | mg/L | $C_{D,p} = (1 - R_{RO/NF,D})C_{D,out}$ |
| Draw solute replenishment rate, $m_{D,R}$ | $mass/time$ | $m_{D,R} = Q_p(SRSF_D + C_{D,p})$ |

- * RR_{FO} : FO feed recovery rate
- * Q_p : Permeate/Capacity
- * $P_{RO/NF}$: Applied pressure
- * $\Delta\pi$: Net osmotic pressure
- * $RR_{RO/NF}$: RO/NF feed recovery rate
- * $C_{D,in}$: Initial DS concentration
- * $SRSF_D$: Specific reverse solute flux of the draw solute
- * $R_{RO/NF}$: Solute rejection of the RO/NF membranes

Table 6 - 4. Manufacturer specifications of RO and NF membranes used in this study.

| Parameters | SW30 HR-380 | NF90-400/34i | NF270-400/34i |
|---|--------------------|--------------------------|--------------------------|
| Recovery, % | 8 | 15 | 15 |
| Effective membrane area, m ² | 35 | 37 | 37 |
| Minimum NaCl Rejection (MgSO ₄), % | 99.65 ^a | 85-95 (>97) ^b | 40-60 (>97) ^b |
| Maximum applied pressure, bar | 69 | 41 | 41 |
| Permeate flow, m ³ /d | 24.6 ^a | 28.4 ^b | 55.6 ^b |
| Specific water permeability, A (Lm ² h ⁻¹ bar ⁻¹) | 0.53 | 6.66 | 13.04 |

^a Permeate flow and salt rejection based on the following test conditions: 32 g/L NaCl, 55 bar.

^b Permeate flow and salt passage based on the following test conditions: 2 g/L NaCl, 4.8 bar.

6.3. Environmental and economic life cycle assessment

6.3.1. Environmental impact assessment

Life cycle assessment (LCA) is a method to identify potential environmental impacts of selected wastewater treatment and desalination technologies and determine factors that can be reduced (Coday et al., 2015; Hancock et al., 2012; Holloway et al., 2016; Valladares Linares et al., 2016). LCA consists of four phases, including goal and scope definition, life cycle inventory analysis (LCI), life cycle impact assessment (LCIA), and interpretation (Pryshlakivsky & Searcy, 2013). The first two phases define the detailed objectives and input data collection from experimental and simulation results. Finally, the LCIA and its interpretation are discussed in the results and discussion section.

The system boundaries of the current study are shown in Figure 6-2. Material surveys including construction, maintenance and operational phases were undertaken by utilising the currently available data published in the literature (Coday et al., 2015; Hancock et al., 2012; Holloway et al., 2016; Valladares Linares et al., 2016) and Ecoinvent LCA database v. 3.0 and Australian LCA database in Simapro software v. 8.1.1. The detailed and calculated data are shown in Table 6-5. Based on the LCI analysis, the LCIA was carried out using the Australian indicator set v.3.0 and thus an environmental impact was then evaluated using global warming indicator (GW, kg CO₂-eq) (PRé-Consultants, 1998). However, the current study did not include the effect of pre-treatment for mine impaired wastewater and membrane fouling on the performances of the different FO hybrid systems. It has to be noted here that the plant lifetime was assumed based on the literature

(Wittholz et al., 2008) and membrane replacement time was assumed based on our previous long-term operation of FO and NF membrane modules (Phuntsho et al., 2016b).

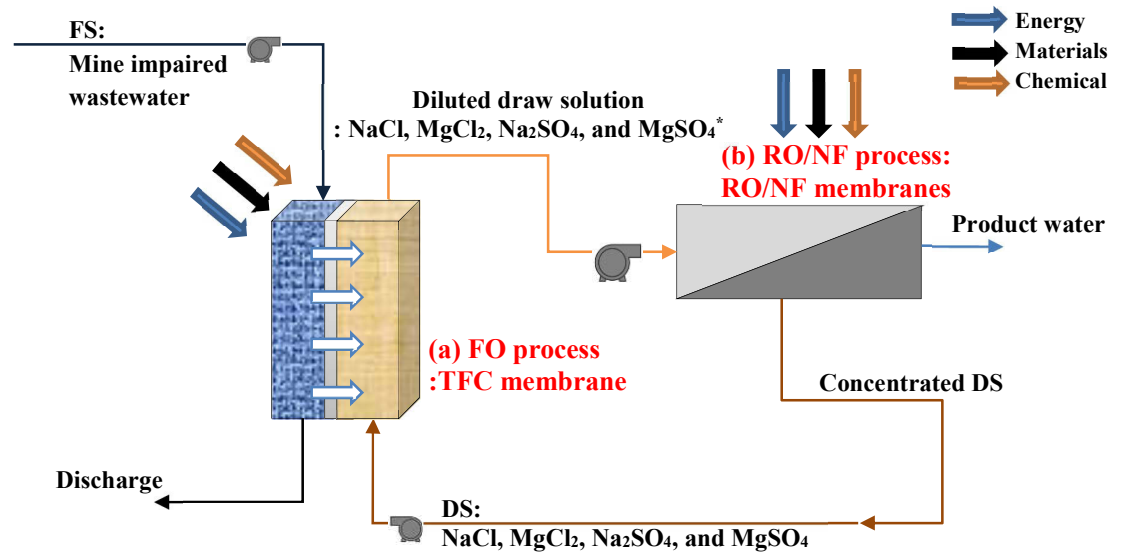


Figure 6 - 2. A schematic diagram of a closed-loop FO and RO/NF hybrid system operation. *MgSO₄ was excluded for a simulation of the post-treatment processes due to its poor performance in the FO process (see Section 6.4.1).

Table 6 - 5. Life cycle inventory data for all unit processes.

| System | Product Flow | Item/material | Grade | SimaPro Material Designation | NaCl, kg/m ³ | MgCl ₂ , kg/m ³ | Na ₂ SO ₄ , kg/m ³ |
|------------------------|---------------------------|---|--|--|--|---------------------------------------|---|
| <i>Forward Osmosis</i> | <i>Infrastructure</i> | Feed strainer housing/basket | Stainless steel, 316, high temp | Stainless steel hot rolled coil, annealed & pickled, elec. arc furnace route, prod. mix, grade 304 RER S | 2.95E-04 | 5.08E-04 | 6.05E-04 |
| | | Pressure vessel middle membrane connector | ABS | Acrylonitrile-butadiene-styrene copolymer, ABS, at plant/RER U | 5.00E-05 | 8.61E-05 | 1.03E-04 |
| | | Pressure vessel end adaptors | CPVC | PVC injection moulding E | 8.47E-05 | 1.46E-04 | 1.74E-04 |
| | | 1" CPVC pipe | Schedule 80 | PVC Pipe E | 3.69E-04 | 6.36E-04 | 7.58E-04 |
| | | 4" CPVC pipe | Schedule 80 | PVC Pipe E | 7.39E-04 | 1.27E-03 | 1.52E-03 |
| | | 3"x3" square tube 1/4" Thick | Mild steel | Hot rolled sheet, steel, at plant/RNA | 7.09E-03 | 1.22E-02 | 1.45E-02 |
| | | 2"x2" square tube 1/4" Thick | Mild steel | Hot rolled sheet, steel, at plant/RNA | 9.81E-03 | 1.69E-02 | 2.01E-02 |
| | | High profile unistrut | Mild steel - zinc coating (gold) | Galvanized steel sheet, at plant/RNA | 3.41E-04 | 5.87E-04 | 7.00E-04 |
| | | Tanks, HDPE | NA | Polyethylene, HDPE, granulate, at plant/RER U | 7.86E-03 | 1.35E-02 | 1.61E-02 |
| | | Pressure vessels | Filament wound, epoxy FRP | Glass fibre reinforced plastic, polyester resin, hand lay-up, at plant/RER U | 5.52E-03 | 9.50E-03 | 1.13E-02 |
| | <i>Membrane Materials</i> | Membrane active layer | Polyamide | Viscose fibres, at plant/GLO U | 6.06E-04 | 1.04E-03 | 1.24E-03 |
| | | Membrane support layer | Polysulfone | Glass fibre reinforced plastic, polyester resin, hand lay-up, at plant/RER U | 3.13E-03 | 5.39E-03 | 6.42E-03 |
| | | Glue | Polyurethane | Polyurethane, flexible foam, at plant/RER U | 2.67E-03 | 4.59E-03 | 5.47E-03 |
| | | Sealant tape | SPVC | Polyvinylchloride, suspension polymerised, at plant/RER U | 1.10E-04 | 1.89E-04 | 2.25E-04 |
| | | Filament tape | Polypropylene backing with fibrglass straps | Oriented polypropylene film E | 3.60E-04 | 6.20E-04 | 7.39E-04 |
| | | Feed spacer | Polystyrene | Polystyrene, general purpose, GPPS, at plant/RER U | 6.24E-03 | 1.07E-02 | 1.28E-02 |
| | | Draw solution spacer | Polyester | Glass fibre reinforced plastic, polyester resin, hand lay-up, at plant/RER U | 1.12E-02 | 1.92E-02 | 2.29E-02 |
| | | Centre core flow adapters and anti-telescoping device | ABS | Acrylonitrile-butadiene-styrene copolymer, ABS, at plant/RER U | 6.04E-04 | 1.04E-03 | 1.24E-03 |
| | | Centre core | CPVC | PVC Pipe E | 1.02E-03 | 1.76E-03 | 2.10E-03 |
| | | <i>Chemical use</i> | DS | NaCl | Sodium chloride,power,at plant/RER U/AusSD U | 6.54E-01 | |
| | | | MgCl ₂ | Chlorine, Liquid (Afshin Hemmatyar & Farzaneh) magnesium production,electrolysis Alloc Def, U | | 2.92E-01 | |
| | | | Na ₂ SO ₄ | Sodium sulphate,power,production mix,at plant/RER U/AusSD U | | | 2.82E-01 |
| | | | HCl | Hydrochloric acid,from Mannheim process,at plant/RER U/AusSD U | 3.84E-05 | 6.58E-05 | 7.67E-05 |
| Cleaning | NaOH | | Sodium hydroxide,50% in H ₂ O, production mix, at plant/RER U/AusSD U | 3.84E-05 | 6.58E-05 | 7.67E-05 | |
| <i>Reverse Osmosis</i> | <i>Infrastructure</i> | 1" CPVC pipe | Schedule 80 | PVC Pipe E | 1.28E-04 | 1.30E-04 | 1.27E-04 |
| | | 1 1/2" CPVC pipe | Schedule 80 | PVC Pipe E | 1.24E-04 | 1.25E-04 | 1.23E-04 |

| System | Product Flow | Item/material | Grade | SimaPro Material Designation | NaCl, kg/m ³ | MgCl ₂ , kg/m ³ | Na ₂ SO ₄ , kg/m ³ |
|------------------------------|---------------------------|---|----------------------------------|---|-------------------------|---------------------------------------|---|
| | | 1" 316 SS pipe | 316 SS | Stainless Steel hot rolled, annealed & pickled, elec. Arc furnace... | 1.53E-04 | 1.54E-04 | 1.51E-04 |
| | | I-Beam - wide flange, 6", 20# | Mild steel | Hot rolled sheet, steel, at plant/RNA | 8.83E-04 | 8.92E-04 | 8.72E-04 |
| | | I-Beam - wide flange, 4", 13# | Mild steel | Hot rolled sheet, steel, at plant/RNA | 7.04E-03 | 7.11E-03 | 6.95E-03 |
| | | 2"x2" square tube 1/4" Thick | Mild steel | Hot rolled sheet, steel, at plant/RNA | 2.03E-03 | 2.05E-03 | 2.00E-03 |
| | | High profile unistrut | Mild steel - zinc coating (gold) | Galvanized steel sheet, at plant/RNA | 5.87E-05 | 5.93E-05 | 5.80E-05 |
| | | Low profile unistrut | Mild steel - zinc coating (gold) | Galvanized steel sheet, at plant/RNA | 2.40E-04 | 2.43E-04 | 2.37E-04 |
| | | Pressure vessels | Filament wound, epoxy FRP | Glass fibre reinforced plastic, polyester resin, hand lay-up, at plant/RER U | 2.43E-03 | 2.68E-03 | 2.19E-03 |
| | <i>Membrane Materials</i> | Membrane active layer | Polyamide thin film composite | Polyamide 6.6 fibres (PA 6.6), from adipic acid and hexamethylene diamine (HDMA), prod. Mix, EU-27S | 5.46E-04 | 6.03E-04 | 4.92E-04 |
| | | Glue | Epoxy | Polyurethane, flexible foam, at plant/RER U | 1.19E-07 | 7.85E-07 | 6.40E-07 |
| | | Feed spacer | Polyethylene. | Polyethylene, HDPE, granulate, at plant/RER U | 4.38E-04 | 1.00E-03 | 8.15E-04 |
| | | Permeate spacer | Polyethylene. | Polyethylene, HDPE, granulate, at plant/RER U | 2.50E-04 | 5.99E-04 | 4.88E-04 |
| | | End caps | PVC | PVC injection moulding E | 3.04E-05 | 3.35E-05 | 2.73E-05 |
| | | Fiber glass shell | Fiber glass | Glass fibre reinforced plastic, polyester resin, hand lay-up, at plant/RER U | 5.28E-04 | 5.83E-04 | 4.75E-04 |
| | | PVC (permeate tube) | PVC | PVC pipe E | 1.32E-04 | 1.45E-04 | 1.18E-04 |
| | <i>Chemical use</i> | | NaCl | | 2.30E-02 | | |
| | | DS | MgCl ₂ | | | 1.00E-02 | |
| | | | Na ₂ SO ₄ | | | | 8.00E-03 |
| | | Cleaning | HCl | Hydrochloric acid,from Mannheim process,at plant/RER U/AusSD U | 4.38E-05 | 4.38E-05 | 4.38E-05 |
| | | | NaOH | Sodium hydroxide,50% in H ₂ O, production mix, at plant/RER U/AusSD U | 4.38E-05 | 4.38E-05 | 4.38E-05 |
| <i>Nanofiltration (NF90)</i> | <i>Infrastructure</i> | Bosch Rexroth aluminum structural framing | Aluminum 4545 (8981 004 744) | Aluminum, primary, ingot, at plant/RNA | 1.59E-03 | 1.72E-03 | 1.55E-03 |
| | | 1" CPVC pipe | Schedule 80 | PVC Pipe E | 3.63E-04 | 3.93E-04 | 3.55E-04 |
| | | 3/4" 316 SS tubing | 316L Sch 40 | Stainless Steel hot rolled, annealed & pickled, elec. Arc furnace... | 6.64E-04 | 7.18E-04 | 6.49E-04 |
| | | Pressure vessels | Filament wound, epoxy FRP | Glass fibre reinforced plastic, polyester resin, hand lay-up, at plant/RER U | 1.96E-03 | 2.39E-03 | 1.96E-03 |
| | <i>Membrane Materials</i> | Membrane active layer | Polyamide thin film composite | Polyamide 6.6 fibres (PA 6.6), from adipic acid and hexamethylene diamine (HDMA), prod. Mix, EU-27S | 9.74E-06 | 1.18E-05 | 9.71E-06 |
| | | Glue | Epoxy | Polyurethane, flexible foam, at plant/RER U | 6.80E-06 | 2.96E-06 | 2.43E-06 |
| | | Feed spacer | Polyethylene. | Polyethylene, HDPE, granulate, at plant/RER U | 6.14E-05 | 1.94E-05 | 1.59E-05 |
| | | Permeate spacer | Polyethylene. | Polyethylene, HDPE, granulate, at plant/RER U | 5.87E-05 | 6.04E-05 | 4.96E-05 |
| | | End caps | PVC | PVC injection moulding E | 2.45E-05 | 1.83E-05 | 1.50E-05 |

| System | Product Flow | Item/material | Grade | SimaPro Material Designation | NaCl, kg/m ³ | MgCl ₂ , kg/m ³ | Na ₂ SO ₄ , kg/m ³ |
|-------------------------------|---------------------------|---|---------------------------------|---|-------------------------|---------------------------------------|---|
| | | Fiber glass shell | Fiber glass | Glass fibre reinforced plastic, polyester resin, hand lay-up, at plant/RER U | 1.50E-05 | 1.27E-05 | 1.04E-05 |
| | <i>Chemical use</i> | PVC (permeate tube) | PVC | PVC pipe E | 1.04E-05 | 1.27E-05 | 1.04E-05 |
| | | DS | NaCl | | 7.55E-01 | | |
| | | | MgCl ₂ | | | 4.43E-01 | |
| | | | Na ₂ SO ₄ | | | | 2.45E-01 |
| | | Cleaning | HCl | Hydrochloric acid,from Mannheim process,at plant/RER U/AusSD U | 4.38E-05 | 4.38E-05 | 4.38E-05 |
| | | | NaOH | Sodium hydroxide,50% in H ₂ O, production mix, at plant/RER U/AusSD U | 4.38E-05 | 4.38E-05 | 4.38E-05 |
| <i>Nanofiltration (NF270)</i> | <i>Infrastructure</i> | Bosch Rexroth aluminum structural framing | Aluminum 4545 (8981 004 744) | Aluminum, primary, ingot, at plant/RNA | 6.30E-04 | 1.37E-03 | 1.09E-03 |
| | | 1" CPVC pipe | Schedule 80 | PVC Pipe E | 1.44E-04 | 3.13E-04 | 2.48E-04 |
| | | 3/4" 316 SS tubing | 316L Sch 40 | Stainless Steel hot rolled, annealed & pickled, elec. Arc furnace... | 2.63E-04 | 5.73E-04 | 4.54E-04 |
| | | Pressure vessels | Filament wound, epoxy FRP | Glass fibre reinforced plastic, polyester resin, hand lay-up, at plant/RER U | 2.71E-04 | 5.90E-04 | 4.67E-04 |
| | <i>Membrane Materials</i> | Membrane active layer | Polyamide thin film composite | Polyamide 6.6 fibres (PA 6.6), from adipic acid and hexamethylene diamine (HDMA), prod. Mix, EU-27S | 3.31E-06 | 7.22E-06 | 5.71E-06 |
| | | Glue | Epoxy | Polyurethane, flexible foam, at plant/RER U | 9.38E-07 | 2.04E-06 | 1.62E-06 |
| | | Feed spacer | Polyethylene. | Polyethylene, HDPE, granulate, at plant/RER U | 4.15E-07 | 9.04E-07 | 7.15E-07 |
| | | Permeate spacer | Polyethylene. | Polyethylene, HDPE, granulate, at plant/RER U | 3.97E-07 | 8.64E-07 | 6.84E-07 |
| | | End caps | PVC | PVC injection moulding E | 2.45E-05 | 2.45E-05 | 2.45E-05 |
| | | Fiber glass shell | Fiber glass | Glass fibre reinforced plastic, polyester resin, hand lay-up, at plant/RER U | 2.07E-06 | 4.51E-06 | 3.57E-06 |
| | <i>Chemical use</i> | PVC (permeate tube) | PVC | PVC pipe E | 1.43E-06 | 3.13E-06 | 2.48E-06 |
| | | DS | NaCl | | 3.68E+00 | | |
| | | | MgCl ₂ | | | 4.23E+00 | |
| | | | Na ₂ SO ₄ | | | | 1.86E+00 |
| | | Cleaning | HCl | Hydrochloric acid,from Mannheim process,at plant/RER U/AusSD U | 2.19E-05 | 4.38E-05 | 4.38E-05 |
| | | | NaOH | Sodium hydroxide,50% in H ₂ O, production mix, at plant/RER U/AusSD U | 2.19E-05 | 4.38E-05 | 4.38E-05 |

6.3.2. Economic life cycle assessment

An economic analysis on CAPEX and OPEX of three different hybrid systems: FO-RO, FO-NF90 and FO-NF270 (90 and 270 refer to two different types of commercial NF membranes, Filmtech Dow Chemicals), was conducted. The total water cost ($\$/\text{m}^3$) of each hybrid system was compared based on a production capacity of 100,000 m^3/day . The results of the FO hybrid systems were compared with the results of a conventional reverse osmosis hybrid system.

The capital construction costs may vary if considering the logistics and impacts of transporting chemicals and materials to the site. Thus, the CAPEX cost analysis was conducted without considering a specific site. This study used literature information with approximations based on global trends and real data from the commercially available products in the market (e.g. cost of membrane modules and chemicals). The unit cost of each FO, RO, and NF membrane module was found in the literature as presented in Table 6-6 (Bigbrandwater, 2016; Coday et al., 2015).

The cleaning strategies for RO and NF were considered to be periodic chemical cleaning (once a year). FO membrane cleaning strategies were considered to be periodic hydraulic cleaning and eventual chemical cleaning although recent studies demonstrated that physical cleaning was very efficient and easy to apply for FO process (Lotfi et al., 2017; Phuntsho et al., 2016b). The amount of chemical required for cleaning process was calculated based on the manufacturer's recommendation (DowChemical, 2017). From the process performance simulation, the number of elements and pressure vessels was obtained. Then, a size of a cleaning tank (i.e. cleaning solution volume) was roughly calculated using the empty pressure vessels volume. The chemical cost was therefore evaluated based on the amount of the cleaning chemical during the cleaning process, and this study considered NaOH and HCl as cleaning chemicals for hybrid systems. It has to be acknowledged that cleaning strategies for the FO process should be determined by its applications as it affects the environmental and economic assessment of the whole process. In addition, DS replenishment cost was calculated using a specific RSF value (SRSF, J_s/J_w , g/L), which is directly related to the process efficiency and sustainability. The specific cost of each draw solute was determined based on the mass of solute needed to

produce one litre of diluted DS with an initial concentration of 1 M. An illustrative summary of the cost parameters considered for the economic analysis is shown in Figure 6-3, and specific economic values are presented in Table 6-6.

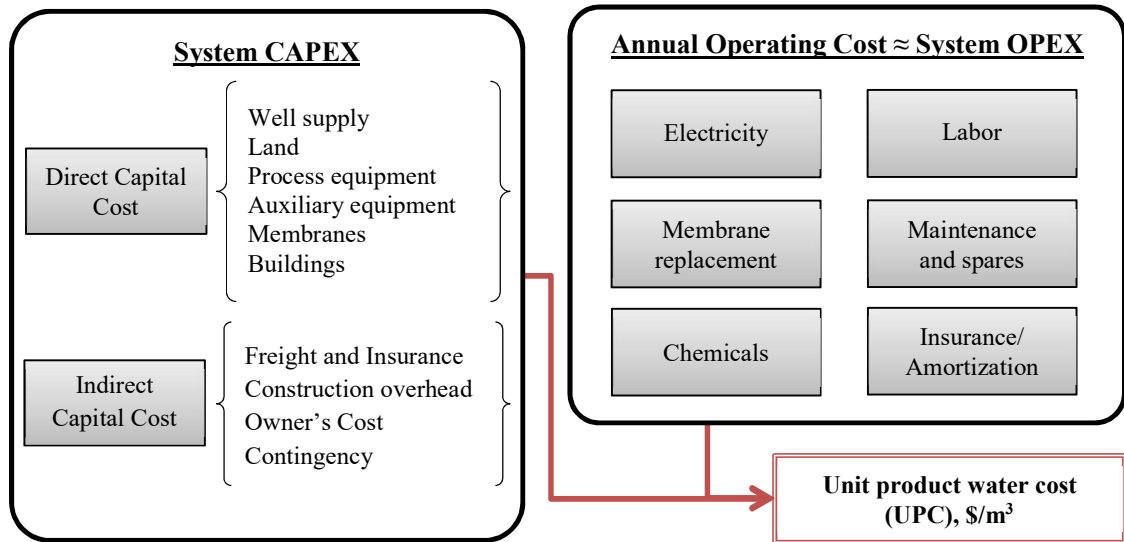


Figure 6 - 3. Specific parameters for cost estimation for desalination processes.

Table 6 - 6. Economic values used in cost analysis for desalination processes (Australian dollar).

| Parameters | Unit | Values |
|---|--------------------------------|---------------------|
| Plant | | |
| Plant capacity | m ³ /day | 100,000 |
| Plant availability (Wittholz et al., 2008) | | 0.95 |
| Plant lifetime (Wittholz et al., 2008) | year | 20 |
| ^a Electricity price (Mountain, 2012) | \$/kWh | 0.29 |
| Membranes | | |
| RO membrane element cost (Filter, 2016) | \$ | 1,161 |
| NF 90 membrane element cost (Filter, 2016) | \$ | 1,092 |
| NF 270 membrane element cost (Americanro, 2016) | \$ | 987 |
| ^b FO membrane element cost | \$ | 1,161 |
| Pressure vessel (7elements/PV) (Moch et al., 2008; Valladares Linares et al., 2016) | \$ | 1,690 |
| Draw solution (Achilli et al., 2010) | | |
| | Unit cost ^c , \$/kg | Specific cost, \$/L |
| NaCl | 19 | 1.11 |
| MgCl ₂ | 37 | 3.52 |
| Na ₂ SO ₄ | 11 | 1.56 |
| MgSO ₄ | 68 | 8.19 |

^a Electricity price in Australia.

^b FO membrane cost was assumed to be the same as the cost of RO module.

^c USD 1\$ = AUD 1.3\$: August. 2016

The CAPEX cost for FO process was calculated using the specific cost of economic parameters of FO process reported in the recent studies (Coday et al., 2015; Valladares Linares et al., 2016). In addition, the CAPEX cost for RO and NF processes was estimated using a capacity and capital cost correlation used in engineering practice was utilized. This is called the power law rule as followed:

$$\left(\frac{\text{Capital cost}_{\text{plant 1}}}{\text{Capital cost}_{\text{plant 2}}}\right) = \left(\frac{\text{Plant capacity}_{\text{plant 1}}}{\text{Plant capacity}_{\text{plant 2}}}\right)^m \quad (6-1)$$

where the power law exponent, m , is usually 0.8 and 0.74 for SWRO and brackish water RO (BWRO), respectively. Those values were determined from the cost database analysis conducted elsewhere (Chilton, 1950; Wittholz et al., 2008). In the present study, 0.74 was therefore used for RO and NF processes. Mathematical formulations used to calculate the annualized capital cost ($\$/\text{m}^3$) are shown as follow (Poullikkas, 2001):

$$\text{Capital amortization } (\alpha) = \frac{i(1+i)^n}{(1+i)^n - 1} \quad (6-2)$$

$$\text{Capital recovery } (C_R), \$ = \alpha \times \text{Total capital cost } (C_T) \quad (6-3)$$

$$\begin{aligned} \text{Annual capital recovery cost } (C_A), \$/\text{m}^3 \\ = \frac{C_R}{365 \times \text{Plant capacity } (\text{m}^3/\text{d}) \times \text{Plant availability}} \end{aligned} \quad (6-4)$$

where the total cost is the sum of the direct and indirect capital costs in Fig. 2., i is the interest rate of 6%, n is the number of years of the project fixed at 20 years, 365 corresponds to the number of days in a year and 0.95 is plant availability due to down time.

The OPEX costs including membranes, chemicals and electricity were calculated based on the results of a full-scale simulation and ROSA software and the values in Table 2. Labour and maintenance were calculated based on the reported percentages in the literature (Valladares Linares et al., 2016). Finally, the OPEX cost was calculated based on a yearly basis cost. The total cost per m^3 of water is the sum of unit CAPEX and OPEX costs. All the calculated data are presented in Table 6-7.

Table 6 - 7. Typical cost parameters for desalination plant, values of FO hybrid plant were estimated based on the literature, simulation and optimization of currently available desalination plant (100,000 m³/day).

| Parameter Draw solution type | SWRO | FO-RO | | | FO-NF90 | | | FO-NF270 | | |
|---|--------------|--------------|-------------------|---------------------------------|--------------|-------------------|---------------------------------|--------------|-------------------|---------------------------------|
| | | NaCl | MgCl ₂ | Na ₂ SO ₄ | NaCl | MgCl ₂ | Na ₂ SO ₄ | NaCl | MgCl ₂ | Na ₂ SO ₄ |
| Equipment (Major equipment, auxiliary equipment, and land and construction) | 145.9 | | 215.1 | | | 190.6 | | | 190.6 | |
| ¹ Membranes | | | | | | | | | | |
| Elements | 8.6 | 29.0 | 46.3 | 54.1 | 30.6 | 48.4 | 55.6 | 26.3 | 46.4 | 53.2 |
| Pressure vessels | 2.4 | 6.0 | 9.6 | 11.2 | 6.4 | 10.2 | 11.6 | 5.6 | 9.8 | 11.2 |
| a.Total Direct Capital Cost | 156.9 | 250.0 | 271.0 | 280.4 | 227.6 | 249.1 | 257.8 | 222.5 | 246.8 | 255.0 |
| ² Freight and Insurance | 7.8 | 12.5 | 13.6 | 14.0 | 11.4 | 12.5 | 12.9 | 11.1 | 12.3 | 12.8 |
| ³ Construction overhead | 23.5 | 37.5 | 40.7 | 42.1 | 34.1 | 37.4 | 38.7 | 33.4 | 37.0 | 38.3 |
| ⁴ Owner's cost | 15.7 | 25.0 | 27.1 | 28.0 | 22.8 | 24.9 | 25.8 | 22.2 | 24.7 | 25.5 |
| ⁵ Contingency | 15.7 | 25.0 | 27.1 | 28.0 | 22.8 | 24.9 | 25.8 | 22.2 | 24.7 | 25.5 |
| b.Total Indirect Capital Cost | 62.8 | 100.0 | 108.4 | 112.2 | 91.0 | 99.6 | 103.1 | 89.0 | 98.7 | 102.0 |
| CAPEX:Fixed capital investment (a+b) | 219.7 | 350.1 | 379.4 | 392.6 | 318.6 | 348.8 | 360.9 | 311.4 | 345.5 | 357.0 |
| Electrical energy price | 150.9 | 26.4 | 27.3 | 24.9 | 7.9 | 8.8 | 5.6 | 8.4 | 9.3 | 6.2 |
| Membrane replacement | 12.4 | 4.4 | 6.9 | 8.0 | 4.7 | 7.3 | 8.3 | 3.9 | 6.9 | 7.8 |
| Chemicals | 19.5 | 36.5 | 83.5 | 31.1 | 36.5 | 83.5 | 31.2 | 36.5 | 83.6 | 31.2 |
| Labour | | | | | | | | | | |
| Cartridge Filters | | | | | | | | | | |
| Repairs and Replacement | 32.3 | 11.9 | 20.8 | 11.3 | 8.7 | 17.6 | 8 | 8.6 | 17.6 | 8 |
| Insurance | | | | | | | | | | |
| Lab fees | | | | | | | | | | |
| OPEX:Annual operating and maintenance | 215.1 | 79.2 | 138.4 | 75.4 | 57.8 | 117.2 | 53.1 | 57.4 | 117.4 | 53.2 |
| Total cost per m³ of water produced | 1.04 | 1.03 | 1.24 | 1.12 | 0.90 | 1.11 | 0.99 | 0.88 | 1.11 | 0.98 |

¹ RO and NF: 7 modules/pressure vessel and FO: 7 modules/pressure vessel (PV).

² 5% of the direct capital costs (Ettouney et al., 2002).

³ 15% of the direct capital costs (Ettouney et al., 2002).

⁴ 10% of the direct capital costs (Ettouney et al., 2002).

⁵ 10% of the direct capital costs (Ettouney et al., 2002).

6.4. Results and discussion

6.4.1. Draw solute performances

In order to fairly confirm the performances of the DS recovery processes (i.e. RO and NF), the similar osmotic pressure of NaCl and Na₂SO₄ (i.e. monovalent and divalent ions) was assumed. Besides it was assumed that MgCl₂ and MgSO₄ have the same molar concentration with NaCl and Na₂SO₄ as their osmotic pressure was around two times higher (for MgCl₂) and lower (for MgSO₄). It is therefore expected to have further savings in operational costs in terms of FO membrane cost and DS replenishment cost.

Table 6-8 shows the water flux, RSF and SRSF in the FO process using four different DSs with FS concentration of around 5.6 g/L BGW. The water flux and RSF followed the order of NaCl > MgCl₂ > Na₂SO₄ > MgSO₄, corresponding to osmotic pressures of 46.7, 92.5, 46.0, and 23.3 bar for 1 M DSs. Although the osmotic pressure of MgCl₂ shows the highest, the water flux was significantly lower than with NaCl (around 38% lower). This is mainly due to the viscosity of NaCl; 0.97, 1.27, 1.26, and 1.71 cP for 1M NaCl, MgCl₂, Na₂SO₄ and MgSO₄, respectively (Achilli et al., 2010; Johnson et al., 2017; Li et al., 2014; Phuntsho et al., 2013b). This result underscores the importance of having a low viscosity draw solute as this allows easy pumping around the system and higher water flux. The reason why MgSO₄ had the lowest water flux and RSF is due to its lowest osmotic pressure and highest viscosity. In addition to that, DSs containing larger-sized hydrated anions (i.e. MgSO₄ and Na₂SO₄) showed the lowest RSF values, regardless of their paired cations and this is consistent with a previous study (Achilli et al., 2010). Based on this experimental evaluation, MgSO₄ was excluded for further investigations due to its poor performance results.

Table 6 - 8. FO experimental water flux (J_w), RSF (J_s), and SRSF (J_s/J_w) behaviors using 1 M DSs with BGW as FS in the FO process.

| DSs | $J_w, \text{Lm}^{-2}\text{h}^{-1}$ | $J_s, \text{gm}^{-2}\text{h}^{-1}$ | $J_s/J_w, \text{g/L}$ |
|---------------------------------|------------------------------------|------------------------------------|-----------------------|
| NaCl | 14.54 | 9.49 | 0.65 |
| MgCl ₂ | 9.00 | 2.61 | 0.29 |
| Na ₂ SO ₄ | 7.02 | 1.98 | 0.28 |
| MgSO ₄ | 3.99 | 0.84 | 0.21 |

6.4.2. Evaluation of the DS reconcentration in RO and NF processes

Table 6-9 shows the performance results of RO and NF processes obtained from the ROSA software. The RO process shows the highest removal efficiency of Na₂SO₄, which is around 98.8% followed by MgCl₂ and NaCl (98.3 and 97.7%, respectively). Therefore, when Na₂SO₄ is used as DS in the FO process, utilizing the RO process as a DS recovery process would be more beneficial to obtain high quality of product water.

However, the NF processes with two different NF membrane modules of NF90 and NF270 show poor rejection rate of NaCl (71.4% for NF90 and 48.1% for NF270). This indicates that utilizing NaCl as DS in the FO process would result in poor rejection rates of the NF processes. Nevertheless, the NF processes show much higher rejection rates with Na₂SO₄, 88.0% for NF90 and 76.8% for NF270. These results indicate that the use of divalent ions in an FO hybrid system could be more advantageous as it shows lower DS loss in FO and higher rejection in RO/NF (Johnson et al., 2017). This confirms that the physio-chemical properties of the draw solutes including a high osmotic pressure, a low viscosity and a high diffusion coefficient are of paramount importance.

Table 6 - 9. ROSA software simulation results of RO and NF processes using different RO and NF membrane modules (Version 9.1, Filmtech Dow Chemicals, USA).

| Membranes (Filmtech™ membranes) | Feed solution ^a | Rejection, % | Permeate, mg/L TDS |
|---------------------------------------|--|--------------|-----------------------|
| SW30HR-380 | NaCl | 99.6 | 23 |
| | MgCl ₂ | 99.9 | 10 |
| | Na ₂ SO ₄ | 99.9 | 8 |
| NF 90-400/34i | NaCl | 87.1 | 755 |
| | MgCl ₂ | 94.0 | 443 |
| | Na ₂ SO ₄ | 96.5 | 245 |
| NF 270-400/34i ^b | NaCl ^b | 48.1 | 3,024 |
| | MgCl ₂ | 46.8 | 3,947 |
| | Na ₂ SO ₄ ^b | 76.8 | 1,577 |

^a The concentrations of the feed solution in RO and NF processes corresponded to the osmotic pressure of feed water in FO process under the osmotic equilibrium condition (≈ 3.96 bar).

^b The ROSA was not able to conduct on NF270 with NaCl and Na₂SO₄ thus the RO experiments were conducted under the conditions of flow rate of 400 mL/min, temperature of 25°C, membrane cell area of 0.0068 m² and operating pressure of 25 bar.

6.4.3. Environmental impact assessment of FO hybrid systems

6.4.3.1. Baseline environmental life cycle assessment

The environmental impact of FO-hybrid systems in terms of global warming (GW, kg CO₂-eq) was evaluated for the production of 100,000 m³/day of reusable water. Figure 6-4 shows the relative contribution analysis of the FO hybrid systems to GW impact without (Figure 6-4 (a)) and with (Figure 6-4 (b)) DS replenishment in the FO process.

Figure 6-4 (a) clearly shows that the predominant contribution to the GW impact comes from FO membrane material required and RO and NF energy use for all hybrid systems. These results are similar to previous research conducted by other research groups (Coday et al., 2015; Hancock et al., 2012; Raluy et al., 2005c).

However, in a closed-loop hybrid system, the draw solute loss during the system operation must be replenished to maintain the same initial DS concentration in the FO process (Achilli et al., 2010; Holloway et al., 2015a). Using a simple mass balance relationship in the FO process, the mass of the total draw solute replenishment ($m_{D,R}$, kg/d) was estimated using equations described in Table 6-3. Figure 6-4 (b) therefore shows that when considering the DS replacement for each hybrid system, the contribution of chemical use to the GW impact becomes significant compared to the results presented in Figure 6-4 (a).

Specifically, the contribution of the total DS replenishment in FO-RO hybrid system with all DSs shows the lowest mainly because of the higher salt rejection in the RO process (i.e. the lowest draw solute loss via RO permeate). However, FO-NF hybrid systems with all DSs show the greatest increase in the total chemical contribution (FO and NF) to the GW impact. For example, the contribution of the chemical use in the FO-NF90 is around 30% while that in the FO-NF270 is around 55%. This is because the draw solute loss through NF permeate is more significant than RO permeate. Interestingly, Na₂SO₄ shows a slightly higher contribution to the GW impact despite its lower SRSF in FO and higher rejection rates in RO and NF. These results indicate that the manufacturing process required to produce Na₂SO₄ could have more negative impacts on the environment. Thus,

the FO hybrid system with Na₂SO₄ does not appear environmentally favorable. Although the results suggest that the overall environmental impacts of all three hybrid systems would be attributed to the amount of DS replenishment needed, the DS replenishment cost in each hybrid process has to be considered as one of the main OPEX cost parameters (Achilli et al., 2010). Hence, a cost analysis of each hybrid system with different DSs will be discussed in the following section 6.3.4.

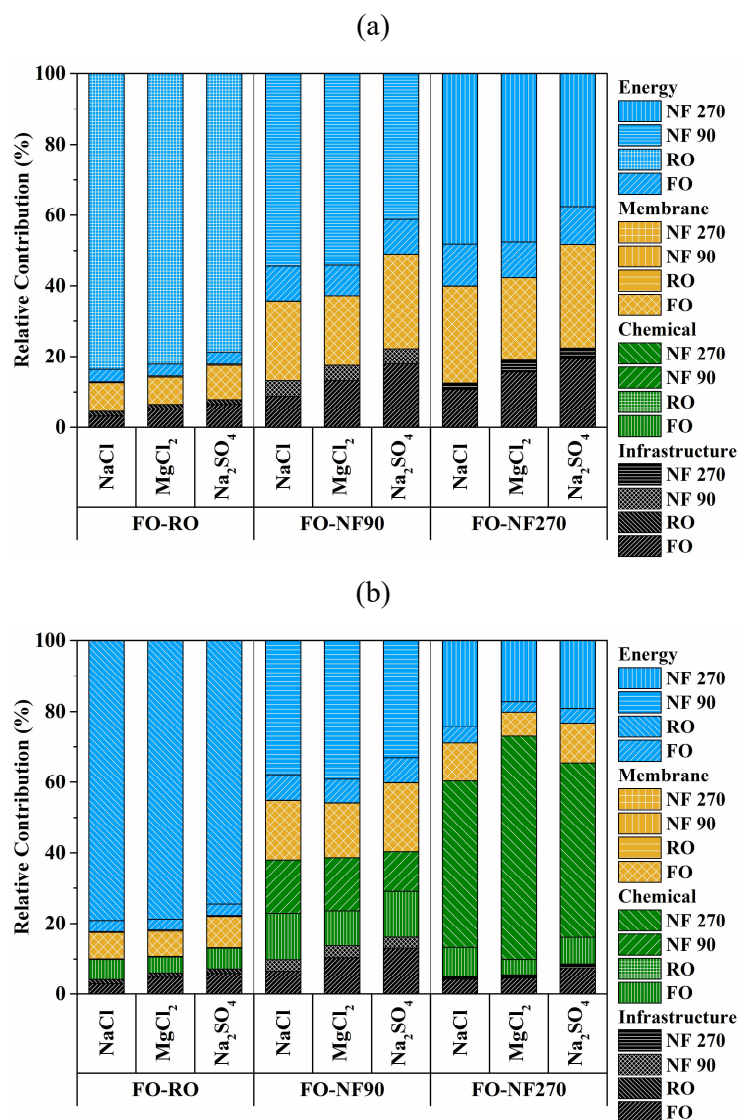


Figure 6 - 4. Relative contribution analysis of various components of the FO-RO and FO-NF hybrid systems with DSs to global warming impact (a) without DS replenishment and (b) with DS replenishment in FO hybrid systems.

6.4.3.2. Impact of operational adjustment of FO-NF hybrid system

The required potable water quality targeted in this study was a TDS concentration of less than 500 mg/L (NHMRC 2011) whereas, the required non-potable water quality was a TDS concentration of less than 1,000 mg/L, which can be applied for most turf grass irrigation (Holloway et al., 2016; Phuntsho et al., 2012 a). Although energy requirement of the FO-RO hybrid systems was higher than other hybrid systems, the final water quality was much lower than 500 mg/L TDS (data are shown in Table 4). Thus, this indicates that the final product water from the FO-RO hybrid system is reusable water (potable and/or non-potable). In this section, the initial performance of NF process with NF90 and NF270 membrane modules was therefore adjusted to achieve NF permeate quality as good as RO permeate (around 100 mg/L). Power consumptions for each FO-NF hybrid system were calculated based on producing final target concentration of 100 mg/L TDS. It has to be understood that there is a slight difference between the SEC of the FO hybrid systems due to the fact that the osmotic pressures of DSs are different under the similar TDS concentrations (as shown in Figure 6-1).

Figure 6-5 (a) and (b) shows that the highest energy use and GW for the FO-NF hybrid systems with NaCl and MgCl₂ were calculated for a system operation with a final concentration of 100 mg/L and 0.6 M NaCl brine concentration. Whereas, the lowest energy use and GW impact were Na₂SO₄ before and after adjusting the process, and FO-NF hybrid systems are still lower than FO-RO hybrid systems. These results clearly show that NF membrane application in FO hybrid systems would be more promising to reconcentrate the draw solute at relatively lower energy consumption and with less environmental impacts.

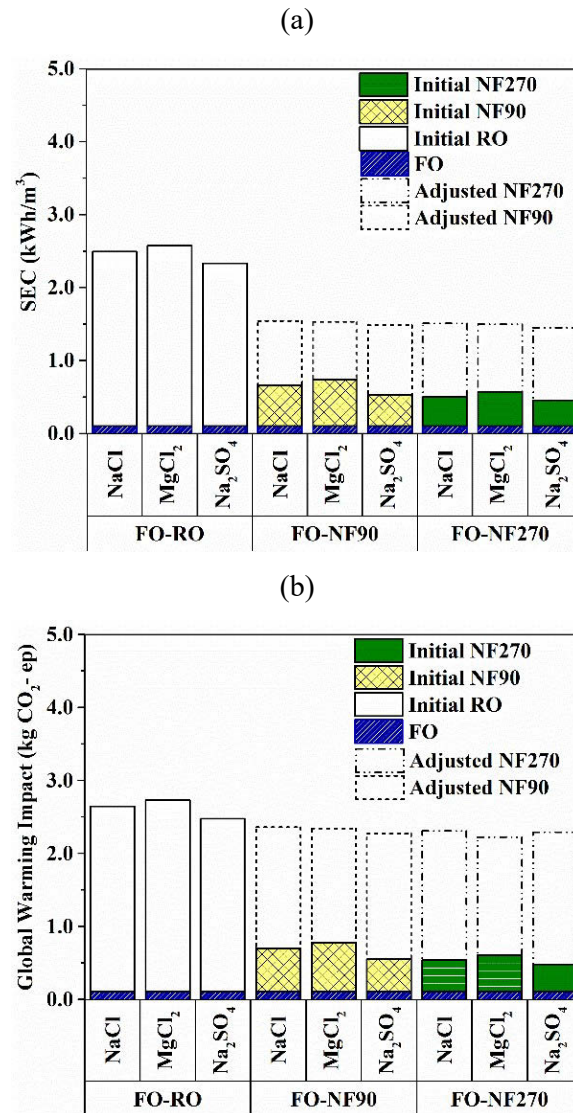


Figure 6 - 5. Initial and optimized (a) energy use and (b) global warming impact for FO-NF hybrid systems with different DSs. Target data: final product concentration of 100 mg/L TDS and brine concentration of 0.6 M NaCl (i.e. seawater osmotic pressure).

6.4.3.3. Impact of FO brine disposal on environmental potential

Energy and GW impacts were evaluated for FO hybrid systems by considering a direct discharge of brine into the oceans and using brine injection wells. The direct discharge to the sea was assumed to be a disposal at a pressure of almost 0 bar (referred to without FO brine disposal in Figure 6-6) while the disposal pressure of deep well injections was assumed to be the one of FO brine concentrate at FO recovery rate of 50% in the FO

process. The FO brine concentration was calculated using solute mass balance relationships described in Table 6-3.

Figure 6-6 shows the impact of FO brine disposal pressure on energy use and GW for all FO hybrid systems using different DSs. FO hybrid systems with NaCl showed the highest increase of the brine pressure on energy use and GW (6, 10, and 10% with RO, NF 90 and 270, respectively). In a closed-loop system, feed stream concentration increases over operation time due to increasing FO feed recovery and diffusing draw solutes from the draw side of membrane modules (Phuntsho et al., 2016b). Such accumulated draw solute in the feed stream can be reduced by controlling the FO feed recovery rate (lower than 80% recovery rate) and using FO membranes with a high reverse flux selectivity such as a TFC FO membranes (Achilli et al., 2010; Phuntsho et al., 2016b). It has to be acknowledged that a specific composition of FO brine is not considered in the current study due to the lack of real sample analysis and background data. Based on this study, further research needs to be conducted on the management of FO brine depending on its specific composition to prevent any additional environmental issues.

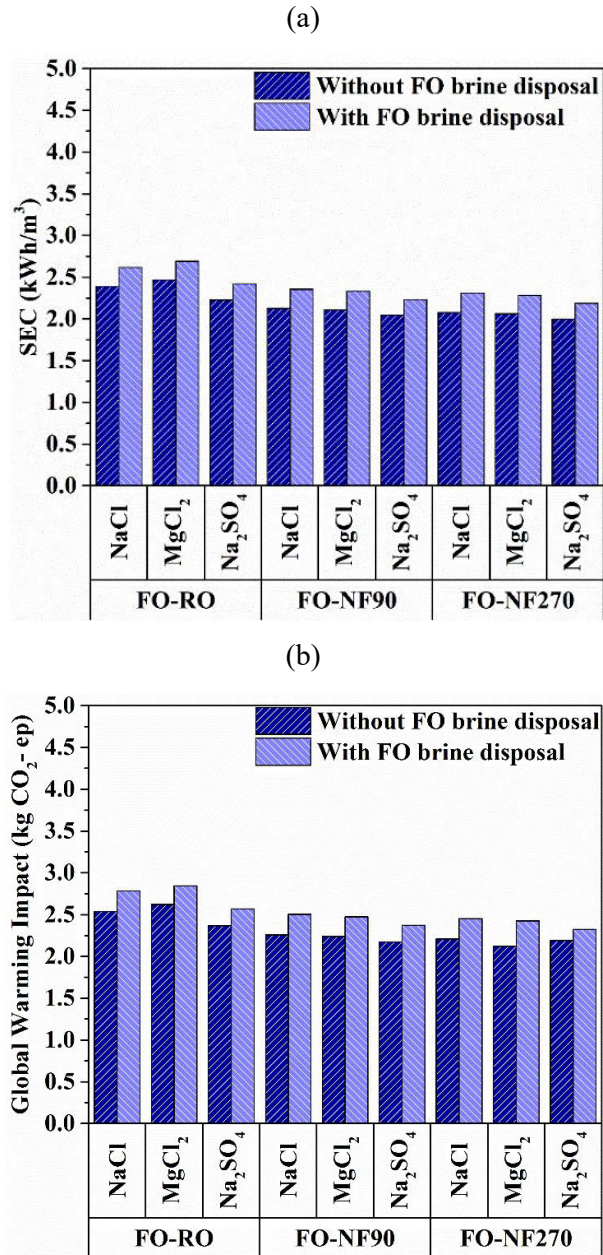


Figure 6 - 6. The impact of FO brine disposal on (a) energy and (b) global warming per unit of water produced for each hybrid system with different DSs. FO brine disposal energy was calculated based on the optimized conditions of FO hybrid system: final product concentration of 100 mg/L TDS and brine concentration of 0.6 M NaCl (i.e. seawater osmotic pressure).

6.4.4. CAPEX and OPEX cost evaluation

The contribution of various components to the total water cost of each hybrid system was evaluated by assuming the whole hybrid process recovery of 50%. Detailed calculations on the CAPEX and OPEX can be found in Table 6-7. Overall, Figure 6-7 (a) shows that the CAPEX cost of FO hybrid systems was around 37.5% higher on average than that of SWRO due to the larger number of FO membrane modules required. However, the OPEX cost of FO hybrid systems was around 62% lower on average than that of SWRO due to lower operating energy requirement (no hydraulic pressure required).

More specifically, FO hybrid systems with MgCl_2 showed the highest OPEX cost and thus the highest total water cost (Figure 6-7 (a)). As shown in Table 6-8, MgCl_2 had around 55% lower SRSF in the FO process and hence it can be clearly seen that the amount of MgCl_2 replenishment is considerably lower than that of NaCl. However, the FO hybrid systems with NaCl show the lowest total water cost. This is because the specific cost of MgCl_2 draw solute is around 67.0% higher than that of NaCl, thus leading to a significant cost for replenishing MgCl_2 in FO hybrid systems in the closed-loop operation.

In addition, although NaCl has the highest SRSF, FO hybrid systems with NaCl show the lowest total water cost. This is because NaCl produces higher water flux, resulting in the lowest contribution of FO membrane modules required to the total water cost. These results indicate that a DS with low initial cost and high water flux can provide a potential for further reducing the total water cost of an FO hybrid system.

Figure. 6-7 (b) shows the impact of SRSF on the OPEX cost of each hybrid system. SRSF values used for the baseline are shown in Table 6-8. It was assumed that the SRSF for each DS can be further reduced if utilizing an FO membrane with higher selectivity. Hence, the SRSF was assumed to be 0.1 g/L. It has to be noted that the energy penalty to achieve the target product water (100 mg/L) was not considered to clearly see the benefit of having a low SRSF in the system. The result clearly indicates that the OPEX cost decreases with the reduction in the SRSF value at similar water flux with the baseline. For example, for NaCl, when the SRSF is down to 0.1 g/L, the OPEX cost of FO-RO

hybrid system decreases from $\$0.22/\text{m}^3$ to $\$0.16/\text{m}^3$, which is around 30% reduction. In addition, for Na_2SO_4 , which has the lowest SRSF value of 0.28 g/L, when the SRSF decreases from 0.28 to 0.1 g/L, the OPEX cost of FO-RO hybrid system decreases from $\$0.19/\text{m}^3$ to $\$0.17/\text{m}^3$ (i.e., 10% reduction). These results clearly show that decreasing the SRSF in the FO process can reduce the DS replenishment cost and thus the overall OPEX costs. From an economic aspect, this confirms that the specific DS cost plays a significant role in the OPEX cost in terms of the total chemical cost required. Therefore, these results suggest the need for draw solutes with lower SRSF, FO membranes with higher selectivity, and lower solute price for further reducing environmental and economic impacts of FO hybrid systems.

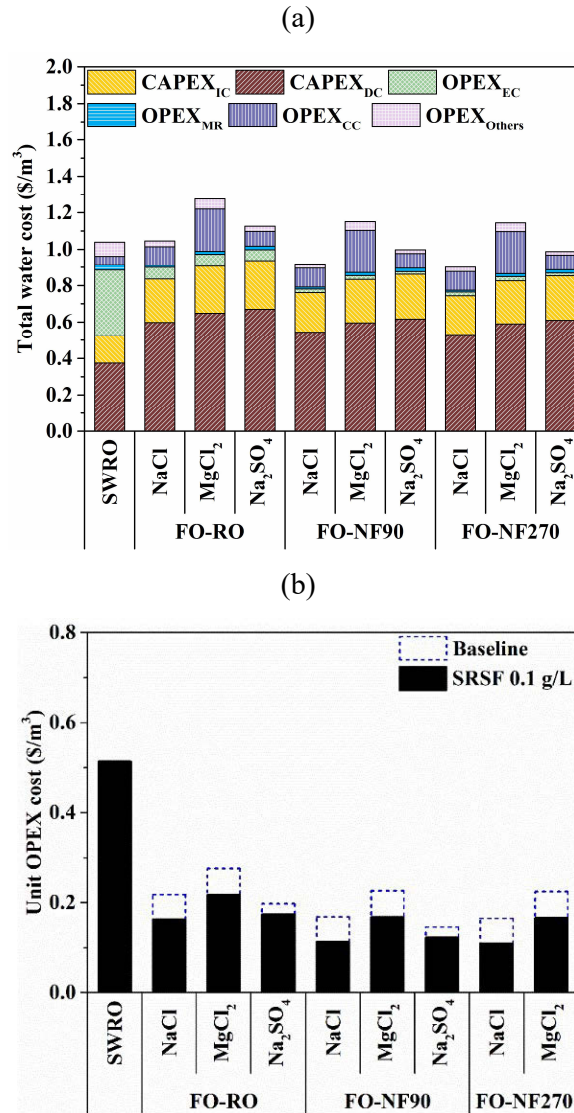


Figure 6 - 7. (a) Life cycle cost analysis ($\$/\text{m}^3$ water produced) and (b) impacts of SRSF on the OPEX cost of each hybrid desalination system based on a plant capacity of 100,000 m^3/d . The SRSF was down to 0.01 g/L. The RO and NF permeates were assumed to be the same for all hybrid systems (≈ 500 mg/L).

RO and NF recovery rates are directly related to the water productivity of the FO process since higher recovery rate in RO and NF leads to higher recycled DS concentration. In FO hybrid system under closed-loop operation, recovery rate of the DS reconcentration process is also an important factor to optimize to reach a cost-effective FO hybrid systems.

Based on the environmental and economic analysis results presented in previous sections, FO-NF 90 has a great potential to be the most sustainable hybrid system for mine impaired

water treatment. Figure 6-8 shows a comparison between the total water cost for the FO-NF 90 hybrid system with NaCl, MgCl₂ and Na₂SO₄, given variations in the NF recovery rate, which was varied from 80% to 99%. The total water cost of the FO hybrid system decreased rapidly with an increase on the NF recovery rate and gradually increased above 90% for NaCl, 93% for MgCl₂ and 95% for Na₂SO₄. The optimum NF feed recovery rate was observed to be about 90% with a total water cost of AUD \$0.9/m³ for the FO-NF 90 hybrid system with NaCl. The optimum NF feed recovery rate of the FO-NF 90 hybrid system with Na₂SO₄, however, was observed to be about 95% with a total water cost of AUD \$0.98/m³. Such high recovery rate would result in a proportionately higher concentration of the recycled DS, which in turn increases the osmotic driving force of the FO process. However, operating the NF process at such higher recovery rates will result in higher operating energy.

As mentioned earlier, although DS loss through RO and NF permeate is not significant, it has to be included when calculating the total DS replenishment costs in the FO hybrid systems. Figure 6-8 also shows the impact of NF permeate concentration on the total water cost of the hybrid systems. NF permeate quality was assumed to be 500 and 100 mg/L of TDS. Overall, the total water cost of the FO-NF 90 hybrid system, with all three DSs, increases with the increase in the NF permeate concentration to 500 mg/L. It can be clearly seen that NF membrane performance in terms of salt rejection can be a major contributor responsible for the total DS replenishment cost and thus the total water cost of FO hybrid systems. These results indicate that the DS performance and replenishment cost should be considered to select DS in the design of a real FO hybrid system.

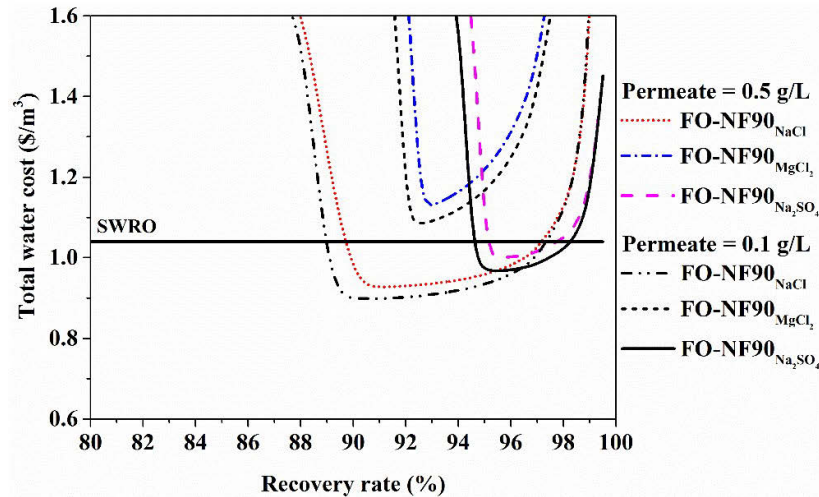


Figure 6 - 8. Total water cost of the FO-NF90 hybrid system with different DSs (NaCl, MgCl₂, and Na₂SO₄) to produce 100,000 m³/d.

6.5. Concluding remarks

In this chapter, environmental and economic analysis of hybrid FO-RO and FO-NF systems for mine impaired water treatment was conducted using different draw solutions. The following conclusions have been drawn from this chapter:

- Environmental impact assessment showed that the DS replenishment is one of the most important contributors to chemical use for the operating of a continuous closed-loop FO hybrid system. Reverse diffusion of draw solutes towards the feed brine could play a crucial role in reducing the environmental impact of the FO hybrid systems.
- The lowest increase in energy use and GW impact was observed with FO-NF90 using Na₂SO₄ as DS when considering the additional energy consumption in the NF processes to achieve a final target concentration (similar to RO permeate).
- In addition, although the contribution of the FO brine disposal pump energy to the total energy and the GW impact was not significant, the impact of specific chemicals in the FO brine on the environmental impacts of the FO hybrid systems needs to be further investigated.

- The amount of DS replenishment required to maintain the initial DS concentration relies on the salt selectivity of the FO membranes. NaCl shows the highest DS replenishment amount while its replenishment cost is lower than Na₂SO₄ and MgCl₂ because of its relatively low costs. Reducing the SRSF results in further savings in OPEX cost for all hybrid systems and this finding underlines the importance of having a high salt selectivity of the FO membranes. Therefore, this study highlights the importance of optimizing the FO process for reducing the DS replenishment cost.
- In a closed-loop operation mode, the FO-NF90 hybrid system with Na₂SO₄ does seem to have more benefits to make the process environmentally and economically favorable for mine impaired water treatment application. However, based on this study, it is clear that further study should focus on feed and draw solute behaviors, effective cleaning strategies, cleaning wastewater discharge and hydrodynamics at a larger-scale FO process to improve and achieve more accurate, reliable and realistic operational data.

CHAPTER 7

PRACTICAL CONSIDERATIONS FOR OPERABILITY OF SPIRAL WOUND FORWARD OSMOSIS MODULE: HYDRODYNAMICS FOULING BEHAVIOUR AND CLEANING STRATEGY

This chapter was published as: **Kim, J.E.**; Blandin, G.; Phuntsho, S.; Verliefde, A.; Le-Clech, P.; Shon, H., Practical considerations for operability of an 8" spiral wound forward osmosis module: Hydrodynamics, fouling behaviour and cleaning strategy. *Desalination* **2017**, *404*, 249-258.

7.1. Introduction

The first commercially available and specifically tailored forward osmosis (FO) membranes, based on cellulose triacetate (CTA), were developed by Hydration Technology Innovations (HTI, Albany, OR), and have been examined in various applications by numerous research groups (Alturki et al., 2012; Blandin et al., 2016a; Kim et al., 2016; McCutcheon et al., 2006a; Phuntsho, 2012; Tan & Ng, 2010). More recently, thin film composite (TFC) FO membranes were designed with a polyamide selective layer, and these feature higher water flux and better solute rejection compared to CTA membranes (Gu et al., 2013; Wang et al., 2010b; Wei et al., 2011b; Yip et al., 2010). In addition, TFC membranes were found to be more pH stable and were more resistant to hydrolysis and biological degradation (Geise et al., 2010; Gu et al., 2013; Wang et al., 2015b). In contrast, previous studies have reported that TFC membranes showed higher fouling tendency than CTA membranes due to the increased surface roughness (Gu et al., 2013; Vrijenhoek et al., 2001; Wang et al., 2015b; Zhu & Elimelech, 1997). As such opportunities to increase flux with commercially available membrane exists, but long-term fouling studies are required. An optimized FO module design is expected to feature high membrane packing density, lower concentration polarization (i.e. high mass transfer coefficient) and high water permeation (Lutchmiah et al., 2014). Performance of several commercial FO membranes (i.e. Porifera and Toyobo) has been widely reported in the literature on small membrane samples but information regarding module design is still limited since most commercial FO membrane modules are still under development. Only the performance of SW FO modules developed by HTI has been reported for a variety of feed and draw spacers (fine, medium and corrugated spacer) (Blandin et al., 2016a) while detailed information on other suppliers module configurations are not available. This clearly indicates that CTA and TFC membrane modules were the most mature and developed membranes during the time of this FO study. In this regard, most studies so far were conducted using small flat sheet membrane coupons which are not always representative of behavior in full-scale modules. Therefore, a better understanding of FO behavior in larger modules is needed to provide more practical insight for full-scale FO operation.

A large-scale spiral wound (SW) FO module typically requires four ports: two inlets and two outlets for both the FS and DS. In SW FO modules, the FS circulates in the feed channel between the rolled layers, and the DS flows through the central tube into the inner side of the membrane envelope (Kim et al., 2014a). Therefore, flow patterns and flow resistance in the feed and draw channels can be different and affected by specific module design. In particular, a more detailed study linking operating conditions (flow rates, inlet pressures) to resulting performances (water flux, reverse salt flux, fouling and cleaning efficiency) of SW FO modules will provide important insights in the operability of current SW FO modules on full-scale.

Very limited pilot-scale FO studies using SW FO modules currently exist in literature (Kim et al., 2014a; Kim & Park, 2011b; McGinnis et al., 2012). However, these pilot studies are of crucial importance for further FO development since the operation of SW modules in industrial plants is affected by several factors such as the number of membrane leaves, feed and draw channel height, spacers that affect mass transfer and pressure loss, but also fouling potential (Schwinge et al., 2004). To the best of the author's knowledge, so far only two studies have been reported in literature using 4040 SW (4" in diameter and 40" in length) (Kim & Park, 2011b) and 8040 SW (8040, 8" inch in diameter and 40" in length) (Kim et al., 2014a) HTI CTA FO modules. Those studies mainly focused on the optimization of a large-scale SW FO module (Kim & Park, 2011b) and of a newly proposed fertilizer drawn forward osmosis process for a specific application (Kim et al., 2014a; Phuntsho et al., 2012a). However, the susceptibility of SW FO modules to membrane fouling during the long-term FO operation has not been considered in those studies, which could consequently exacerbate the performance of in full-scale FO stand-alone or hybrid process. Although membrane fouling on the feed side in FO happens less and is easily removed by simple physical cleaning (Hancock et al., 2013; Lee et al., 2010; Valladares Linares et al., 2013b), the effect of osmotic backwash seems to be unclear. Some studies have reported that the osmotic backwash could lead to an adverse effect on the driving force due to the accumulation of the reversed solutes within the fouling layer (Arkhangelsky et al., 2012; Valladares Linares et al., 2013a; Valladares Linares et al., 2013b). Nevertheless, the specific combination of osmotic backwash with subsequent physical cleaning could be more effective to restore a significant portion of water productivity after fouling occurred (Blandin et al., 2015a). Thus, there is a critical need

to control operating conditions and assess performances of SW FO modules more systematically including fouling behavior and cleaning strategies for sustainable FO operation.

As an alternative to FO, a new FO-derived concept called pressure assisted osmosis (PAO) has recently been developed. PAO is aimed at increased water production compared to FO for more favorable economics for further commercialization (Blandin et al., 2015a; Blandin et al., 2013; Lutchmiah et al., 2015; Oh et al., 2014; Sahebi et al., 2015). In PAO, hydraulic pressure is applied on the feed side of the membrane to enhance the water flux through the synergistic effects of hydraulic pressure and osmotic pressure (Blandin et al., 2015a; Blandin et al., 2013; Lutchmiah et al., 2015; Oh et al., 2014; Sahebi et al., 2015). Overall, it has been demonstrated that by increasing the applied pressure, the water flux was significantly improved despite higher ICP. Even more than for FO, the role of a spacer in the PAO process is important to prevent the deformation and damage of the membrane caused by the applied hydraulic pressure on the feed side of the membrane (Duan et al., 2014; Oh et al., 2014; Sahebi et al., 2015). This reinforces the need to evaluate the impact of hydraulic pressure on the module-scale FO and PAO operations.

Accordingly, there is a clear need for a detailed assessment of the impact of hydrodynamic conditions on pressure behavior of an SW FO module (i.e. build-up in draw stream and drop along feed line). This chapter therefore systematically outlined the performances of two commercial SW FO modules (CTA from HTI and TFC from Toray Industries Inc). An assessment of the water flux and reverse salt flux behaviors as a function of operating conditions in both FO and PAO operation was conducted to evaluate the performance of both modules compared to lab-scale experiments. Fouling studies were performed with a mixture of model organic foulants was then used to evaluate the fouling behavior and cleaning strategies for the modules operated in a seawater dilution application. To our best knowledge, this is the first study addressing the practical operations of commercially available 8" SW FO modules and providing a comparative assessment of long-term fouling behavior in large-scale FO process. Therefore, the results reported in this chapter can be very useful for further investigation of the fouling control by chemical cleaning and/or pre-treatment in full-scale FO operation.

This chapter is an extension of the research article published by the author in Desalination (Kim et al., 2017a).

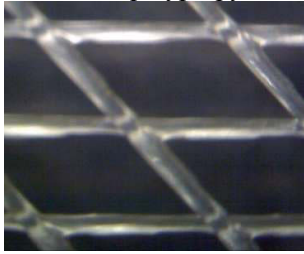
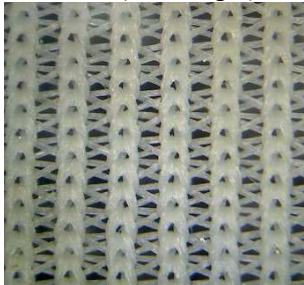
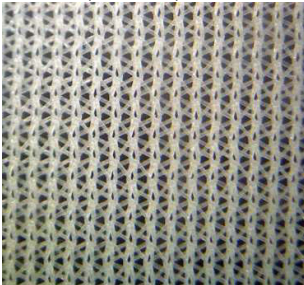
7.2. Materials and Methods

7.2.1. Spiral wound FO membrane module

Two different 8" SW FO modules were used (Table 7-1): one CTA module manufactured by HTI and one TFC polyamide module manufactured by Toray Industries, Korea. In both modules, the rejection layer of the membrane faces the FS and the porous support layer of the membrane faces to the DS. Feed and permeate spacers were present to keep the membrane leaves apart (Kim et al., 2014a; Kim & Park, 2011b).

As presented in Table 7-1, the CTA module had a corrugated feed spacer made of 2.5 mm polystyrene chevron and an effective membrane area of 9 m² with six membrane leaves. The TFC module had a feed spacer made of a 1.19 mm diamond type polypropylene mesh and an effective membrane area of 15 m² with ten membrane leaves. In addition, both modules had different permeate spacers: the CTA module had three tricot spacers, while the TFC module featured a draw channel containing one diamond type spacer wedged in between two tricot type spacers. If a net spacer is used inside of the envelope in the SW FO module and the DS side is pressurized, the feed flow channel may be blocked by membrane deformation. Accordingly, a tricot fabric spacer is used inside the envelope like a permeate carrier of an SW RO module and prevents the membrane deformation and this structure has been already utilized for pressure-retarded osmosis application (Kim et al., 2013b). Water permeability (A) for both FO modules was measured in RO mode in a pilot-scale FO unit (tap water - conductivity $240 \pm 20 \mu\text{m/cm}$ - in the feed and draw sides). The tests were conducted at increasing feed pressures (in intervals of 0.5 bar up to 2.5 bar). A_{CTA} and A_{TFC} were found to be 1.6 ± 0.2 and $8.9 \pm 0.14 \text{ Lm}^{-2}\text{h}^{-1}\text{bar}^{-1}$, respectively. Additional information on the properties of the CTA and TFC FO membranes such as water and salt permeability (A and B values), feed rejection (R), structural parameter (S) and membrane total thickness are all provided in Table 7-2.

Table 7 - 1. Specifications of two spiral wound forward osmosis membrane modules employed in this study.

| Parameter | CTA (HTI) | TFC (Toray) |
|--|---|--|
| Water permeability(A), $\text{Lm}^{-2}\text{h}^{-1}\text{bar}^{-1}$ | 1.6 ± 0.2 | 8.9 ± 0.1 |
| Effective membrane area, m^2 | 9 | 15 |
| Number of leaves in the assembly | 6 | 10 |
| Feed spacer thickness, mm | 2.5 | 1.19 |
| Feed spacer type | Corrugated polystyrene | Diamond polypropylene |
| *Image of feed spacer | n.a. |  |
| Draw spacer type | Tricot(dense/rigid) | Tricot(flexible)/Diamond |
| *Image of draw spacer |  |  |

*Microscope measurement (5MP USB 2.0 Digital Microscope) and the spacers obtained from the SW FO module autopsy.

Table 7 - 2. HTI CTA and Toray TFC FO membrane properties (i.e., water and salt (NaCl) permeability coefficients and rejection of the active layer, the structural parameter of the support layer and membrane thickness).

| | Water permeability coefficient, A ($\text{L}/\text{m}^2/\text{h}/\text{bar}$) | Salt permeability coefficient, B ($\text{L}/\text{m}^2/\text{h}$) | Structural parameter, S (10^{-6} m) | Red Sea Salt Rejection (%) | Thickness of AL* (μm) (Wang et al., 2015b) | Thickness of SL* (μm) (Wang et al., 2015b) |
|------------------|--|--|---|----------------------------|--|--|
| HTI CTA | 1.6 ± 0.2 | 0.46 ± 0.3 | 507 | 76% | 6.1 ± 2.0 | 51.4 ± 6.7 |
| Toray TFC | 8.9 ± 0.14 | 5.68 ± 0.14 | 466 | 85% | 4.9 ± 1.1 | 47.8 ± 2.5 |

*AL: Active layer, SL: Support layer

7.2.2. Feed and draw solutions

A draw solution at a concentration of 35 g/L of Red Sea salt (RSS) from Red Sea Inc. with an equivalent osmotic pressure of 24.7 bar was prepared and used in all experiments (Blandin et al., 2015a; Blandin et al., 2013). RSS composition is described in Table 7-3. Humic acid and alginate were chosen as model organic foulants, while calcium (as calcium chloride, CaCl₂) was added to further enhance fouling. Model organic foulants used in this study have been known as major organic components in wastewater and have extensively been used to study in fouling behavior in FO process (Ang et al., 2006; Blandin et al., 2015a; Boo et al., 2013). In fouling experiments, the FS was prepared by mixing the following chemicals to tap water: 1.2 g/L RSS, 0.22 g/L CaCl₂ (Ajax Finechem Pty Ltd, Tarend point, Australia), 0.2 g/L humic acid sodium salt (Aldrich, Milwaukee, WIS) and 0.2 g/L alginic acid sodium salt (Sigma Aldrich Co., St Louis, MO). The total organic carbon (TOC) concentration of the feed was 94 mg/L. Before and after the fouling experiments, baseline experiments were conducted using tap water and 35g/L RSS as FS and DS, respectively.

Table 7 - 3. Sea Salt of 35 g/L prepared in Milli-Q Water (Blandin et al., 2013).

| Composition | Concentration (mg/L) |
|--------------------|-----------------------------|
| Cl | 18,772 |
| Na | 10,692 |
| Mg | 1,320 |
| Ca | 480 |
| K | 390 |
| S | 890 |
| C (inorganic) | 45 |
| Br | 15 |

7.2.3. Pilot-scale system and experimental procedure

As shown in Figure 7-1, a pilot-scale FO system was used for the experiments. Details about the design and control of the pilot-scale FO system are provided in our previous study (Kim et al., 2014a). Flow meters, pressure gauges and electrical conductivity (EC) meters were installed at both the inlet and outlet points of the module and connected to a computer for online data recording and monitoring. Although the feed and draw flow rates were varied between 17 and 100 L/min and between 4 and 15 L/min, respectively, the cross-flow velocity of each module shows difference due to their different module

designs. The converted feed and draw cross-flow velocities for both are presented in Table 7-4.

The impact of feed and draw flow rates on pressure-drop were successively evaluated. For this evaluation, 500 L of FS and DS were prepared with tap water, and each experiment was carried out at a fixed draw flow rate, while the feed flow rate was varied and vice versa. Details of the experimental conditions are summarized in Table 7-4.

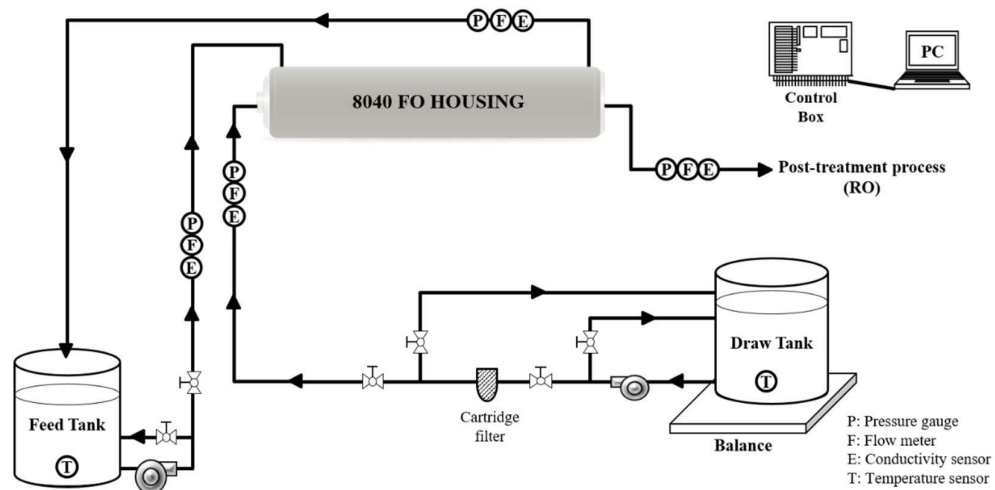


Figure 7 - 1. Schematic diagram of the pilot-scale FO experimental set up and illustration of 8040 spiral wound FO modules: (a) CS CTA and (b) MS TFC (CS: corrugated feed spacer and MS: medium diamond shape feed spacer).

Table 7 - 4. Experimental conditions for module hydrodynamic tests.

| Module | Test No. | Feed cross-flow velocity, m/s (L/min) | Draw cross-flow velocity, m/s (L/min) | FS and DS |
|--------|----------|---------------------------------------|---------------------------------------|--------------------|
| CTA | Test 1 | 0.08-0.44 (17-100) | 0.04 (10) | Tap water of 500 L |
| | Test 2 | 0.18 (40) | 0.02-0.07 (4-15) | |
| TFC | Test 3 | 0.16-0.91 (17-100) | 0.09 (10) | |
| | Test 4 | 0.37 (40) | 0.04-0.14 (4-15) | |

PAO operation was also tested to assess the effect of the hydraulic pressure in the feed channel. Feed pressure was changed by adjusting the back pressure valve for fixed feed and draw flow rates. The maximum operating pressure used in this study was 2.5 bar as feed inlet pressure. The PAO experiments were performed with 200 L of 35 g/L RSS as

DS and 500 L of tap water as FS. The feed and draw flow rates were constant and fixed based on the optimized conditions defined in the initial SW FO module experiments.

Water fluxes ($J_w, \text{Lm}^{-2}\text{h}^{-1}$) were calculated by using the following formula:

$$J_w = \frac{\text{Change in DS volume (L)}}{A_m(\text{m}^2) \times \Delta t (\text{hr})} \quad (7-1)$$

where A_m is the effective membrane surface area (m^2) and Δt is the operation time (hr). In addition, the recovery rate (%) during the operation in FO and PAO modes was defined as

$$\text{Recovery rate} = \frac{\text{Permeated volume (PV,L)}}{\text{Initial FS volume (L)}} \times 100 \quad (7-2)$$

When tap water was used as FS in FO and PAO modes, the change in FS salt concentration (and thus reverse salt flux) was determined based on conductivity measurements (using a multimeter CP-500L, ISTEK, Korea) (Phuntsho et al., 2011). The concentration change in the feed solution at the beginning and end of each experiment was measured. The measured value was used to calculate the specific reverse solute flux (SRSF), which is defined as a ratio of reverse salt flux ($J_s, \text{gm}^{-2}\text{h}^{-1}$) and water flux ($J_w, \text{Lm}^{-2}\text{h}^{-1}$) (Phillip et al., 2010; Sahebi et al., 2015). SRSF ($J_s/J_w, \text{g/L}$) was then calculated using the following formula:

$$\text{SRSF} = \frac{1}{J_w} \left(\frac{C_f V_f - C_i V_i}{A_m \Delta t} \right) \quad (7-3)$$

where C_i and C_f are the initial and final feed solute concentration (g/L), and V_i and V_f are the initial and final volume of the feed water (L). When DI water was used as FS, the RSF/SRSF was determined by measuring the increased electrical conductivity of the FS between the start and end of each batch experiment. The electrical conductivity was then converted into mass concentration using calibration curve for the RSS concentration versus conductivity as shown in Figure 7-2.

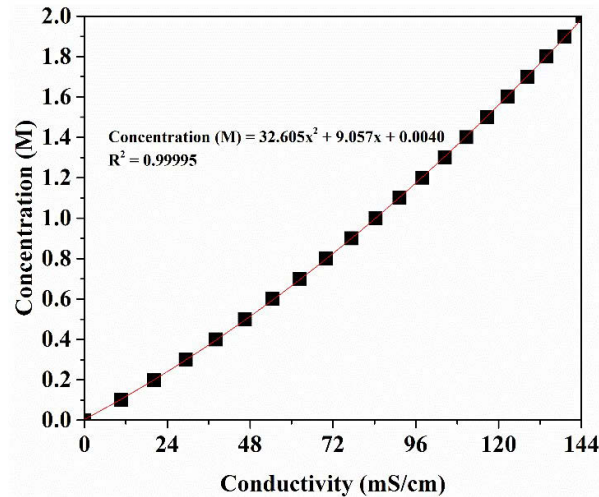


Figure 7 - 2. Variation of NaCl concentration with NaCl conductivity.

7.2.4. Fouling cycles and cleaning experimental procedure

Fouling behavior was evaluated in FO operation (no hydraulic pressure added, i.e. back pressure valve opened) for both modules. All experiments were conducted with 200 L of 35 g/L RSS as DS and 500 L mixed fouling solution (as described in Section 7.2.2) as FS. After 400 L of water permeated (i.e. after 80% recovery feed water reached), the test was stopped and new feed and draw solutions were prepared and a new fouling cycle was initiated (without cleaning in-between cycles). Fouling runs were repeated for three cycles in total before cleaning took place. Operation time for the CTA module was much longer than for the TFC module due to its low water permeability (since similar permeation volumes were aimed at).

Osmotic backwashing was conducted after the three fouling cycles, using 200 L of 35 g/L RSS as cleaning DS (replacing the feed water) and tap water as cleaning feed solution (replacing the DS) for 60 min to remove the fouling layer from the membrane surface at the same feed and draw flow rates of 40 and 10 L/min, respectively for both modules (cross-flow velocities for each module are shown in Table 7-4). After the osmotic backwash, physical cleaning at 100 L/min of feed flow rate (0.44 and 0.91 m/s for CTA and TFC modules, respectively) was performed for 5 min using tap water to flush the dislodged foulants from the feed channel (Blandin et al., 2015a). During the physical cleaning, samples of the feed side (used as draw side during the backwashing) were

collected every 1 min (100 L flushing), and analyzed using a total organic carbon (TOC) analyzer (SGE Anatoc TOC II Analyser). Before each fouling run, as well as before and after cleaning, the baseline flux was measured by operation with tap water as FS and 35 g/L as DS for 30 min to assess the influence of fouling on membrane permeability and inlet pressure (and pressure-drop) in the feed channel.

7.3. Results and discussion

7.3.1. Impact of operating conditions on module hydrodynamics

7.3.1.1. Impact of feed and draw flow rates on pressure-drop (without permeation)

It should be noted that the flow rate range is much lower in the draw channel, as recommended in (Kim et al., 2014a; Kim & Park, 2011b). Results for the CTA module (Figure 7-3 (a)) indicate that the effect of feed flow rate increase on the pressure-drop was moderate (at constant draw cross-flow velocity of 0.04 m/s). When the feed cross-flow velocity was increased from 0.08 to 0.44 m/s, the feed inlet pressure was increased from 0.17 to 0.27 bar. In addition, as shown in Figure 7-3 (b), when the draw cross-flow velocity was increased from 0.03 to 0.05 m/s (much lower range than for feed stream), the draw inlet pressure was more linearly increased from 0.39 to 0.74 bar. This demonstrates that much higher flow resistance occurs in the draw channel of the CTA module, which is mainly due to the use of dense and thick draw tricot spacers with lower cross-flow velocities in both sides of the module (Tables 7-1 and 7-4) (Cipollina & Micale, 2016).

When the feed cross-flow velocity was increased from 0.16 to 0.91 m/s in the TFC module (Figure 7-3 (c)), the feed inlet pressure was increased from 0.22 to 0.39 bar. Specifically, under much higher feed cross-flow velocity of 0.91 m/s (Table 7-4), the feed inlet pressure with the TFC module is slightly higher (0.39 bar) than that with the CTA module (0.27 bar), which corroborates with the fact that the spacer used in the feed channel of the TFC module is thinner (1.19 mm) with higher packing density leading to lower feed channel height (0.00258 mm for TFC and 0.00394 mm for CTA), resulting in higher feed

inlet pressure (Park & Kim, 2013; Schwinge et al., 2004; Shakaib et al., 2007). Pressure-drop in the draw channel of the TFC module was not only lower but also much less sensitive to flow rate variation than in the CTA module, mainly due to the presence of one layer of diamond spacer with much lower resistance in the draw channel (Figure 7-3 (d)).

As such, it is clear that spacer design is of crucial importance for pressure-drop in the SWFO module. The tested CTA module with a corrugated spacer in the feed channel does allow a very low pressure drop in the feed channel, but this comes at the cost of a low packing density. Most likely, this is only justifiable economically if feed waters with a very high load of foulants and potential clogging problems are treated. In that aspect, the diamond spacer used in the TFC module appears to be a better compromise that allows for higher packing densities at moderate pressure drop. The permeate spacers used in the CTA module resulted in a very large pressure drop, even at a low flow rate. Combinations of tricot permeate spacers to support the membrane and limit deformation and a diamond spacer to limit pressure-drop (as in the TFC module) (Table 7-4) allows using higher draw flow rates.

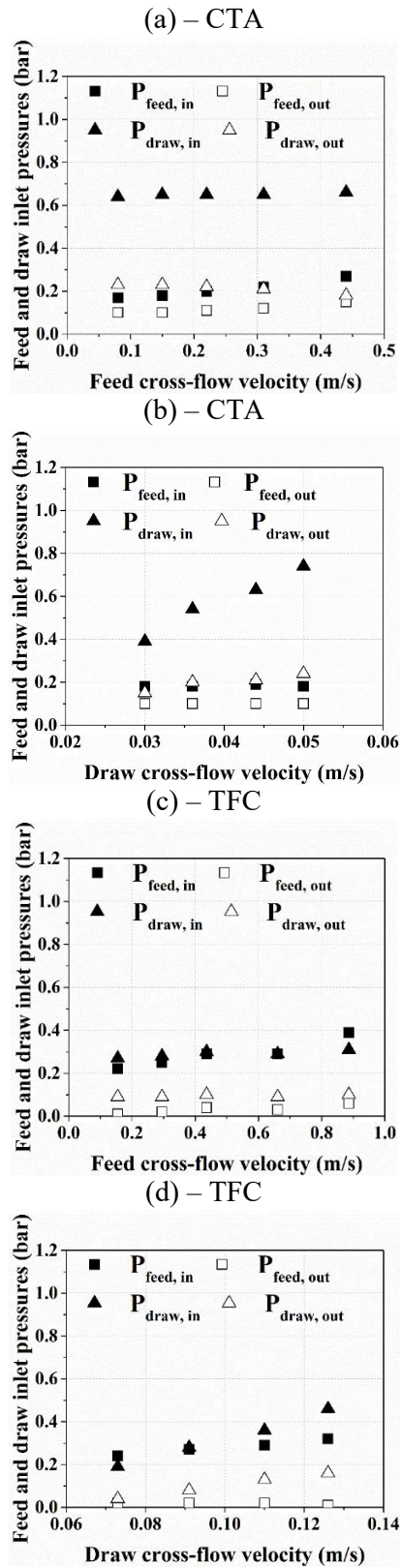


Figure 7 - 3. Effect of feed and draw cross-flow velocities on pressure build-up in CTA (a and b) and TFC (c and d) modules. Tap water was used as FS and DS.

7.3.1.2. Impact of feed and draw channel pressurization on pressure-drop

In these experiments, the system was operated by adjusting the feed inlet pressure using the back pressure valve of the feed side. Figure 7-4 shows the impact of the feed inlet pressure on the feed and draw channel inlet and outlet pressures for both modules. For both modules (Figure 7-4 (a) and (b)), the draw inlet pressure was increased when the pressure was applied on the feed side. Interestingly, both modules have very distinct behavior with regards to this “pressure transfer.” For the CTA module, the draw inlet pressure increase is already maximal at lower hydraulic pressures (1 bar), and remains constant even when further increasing the feed pressure (up to 2.5 bar). This appears to indicate that the pressurization of the draw side in the CTA module is more likely a consequence of draw channel pressurization on the tricot type support on the draw side. At higher pressures, further reduction of the channel is not possible as the tricot support could not be more compacted. For the TFC module, a more linear increase in the draw inlet pressure was observed with increasing feed pressure (Figure 7-4 (b)). Here, it could thus be hypothesized that the diamond type spacer is less supportive and allows for more channel reduction (Blandin et al., 2013; Kim & Elimelech, 2012). To identify the reason behind the increases in draw pressure for both modules, RO tests with the modules were compared to tests in FO mode (using tap water as FS and DS).

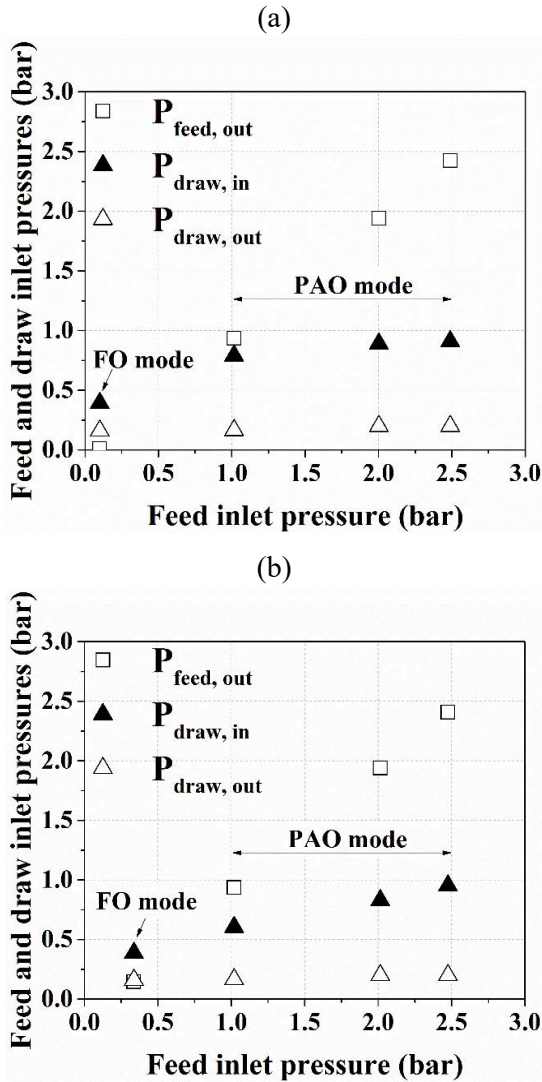


Figure 7 - 4. Impact of feed inlet pressure on the feed and draw channel pressurization with (a) CTA and (b) TFC modules. Feed cross-flow velocity was constant at 0.18 m/s for CTA and 0.37 m/s for TFC, while the draw flow cross-flow velocities for CTA and TFC modules were 0.04 and 0.09 m/s, respectively. Tap water was used as FS and DS.

7.3.2. Relative contribution of hydraulic pressure to permeation flux

FO and PAO tests were carried out using CTA and TFC modules (Figure 7-5), and now with tap water as FS, and 35 g/L RSS as DS. The water fluxes in FO and PAO modes with the TFC module were significantly higher than that with the CTA module. For example, in FO mode (no hydraulic pressure applied), the flux with the TFC module was around $16.6 \text{ Lm}^{-2}\text{h}^{-1}$, while the flux with the CTA module was around $5.4 \text{ Lm}^{-2}\text{h}^{-1}$. The higher performance of the TFC membranes compared to CTA membranes corroborates findings from literature (Coday et al., 2013; Yip et al., 2010).

In PAO mode (Figure 7-5), as expected, the water flux improved with increasing applied pressures. For the CTA module, the flux increase with applied pressure was moderate, i.e., from 6.72 to $7.3 \text{ Lm}^{-2}\text{h}^{-1}$ (at 2.5 bars of applied pressure) and remained much lower than the fluxes obtained with the TFC module. For the TFC module, the impact of the applied pressure on the water flux was significant, already at low applied pressure (flux increased from 19 to $24.5 \text{ Lm}^{-2}\text{h}^{-1}$ at 1 and 2.5 bar, respectively). This confirms that the TFC membranes not only has higher permeation flux in FO mode, but is also more responsive to the use of hydraulic pressure (PAO mode) due to its higher water permeability. Although additional energy is required to pressurise the feed solution in PAO, the significant increase in performance could lead to additional cost savings, in particular by a reduction of the number of membrane modules required (Blandin et al., 2015b).

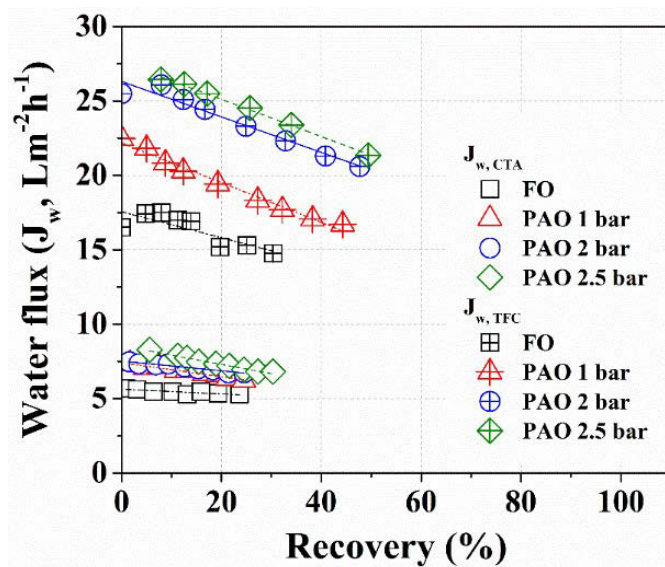


Figure 7 - 5. Comparison of flux behavior in pilot-scale FO and PAO processes using two different SW FO modules. Experimental conditions: feed flow rate: 0.18 and 0.37 m/s for CTA and TFC, respectively, draw flow rate: 0.04 m/s for CTA and 0.09 m/s for TFC, and applied pressure in PAO: 1, 2 and 2.5 bar, 35 g/L RSS as DS and tap water as FS.

Table 7-5 shows the comparison of the specific reverse salt flux (SRSF) behavior for FO and PAO modes using the two different SW FO modules. Compared to the CTA module, the TFC module had much lower SRSF, and thus not only had a higher flux but also a higher selectivity than the CTA module. As expected from the previous lab experiments, the results show a significant decrease in the SRSF for both modules with increasing applied pressure. For example, the SRSF were 1.22 and 0.37 g/L for CTA and TFC, respectively in FO mode, and decreased down to 0.64 and 0.10 g/L for CTA and TFC, respectively in PAO mode with a feed inlet pressure of 2.5 bar (Blandin et al., 2013; Oh et al., 2014; Sahebi et al., 2015). This corroborates previous findings that reverse transport of the draw solutes through the membranes is significantly decreased by the enhanced water permeation. The effect of hydraulic pressure on the RSF for the TFC is even more propounded compared to the CTA, due to the higher water permeability of the TFC. Also, the CTA module could have the risk of irreversible fouling on the support layer caused by more solute diffusing from DS into FS in which the enhanced salt accumulation on the feed side of the CTA module and is mainly promoted by the reverse diffusion of Na^+ (Mi & Elimelech, 2008; Xie et al., 2013b). Such reverse solute flux through the FO membranes can have a significant economic impact on the FO process. Draw solute

leakages through SRSF in the FO process is one of the major contributors to draw solute replenishment cost in a continuous closed-loop configuration (Achilli et al., 2010). A recent study conducted by Phuntsho et al (Phuntsho et al., 2016b) has pointed out that accumulation of draw solutes in the feed brine would be one of the significant environmental challenges for brine disposal, especially for FO membranes with lower reverse flux selectivity. This indicates that, CTA with lower reverse flux selectivity (as shown in Table 7-5) would result in much higher accumulation of draw solutes in the feed brine thus leading to higher draw replenishment and brine treatment costs. These studies clearly show that the TFC FO membrane with much higher reverse flux selectivity than CTA FO membrane would be more beneficial for FO hybrid systems.

Table 7 - 5. Comparison of specific reverse salt flux (SRSF, J_s/J_w) behaviour in pilot-scale FO and PAO processes using two different SW FO modules: CTA and TFC.

| Operation mode | CTA module | | | TFC module | | |
|----------------|---|---|--------------------|---|---|--------------------|
| | J_w, CTA (Lm^2h^{-1}) | J_s, CTA (gm^2h^{-1}) | J_s/J_w (g/L) | J_w, TFC (Lm^2h^{-1}) | J_s, TFC (gm^2h^{-1}) | J_s/J_w (g/L) |
| FO | 5.4 | 6.58 | 1.22 | 16.6 | 6.1 | 0.37 |
| PAO | | | | | | |
| 1 bar | 6.7 | 6.12 | 0.91 | 19.0 | 4.1 | 0.22 |
| 2 bar | 7.1 | 5.47 | 0.77 | 23.6 | 2.6 | 0.11 |
| 2.5 bar | 7.3 | 4.66 | 0.64 | 24.5 | 2.5 | 0.10 |

7.3.3. Fouling behavior in SW FO modules and impact on hydraulic performance

The water flux as a function of permeate volume is presented in Figure 7-6 (a) and (c) while permeate volume and recovery rate as a function of operation time is shown in Figure 7-6 (b) and (d). During each batch, flux decreased significantly with time (and increasing recovery) due to a combination of the osmotic dilution of the DS and potentially fouling. Only when comparing initial permeation fluxes for batches, the occurrence of fouling can be individually assessed. No significant initial permeation flux decline with batches was observed for neither of the tested modules, even after three batches of operation without cleaning in between. As such, despite the relatively long time of operation, especially for the CTA module, and the high load of foulant used, a faster flux decline was noticed at early stages of operation but between fouling experiments the flux decline was relatively small (Figure 7-6 (a)). For the TFC module (Figure 7-6 (b)), fouling was limited, although a higher impact of fouling was initially

expected due to the higher roughness of the membrane and the higher permeation flow compared to the CTA (Blandin et al., 2016b; She et al., 2016). Such little flux decline for TFC module shows that the fouling happening in the SW FO module is clearly different from the results reported in existing literature, which was conducted using small FO membrane coupons (Mi & Elimelech, 2010; Tang et al., 2007; Vrijenhoek et al., 2001). This study seems to suggest that the membrane surface properties play a less dominant role in SW FO module fouling.

Nevertheless, there was the steep decrease of the initial water flux was observed with CTA module, and the initial recovery rate between the CTA and TFC modules was significantly different (recovery rate of 10 % and 2% for CTA and TFC modules, respectively), resulting in the huge difference of operation time for CTA and TFC modules (i.e. 20 times higher). This was more likely because of two reasons; the impact of ECP on the membrane surface of the CTA module mainly due to higher RSF (discussed in Section 7.3.2) and that the CTA module used in this study has been operating several times before we conducted the fouling experiments, thus it could already have a fouling layer on the membrane surface to some extent even though the flux was almost fully restored after hydraulic cleaning (Phuntsho et al., 2016b). More specifically, it was observed that the recovery rate of the CTA module after 10 hrs operation was around 1% with water flux of lower than $1 \text{ Lm}^{-2}\text{h}^{-1}$ and thus there was no meaning to operate CTA module longer than 10 hrs (Figure 7-6 (a)). From this aspect, CTA and TFC module configuration in a full-scale FO desalination plant cannot be the same and it is dependent on the performance of FO membrane modules. Thus, it is more preferred that CTA modules should be paralleled in a full-scale FO desalination plant.

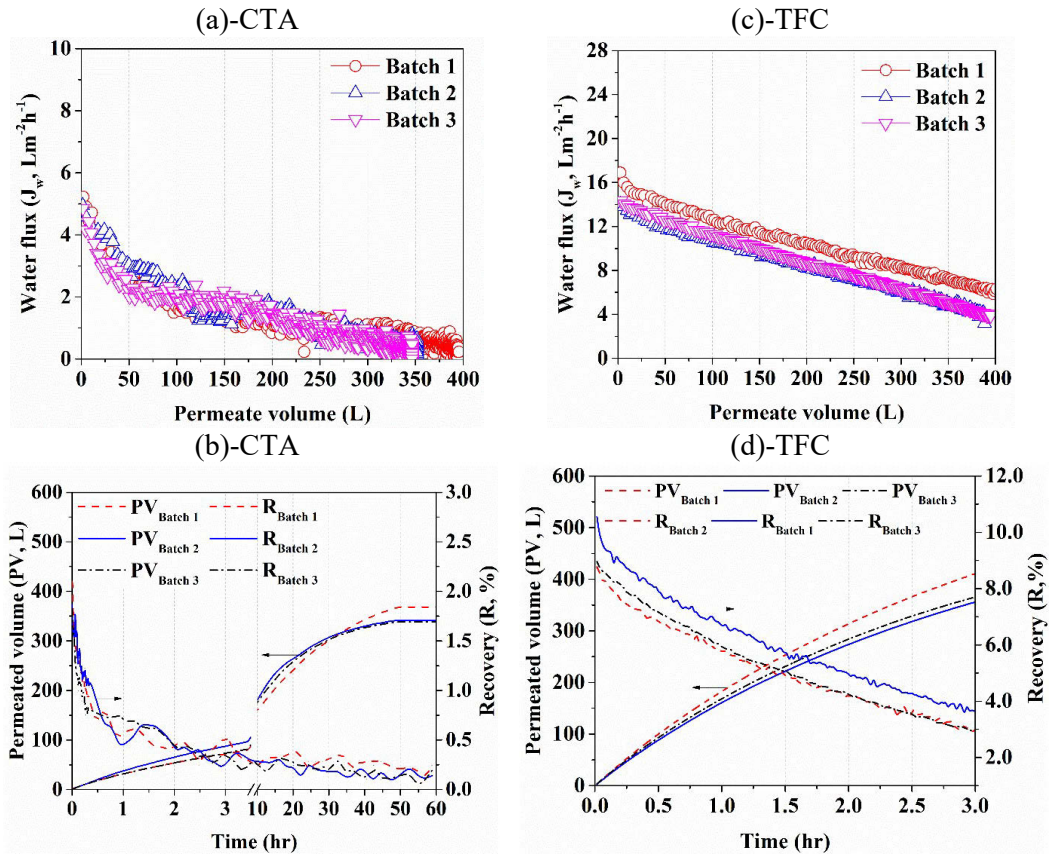


Figure 7 - 6. Effect of organic foulant in feed solution on FO fouling of CTA (a and b) and TFC (c and d) modules. (a) and (c) water flux (J_w) as a function of permeate volume (L); (b) and (d) permeate volume (L) and recovery rate (R) as a function of operation time. Fouling experiments were conducted using 35 g/L RSS as DS and feed fouling solution prepared by addition of 1.2 g/L RSS, 0.22 g/L CaCl_2 , 0.2 g/L alginate, 0.2 g/L humic acid.

To get further insight in the behavior of the SW FO modules during the fouling (as no real decrease in water permeability was noticed over the batches), feed inlet pressure was compared before and after the fouling experiments. Figure 7-7 compares the feed inlet pressure during fouling experiments with the feed pressure using pure water as feed before and after the third batch of fouling. As shown in Figure 7-7, as soon as the foulant mixture was used as FS, a much higher feed inlet pressure was observed in the module, due to higher viscosity resulting in an increased flow resistance and pressure-drop along the membrane channel on the feed side. This feed pressure increase most likely indicates foulant deposition, although no decrease in permeation flux was noticed. This would indicate that fouling occurs more in the channel spacers rather than on the membrane surface. Most likely, the foulants accumulated in dead zone of the feed spacer, and consequently, the cross-flow velocity and the required pressure increased in the feed

channel. Despite the fact that no decrease in membrane water permeability is seen, the increased pressure-drop in the feed channel is of course unwanted. Increased pressure drops lead to higher energy consumption for the pump to maintain the water circulation (Schwinge et al., 2004). As such, controlling fouling in the feed channel, and avoiding unwanted pressure-drop will be a key parameter for real-life FO operation, especially on challenging feed streams. By comparing feed pressure (with tap water as FS) before and after fouling experiments, it is clear that for the TFC module, pressure-drop increased much more than for the CTA one (i.e. 1 and 0.25 bar, respectively). As discussed earlier, the corrugated spacer used in the CTA module leads to an increased channel thickness with lower initial pressure-drop and most likely less sensitivity to fouling deposition with much longer operation time. In addition, since the CTA module has shown lower cross-flow velocity of around 0.18 m/s compared to the TFC module (0.37 m/s) corresponding to the flow rate of 40 L/min, thus showing that mass transfer coefficient of TFC module (3.04×10^{-5} m/s) is higher than that of CTA module (2.40×10^{-5} m/s). Consequently, the loose fouling layer in the corrugated spacer can be flushed to some extent or changed by hydrodynamics due to its spacer geometry (Figure 7-7).

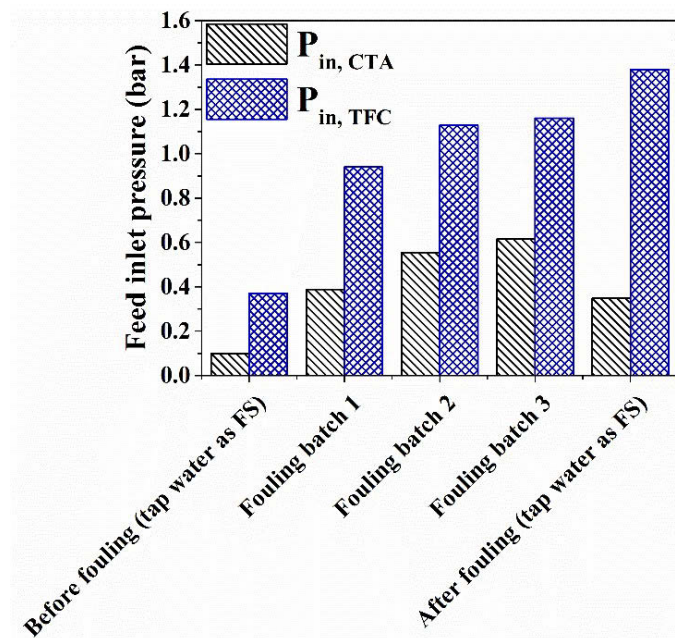


Figure 7 - 7. Feed inlet pressure change with CTA and TFC modules. Fouling experiments were conducted using 35 g/L RSS as DS and feed fouling solution prepared by addition of 1.2 g/L RSS, 0.22 g/L CaCl_2 , 0.2 g/L alginate, 0.2 g/L humic acid.

7.3.4. Fouling reversibility by osmotic backwash

As discussed in Section 7.3.3, no significant impact of fouling was observed on permeation flux, indicating that fouling occurs more in the spacers rather than on the membrane surface in the SW FO modules. Therefore, it is unclear whether osmotic backwashing will have a clear effect on fouling remediation. To assess this, not only the water permeability was monitored, but also the potential recovery of the pressure-drop in the feed channel. The cleaning strategy consisted of a combination of osmotic backwash followed by feed channel water flushing at high cross flow velocity (Section 7.2.4). During the osmotic backwash, the feed pressure drop remained relatively constant for the CTA module, but was observed to decrease slightly for the TFC module (see Figure 7-8 (a)). This indicates that the osmotic backwashing could be efficient to recover materials accumulated in the feed channel during operation, especially for TFC membrane module. Besides, as shown in Figure 7-8 (a), significant reverse flux difference between CTA and TFC modules was observed during the osmotic backwash. For instance, the reverse water permeation in the TFC module (average of $14.5 \text{ Lm}^{-2}\text{h}^{-1}$) was much higher than that in the CTA module (average of $2.8 \text{ Lm}^{-2}\text{h}^{-1}$), indicating that reverse flux assisted dissociation and dislodging of the foulant layer from the membrane surface could be more pronounced in the TFC FO membrane modules. The results in Figure 7-8 (b) therefore have confirmed that the feed inlet pressure was dramatically decreased after osmotic backwashing and flushing the feed channel under the highest cross flow velocity for each module, i.e. from 1.4 to 0.8 and from 0.35 to 0.25 for TFC and CTA modules, respectively. Still, the feed pressure was not restored to its original level for the clean module, thus indicating that almost full recovery was achieved or modification of the pressure balance in the module happened.

In order to compare the efficiency of the cleaning and estimate required durations for both modules, TOC concentrations flushed out of the module after each minute (i.e. 100 L) are presented in Figure 7-8 (c). The results indicate that a very high load of foulants is removed in the early stage of physical cleaning and after 3 min (300 L), the TOC level returns to that of the incoming tap water and no more foulants are flushed out the module. As such, it is clear that for the foulants used in this study, only a very short period of physical cleaning is required after osmotic backwash. Consequently, the combination of

osmotic backwash and physical cleaning has proven to be an efficient cleaning strategy for the SW FO modules.

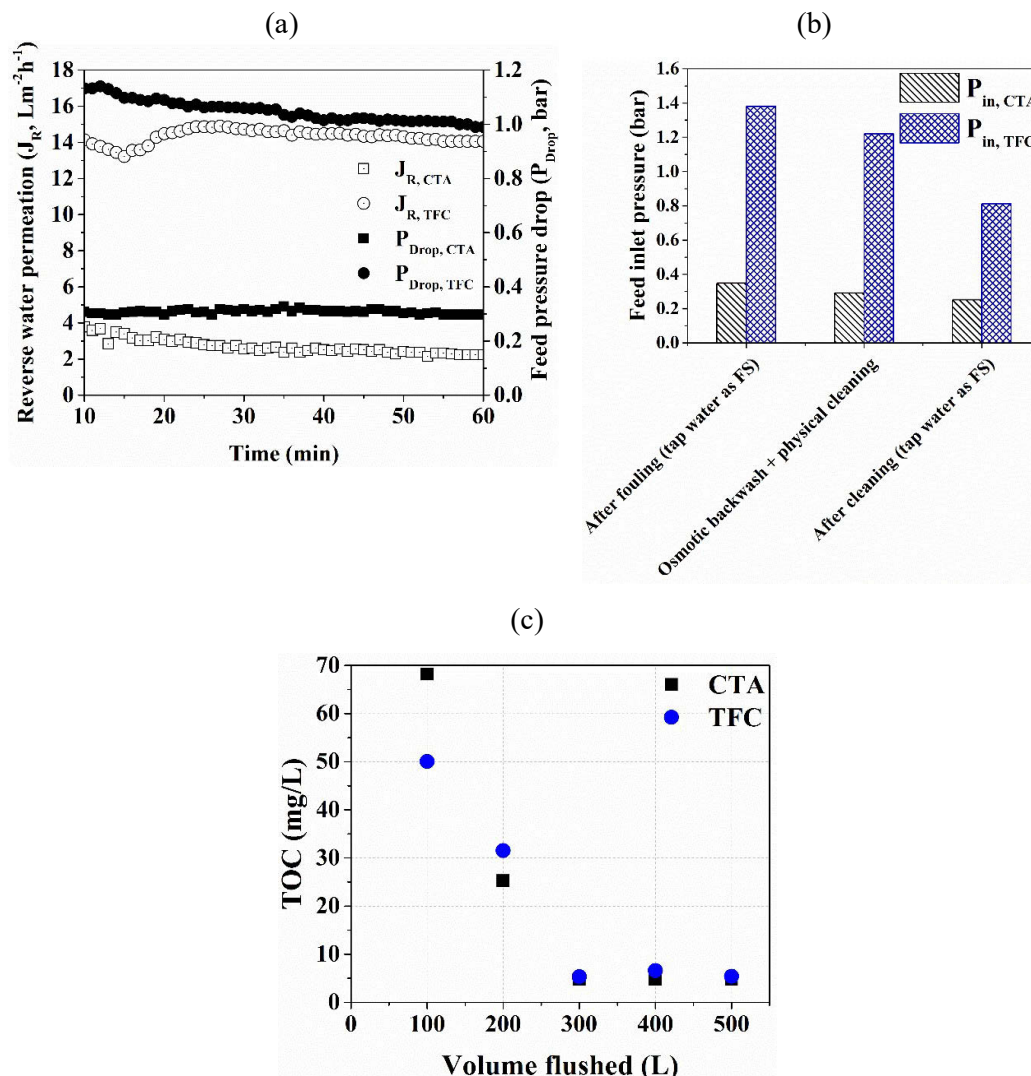


Figure 7 - 8. (a) Variation of reverse water flux and feed pressure drop with osmotic backwash operation time, (b) effect of osmotic backwash and physical cleaning on the feed inlet pressure recovery and (c) total organic carbon (TOC, mg/L) concentration as a function of the water volume flushed (L). Physical cleaning with maximum feed cross-flow velocity of 0.44 and 0.91 m/s for CTA and TFC, respectively was performed for 5 min using tap water. The TOC of the feed was around 94 mg/L.

7.4. Concluding remarks

This chapter presented practical considerations of SW FO modules with different membrane properties (CTA and TFC). The evaluation of two modules was conducted to establish hydrodynamic conditions under different feed and draw flow rates. In addition, the performances of two SW FO modules under different operation modes (FO and PAO modes) were compared. Finally, the effectiveness of the combined osmotic backwash and physical cleaning on the flux recovery was evaluated. The following conclusions have been drawn from this chapter:

- The draw side of the CTA module was more sensitive to flow rate due to the use of permeate spacers thick tricot creating more resistance to the flux. The operation of the draw side of the TFC module is less restrictive thanks to a mesh spacer but then less mechanical support is provided to the feed stream in the module. Also, pressure transfer from the feed to the draw channel was observed in PAO operation due to the potential compaction and narrowing of the draw channel.
- In PAO mode, enhanced water permeation caused by the additional hydraulic pressure on the feed side of the TFC module led to less RSF which is beneficial for process efficiency and potentially to limit (RSF enhanced) fouling propensity.
- Fouling tests demonstrated that fouling occurs even when only limited impact on permeation is observed. Pressure-drop can be an important indicator of fouling occurrence for practical SW FO operation. The combination of osmotic backwash and physical cleaning confirmed to be very efficient and easy to implement on a module scale.

CHAPTER 8

FORWARD OSMOSIS MEMBRANE MODULAR CONFIGURATIONS FOR OSMOTIC DILUTION OF SEAWATER BY FORWARD OSMOSIS AND REVERSE OSMOSIS HYBRID SYSTEM

This chapter was published as: **Kim, J. E.**; Phuntsho, S.; Ali, S. M.; Choi, J. Y.; Shon, H. K., Forward osmosis membrane modular configurations for osmotic dilution of seawater by forward osmosis and reverse osmosis hybrid system, *Water research* **2018**, *128*, 183-192

8.1. Introduction

Most FO studies have been so far conducted in a lab-scale level using small membrane coupons and the performance data from such studies are difficult to translate to large or full-scale FO systems. Performance demonstration and simulation of module-scale FO operation is, therefore, essential for providing a better understanding of its process performance and also in their economic and environmental impact assessments. Few FO studies have reported using commercial 4040 (4-inch diameter and 40-inch length) and 8040 (8-inch diameter and 40-inch length) spiral wound FO membrane element and module (Kim et al., 2014a; Kim & Park, 2011b). These studies have demonstrated the significant influence of the operational parameters such as solute concentrations, solution flow rates, and pressures on the permeate flow rate across the FO membrane. The changes in the solution flow rates could affect the pressure drop along the DS and FS channels which could become more significant in a multi-element FO module operation. The results obtained from a pilot-scale FO operation or module-scale simulation could be more realistic and useful for evaluating the economic and environmental viability of the FO-RO hybrid systems. Although there are several studies on the economic and environmental assessment of FO hybrid systems (Hancock et al., 2012; Valladares Linares et al., 2016), the issues and impact of the FO membrane element arrangement such as the number of membrane elements per housing and the optimum stages at which hydraulic pressure should be applied for PAO operation and their impact on the economic and environmental feasibility has not yet been evaluated in greater details.

The objective of this study is therefore to evaluate the performance of the FO module with multiple FO membrane elements arranged in series in a housing under different volumetric flow rates and the pressure differentials. In order to establish a correlation between the operational parameters of multiple FO elements in series, pilot-scale FO operation was conducted. The experimental data were then used to obtain an empirical correlation that can be used to extrapolate for determining the modular arrangement design scenarios in the FO process and its performance simulation, as well as a sensitivity analysis for the FO/PAO-RO hybrid system based on the different channel spacer and additional hydraulic pressure. Based on the performance simulation, the effect of module arrangement scenarios on the economics of FO hybrid systems is evaluated. This study,

therefore, provides a better understanding of the practical issues in the system design of a full-scale FO process.

This chapter is an extension of a research article published by the author in Water Research (Kim et al., 2017b).

8.2. Materials and Methods

8.2.1. Spiral wound FO membrane element

A commercial 8040 spiral wound polyamide based thin film composite (TFC) FO membrane element (Toray Industries, Korea) was used for pilot-scale FO and PAO experiments. The effective membrane area used for experiments and simulation is shown in Table 8-1. Each polyvinyl chloride housing contained single 8040 FO membrane element and the more detailed configuration of the FO membrane module used in this study can be found in our previous studies (Kim et al., 2014a; Phuntsho et al., 2016b). FO process was operated with the active layer of the TFC FO membrane facing the feed solution (FS) and the porous support layer of the membrane facing the draw solution. Finally, all FO tests were conducted under the co-current mode of cross-flow operation due to technical restrictions of our FO pilot unit for operating under the counter-current mode of crossflow direction.

Table 8 - 1. Input data for the performance simulation of FO and PAO processes.

| Parameters | Unit | Values |
|---|-------------------------|-----------------|
| Operating conditions | | |
| Feed flow rate | L/min | 30 – 60 |
| Draw flow rate | L/min | 2 – 6 |
| Feed inlet pressure (PAO) | bar | 4 |
| Temperature | °C | 25 |
| Membrane Material | | |
| Pure water permeability, A_{TFC} | $Lm^{-2}h^{-1}bar^{-1}$ | 5.54 ± 0.14 |
| Salt permeability, B_{TFC} | $Lm^{-2}h^{-1}$ | 2.26 ± 0.11 |
| Spacer channel height | mm | 1.19/3 |
| Effective membrane module area | m^2 | 15/8 |
| FS, Wastewater concentration ($\approx NaCl$) | M | 0.02 |
| DS, Seawater concentration ($\approx NaCl$) | M | 0.6 |

8.2.2. Feed and draw solutions

DS consisted of sodium chloride (NaCl) solution prepared using tap water to make it similar to the seawater (osmotic pressure of 27.8 bar at 0.6 M concentration). The FO hybrid systems in this study were assumed to treat wastewater effluent with an osmotic pressure of around 0.99 bar first by osmotic dilution using FO process and the downstream RO process to desalinate the diluted seawater (Phuntsho et al., 2016b). However, for this particular study, the FS was prepared by using NaCl only to have the osmotic pressure of 0.99 bar (i.e. 0.02 M NaCl) without the presence of any organics. The osmotic pressures of the solutions were calculated using the thermodynamic modelling software OLI Stream Analyser (Version 9.5 OLI Systems, Inc., Morris Plains, NJ). The initial volumes of the feed and draw solutions were 1,000 L and 500 L, respectively.

8.2.3. Pilot-scale experimental procedure

A schematic diagram of pilot-scale FO experimental set-up in which low-pressure pumps were used to circulate the feed and draw solutions has shown in Figure 3-5 (Chapter 3). The pressure, flow rate, electrical conductivity, and temperature of solutions were recorded online using sensors connected to a PC data acquisition system. The feed and draw inlet pressures were initially adjusted based on the specifications recommended by the manufacturer (Kim et al., 2014a).

The outlet solution parameter of the first module was used as the inlet parameters of the second module and so on. The parameters include the flow rates, pressures and concentrations of the both the DS and FS (Kim et al., 2014a). In total, experiments were conducted to simulate the series operation of up to 4 elements beyond which the experiment could not be carried out further, as the pressure differential exceeded the pressure recommended by the manufacturer (Kim et al., 2017a). The module in this study refers to all the FO membrane elements loaded in the housing while FO element refers to a single FO element.

8.2.4. Determination of pure water permeability and salt rejection

Pure water permeability (A_{TFC}) and NaCl rejection (R) of the FO element was evaluated in RO mode of operation by applying hydraulic pressure from 0.5 to 2.5 bar on the feed side. A_{TFC} value was measured using tap water on both sides of the membrane while rejection rate was measured using 1.2 g/L NaCl as feed and with hydraulic pressure on the feed side of the membrane. A_{TFC} and R for 8040 FO membrane element were found to be $5.54 \pm 0.14 \text{ Lm}^{-2}\text{h}^{-1}\text{bar}^{-1}$ (LMH) and 87%, respectively. Input data for FO and PAO performance simulation are shown in Table 8-1. The water fluxes in FO experiments were determined by measuring the difference in the draw flow rates between inlet and outlet of the FO membrane module which was further confirmed through the measurement of change in the mass of the DS in the DS tank.

Module-scale analysis in terms of water flux (J_w , $\text{Lm}^{-2}\text{h}^{-1}$, LMH) and salt flux (J_s , $\text{gm}^{-2}\text{h}^{-1}$, gMH) was performed to establish possible series element arrangement scenarios in the FO process. J_w can be expressed using the A value and feed and draw bulk osmotic pressures ($\pi_{F,b}$ and $\pi_{D,b}$, respectively). In addition, J_s can be expressed using the solute permeability coefficient (B) and the feed and draw concentrations ($C_{F,b}$ and $C_{D,b}$, respectively):

$$J_w = A(\pi_{D,b} - \pi_{F,b}) \quad (8-1)$$

$$J_s = B(C_{D,b} - C_{F,b}) \quad (8-2)$$

However, J_w and J_s should consider the effect of concentration polarization (CP) and RSF (Deshmukh et al., 2015). A mass transfer coefficient, k_F , represents the hydrodynamics of the feed flow in the feed channel thus indicating the occurrence of the concentrative external CP (CECP) on the feed side of the module. k_F is determined using Sherwood-Reynolds-Schmidt correlations (Deshmukh et al., 2015; Phuntsho et al., 2014b).

$$\pi_{F,m} = \pi_{F,b} \exp\left(\frac{J_w}{k_F}\right) \quad (8-3)$$

The structural parameter, S , of the porous support layer and the diffusivity, D , of the draw solute in water represents the dilutive internal CP (DICP) on the draw side. S is incorporated with the thickness, t_s , tortuosity, τ , and porosity, ε of the support layer (Phuntsho et al., 2014b).

$$\pi_{D,i} = \pi_{D,b} \exp\left(-\frac{J_w S}{D}\right) \quad (8-4)$$

The osmotic driving force is influenced by RSF due to an accumulation of draw solutes in the feed and thus reducing the water flux. This effect is mainly attributed to the degree of feed-side CECP because the increased cross-flow velocity in the feed channel reduces the reverse diffusion of the draw solute. Therefore, Eq. (8-5) and (8-6) incorporate the effects of the ECP and ICP:

$$J_w = \frac{A \left[\pi_{D,b} \exp\left(-\frac{J_w S}{D}\right) - \pi_{F,b} \exp\left(\frac{J_w}{k_F}\right) \right]}{1 + \frac{B}{J_w} \left[\exp\left(\frac{J_w}{k_F}\right) - \exp\left(-\frac{J_w S}{D}\right) \right]} \quad (8-5)$$

$$J_s = \frac{B \left[C_{D,b} \exp\left(-\frac{J_w S}{D}\right) - C_{F,b} \exp\left(\frac{J_w}{k_F}\right) \right]}{1 + \frac{B}{J_w} \left[\exp\left(\frac{J_w}{k_F}\right) - \exp\left(-\frac{J_w S}{D}\right) \right]} \quad (8-6)$$

The water flux shown by Eq. (8-1) has been modified to take into account the hydraulic pressure, which generates the transmembrane pressure (ΔP), and CECP (Eq. (8-3)) and DICP (Eq. (8-4)) phenomenon. The water flux ($J_{w, PAO}$) under PAO mode can be expressed as follows (Lutchmiah et al., 2015; Sahebi et al., 2015):

$$J_{w,PAO} = A \left[\Delta P + \pi_{D,b} \exp(-J_w K) - \pi_{F,b} \exp\left(\frac{J_w}{k}\right) \right] \quad (8-7)$$

Thus, the validation of pilot experimental flux and predicted flux for FO TFC membrane module under FO and PAO operations is also shown in Figure 8-1.

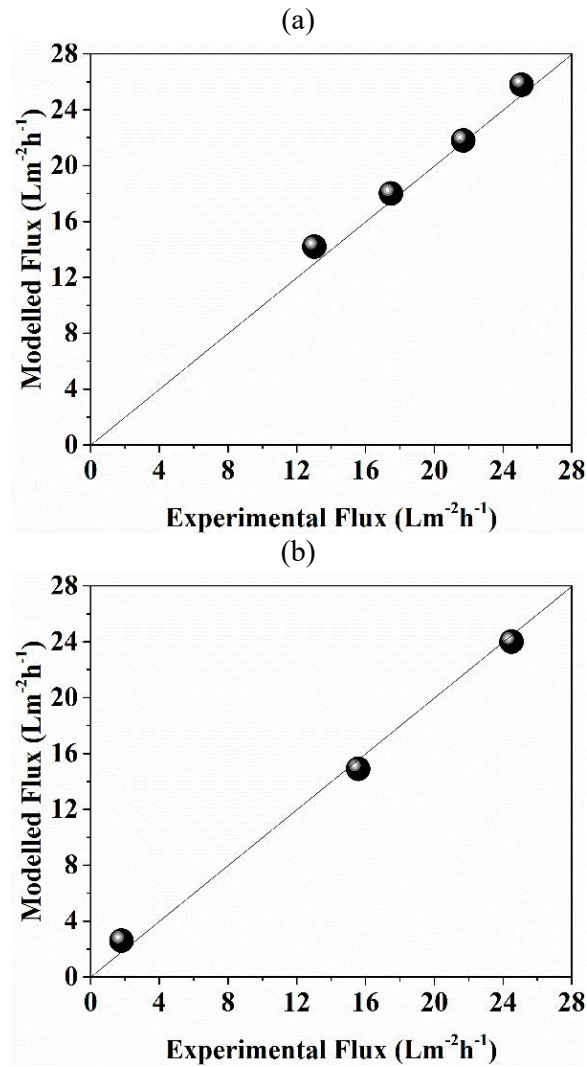


Figure 8 - 1. Validation of pilot experimental flux and predicted flux for FO TFC membrane module under (a) FO and (b) PAO operations.

8.3. Results and discussion

8.3.1. Correlation between the operational parameters of an FO module operation

Figure 8-2 shows the variations of average water flux, the FS and DS concentrations at the outlet of each FO element operated using a single element. The pilot-scale FO process was able to operate up to four number of 8040 FO membrane elements in series due to the operational limitation of FO process to keep the DS pressure within the safe operating

limit (Kim et al., 2017a; Kim & Park, 2011b). The highest average water flux of 25.1 LMH was observed for the first element which is expected due to the highest osmotic driving force available, however, the average water fluxes of each FO element decrease for the subsequent elements. The decline in the FO average water flux of the downstream elements is attributed to a cumulative decrease in the osmotic driving force due to the change in the solute concentrations of the FS and DS along the module as presented in the secondary axis of Fig. 2 (a). The DS concentration decreases along the elements due to dilution by the water flux coming from the feed side. The increase in the FS concentration was only slightly noticeable since the FS flow rate used in the pilot unit was much higher than the DS flow rate, because of which the feed recovery rate was low for the pilot operation. The water fluxes of each element refer to the cumulative average water fluxes of each FO element with a membrane area of 15 m².

It is important to note from the average flux results that under co-current FO operation (as applied in this study), the presence of large driving force in the first element is likely to produce very high water flux which would promote membrane fouling or scaling especially if it exceeds the critical flux of the membrane. This could result in increased cleaning frequency and hence reduce the membrane life (Phuntsho et al., 2014b). However, the current study did not include the effect of fouling on the performances in the FO process of the different FO hybrid system scenarios. The current design of the FO pilot unit also made it difficult to operate in the counter-current mode of operation.

Figure 8-2 (b) shows the pilot-scale experimental data of the inlet pressure for the single FO element in a housing at different inlet FS and DS flow rates conducted using 0.6 M NaCl as DS and 0.02 M NaCl as FS. It can be seen that when a higher FS and DS flow rates are used at the inlet of an FO element, the inlet pressure increases significantly with their respective flow rates. It must be noted here that the maximum feed inlet pressure of the FO process is 4 bar as recommended by the manufacturer. The feed inlet pressure decreases along the subsequent FO elements. However, the DS flow rate increases cumulatively along the FO channel along the module due to incoming water flux, this will lead to significant increase in the pressure at the inlet of the subsequent FO elements of a housing containing multiple elements in series. At the DS inlet flow rate of 5.7 LPM (liter per minute), the inlet pressure is 0.2 bar which increases to 0.60 bar when the inlet

flow rate reaches above 10 LPM. This pressure build-up is seen as one of the most critical operational parameters for FO module operation as it affects the pressure difference between the FS and DS that could undermine the integrity of the FO membrane. If the DS channel pressure increases above critical operational limit recommended by the manufacturer or the pressure increase above the feed pressure, the thin film polyamide active layer of the FO membrane is likely to delaminate as it is not supported on the opposite side or the feed side of the FO membrane. Besides, the initial DS flow rates and the pressure build-up along the membrane module will also depend on the initial DS concentration used and the number of membrane elements in a series in a single housing or stage. Even at similar inlet DS flow rates, if higher DS concentration is used, the water flux will be higher due to the increased driving force which increases the cumulative DS flow rates along the channel thereby further contributing to the pressure build-up as shown in Figure 8-2 (b). However, given that this study is limited to using seawater as DS, the concentration will not significantly change and hence the osmotic driving force is almost fixed. Increasing the number of elements in series within a single stage therefore increases the cumulative permeate flow rates at the last elements, which contributes towards higher pressure build-up. This pressure build-up is, therefore, likely to determine the maximum number of elements in series that can be safely accommodated in a single housing. This number of elements in a single housing will ultimately affect the feed recovery rates and the DS dilution factor (i.e. final diluted DS concentration) that can be achieved in a single stage FO process. The DS dilution factor and the concentration of the diluted DS are significant because it directly affects the energy consumption of the downstream RO process. At a lower dilution factor, the concentrations of the diluted DS will be higher which will ultimately increase the operating energy of the subsequent RO process which is not desirable.

A correlation between the initial FS and DS flow rates and its inlet pressures was developed by fitting the experimental data collected during the pilot-scale FO operation as shown in Figure 8-2 (b). The curve fitting provides the following empirical correlation equations that can be used to simulate and predict the variations of pressure in the housing containing multiple FO membrane elements in series at different inlet FS and DS flow rates, valid for specific operating conditions of 0.6 M NaCl as DS and 0.02 M NaCl as FS using 8040 TFC FO membrane elements are presented in Figure. 8-2. However, the

empirical correlation can be represented in a more general form of the equation that could be applicable to other configurations using the same membrane module as follows:

$$P_{FS}(\text{bar}) = K_1 Q_{FS}^2 - K_2 Q_{FS} + K_3 \quad (8-8)$$

$$P_{DS}(\text{bar}) = C_1 Q_{DS}^2 + C_2 Q_{DS} - C_3 \quad (8-9)$$

where P_{FS} and P_{DS} are the FS and DS inlet pressures and Q_{FS} and Q_{DS} are the FS and DS flow rates at the inlet of FO membrane element. K and C are the constants that could depend on various operational parameters such as DS and FS properties and membrane and geometric configuration of spacer and elements. Equations (8-8) and (8-9) can be therefore used in simulating the pressure build-up for a housing containing multiple elements in series. These quadratic equations, in fact, resemble a standard Bernoulli's equation of the fluid in a closed conduit where the pressure drop varies to the square of the flow rate (flow velocity) and clearly indicate the significant impact of the flow rates on the DS operating pressure during the FO operation. However, since the scope of this study is limited to the osmotic dilution of seawater using wastewater effluent, the K and C values obtained from the above empirical correlations are only to this particular scenario since the only major operating parameters available for variations are the DS and FS flow rates (or cross flow) as the DS or FS concentrations do not vary significantly. The mass balance relationship in a continuous mode of operation (Liyanaarachchi et al., 2016) along with the above empirical module-scale model (Deshmukh et al., 2015) can fairly simulate the performances of the FO process to suggest several modular options for system design of the FO process.

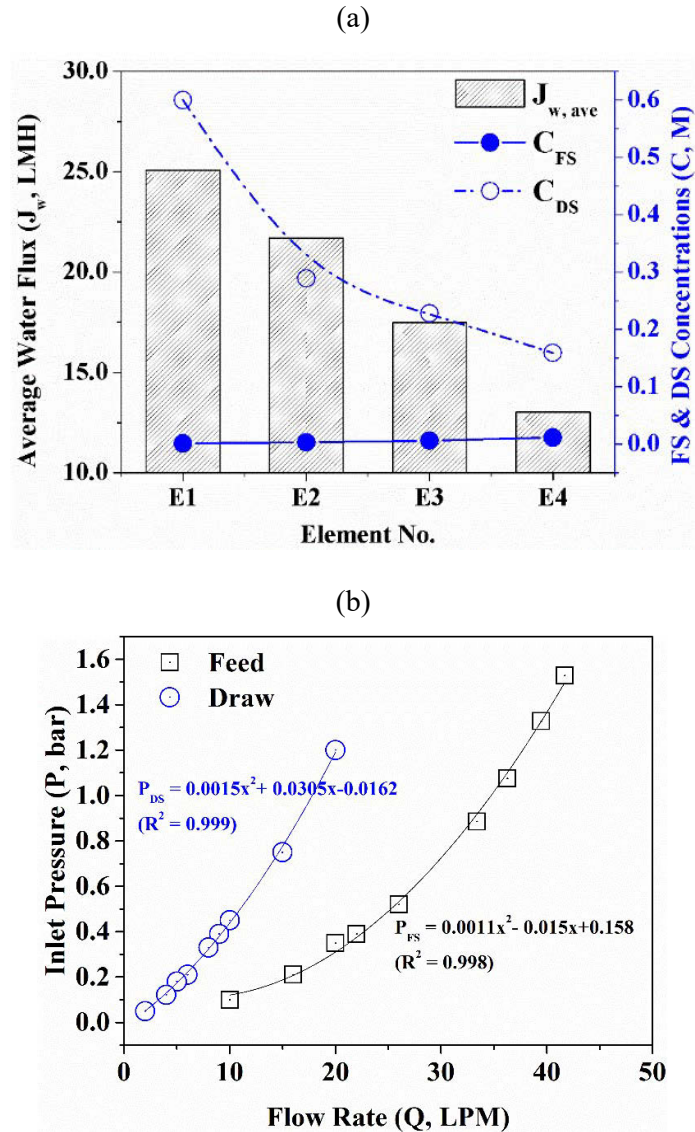


Figure 8 - 2. (a) Variations of average water flux and feed and draw solution concentrations along the number of elements and (b) variation of feed and draw inlet pressures (this is related to the feed and draw flow rates of the first element) as a function of feed and draw flow rates. This relationship data was obtained from pilot-scale FO operations. FO experimental conditions: 0.6 M NaCl as DS (seawater), 0.02 M NaCl as FS (wastewater), room temperature, and co-current cross-flow condition.

8.3.2. Determination of possible element arrangement options in series

8.3.2.1. Simulating the variations of flow rate and pressure along the FO module

In a typical RO plant, up to 8 elements are connected in series in a single housing (DowFilmtec, 2016; Wilf & Klinko, 2001) and the aim here is to evaluate the possibilities of a similar module arrangement for FO process simulation. In module-scale FO operation, it has been observed that the feed and draw inlet pressures are critical (Kim et al., 2017a). As this pressure variation depends on the flow rates, it is important to understand how this pressure would impact the elemental arrangement within the housing to form an FO membrane module. The initial FS and DS flow rates and the permeation flow rates are therefore likely to be more critical in contributing to the pressure variation in the FO membrane elements. Since permeate flow rates cumulate along the element in series in a housing, it depends on the water flux which in turn depends on the osmotic driving forces (DS concentration). It is, therefore, important to simulate the pressure build-up by considering all these major parameters.

Figure 8-3 (a) shows the variations of feed flow rates, DS flow rates and permeate flow rates ($Q_{p/\text{element}}$) along the FO elements in the housing containing 8 elements in series. As the initial DS flows ($Q_{DS,\text{in}}$) through the DS channel, it picks up the permeate water from the feed increasing its flow ($Q_{DDS} = Q_{D,\text{in}} + Q_p$) which then becomes a diluted DS. As the water flux is generated throughout the length of the module, the DS flow rate increases cumulatively along the FO module passing through each FO membrane element. This cumulative increase in the DS flow rates along the downstream of the DS channel can significantly contribute towards the pressure build-up. The simulation shows that the DS and FS flow rates become equal at about 4th FO element in series in the housing. If the point at which the FS and DS flow rates becomes equal is to be considered as the limit for the FO operation, then it appears that the maximum number of FO element under the conditions simulated in this study is only four FO elements in one housing. If the housing contains more than four elements, the DS flow rate could exceed the feed flow rates likely creating a negative pressure differential that could undermine the FO membrane integrity. This is likely to be highly critical for fixing the operational conditions of the FO process.

Figure 8-3 (b) shows variations of the simulated feed and draw inlet pressures along the elements in a housing under different feed inlet flow rates (30-60 LPM) but at fixed initial draw flow rate of 2 LPM, which was the lowest flow rate we could operate in the pilot-scale FO unit used for this study. When the feed flow rate increases from 30 to 60 LPM, the inlet feed pressure also correspondingly increases, however, the feed inlet pressure of each FO element decreases gradually after about 5th element in series in the same housing. This pressure drop along the FO module is expected firstly due to the decrease in the feed flow rate along the feed channel as water is extracted continuously by the DS and secondly due to frictional loss within the hydraulic channel of the feed inside the membrane element. If this pressure drop on the feed side is large, it could likely have an impact on the pressure differential across the membrane as the pressure on the DS side will increase along its housing (Figure 8-2 (b)). At about the 5th element, the draw inlet pressure becomes equal (at inlet DS flow rate of 2 LPM) to the feed inlet pressure of around 1.4 bar (at inlet FS flow rate of 60 LPM) due to pressure build-up as a result of cumulative permeate flow (Kim & Park, 2011b; Phuntsho et al., 2014b). This is, in fact, the similar point at which the DS and FS flow rates become equal based on the simulation results in Figure 8-3 (a), for the initial feed flow rate of 60 LPM. This pressure build-up may not significantly affect the DS pumping energy as the increased permeate flow rate would naturally generate adequate hydraulic energy to drive out the diluted DS through the DS channel without the need of additional pumping load to the DS. However, this increased diluted DS flow rate could contribute to the pressure differential that can impact the membrane integrity which needs careful consideration.

When lower inlet FS flow rates are used, the number of elements in series that can be safely accommodated in a single housing further decreases to 4, 3, and 2 at inlet FS flow rates of 50, 40, and 30 LPM. This is because at these lower FS flow rates, the inlet feed pressure is also correspondingly low and hence the increased inlet DS pressure could easily exceed the inlet feed pressure along the module. Therefore, the only approach here is to operate the FS at a suitable and fixed inlet pressure even when lower initial FS flow rates used. Although using a higher initial FS flow rate could increase the inlet feed pressure, however, this option will also increase the head loss in the system and also reduce the feed recovery rate of the system. These results therefore suggest that if lower

feed flow rates are to be used to enhance feed recovery rates of the FO system, the only way is to operate the feed at slightly elevated feed pressure and this means subjecting the FO process under the PAO mode of operation. This pressure differential developed in the module would, however, be different for those modules operated under co- and counter-current cross-flow directions. The pressure differential along the membrane module would not vary significantly when operated in a counter-current crossflow mode since the feed direction on which pressure drop occurs is associated with the direction of the DS at the inlet side where the initial pressure is also lower.

The influence of the initial DS flow rate on the feed and draw inlet pressure (at fixed FS flow rate of 60 LPM) for the number of membrane elements in series in the housing is shown in Figure 8-3 (c). The number of FO membrane elements that can be safely accommodated in a single housing (without exceeding the inlet feed pressure) decreases with the increase in the initial DS flow rate used in the FO process. For example, the maximum number of elements is 5 for an initial DS flow rate of 2 LPM but decreases to 4 at an initial DS flow rate of 4 to 6 LPM. These indicate that FO process must use lower initial DS flow rates if a higher number of FO elements is to be safely accommodated in the housing to enhance feed recovery rates. However, for an FO desalination plant of fixed capacity, the initial DS flow rate and concentration correlate inversely (Phuntsho et al., 2017a) and hence it must be complemented by higher DS concentration. However, this could be a challenge for a situation such as in this study where seawater used as DS has almost fixed concentration. Therefore, this study shows that the initial DS flow rate plays a significant role in determining the number of membrane elements in series per housing for the FO process in order to maintain safe operating pressure differential. Based on the results in Figure 8-3 (c), the initial DS flow rate of 4 LPM was therefore selected for further simulation for 4 membrane elements in series (under the conditions used in the study) to maintain the least draw pressure build-up even though using higher draw inlet flow rate enhances the water extraction capacity and the feed recovery rate (Phuntsho et al., 2014b).

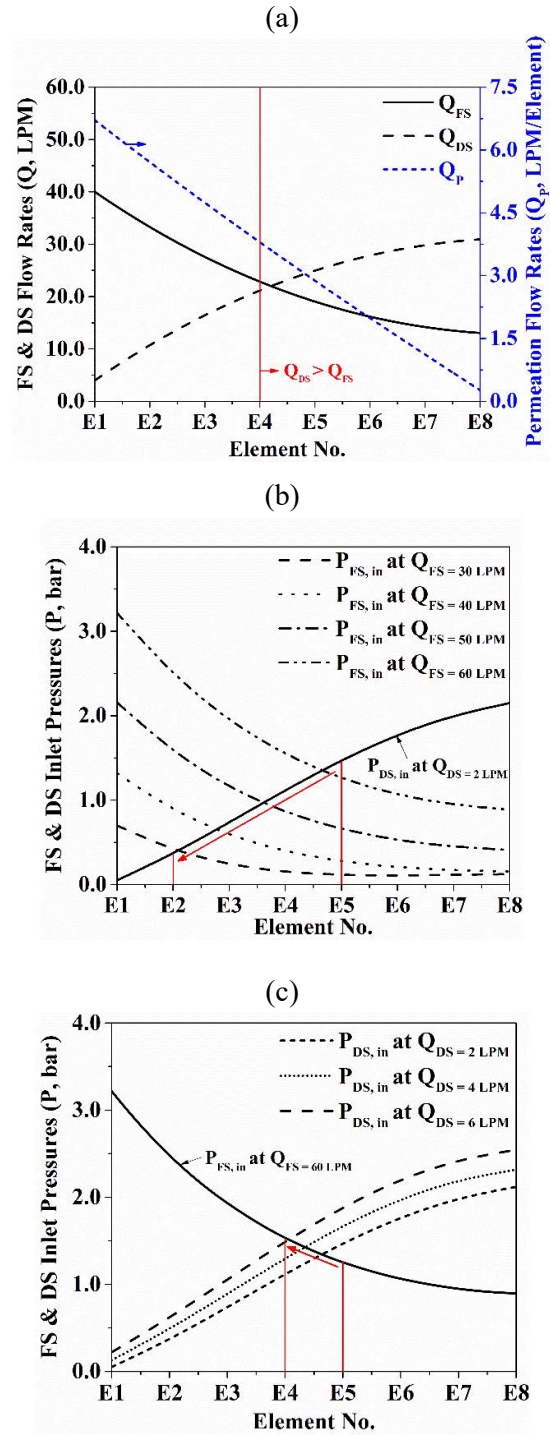


Figure 8 - 3. (a) Variations of the initial flow rates along the DS channel and feed and draw inlet pressures with the number of elements under different (b) feed and (c) draw flow rates.

8.3.2.2. Exploring different FO element arrangement scenarios: sensitivity analysis

Providing more number of elements in each housing helps increase the feed recovery rates, increases the production capacity and plant compactness. The results from Figures 8-2 and 8-3, however, indicate that the total number of FO membrane elements in a single housing will be limited due to pressure build-up inside the DS channel which otherwise could undermine the integrity of the FO membrane during the operations. The elemental arrangement for an FO module may not be suitable if it is simply based on the established RO module and hence is likely to require certain modifications to suit its process performance. Several possible modular design options are proposed as shown in Figure 8-4 and these options are based on the following criteria:

- The hydraulic pressure of the DS should not exceed the hydraulic pressure of the FS due to pressure drop in each solution channel and this is essential to protect the integrity of the thin rejection layer of FO membrane due to likely delamination.
- The diluted DS should have the lowest possible concentration as this determines the energy for any post-treatment by the RO process.

Pressure drops inside the DS and FS channels is mainly responsible for the pressure difference between the two channels and hence the proposed design options mostly looked at the factors responsible for these pressure drops. Some of the major factors responsible for pressure drop are the channel thickness, initial FS and DS concentrations and its flow rates, water flux through the membrane (which in turn depends on the osmotic driving force and the membrane performance), feed recovery rates and DS dilution factor and number of membrane elements in a single housing. Maintaining positive pressure difference (higher pressure for FS channel) therefore would involve controlling these factors that affect the pressure drop inside the channels. The fluid velocity directly affects the pressure drop inside the channel (pressure drop proportional to the square of the velocity) and hence controlling fluid velocity is one way of controlling the pressure drop. Hence, one way of limiting pressure on the DS channel is to start the FO process with lower initial DS flow rate at the inlet of the first element but this is not applicable for the current FO process where its target application is for osmotic dilution of seawater using

wastewater and seawater concentration is fairly constant. The second option is to use FO membrane element with different channel thickness either in a single housing or different stages so as to limit the pressure drop inside the channel due to change in the solution flow rates. Another option is to elevate the hydraulic pressure of the FS (i.e. under the PAO mode) to negate the pressure increase on the DS side of the FO membrane. A total of six different modular design options have been proposed and compared in this study as described in Figure 8-4 and Table 8-2.

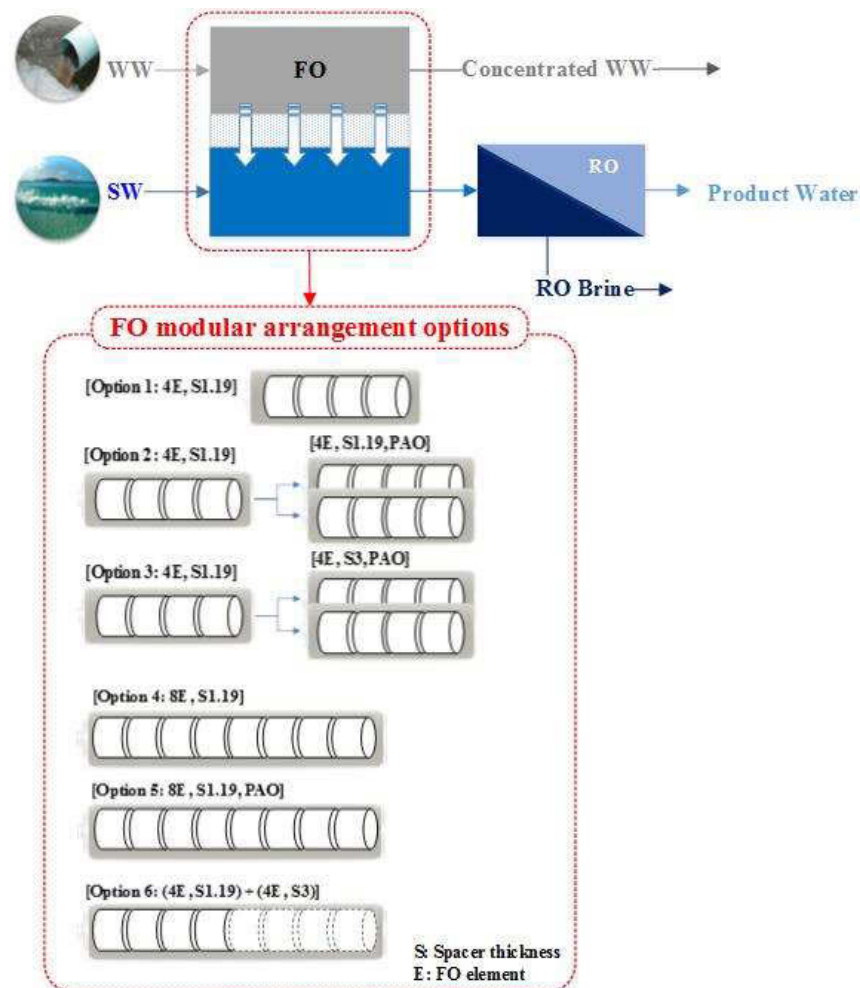


Figure 8 - 4. Schematic of possible modular design options of the FO process with the integration of PAO process. N.B. WW: Wastewater, SW: Seawater.

Table 8 - 2. Six different modular configuration options for sensitivity analysis.

| Possible Modular Options | Description |
|--------------------------|---|
| Option 1 | one stage containing 4 elements in series per housing with a uniform channel thickness of 1.19 mm. This option based on our earlier observation discussed under Section 3.2. |
| Option 2 | two stages FO modular arrangement. The first stage contains one PV with 4 elements (exactly as option 1) and the second stage contains two housing in parallel each with 4 elements. All the FO membrane elements have the same spacer thickness of 1.19 mm. The second stage is however subjected to PAO mode at a feed pressure of 4 bar based on the recent study by Blandin et al. (2015b). |
| Option 3 | similar modular arrangements as in option 2 except for the much larger channel spacer thickness used for all the membrane elements in the second stages with 3 mm instead of 1.19 mm. |
| Option 4 | one stage containing 8 elements per housing in series with the same channel spacing of 1.19 mm throughout. |
| Option 5 | a similar arrangement as option 4 except that the housing is subjected to PAO at 4 bar applied pressure. |
| Option 6 | one stage containing 8 elements in a single housing but the first 4 elements have channel spacers of 1.19 mm and the last 4 elements with 3 mm spacer thickness. |

8.3.3. Performance simulations of the different modular options

As expected, Figure 8-5 (a) shows that the feed inlet pressure for each FO element decreases while the draw inlet pressure increases gradually but the DS inlet pressure does not exceed the feed inlet pressure for elements arranged in series of up to 4 elements per housing for options 1 to 3. In the second stage, two housings are provided in parallel with each housing containing 4 elements but of different spacer thickness for options 2 and 3 and operated under PAO mode in order to compensate the loss of osmotic driving force. The idea here is to divide the flow rates in order to reduce both the feed and draw inlet pressures and lower the pressure difference so that second stage can be operated safely with positive pressure difference. The feed inlet was elevated to 4 bar by applying external hydraulic pressure which decreased to 3.6 bar at the last element for both options 2 and 3. It can be seen that the draw inlet pressure for option 2 increases much more rapidly compared to option 3 because of the smaller spacer thickness used and reaching almost

similar to the inlet feed pressure at the end of the 8th element (4th element in the second stage). The draw inlet pressure at the end of the 8th element (4th element in the second stage) for option 3 is only about 3.2 bar which is much lower than the feed inlet pressure at that point. These results show that by using larger channel spacer thickness and enhanced hydraulic pressure in the second stage, the DS pressure build-up can be mitigated and thus able to accommodate more than 4 elements in the second stage thereby increasing the feed recovery rate. Our estimate shows (data not presented) that up to 6 elements can be easily accommodated in the second stage for option 3 which could help further enhanced feed recovery rates of the FO modules.

It was shown in Figure 8-5 (a) that by using larger spacer thickness or by operating the FO module under PAO mode or both, the pressure differences between the FS and DS can be maintained positive for the safe operation of the FO module. This technique has been applied in options 4, 5, and 6 to see whether FO modular operations can be conducted safely in a standard single stage, 8 elements per housing as shown in Figure 8-4.

Option 4 is, in fact, an extension of the option 1 to 8 elements per housing as a means for comparison. It is obvious from Figure 8-5 (b) that without any modification, the first stage housing cannot accommodate more than 4 elements in series as the DS pressure would easily exceed the feed pressure. When the same module is operated under the PAO mode as in option 5 at about 4 bar feed inlet applied pressure, a higher positive pressure difference can be maintained between FS and DS compared to option 4 however, the DS pressure still increases above the feed pressure after the 4th FO element. This shows that even by elevating the feed pressure, the first stage FO module still cannot accommodate more than 4 elements per housing. This is because of the very high water flux generated under the combined osmotic driving force and applied hydraulic pressure that results in higher permeate flow rates in the DS thereby rapidly increasing the draw pressure significantly. This is evident from the very high cumulative permeate flow rates shown in Figure 8-5 (c) for option 5.

A larger spacer thickness (3 mm) is used for the last four FO elements of the 8 elements in a housing in option 6. The results in Figure 8-5 (b) shows that even using larger feed

spacer thickness from the 5th element onwards, the feed inlet pressure for element E5 remains almost same as the feed outlet of E5. This is expected because entry pressure is not expected to change although the pressure-drop or build-up inside the last four elements will change as evident from the results in the Figure where the draw pressure build-up is very gradual compared to option 5. Although the draw pressure in the last three is lower compared to option 4 however, it still exceeds the feed pressure above 4th elements of the housing and hence option 6 cannot be operated safely with 8 elements in a single housing. Using a larger spacer thickness for all the eight elements could be one way of keeping the draw pressure below feed if option 6 is to be operated safely, however, this will also significantly decrease the effective membrane area thereby decreasing the throughput and feed recovery rates and decreasing the footprint.

The results in Figure 8-5 (c) show that the permeate throughput of the FO module is highest for option 5 because of the additional permeate flux due to applied pressure subjected to all the membrane elements in the module. This, therefore, results in the highest DS dilution and hence the lowest concentration of the diluted DS with a final concentration of about 0.044 M as shown in Figure 8-5 (d). The extent of DS dilution is important as this has direct implications on the energy of the RO post-treatment process. The results also show that the next highest permeate throughput is obtained for option 2 followed by option 3 as shown in Figure 8-5 (c) and hence, correspondingly lower DS dilution with a final diluted DS concentration of 0.049 M and 0.064 M, respectively (Figure 8-5 (d)). Although options 2 and 3 use the same modular configurations and hydraulic pressure, option 2 shows the higher permeate throughput than option 3 due to its larger effective membrane area in the element when smaller spacer thickness is used. These results show that, by slightly elevating the feed hydraulic pressure, it can compensate for the loss of osmotic driving force in the second stage and therefore enhance the throughput and hence the extent of dilution. Besides, it also helps maintain a positive pressure difference between FS and DS. The lowest permeate throughput was observed for options 4 and 6 as shown in Figure 8-5 (c) because of which they also resulted in lower final DS dilution as presented in Figure 8-5 (d).

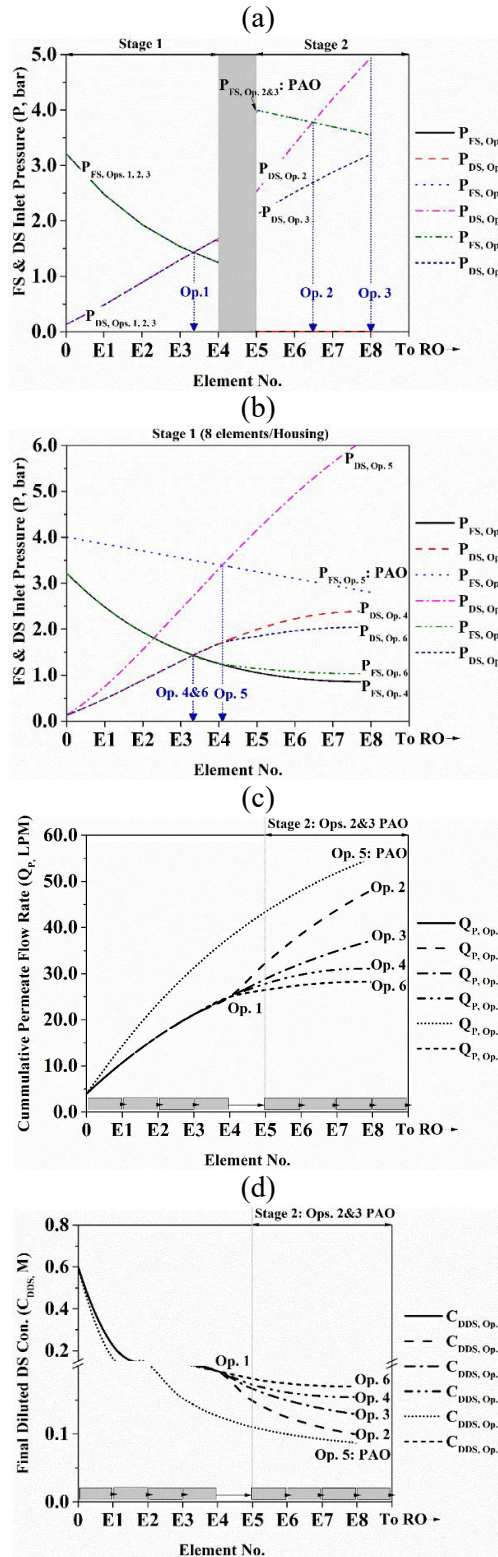


Figure 8 - 5. Variations of the feed and draw inlet pressures, P_{FS} and P_{DS} (a) in options 1, 2, and 3 and (b) in options 4, 5, and 6, (c) the cumulative permeation flow rate, Q_p , and (d) the final diluted DS concentration, C_{DDS} under different module design options as shown in Figure 8-4.

8.3.4. Implications of the configuration options

The results in Figure 8-5 clearly demonstrated that combining FO membranes with different channel spacer thickness in the same housing or in different stage housing can help reduce the pressure build-up in the draw channel and thus their implications to the overall system should be assessed and discussed. Using membrane elements with larger spacer thickness reduce the packing density of the FO module (increases plant footprint) and reduce the feed recovery rates. However, operating the FO modules under PAO mode not only helps maintain a positive pressure difference but also increase the permeate throughput thereby lowering the plant footprint and enhancing feed recovery rates. It must also be pointed out that applying external hydraulic pressure on the feed not only incurs additional energy cost to the system but also can lower the osmotic process efficiency due to enhanced dilutive ICP when operated at higher water flux than the normal osmotic flux. Option 5 has a similar configuration of the established RO and NF membrane processes and hence could be the most preferred configuration for FO process. However, based on the results in Figure 8-5, options 2 and 3 are the most suitable modular configurations for FO process under the conditions simulated in this study. These options are capable of not only maintaining positive pressure differences between the feed and draw solutions for up to a total of 8 elements in two stages, it could also accommodate more than 4 elements in the second stages in a single housing thereby helping further enhance the system capacity.

For a fair comparison, Figure 8-6 presents the total membrane area required and specific energy consumption (SEC) of the combined FO and RO hybrid system without energy recovery device for the six different configuration options described in Figure 8-4. Assuming a plant capacity of 100,000 m³/day at 50% feed recovery rate and pump efficiency of 85%. The SEC of seawater RO (SWRO) process alone was taken at 3.9 kWh/m³ (Kim et al., 2015a) for comparison in this study.

Figure 8-6 (a) clearly shows that the total membrane area required for option 1, 2, 3, and 5 are comparable while the total membrane area required for options 4 and 6 are significantly higher confirming the advantage of PAO mode in lowering the plant footprint. The total SEC of all the options shown in Figure 8-6 (b) indicates that the SECs

of the FO hybrid systems are still much lower than the conventional SWRO desalination process. This is expected due to the osmotic dilution of the seawater by the FO process before desalination by the RO process. The total SEC for options 1, 4 and 6 are the highest mainly because of the final diluted DS concentration which were higher that increases the SEC of the RO process and this further confirms that these modular configurations are not suitable. The SEC of options 2 (1.38 kWh/m³) and 3 (1.45 kWh/m³) are slightly lower than most other options which further support their suitability for system configuration for modular operations of the FO-RO hybrid system. For all the six hybrid options considered in this study, SEC of RO process forms the largest proportion of the total SEC and the contribution of FO and PAO processes were less significant. Although options 1 and 6 resulted in the highest SECs, overall however, the SEC between the six options were not drastically different indicating that the suggested modular configuration of the FO-RO hybrid system can be suitably adopted for FO system design. It is therefore expected that with optimization in the spacer thickness and applied hydraulic pressure, there could still be potential for further reduction in the membrane and energy cost which needs further investigation including the effect of using different thickness for DS and FS channels.

However, it must be noted that this simulation study is limited to the FO operation conditions under the co-current crossflow and the results might slightly different as the directions of pressure drop changes. The principles of pressure drop (pressure build-up for DS and pressure drop/decrease for FS) for FO modular operation will however still apply universally whichever configuration or cross-flow directions are used.

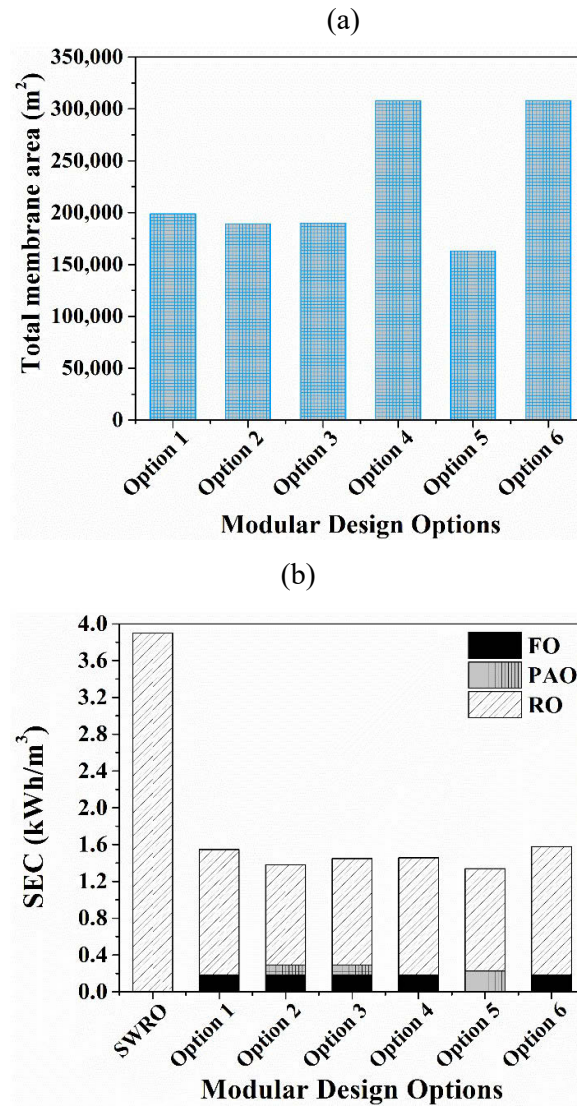


Figure 8 - 6. Evaluation of (a) total membrane area required (m²) and (b) specific energy consumption (kWh/m³) of different FO hybrid process options.

8.4. Concluding remarks

This study evaluated the various options for full-scale modular configuration of FO process for osmotic dilution of seawater by wastewater for simultaneous desalination and water reuse through FO-RO hybrid system. The following conclusions are drawn from this study:

- During FO module operation, feed flow rate decreases (pressure drops) while the draw flow rates increases (pressure build-up) along the membrane housing thereby reducing the pressure differences across the membrane. Experimental study shows that the initial DS flow rate is a very important operating parameter as it significantly affects the pressure build-up along the FO housing and hence determines the safe number of FO membrane elements that can be accommodated in series in a single housing.
- Experimental studies under the conditions tested in this study show that a single housing cannot accommodate more than 4 elements as the draw pressure exceeds the feed pressure indicating that normal single housing with 8 elements is not likely to be practical for safe FO operation.
- Six different FO modular configurations simulated in this study show that 2-stage FO configuration with multiple housings (in parallel) in the second stage using same or larger spacer thickness can help reduce the draw pressure build-up due to reduction of the draw flows in the second stage thereby allowing 4 or more FO elements in the second stage housing to be safely accommodated.
- Operating the second stage FO under slightly elevated feed hydraulic pressure (PAO) not only compensates the loss of osmotic driving force but also enhances permeate flux and maintains positive pressure differences.
- The energy penalty posed by the PAO mode of FO operation is compensated by enhanced permeate throughput, reduced membrane area, and plant footprint.

- The contribution of FO/PAO to the total SEC of the FO-RO hybrid system was not significant compared to the SEC of the RO process which still formed about 90% of the total SEC indicating that the proposed two-stage FO modular configuration is one way of making the FO full-scale operation practical for FO-RO hybrid system.

CHAPTER 9

CONCLUSIONS AND RECOMMENDATIONS

9.1. Conclusions

Although the studies on the application of the FO process has been gaining popularity recently however the study on how the FO process would perform as a system is still yet to be fully understood due to limited literature on the performances of the module-scale operations. This study therefore makes significant contributions towards understanding the FO module-scale operation including identifying the limitations and options to overcome during the full-scale operations. In order to process the FO technology to commercial readiness, there is a clear need for technological, environmental and economic assessment to not only understand its own system performances but also to understand its comparative advantages over the existing technologies such as state of the art RO technologies. The following sections provide brief conclusions drawn from this study and some of the recommendations for future studies to further progress this technology.

9.1.1. Long-term module-scale operation of forward osmosis and nanofiltration hybrid system in the field

The FDFO-NF hybrid system was operated in the field at one of the coal mining sites in New South Wales, Australia for about six months

This study (Chapter 4) showed that FDFO desalination can be operated long-term with minimal chemical cleaning frequency because simple hydraulic cleaning was observed effective in restoring the water flux due to organic fouling. As the FO converts impaired water sources into high quality treated water for the post-treatment process, the NF process performed efficiently without any issue of fouling or scaling, indicating that chemical cleaning costs will be significantly reduced or eliminated for the NF process when combined with the FO process. However, this study also observed that the reverse diffusion of fertilizer draw solutes containing nutrients (N or P) in the feed brine would be one of the significant challenges for brine management hence requiring special and expensive brine management system. In fact the fertilizer concentration becomes even worst when the FO process is operated at higher feed recovery rates. In addition, a low feed solute rejection could result in the accumulation of feed salts in the draw solution

when the FO is operated under a closed-loop system and thus impairing the final product water quality for fertigation. This study, therefore, demonstrates the significance of a need to develop an FO membrane with much higher water flux and solute flux.

9.1.2. Environmental and economic feasibility of the FO hybrid system

The long-term operation of the FDFO-NF hybrid system indicates the technological feasibility of the system for fertigation. However, for a commercial reality, the environmental and economic life cycle assessment for the FDFO-NF hybrid system is essential to understand its advantages and competitiveness over the existing technology such as microfiltration (MF)-reverse osmosis (RO) or MF-RO and ultrafiltration (UF)-RO or UF-RO using as pre-treatment to RO process. The study in Chapter 5 showed that the FDFO-NF hybrid system has a lower environmental impact and economic cost compared to the conventional MF/UF-RO hybrid systems mainly due to lower energy consumption and cleaning chemicals given the feed water and draw solution conditions considered in this study. However, the types of FO membrane and its performances play a significant role in the environmental impact and its economic costs. In closed-loop FO hybrid system, the economic cost of the FDFO-NF process using a thin-film composite FO (TFC-FO) membrane with an optimum NF recovery rate of 85% was observed to be the lowest at a given feed and draw solute conditions used in this study. The performance of FO membranes in terms of water flux and salt selectivity had significant implications on the capital and operational costs of the entire process. Sensitivity analysis of the FDFO-NF hybrid system indicates that the key parameters to further reduce the CAPEX and OPEX are the cost of the FO module, the average water flux, and the recovery rate of the NF process and this indicates that there is still plenty of room to further lower its environmental impact and economics by improving the FO membrane performances.

9.1.3. Different types of inorganic draw solutes in the life cycle assessment of the FO hybrid systems

A closed-loop FO-RO/NF system was evaluated for treating coal mine impaired water using different types of draw solutes in order to understand their comparative

performances and their choice of suitability based on the environmental and economic life cycle assessment (LCA) (Chapter 6).

A performance of the draw solutes must be assessed under both the FO and RO or NF process as this could have a significant environmental and economic (OPEX and CAPEX costs) impacts. Based on the performances of the draw solutes with the RO and NF post-treatment process (i.e. DS separation and reconcentration), divalent draw solutes such as Na_2SO_4 would be provide greater benefits such as lower DS replenishment cost and better quality of product water because of the high rejection of the solutes by the post-treatment process like RO or NF. The loss of draw solute by reverse diffusion and the feed rejection rates of RO and NF process (permeate concentration) would significantly influence the draw solute replenishment cost in a closed-loop FO hybrid system. The environmental impact of FO hybrid systems indicates that the dominant contribution to the global warming impact is due to the energy consumption of the RO or NF process.

The CAPEX cost of the FO hybrid systems was found around 37.5% higher on average than that of the seawater RO due to the significant membrane area required for the FO process based on the membrane performance used in this study. However, the operational cost of FO hybrid system is about 62 % lower than that of seawater RO system, mainly due to much lower operating energy of the FO hybrid system. In a closed-loop FO hybrid system, the specific reverse salt flux and draw solute cost is crucial in reducing the environmental and economic impacts of the FO hybrid systems.

Capital cost evaluation indicated that the capital cost of FO hybrid systems showed around 37.5% higher on average than that of seawater RO due to the significant FO membrane area required. However, the operational cost of FO hybrid systems showed around 62% lower on average than that of seawater RO, mainly due to much lower operating energy consumption. Overall, in a closed-loop system, specific reverse salt flux and draw solute cost play a crucial role in reducing the environmental and economic life cycle impacts of the FO hybrid systems. Developing novel draw solutes or an appropriate draw solution needs to be used to further reduce the DS loss cost in the FO process and the energy usage in the reconcentration process (RO or NF).

9.1.4. Spiral wound forward osmosis membrane module operation: hydrodynamics, fouling behavior and cleaning strategy

Understanding the performances of a module-scale FO process operation is important for designing an optimum configuration for a full-scale system. The module-scale performance could depend on several operating parameters such as feed and draw water properties, required product water quality, the following configuration, membrane element type, etc.

Chapter 7 investigated two different 8-inch SWFO modules (CTA and TFC based membrane modules) in terms of their hydrodynamics, operating pressure, water and solute fluxes, fouling behavior and cleaning strategy. The results show that for a module-scale FO operation, we must use a significantly lower initial DS flow rate compared to the feed water flow rate since the pressure-drop (pressure build-up) is likely to occur in the draw channel as the flow rates drastically increase along the channel. Increasing the draw pressure above the feed can damage the membrane and hence suffer the membrane from integrity issues. Based on the spacer thickness between the CTA and TFC membrane modules. The results clearly indicated that spacer design is crucial for pressure control in the SWFO module.

Since it is impractical to reach osmotic equilibrium by the osmotic process alone (infinite membrane area and feed volume required) without the external influence, the FO membrane module was also operated under the influence of an external hydraulic pressure (max of 2.5 bar in this study) or under the pressure assisted osmosis (PAO) mode of operation. The advantage of this concept is that the applied pressure can improve the water flux especially as the driving force of the DS decreases along the DS channel due to dilutive effect and hence reduce the membrane area required and the capital cost. Under both FO and PAO (applied pressure up to 2.5 bar) operations, the TFC module showed a significantly higher water flux and lower reverse salt flux than the CTA FO membrane module.

The study on the fouling behavior of the SWFO modules showed that the feed inlet pressure could be more sensitive to foulant deposition than the water flux as the fouling

deposition appears to occur in the feed channel rather than on the membrane surface under the conditions considered in this study. Osmotic backwashing combined with physical cleaning was conducted to assess whether osmotic backwashing would have a clear effect on restoring the water flux of the membrane after subjecting the membrane to fouling tests. The combination of osmotic backwashing and physical cleaning can be a very effective approach and can be adapted to large-scale FO operation for the FO process.

9.1.5. FO membrane module configuration options for osmotic dilution of seawater by FO-RO hybrid system

In a typical RO plant, up to 8 elements are connected in a series in a single housing and the study in Chapter 8 was aimed at understanding whether similar FO membrane element arrangement is practical for the FO process and if not evaluate options for full-scale modular configuration of FO process for osmotic dilution of seawater by wastewater for simultaneous desalination and wastewater reuse through FO-RO hybrid system. Our earlier studies have shown that the feed and draw inlet pressures and the pressure difference between the feed and draw along the membrane module are considered critical for the module-scale operations. Due to lack of a FO pilot unit with a full-scale membrane module configuration, the study was conducted using empirical relationships obtained from a single FO membrane element operation where the outlet parameters of the first 8040 FO membrane element was used as the input parameter of the second and so on for the FO elements arranged in series. This empirical equation was then extrapolated and then used to simulate the operational performances of different FO module configuration.

During the FO module operation, the feed flow rate decreases (pressure drops) while the draw flow rates increase (pressure build-up) along the membrane housing thereby reducing the pressure differences across the membrane which could significantly undermine the integrity of the FO membrane. The experimental study showed that the initial DS flow rate is a very important operating parameter as it significantly affects the pressure build-up along the FO housing and hence determines the safe number of FO membrane elements that can be accommodated in series in a single housing. The experimental studies under the conditions tested in this study showed that a single

housing cannot accommodate more than 4 elements as the draw pressure exceeds the feed pressure and this clearly indicates that a normal single housing with 7 or 8 elements similar to the RO process is not likely to be practical for the safe operation of the FO membranes. Six different FO modular configuration options were simulated in this study and it shows that a two-stage FO configuration with multiple housings (in parallel) in the second stage using same or larger spacer thickness can help reduce the draw pressure build-up due to the reduction of the draw flows in the second stage accommodated. Operating a second stage FO module under slightly elevated feed hydraulic pressure or PAO mode not only compensates the loss of osmotic driving force but also enhances permeate flux and maintains positive pressure differences. The energy penalty posed by the PAO mode of FO operation is compensated by enhanced permeate throughput, reduced membrane area, and plant footprint. The contribution of FO/PAO to the total SEC of the FO-RO hybrid system was not significant compared to the SEC of the RO process which still formed about 90% of the total SEC indicating that the proposed two-stage FO modular configuration is one way of making the FO full-scale operation practical for FO-RO hybrid system.

9.2. Recommendations

Based on the comparative life cycle assessment and economic analysis, the FO hybrid technology could be highly competitive with the current RO hybrid technology. However, to further advance the FO technology for commercial applications, significant research efforts are still needed. Although a module-scale pilot FO unit (2 membrane elements only) was used in all the studies above, however, these studies were constrained because this pilot unit was not a full-scale FO system and hence operating the system in a batch mode provided limited operational and performance data directly relevant and applicable to the real commercial plants.

The following are the recommendations based on the studies detailed here in this thesis.

- A full-scale FO process operation is essential to more accurately understand and develop confidence in the module-scale performances of the FO or FO hybrid system. Few pilot-scale operations including in this study relied on one or two membrane

elements which are not feasible to operate in a continuous process like in the full-scale system. Therefore, the future studies must be conducted using a full-scale FO pilot system instead of just one or two membrane elements.

- Membrane performance is one of the significant areas of consideration for the successful application of the FO technology in the future. While high water flux performance is significant in reducing the CAPEX cost however salt rejecting properties of the membrane is expected to be more crucial for successful application of the technology as this has several implications such as on the issue of brine management and the quality of the final product water from the FO or FO hybrid system. Therefore the future research should focus on the developing novel TFC FO membranes with high reverse solute selectivity which means membranes with high water permeability, high FO water flux performance, very low specific reverse solute flux and very high feed solute rejection. Without such membranes, the FO hybrid system would suffer greatly from contaminated feed brine management issues and feed salinity build-up in the draw solution in a closed-loop FO hybrid system that undermines the final water quality.
- The principle of the FO process is different from the established membrane processes such as RO and NF processes even though the process configuration may appear similar in modular arrangements. As the FO technology reaches towards commercialization (few niche applications have been already reported although the technical details are still not available), there is a need to have a process simulation software that can perform the system analysis and conduct full-scale modular design and performance modeling. Such a software could be useful in understanding how the FO hybrid system would perform given the number of parameters involved in the operations most of which are implicit when analyzed in module-scale FO configurations.
- The structural framework for the development of FO simulation software is proposed as shown in Figure 9-1. A comprehensive mathematical framework of a full-scale FO process should be developed by employing the mass balance equations of the process and the solution-diffusion models modified with the thin film theory. Specifically, this simulation software is proposed based on module-scale FO operation (Chapter 7), a correlation between the operational parameters of multiple FO elements in series (Chapter 8), and a simple mass balance of the volumetric flows, draw solutes and the

feed solutes (Phuntsho et al., 2016a). A graphical user interface (GUI) used in this research can make the design process easy, economical and efficient by reducing the time to design, estimating the performance before fabrication and by comparing different configurations (Zaina & Álvaro, 2015). The simulation software must also consider modelling the hydrodynamic conditions that occur within the FS/DS channels in the presence of spacers that significantly affects the pressure drop across the FO elements.

- As shown in Figure 9-2, it consists of seven different steps. The first step of this software is “Project Info” which user can put all the information of the project. The second and third steps conduct the calculation of osmotic pressure of the feed and draw solutions using a correlation between total dissolved solids (TDS) and osmotic pressure and user’s input data. Then the user can select flow configuration for the system. There are two configurations; co-current and counter-current cross flow modes. In the “FO configuration” step, elements are selected according to feed water properties, fouling propensity and required rejection. The performance of the FO membrane module selected for the system is estimated using Matlab numerically including water flux, draw solution dilution factor and feed solution concentration. The estimated FO performance will be then used for calculating the number of elements and pressure vessels needed. In the “FO simulation” step, the chosen system configuration needs to be analyzed to find the optimum conditions. Finally, a graphical user interface would be developed to easily receive the input from the user and to display the output as a formatted report, which can be saved for documentation purposes.
- FO process has emerged as one of the most promising solutions in wastewater purification, seawater/brackish desalination, food processing, and power generation. However, to commercialize FO, we first need to recognize a huge guarantee of its full-scale implementation in terms of process efficiency and economics. The development of FO simulation software will allow conducting pre-evaluation of process performance and thus the optimum operating conditions. Therefore, the development and commercialization of FO simulation software will provide more opportunities to commercialize FO process in the near future.

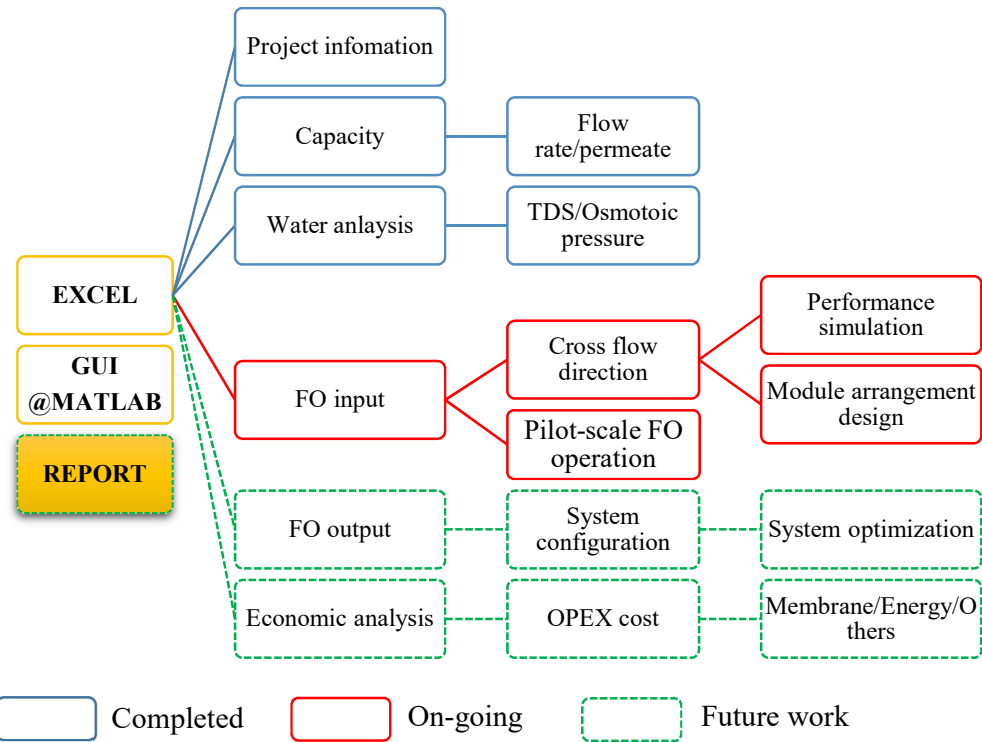


Figure 9 - 1. Diagram of the progress of development of a commercial FO simulation software

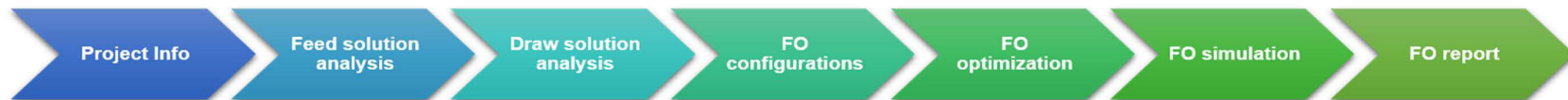
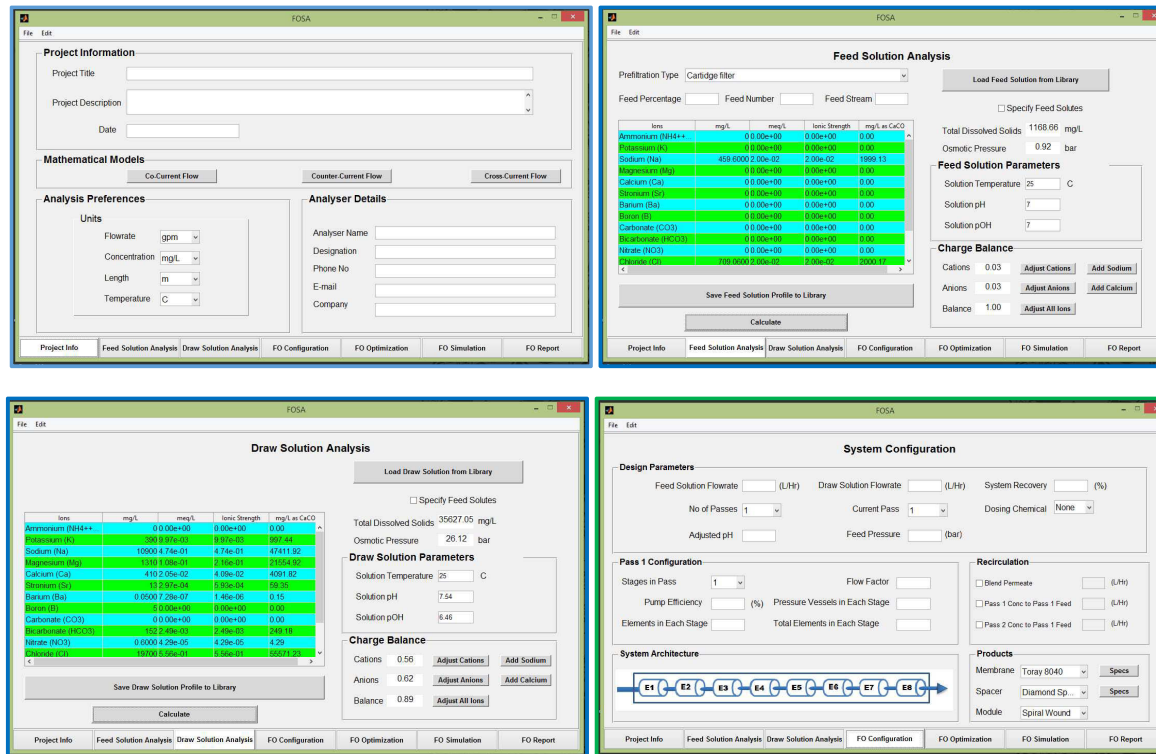


Figure 9 - 2. Developed Matlab graphical user-friendly interface (GUI) FO simulation software

REFERENCES

- World Population Prospects 2017, UNITED NATIONS.
- Achilli, A., Cath, T.Y., Childress, A.E. 2009a. Power generation with pressure retarded osmosis: An experimental and theoretical investigation. *Journal of Membrane Science*, **343**(1), 42-52.
- Achilli, A., Cath, T.Y., Childress, A.E. 2010. Selection of inorganic-based draw solutions for forward osmosis applications. *Journal of Membrane Science*, **364**(1), 233-241.
- Achilli, A., Cath, T.Y., Marchand, E.A., Childress, A.E. 2009b. The forward osmosis membrane bioreactor: A low fouling alternative to MBR processes. *Desalination*, **239**(1), 10-21.
- AEMC. 2013. Final Report: 2013 Residential Electricity Price Trends. *Australian Energy Market Commission (AEMC)*.
- Afshin Hemmatyar, A.M., Farzaneh, F. 2008. A new analytical approach in modeling of multi-loop feed-forward linearized microwave power amplifiers. *AEU - International Journal of Electronics and Communications*, **62**(6), 421-429.
- Akther, N., Sodiq, A., Giwa, A., Daer, S., Arafat, H.A., Hasan, S.W. 2015. Recent advancements in forward osmosis desalination: A review. *Chemical Engineering Journal*, **281**, 502-522.
- Alnaizy, R., Aidan, A., Qasim, M. 2013. Copper sulfate as draw solute in forward osmosis desalination. *Journal of Environmental Chemical Engineering*, **1**(3), 424-430.
- Altaee, A., Hilal, N. 2014. Dual-stage forward osmosis/pressure retarded osmosis process for hypersaline solutions and fracking wastewater treatment. *Desalination*, **350**, 79-85.
- Altaee, A., Mabrouk, A., Bourouni, K. 2013. A novel Forward osmosis membrane pretreatment of seawater for thermal desalination processes. *Desalination*, **326**(0), 19-29.
- Altaee, A., Mabrouk, A., Bourouni, K., Palenzuela, P. 2014a. Forward osmosis pretreatment of seawater to thermal desalination: High temperature FO-MSF/MED hybrid system. *Desalination*, **339**(0), 18-25.

- Altaee, A., Zaragoza, G. 2014a. A conceptual design of low fouling and high recovery FO–MSF desalination plant. *Desalination*, **343**, 2-7.
- Altaee, A., Zaragoza, G. 2014b. A conceptual design of low fouling and high recovery FO–MSF desalination plant. *Desalination*, **343(0)**, 2-7.
- Altaee, A., Zaragoza, G., van Tonningen, H.R. 2014b. Comparison between Forward Osmosis-Reverse Osmosis and Reverse Osmosis processes for seawater desalination. *Desalination*, **336**, 50-57.
- Alturki, A., McDonald, J., Khan, S.J., Hai, F.I., Price, W.E., Nghiem, L.D. 2012. Performance of a novel osmotic membrane bioreactor (OMBR) system: Flux stability and removal of trace organics. *Bioresource Technology*, **113**, 201-206.
- Alturki, A.A., McDonald, J.A., Khan, S.J., Price, W.E., Nghiem, L.D., Elimelech, M. 2013. Removal of trace organic contaminants by the forward osmosis process. *Separation and Purification Technology*, **103**, 258-266.
- Americanro. 2016. Membrane cost, Vol. 2016.
- Amini, M., Jahanshahi, M., Rahimpour, A. 2013. Synthesis of novel thin film nanocomposite (TFN) forward osmosis membranes using functionalized multi-walled carbon nanotubes. *Journal of Membrane Science*, **435(0)**, 233-241.
- Ang, W.S., Lee, S., Elimelech, M. 2006. Chemical and physical aspects of cleaning of organic-fouled reverse osmosis membranes. *Journal of Membrane Science*, **272(1)**, 198-210.
- ANZ-ECC, ARMCANZ. 2000. National water quality management strategy: An introduction to Australian and New Zealand Guidelines for Fresh and Marine Water Quality - 4A, Australian and New Zealand Environment and Conservation Council (ANZ-ECC) and Agriculture and Resource Management Council of Australia and New Zealand (ARMCANZ).
- APHA. 2005. *Standard methods for the examination of water and wastewater*. American Public Health Association.
- Arena, J.T., McCloskey, B., Freeman, B.D., McCutcheon, J.R. 2011a. Surface modification of thin film composite membrane support layers with polydopamine: enabling use of

reverse osmosis membranes in pressure retarded osmosis. *Journal of Membrane Science*, **375**(1), 55-62.

Arena, J.T., McCloskey, B., Freeman, B.D., McCutcheon, J.R. 2011b. Surface modification of thin film composite membrane support layers with polydopamine: Enabling use of reverse osmosis membranes in pressure retarded osmosis. *Journal of Membrane Science*, **375**(1-2), 55-62.

Arévalo, J., Garralón, G., Plaza, F., Moreno, B., Pérez, J., Gómez, M.Á. 2009. Wastewater reuse after treatment by tertiary ultrafiltration and a membrane bioreactor (MBR): a comparative study. *Desalination*, **243**(1-3), 32-41.

Arkhangelsky, E., Wicaksana, F., Chou, S., Al-Rabiah, A.A., Al-Zahrani, S.M., Wang, R. 2012. Effects of scaling and cleaning on the performance of forward osmosis hollow fiber membranes. *Journal of Membrane Science*, **415-416**, 101-108.

Arvanitoyannis, I.S. 2008. 3 - ISO 14040: Life Cycle Assessment (LCA) – Principles and Guidelines. in: *Waste Management for the Food Industries*, (Ed.) I.S. Arvanitoyannis, Academic Press. Amsterdam, pp. 97-132.

Ayers, R.S., Westcot, D.W. 1985. Water quality for agriculture, Vol. FAO irrigation and drainage paper 29, Food and Agriculture Organization, United Nations. Rome.

Bai, H., Liu, Z., Sun, D.D. 2011. Highly water soluble and recovered dextran coated Fe₃O₄ magnetic nanoparticles for brackish water desalination. *Separation and Purification Technology*, **81**(3), 392-399.

Bamaga, O.A., Yokochi, A., Zabara, B., Babaqi, A.S. 2011. Hybrid FO/RO desalination system: Preliminary assessment of osmotic energy recovery and designs of new FO membrane module configurations. *Desalination*, **268**(1), 163-169.

Benavides, S., Oloriz, A.S., Phillip, W.A. 2014. Forward Osmosis Processes in the Limit of Osmotic Equilibrium. *Industrial & Engineering Chemistry Research*.

Bengtsson, J., Howard, N. 2010. A Life Cycle Impact Assessment Method for Use in Australia—Classification, Characterisation and Research Needs.

Bigbrandwater. 2016. Bigbrandwater.

- Biswas, W.K. 2009. Life Cycle Assessment of Seawater Desalination in Western Australia. *World Academy of Science, Engineering & Technology*, **56**, 369-375.
- Blandin, G., Verliefde, A., Comas, J., Rodriguez-Roda, I., Le-Clech, P. 2016a. Efficiently Combining Water Reuse and Desalination through Forward Osmosis—Reverse Osmosis (FO-RO) Hybrids: A Critical Review. *Membranes*, **6**(3), 37.
- Blandin, G., Verliefde, A.R., Le-Clech, P. 2015a. Pressure enhanced fouling and adapted anti-fouling strategy in pressure assisted osmosis (PAO). *Journal of Membrane Science*, **493**, 557-567.
- Blandin, G., Verliefde, A.R., Tang, C.Y., Le-Clech, P. 2015b. Opportunities to reach economic sustainability in forward osmosis–reverse osmosis hybrids for seawater desalination. *Desalination*, **363**, 26-36.
- Blandin, G., Verliefde, A.R.D., Tang, C.Y., Childress, A.E., Le-Clech, P. 2013. Validation of assisted forward osmosis (AFO) process: Impact of hydraulic pressure. *Journal of Membrane Science*, **447**, 1-11.
- Blandin, G., Vervoort, H., Le-Clech, P., Verliefde, A.R.D. 2016b. Fouling and cleaning of high permeability forward osmosis membranes. *Journal of Water Process Engineering*, **9**, 161-169.
- BOM. 2015. Climate data online. Bureau of Metreology, Australian Government., Bureau of Meteorology, Australia. www.bom.gov.au.
- Bonton, A., Bouchard, C., Barbeau, B., Jedrzejak, S. 2012. Comparative life cycle assessment of water treatment plants. *Desalination*, **284**(0), 42-54.
- Boo, C., Elimelech, M., Hong, S. 2013. Fouling control in a forward osmosis process integrating seawater desalination and wastewater reclamation. *Journal of Membrane Science*, **444**, 148-156.
- Bowden, K.S., Achilli, A., Childress, A.E. 2012a. Organic ionic salt draw solutions for osmotic membrane bioreactors. *Bioresource Technology*, **122**(0), 207-216.
- Bowden, K.S., Achilli, A., Childress, A.E. 2012b. Organic ionic salt draw solutions for osmotic membrane bioreactors. *Bioresource technology*, **122**, 207-216.

- Bui, N.-N., Lind, M.L., Hoek, E.M., McCutcheon, J.R. 2011. Electrospun nanofiber supported thin film composite membranes for engineered osmosis. *Journal of membrane science*, **385**, 10-19.
- Cai, Y., Shen, W., Loo, S.L., Krantz, W.B., Wang, R., Fane, A.G., Hu, X. 2013. Towards temperature driven forward osmosis desalination using Semi-IPN hydrogels as reversible draw agents. *Water Research*, **47**(11), 3773-3781.
- Cath, T., Childress, A. Systems and methods for forward osmosis assisted desalination of liquids, USA patent# Pub, NO Patent US2,006.
- Cath, T., Childress, A., Elimelech, M. 2006a. Forward osmosis: Principles, applications, and recent developments. *Journal of Membrane Science*, **281**(1-2), 70-87.
- Cath, T.Y., Childress, A.E., Elimelech, M. 2006b. Forward osmosis: principles, applications, and recent developments. *Journal of Membrane Science*, **281**(1), 70-87.
- Cath, T.Y., Drewes, J.E., Lundin, C.D. 2009. A novel hybrid forward osmosis process for drinking water augmentation using impaired water and saline water sources. *Water Research Foundation*.
- Cath, T.Y., Hancock, N.T., Lundin, C.D., Hoppe-Jones, C., Drewes, J.E. 2010a. A multi-barrier osmotic dilution process for simultaneous desalination and purification of impaired water. *Journal of Membrane Science*, **362**(1-2), 417-426.
- Cath, T.Y., Hancock, N.T., Lundin, C.D., Hoppe-Jones, C., Drewes, J.E. 2010b. A multi-barrier osmotic dilution process for simultaneous desalination and purification of impaired water. *Journal of Membrane Science*, **362**(1), 417-426.
- Charcosset, C. 2009. A review of membrane processes and renewable energies for desalination. *Desalination*, **245**(1-3), 214-231.
- Chekli, L., Phuntsho, S., Kim, J.E., Kim, J., Choi, J.Y., Choi, J.-S., Kim, S., Kim, J.H., Hong, S., Sohn, J. 2016. A comprehensive review of hybrid forward osmosis systems: Performance, applications and future prospects. *Journal of Membrane Science*, **497**, 430-449.
- Chekli, L., Phuntsho, S., Shon, H.K., Vigneswaran, S., Kandasamy, J., Chanan, A. 2012. A review of draw solutes in forward osmosis process and their use in modern applications. *Desalination and Water Treatment*, **43**(1-3), 167-184.

- Chilton, C.H. 1950. Six-tenths factor applies to complete plant costs. *Chemical Engineering*, **57**(4), 112-114.
- Choi, Y.-J., Choi, J.-S., Oh, H.-J., Lee, S., Yang, D.R., Kim, J.H. 2009. Toward a combined system of forward osmosis and reverse osmosis for seawater desalination. *Desalination*, **247**(1–3), 239-246.
- Chou, S., Shi, L., Wang, R., Tang, C.Y., Qiu, C., Fane, A.G. 2010. Characteristics and potential applications of a novel forward osmosis hollow fiber membrane. *Desalination*, **261**(3), 365-372.
- Cipollina, A., Micale, G. 2016. *Sustainable Energy from Salinity Gradients*. Woodhead Publishing.
- Coday, B.D., Heil, D.M., Xu, P., Cath, T.Y. 2013. Effects of transmembrane hydraulic pressure on performance of forward osmosis membranes. *Environmental Science & Technology*, **47**(5), 2386-2393.
- Coday, B.D., Miller-Robbie, L., Beaudry, E.G., Munakata-Marr, J., Cath, T.Y. 2015. Life cycle and economic assessments of engineered osmosis and osmotic dilution for desalination of Haynesville shale pit water. *Desalination*, **369**, 188-200.
- Coday, B.D., Yaffe, B.G., Xu, P., Cath, T.Y. 2014. Rejection of trace organic compounds by forward osmosis membranes: a literature review. *Environmental Science & Technology*, **48**(7), 3612-3624.
- Cornelissen, E., Harmsen, D., De Korte, K., Ruiken, C., Qin, J.-J., Oo, H., Wessels, L. 2008. Membrane fouling and process performance of forward osmosis membranes on activated sludge. *Journal of Membrane Science*, **319**(1), 158-168.
- Cornelissen, E.R., Harmsen, D.J.H., Beerendonk, E.F., Qin, J.J., Kappelhof, J.W.M.N. 2011. Effect of draw solution type and operational mode of forward osmosis with laboratory-scale membranes and a spiral wound membrane module. *Journal of Water Reuse and Desalination*, **1**(3), 133.
- Corral, A.F., Yenal, U. 1932. Reverse Osmosis Treatment of Central Arizona Project Water—Brine Minimization Via Vibratory Shear-enhanced Processing.
- D'Haese, A., Le-Clech, P., Van Nevel, S., Verbeken, K., Cornelissen, E.R., Khan, S.J., Verliefde, A.R. 2013. Trace organic solutes in closed-loop forward osmosis

applications: Influence of membrane fouling and modeling of solute build-up. *Water Research*, **47**(14), 5232-5244.

Deshmukh, A., Yip, N.Y., Lin, S., Elimelech, M. 2015. Desalination by forward osmosis: Identifying performance limiting Parameters through module-scale modeling. *Journal of Membrane Science*, **491**, 159-167.

DeWolfe, J. 2003. *Guidance manual for coagulant changeover*. American Water Works Association.

DOW, C. 2014. Product Information for DOW™ Filmtec BW30-440i, DOW™ Filmtec Membranes, DOW Chemicals.

DowChemical. 2017. FILMTEC Membranes - The Dow Chemical Company.

DowFilmtec. 2016. Reverse Osmosis System Analysis (ROSA). in: *Midland*, Vol. 2016.

Duan, J., Litwiller, E., Pinnau, I. 2014. Solution-diffusion with defects model for pressure-assisted forward osmosis. *Journal of Membrane Science*, **470**, 323-333.

Dumée, L., Lee, J., Sears, K., Tardy, B., Duke, M., Gray, S. 2013. Fabrication of thin film composite poly (amide)-carbon-nanotube supported membranes for enhanced performance in osmotically driven desalination systems. *Journal of membrane science*, **427**, 422-430.

Duong, P.H.H., Chung, T.-S. 2014. Application of thin film composite membranes with forward osmosis technology for the separation of emulsified oil–water. *Journal of Membrane Science*, **452**(0), 117-126.

Elimelech, M. 2007. Yale constructs forward osmosis desalination pilot plant. *Membrane Technology*, **2007**(1), 7-8.

Emadzadeh, D., Lau, W.J., Matsuura, T., Rahbari-Sisakht, M., Ismail, A.F. 2014. A novel thin film composite forward osmosis membrane prepared from PSf–TiO₂ nanocomposite substrate for water desalination. *Chemical Engineering Journal*, **237**, 70-80.

Ersu, C.B., Ong, S.K., Arslankaya, E., Lee, Y.-W. 2010. Impact of solids residence time on biological nutrient removal performance of membrane bioreactor. *Water research*, **44**(10), 3192-3202.

- Ettouney, H.M., El-Dessouky, H.T., Faibish, R.S., Gowin, P.J. 2002. Evaluating the economics of desalination. *Chemical Engineering Progress*, **98**(12), 32.
- Filter, B.B.W. 2016. Membrane cost, Vol. 2016.
- Frank, B.S. 1972. Desalination of sea water, Google Patents.
- Frischknecht, R., Jungbluth, N., Althaus, H.-J., Doka, G., Dones, R., Heck, T., Hellweg, S., Hirschler, R., Nemecek, T., Rebitzer, G. 2005. The ecoinvent database: Overview and methodological framework (7 pp). *The International Journal of Life Cycle Assessment*, **10**(1), 3-9.
- Fritzmann, C., Löwenberg, J., Wintgens, T., Melin, T. 2007. State-of-the-art of reverse osmosis desalination. *Desalination*, **216**(1), 1-76.
- Garcia-Castello, E.M., McCutcheon, J.R., Elimelech, M. 2009. Performance evaluation of sucrose concentration using forward osmosis. *Journal of Membrane Science*, **338**(1-2), 61-66.
- Ge, Q., Chung, T.-S. 2013. Hydroacid complexes: a new class of draw solutes to promote forward osmosis (FO) processes. *Chemical communications*, **49**(76), 8471-8473.
- Ge, Q., Ling, M., Chung, T.-S. 2013. Draw solutions for forward osmosis processes: Developments, challenges, and prospects for the future. *Journal of Membrane Science*, **442**(0), 225-237.
- Ge, Q., Su, J., Chung, T.-S., Amy, G. 2010. Hydrophilic superparamagnetic nanoparticles: synthesis, characterization, and performance in forward osmosis processes. *Industrial & Engineering Chemistry Research*, **50**(1), 382-388.
- Ge, Q., Wang, P., Wan, C., Chung, T.-S. 2012. Polyelectrolyte-promoted forward osmosis–membrane distillation (FO–MD) hybrid process for dye wastewater treatment. *Environmental science & technology*, **46**(11), 6236-6243.
- Geise, G.M., Lee, H.S., Miller, D.J., Freeman, B.D., McGrath, J.E., Paul, D.R. 2010. Water purification by membranes: the role of polymer science. *Journal of Polymer Science Part B: Polymer Physics*, **48**(15), 1685-1718.

- Gerstandt, K., Peinemann, K.-V., Skilhagen, S.E., Thorsen, T., Holt, T. 2008. Membrane processes in energy supply for an osmotic power plant. *Desalination*, **224**(1-3), 64-70.
- Glueckstern, P., Priel, M. 1998. A hybrid SWRO/BWRO desalination plant. *Desalination*, **115**(2), 203-209.
- Gomez, J.D., Cath, T.Y. 2011. *Assessment of Osmotic Mechanisms Pairing Desalination Concentrate and Wastewater Treatment*. CH2M HILL.
- Grafton, R., Kowalick, I., Miller, C., Stubbs, T., Verity, F., Walker, K. 2010. Sustainable diversions in the Murray-Darling Basin: an analysis of the options for achieving a sustainable diversion limit in the Murray-Darling Basin. Wentworth Group of Concerned Scientist. *New South Wales*.
- Grant, T., James, K.L., Lundie, S. 2001. Alcas: Australian Lca Society. *The International Journal of Life Cycle Assessment*, **6**(6), 323-324.
- Greenlee, L.F., Lawler, D.F., Freeman, B.D., Marrot, B., Moulin, P. 2009. Reverse osmosis desalination: water sources, technology, and today's challenges. *Water research*, **43**(9), 2317-2348.
- Gu, Y., Wang, Y.-N., Wei, J., Tang, C.Y. 2013. Organic fouling of thin-film composite polyamide and cellulose triacetate forward osmosis membranes by oppositely charged macromolecules. *Water Research*, **47**(5), 1867-1874.
- Guo, C.X., Zhao, D., Zhao, Q., Wang, P., Lu, X. 2014. Na⁺-functionalized carbon quantum dots: a new draw solute in forward osmosis for seawater desalination. *Chemical Communications*, **50**(55), 7318-7321.
- Gwak, G., Jung, B., Han, S., Hong, S. 2015. Evaluation of poly (aspartic acid sodium salt) as a draw solute for forward osmosis. *Water Research*, **80**, 294-305.
- Han, G., Chung, T.-S., Toriida, M., Tamai, S. 2012. Thin-film composite forward osmosis membranes with novel hydrophilic supports for desalination. *Journal of Membrane Science*, **423**, 543-555.
- Han, G., Zhao, B., Fu, F., Chung, T.-S., Weber, M., Staudt, C., Maletzko, C. 2016. High performance thin-film composite membranes with mesh-reinforced hydrophilic

sulfonated polyphenylenesulfone (sPPSU) substrates for osmotically driven processes. *Journal of Membrane Science*, **502**, 84-93.

Hancock, N.T., Black, N.D., Cath, T.Y. 2012. A comparative life cycle assessment of hybrid osmotic dilution desalination and established seawater desalination and wastewater reclamation processes. *Water Research*, **46**(4), 1145-1154.

Hancock, N.T., Cath, T.Y. 2009. Solute coupled diffusion in osmotically driven membrane processes. *Environmental Science & Technology*, **43**(17), 6769-6775.

Hancock, N.T., Phillip, W.A., Elimelech, M., Cath, T.Y. 2011a. Bidirectional Permeation of Electrolytes in Osmotically Driven Membrane Processes. *Environmental Science & Technology*, **45**(24), 10642-10651.

Hancock, N.T., Xu, P., Heil, D.M., Bellona, C., Cath, T.Y. 2011b. Comprehensive bench-and pilot-scale investigation of trace organic compounds rejection by forward osmosis. *Environmental Science & Technology*, **45**(19), 8483-8490.

Hancock, N.T., Xu, P., Roby, M.J., Gomez, J.D., Cath, T.Y. 2013. Towards direct potable reuse with forward osmosis: Technical assessment of long-term process performance at the pilot scale. *Journal of Membrane Science*, **445**, 34-46.

Hartanto, Y., Yun, S., Jin, B., Dai, S. 2015. Functionalized thermo-responsive microgels for high performance forward osmosis desalination. *water research*, **70**, 385-393.

Hau, N.T., Chen, S.-S., Nguyen, N.C., Huang, K.Z., Ngo, H.H., Guo, W. 2014. Exploration of EDTA sodium salt as novel draw solution in forward osmosis process for dewatering of high nutrient sludge. *Journal of Membrane Science*, **455**, 305-311.

Holloway, R.W., Maltos, R., Vanneste, J., Cath, T.Y. 2015a. Mixed draw solutions for improved forward osmosis performance. *Journal of Membrane Science*, **491**, 121-131.

Holloway, R.W., Miller-Robbie, L., Patel, M., Stokes, J.R., Munakata-Marr, J., Dadakis, J., Cath, T.Y. 2016. Life-cycle assessment of two potable water reuse technologies: MF/RO/UV–AOP treatment and hybrid osmotic membrane bioreactors. *Journal of Membrane Science*, **507**, 165-178.

- Holloway, R.W., Wait, A.S., Fernandes da Silva, A., Herron, J., Schutter, M.D., Lampi, K., Cath, T.Y. 2015b. Long-term pilot scale investigation of novel hybrid ultrafiltration-osmotic membrane bioreactors. *Desalination*, **363**, 64-74.
- Hoover, L.A., Phillip, W.A., Tiraferri, A., Yip, N.Y., Elimelech, M. 2011. Forward with osmosis: emerging applications for greater sustainability. *Environmental Science & Technology*, **45**(23), 9824-9830.
- Hoover, L.A., Schiffman, J.D., Elimelech, M. 2013. Nanofibers in thin-film composite membrane support layers: Enabling expanded application of forward and pressure retarded osmosis. *Desalination*, **308**, 73-81.
- Howat, V. 2013. Annual environmental management report 2013: Newstan Colliery.
- Jin, X., Shan, J., Wang, C., Wei, J., Tang, C.Y. 2012. Rejection of pharmaceuticals by forward osmosis membranes. *Journal of Hazardous Materials*, **227**, 55-61.
- Johnson, D.J., Suwaileh, W.A., Mohammed, A.W., Hilal, N. 2017. Osmotic's potential: An overview of draw solutes for forward osmosis. *Desalination*.
- Kim, D.I., Kim, J., Shon, H.K., Hong, S. 2015a. Pressure retarded osmosis (PRO) for integrating seawater desalination and wastewater reclamation: Energy consumption and fouling. *Journal of Membrane Science*, **483**(0), 34-41.
- Kim, D.I., Kim, J., Shon, H.K., Hong, S. 2015b. Pressure retarded osmosis (PRO) for integrating seawater desalination and wastewater reclamation: Energy consumption and fouling. *Journal of Membrane Science*, **483**, 34-41.
- Kim, J., Blandin, G., Phuntsho, S., Verliefe, A., Le-Clech, P., Shon, H. 2017a. Practical considerations for operability of an 8" spiral wound forward osmosis module: Hydrodynamics, fouling behaviour and cleaning strategy. *Desalination*, **404**, 249-258.
- Kim, J.E., Phuntsho, S., Ali, S.M., Choi, J.Y., Shon, H.K. 2017b. Forward osmosis membrane modular configurations for osmotic dilution of seawater by forward osmosis and reverse osmosis hybrid system. *Water Research*.
- Kim, J.E., Phuntsho, S., Chekli, L., Choi, J.Y., Shon, H.K. 2018. Environmental and economic assessment of hybrid FO-RO/NF system with selected inorganic draw solutes for the treatment of mine impaired water. *Desalination*, **429**(Supplement C), 96-104.

- Kim, J.E., Phuntsho, S., Chekli, L., Hong, S., Ghaffour, N., Leiknes, T., Choi, J.Y., Shon, H.K. 2017c. Environmental and economic impacts of fertilizer drawn forward osmosis and nanofiltration hybrid system. *Desalination*, **416**, 76-85.
- Kim, J.E., Phuntsho, S., Lotfi, F., Shon, H.K. 2014a. Investigation of pilot-scale 8040 FO membrane module under different operating conditions for brackish water desalination. *Desalination and Water Treatment*, **53**(10), 2782-2791.
- Kim, J.E., Phuntsho, S., Lotfi, F., Shon, H.K. 2014b. Investigation of pilot-scale 8040 FO membrane module under different operating conditions for brackish water desalination. *Desalination and Water Treatment*, **doi: 10.1080/19443994.2014.931528**.
- Kim, J.E., Phuntsho, S., Shon, H.K. 2013a. Pilot-scale nanofiltration system as post-treatment for fertilizer-drawn forward osmosis desalination for direct fertigation. *Desalination and Water Treatment*(ahead-of-print), 1-9.
- Kim, Y., Chekli, L., Shim, W.-G., Phuntsho, S., Li, S., Ghaffour, N., Leiknes, T., Shon, H.K. 2016. Selection of suitable fertilizer draw solute for a novel fertilizer-drawn forward osmosis–anaerobic membrane bioreactor hybrid system. *Bioresource Technology*, **210**, 26-34.
- Kim, Y.C., Elimelech, M. 2012. Adverse impact of feed channel spacers on the performance of pressure retarded osmosis. *Environmental Science & Technology*, **46**(8), 4673-4681.
- Kim, Y.C., Kim, Y., Oh, D., Lee, K.H. 2013b. Experimental Investigation of a Spiral-Wound Pressure-Retarded Osmosis Membrane Module for Osmotic Power Generation. *Environmental Science & Technology*, **47**(6), 2966-2973.
- Kim, Y.C., Park, S.-J. 2011a. Experimental Study of a 4040 Spiral-Wound Forward-Osmosis Membrane Module. *Environmental Science & Technology*, **45**(18), 7737–7745.
- Kim, Y.C., Park, S.J. 2011b. Experimental study of a 4040 spiral-wound forward-osmosis membrane module. *Environ Science & Technology*, **45**(18), 7737-45.
- Kravath, R.E., Davis, J.A. 1975. Desalination of sea water by direct osmosis. *Desalination*, **16**(2), 151-155.

- kuang, W., Liu, Z., Yu, H., Kang, G., Jie, X., Jin, Y., Cao, Y. 2016. Investigation of internal concentration polarization reduction in forward osmosis membrane using nano-CaCO₃ particles as sacrificial component. *Journal of Membrane Science*, **497**, 485-493.
- Lay, W.C.L., Zhang, J., Tang, C., Wang, R., Liu, Y., Fane, A.G. 2012. Factors affecting flux performance of forward osmosis systems. *Journal of Membrane Science*, **394–395**(0), 151-168.
- Lee, S., Boo, C., Elimelech, M., Hong, S. 2010. Comparison of fouling behavior in forward osmosis (FO) and reverse osmosis (RO). *Journal of Membrane Science*, **365**(1–2), 34-39.
- Lew, C., Hu, J., Song, L., Lee, L., Ong, S., Ng, W., Seah, H. 2005. Development of an integrated membrane process for water reclamation. *Water Science & Technology*, **51**(6-7), 455-463.
- Li, D., Zhang, X., Yao, J., Simon, G.P., Wang, H. 2011a. Stimuli-responsive polymer hydrogels as a new class of draw agent for forward osmosis desalination. *Chem. Commun.*, **47**(6), 1710-1712.
- Li, D., Zhang, X., Yao, J., Zeng, Y., Simon, G.P., Wang, H. 2011b. Composite polymer hydrogels as draw agents in forward osmosis and solar dewatering. *Soft Matter*, **7**(21), 10048-10056.
- Li, X.-M., Zhao, B., Wang, Z., Xie, M., Song, J., Nghiem, L.D., He, T., Yang, C., Li, C., Chen, G. 2014. Water reclamation from shale gas drilling flow-back fluid using a novel forward osmosis–vacuum membrane distillation hybrid system. *Water Science & Technology*, **69**(5), 1036-1044.
- Linares, R.V., Yangali-Quintanilla, V., Li, Z., Amy, G. 2011. Rejection of micropollutants by clean and fouled forward osmosis membrane. *Water Research*, **45**(20), 6737-6744.
- Ling, M.M., Chung, T.-S. 2011a. Desalination process using super hydrophilic nanoparticles via forward osmosis integrated with ultrafiltration regeneration. *Desalination*, **278**(1–3), 194-202.
- Ling, M.M., Chung, T.-S. 2011b. Novel dual-stage FO system for sustainable protein enrichment using nanoparticles as intermediate draw solutes. *Journal of Membrane Science*, **372**(1–2), 201-209.

- Ling, M.M., Chung, T.-S. 2012. Surface-dissociated nanoparticle draw solutions in forward osmosis and the regeneration in an integrated electric field and nanofiltration system. *Industrial & Engineering Chemistry Research*, **51**(47), 15463-15471.
- Ling, M.M., Wang, K.Y., Chung, T.-S. 2010. Highly Water-Soluble Magnetic Nanoparticles as Novel Draw Solutes in Forward Osmosis for Water Reuse. *Industrial & Engineering Chemistry Research*, **49**(12), 5869-5876.
- Liu, P., Zhang, H., Feng, Y., Shen, C., Yang, F. 2015a. Integrating electrochemical oxidation into forward osmosis process for removal of trace antibiotics in wastewater. *Journal of hazardous materials*, **296**, 248-255.
- Liu, P., Zhang, H., Feng, Y., Yang, F., Shen, C. 2015b. Integrating electrochemical oxidation into forward osmosis process for removal of trace antibiotics in wastewater. *Journal of Hazardous materials*, **Article in Press**.
- Liu, X., Ng, H.Y. 2015. Fabrication of layered silica-polysulfone mixed matrix substrate membrane for enhancing performance of thin-film composite forward osmosis membrane. *Journal of Membrane Science*, **481**, 148-163.
- Liu, Z., Bai, H., Lee, J., Sun, D.D. 2011. A low-energy forward osmosis process to produce drinking water. *Energy & Environmental Science*, **4**(7), 2582-2585.
- Liyanaarachchi, S., Jegatheesan, V., Muthukumaran, S., Gray, S., Shu, L. 2016. Mass balance for a novel RO/FO hybrid system in seawater desalination. *Journal of Membrane Science*, **501**, 199-208.
- Lotfi, F., Chekli, L., Phuntsho, S., Hong, S., Choi, J.Y., Shon, H.K. 2017. Understanding the possible underlying mechanisms for low fouling tendency of the forward osmosis and pressure assisted osmosis processes. *Desalination*, **In Press**.
- Luo, H., Wang, Q., Zhang, T.C., Tao, T., Zhou, A., Chen, L., Bie, X. 2014a. A review on the recovery methods of draw solutes in forward osmosis. *Journal of Water Process Engineering*, **4**, 212-223.
- Luo, L., Wang, P., Zhang, S., Han, G., Chung, T.-S. 2014b. Novel thin-film composite tri-bore hollow fiber membrane fabrication for forward osmosis. *Journal of Membrane Science*, **461**, 28-38.

- Lutchmiah, K., Harmsen, D.J.H., Wols, B.A., Rietveld, L.C., Jianjun, Q., Cornelissen, E.R. 2015. Continuous and discontinuous pressure assisted osmosis (PAO). *Journal of Membrane Science*, **476**, 182-193.
- Lutchmiah, K., Verliefde, A.R.D., Roest, K., Rietveld, L.C., Cornelissen, E.R. 2014. Forward osmosis for application in wastewater treatment: A review. *Water Research*, **58**, 179-197.
- Mabrouk, A.-N.A. 2013. Techno-economic analysis of tube bundle orientation for high capacity brine recycle MSF desalination plants. *Desalination*, **320**, 24-32.
- Masters, G.M. 1991. Introduction to environmental engineering and Science Prentice Hall. *Upper Saddle River*.
- Matilainen, A., Vepsäläinen, M., Sillanpää, M. 2010. Natural organic matter removal by coagulation during drinking water treatment: A review. *Advances in Colloid and Interface Science*, **159**(2), 189-197.
- McCormick, P., Pellegrino, J., Mantovani, F., Sarti, G. 2008. Water, salt, and ethanol diffusion through membranes for water recovery by forward (direct) osmosis processes. *Journal of Membrane Science*, **325**(1), 467-478.
- McCutcheon, J.R., McGinnis, R.L., Elimelech, M. 2006a. Desalination by ammonia-carbon dioxide forward osmosis: Influence of draw and feed solution concentrations on process performance. *Journal of Membrane Science*, **278**(1-2), 114-123.
- McCutcheon, J.R., McGinnis, R.L., Elimelech, M. 2006b. Desalination by ammonia-carbon dioxide forward osmosis: Influence of draw and feed solution concentrations on process performance. *Journal of Membrane Science*, **278**(2006), 114-123.
- McCutcheon, J.R., McGinnis, R.L., Elimelech, M. 2005. A novel ammonia-carbon dioxide forward (direct) osmosis desalination process. *Desalination*, **174**(1), 1-11.
- McGinnis, R.L., Elimelech, M. 2007. Energy requirements of ammonia-carbon dioxide forward osmosis desalination. *Desalination*, **207**(1), 370-382.
- McGinnis, R.L., Hancock, N.T., Nowosielski-Slepowron, M.S., McGurgan, G.D. 2012. Pilot demonstration of the NH₃/CO₂ forward osmosis desalination process on high salinity brines. *Desalination*, **312**, 67-74.

- Mehta, G.D. 1982. Further results on the performance of present-day osmotic membranes in various osmotic regions. *Journal of Membrane Science*, **10**(1), 3-19.
- Mezher, T., Fath, H., Abbas, Z., Khaled, A. 2011. Techno-economic assessment and environmental impacts of desalination technologies. *Desalination*, **266**(1), 263-273.
- Mi, B., Elimelech, M. 2008. Chemical and physical aspects of organic fouling of forward osmosis membranes. *Journal of Membrane Science*, **320**(1-2), 292-302.
- Mi, B., Elimelech, M. 2010. Organic fouling of forward osmosis membranes: Fouling reversibility and cleaning without chemical reagents. *Journal of Membrane Science*, **348**(1), 337-345.
- MingáLing, M. 2011. Facile synthesis of thermosensitive magnetic nanoparticles as “smart” draw solutes in forward osmosis. *Chemical communications*, **47**(38), 10788-10790.
- Moch, I., Querns, W.R., Steward, D., Environmental Resources, T., Water Treatment Engineering Research, T., Water Desalination, R., Development, P. 2008. *WT Cost II modeling the capital and operating costs of thermal desalination processes utilizing a recently developed computer program that evaluates membrane desalting, electrodialysis, and ion exchange plants : case study for a seawater 20-million-gallon-per-day (MGD) hybrid system involving 10-MGD multistage flash distillation plus 10-MGD reverse osmosis*. U.S. Dept. of the Interior, Bureau of Reclamation, Technical Service Center, Water and Environmental Services Division, Water Treatment Engineering Research Team ; Available through the National Technical Information Service, Denver, Colo.; Springfield, Va.
- Moody, C.D., Kessler, J.O. 1976. Forward osmosis extractors. *Desalination*, **18**(1976), 283-295.
- Mountain, B. 2012. Electricity prices in Australia: An International Comparison. *A report commissioned by the Energy Users Association of Australia*.
- Munns, R. 2002. Comparative physiology of salt and water stress. *Plant, Cell & Environment*, **25**(2), 239-250.
- Muñoz, I., José Gómez, M., Molina-Díaz, A., Huijbregts, M.A., Fernández-Alba, A.R., García-Calvo, E. 2008. Ranking potential impacts of priority and emerging pollutants in urban wastewater through life cycle impact assessment. *Chemosphere*, **74**(1), 37-44.

- NSW-EPA. 2009. Protection of the Environment Operations (General) Regulation 2009. Version in: *2009 No 211*. New South Wales State, Australia.
- Oh, Y., Lee, S., Elimelech, M., Lee, S., Hong, S. 2014. Effect of hydraulic pressure and membrane orientation on water flux and reverse solute flux in pressure assisted osmosis. *Journal of Membrane Science*, **465**, 159-166.
- Ong, R.C., Chung, T.-S., de Wit, J.S., Helmer, B.J. 2015. Novel cellulose ester substrates for high performance flat-sheet thin-film composite (TFC) forward osmosis (FO) membranes. *Journal of Membrane Science*, **473**, 63-71.
- Organization, I.S. 1997. *ISO 14040: Environmental Management-Life Cycle Assessment-Principles and Framework*.
- Papadopoulos, I. 1999. Fertigation-chemigation in protected agriculture. *Cahiers options Mediterraneennes*, **31**, 275-291.
- Park, M., Kim, J.H. 2013. Numerical analysis of spacer impacts on forward osmosis membrane process using concentration polarization index. *Journal of Membrane Science*, **427**, 10-20.
- Park, S.H., Park, B., Shon, H.K., Kim, S. 2015. Modeling full-scale osmotic membrane bioreactor systems with high sludge retention and low salt concentration factor for wastewater reclamation. *Bioresource technology*, **190**, 508-515.
- Petrotos, K.B., Quantick, P., Petropakis, H. 1998. A study of the direct osmotic concentration of tomato juice in tubular membrane – module configuration. I. The effect of certain basic process parameters on the process performance. *Journal of Membrane Science*, **150**(1), 99-110.
- Phillip, W.A., Yong, J.S., Elimelech, M. 2010. Reverse Draw Solute Permeation in Forward Osmosis: Modeling and Experiments. *Environmental Science & Technology*, **44**(13), 5170-5176.
- Phocaidis, A. 2007. Handbook on pressurized irrigation techniques. 2nd Ed. ed, Food and Agriculture Organization, UN. Rome.
- Phuntsho, S. 2012. A novel fertiliser drawn forward osmosis desalination for fertigation. *Doctoral dissertation*.

- Phuntsho, S., Hong, S., Elimelech, M., Shon, H.K. 2013 a. Forward osmosis desalination of brackish groundwater: Meeting water quality requirements for fertigation by integrating nanofiltration. *Journal of Membrane Science*, **436**, 1-15.
- Phuntsho, S., Hong, S., Elimelech, M., Shon, H.K. 2014a. Osmotic equilibrium in the forward osmosis process: Modelling, experiments and implications for process performance. *Journal of Membrane Science*, **453**, 240-252.
- Phuntsho, S., Hong, S., Elimelech, M., Shon, H.K. 2014b. Osmotic equilibrium in the forward osmosis process: Modelling, experiments and implications for process performance. *Journal of Membrane Science*, **453**(0), 240-252.
- Phuntsho, S., Kim, J.E., Hong, S., Ghaffour, N., Leiknes, T., Choi, J.Y., Shon, H.K. 2017a. A closed-loop forward osmosis-nanofiltration hybrid system: Understanding process implications through full-scale simulation. *Desalination*.
- Phuntsho, S., Kim, J.E., Hong, S., Ghaffour, N., Leiknes, T., Choi, J.Y., Shon, H.K. 2017b. A closed-loop forward osmosis-nanofiltration hybrid system: Understanding process implications through full-scale simulation. *Desalination*, **421**(Supplement C), 169-178.
- Phuntsho, S., Kim, J.E., Hong, S., Ghaffour, N., Leiknes, T., Choi, J.Y., Shon, H.K. 2016a. A closed-loop forward osmosis-nanofiltration hybrid system: Understanding process implications through full-scale simulation. *Desalination*.
- Phuntsho, S., Kim, J.E., Johir, M.A.H., Hong, S., Li, Z., Ghaffour, N., Leiknes, T., Shon, H.K. 2016b. Fertiliser drawn forward osmosis process: Pilot-scale desalination of mine impaired water for fertigation. *Journal of Membrane Science*, **508**, 22-31.
- Phuntsho, S., Sahebi, S., Majeed, T., Lotfi, F., Kim, J.E., Shon, H.K. 2013a. Assessing the major factors affecting the performances of forward osmosis and its implications on the desalination process. *Chemical Engineering Journal*, **231**, 484-496.
- Phuntsho, S., Sahebi, S., Majeed, T., Lotfi, F., Kim, J.E., Shon, H.K. 2013b. Assessing the major factors affecting the performances of forward osmosis and its implications on the desalination process. *Chemical Engineering Journal*, **231**(0), 484-496.
- Phuntsho, S., Shon, H., Hong, S., Lee, S., Vigneswaran, S., Kandasamy, J. 2012a. Fertiliser drawn forward osmosis desalination: the concept, performance and limitations for fertigation. *Reviews in Environmental Science and Bio/Technology*, **11**(2), 147-168.

- Phuntsho, S., Shon, H.K., Hong, S., Lee, S., Vigneswaran, S. 2011. A novel low energy fertilizer driven forward osmosis desalination for direct fertigation: Evaluating the performance of fertilizer draw solutions. *Journal of Membrane Science*, **375**(1–2), 172-181.
- Phuntsho, S., Shon, H.K., Hong, S., Lee, S., Vigneswaran, S., Kandasamy, J. 2012b. Fertiliser drawn forward osmosis desalination: the concept, performance and limitations for fertigation. *Reviews in Environmental Science and Bio/Technology*, **11**(2), 147-168.
- Phuntsho, S., Shon, H.K., Hong, S., Lee, S., Vigneswaran, S., Kandasamy, J. 2012 a. Fertiliser drawn forward osmosis desalination: The concept, performance and limitations for fertigation. *Reviews in Environmental Science and Bio/Technology*.
- Phuntsho, S., Shon, H.K., Majeed, T., El Saliby, I., Vigneswaran, S., Kandasamy, J., Hong, S., Lee, S. 2012c. Blended fertilizers as draw solutions for fertilizer-drawn forward osmosis desalination. *Environmental Science & Technology*, **46**(8), 4567-4575.
- Pickering, K.D., Wiesner, M.R. 1993. Cost model for low-pressure membrane filtration. *Journal of Environmental Engineering*, **119**(5), 772-797.
- Poullikkas, A. 2001. Optimization algorithm for reverse osmosis desalination economics. *Desalination*, **133**(1), 75-81.
- PRé-Consultants, S. 1998. LCA software. *The Netherlands (www.pre.nl/simapro/default.htm)*.
- PRé-Consultants, S. 2008. SimaPro software, SimaPro Version.
- Pryshlakivsky, J., Searcy, C. 2013. Fifteen years of ISO 14040: a review. *Journal of Cleaner Production*, **57**(0), 115-123.
- Qiu, C., Setiawan, L., Wang, R., Tang, C.Y., Fane, A.G. 2012. High performance flat sheet forward osmosis membrane with an NF-like selective layer on a woven fabric embedded substrate. *Desalination*, **287**, 266-270.
- Raluy, R.G., Serra, L., Uche, J. 2005a. Life cycle assessment of desalination technologies integrated with renewable energies. *Desalination*, **183**(1–3), 81-93.
- Raluy, R.G., Serra, L., Uche, J. 2005b. Life Cycle Assessment of Water Production Technologies - Part 1: Life Cycle Assessment of Different Commercial

Desalination Technologies (MSF, MED, RO) (9 pp). *The International Journal of Life Cycle Assessment*, **10**(4), 285-293.

Raluy, R.G., Serra, L., Uche, J., Valero, A. 2005c. Life Cycle Assessment of Water Production Technologies-Part 2: Reverse Osmosis Desalination versus the Ebro River Water Transfer (9 pp). *The International Journal of Life Cycle Assessment*, **10**(5), 346-354.

Razmjou, A., Barati, M.R., Simon, G.P., Suzuki, K., Wang, H. 2013a. Fast deswelling of nanocomposite polymer hydrogels via magnetic field-induced heating for emerging FO desalination. *Environmental science & technology*, **47**(12), 6297-6305.

Razmjou, A., Simon, G.P., Wang, H. 2013b. Effect of particle size on the performance of forward osmosis desalination by stimuli-responsive polymer hydrogels as a draw agent. *Chemical engineering journal*, **215**, 913-920.

Ren, J., McCutcheon, J.R. 2014. A new commercial thin film composite membrane for forward osmosis. *Desalination*, **343**(0), 187-193.

Roy, D., Rahni, M., Pierre, P., Yargeau, V. 2016. Forward osmosis for the concentration and reuse of process saline wastewater. *Chemical Engineering Journal*, **287**, 277-284.

Rutherford, I., Finlayson, B. 2011. Whither Australia: will availability of water constrain the growth of Australia's population? *Geographical Research*, **49**(3), 301-316.

Sahebi, S., Phuntsho, S., Kim, J.E., Hong, S., Shon, H.K. 2015. Pressure assisted fertiliser drawn osmosis process to enhance final dilution of the fertiliser draw solution beyond osmotic equilibrium. *Journal of Membrane Science*, **481**, 63-72.

Sairam, M., Sereewatthanawut, E., Li, K., Bismarck, A., Livingston, A. 2011. Method for the preparation of cellulose acetate flat sheet composite membranes for forward osmosis—desalination using MgSO₄ draw solution. *Desalination*, **273**(2), 299-307.

Saren, Q., Qiu, C.Q., Tang, C.Y. 2011. Synthesis and characterization of novel forward osmosis membranes based on layer-by-layer assembly. *Environmental science & technology*, **45**(12), 5201-5208.

- Schwinge, J., Neal, P.R., Wiley, D.E., Fletcher, D.F., Fane, A.G. 2004. Spiral wound modules and spacers: Review and analysis. *Journal of Membrane Science*, **242**(1–2), 129-153.
- Setiawan, L., Wang, R., Li, K., Fane, A.G. 2011. Fabrication of novel poly (amide–imide) forward osmosis hollow fiber membranes with a positively charged nanofiltration-like selective layer. *Journal of Membrane Science*, **369**(1), 196-205.
- Setiawan, L., Wang, R., Tan, S., Shi, L., Fane, A.G. 2013. Fabrication of poly (amide-imide)-polyethersulfone dual layer hollow fiber membranes applied in forward osmosis by combined polyelectrolyte cross-linking and depositions. *Desalination*, **312**, 99-106.
- Shaffer, D.L., Werber, J.R., Jaramillo, H., Lin, S., Elimelech, M. 2015a. Forward osmosis: Where are we now? *Desalination*, **356**(0), 271-284.
- Shaffer, D.L., Werber, J.R., Jaramillo, H., Lin, S., Elimelech, M. 2015b. Forward osmosis: Where are we now? *Desalination*, **356**, 271-284.
- Shaffer, D.L., Yip, N.Y., Gilron, J., Elimelech, M. 2012. Seawater desalination for agriculture by integrated forward and reverse osmosis: Improved product water quality for potentially less energy. *Journal of Membrane Science*, **415**, 1-8.
- Shahabi, M.P., McHugh, A., Ho, G. 2015. Environmental and economic assessment of beach well intake versus open intake for seawater reverse osmosis desalination. *Desalination*, **357**(0), 259-266.
- Shakaib, M., Hasani, S., Mahmood, M. 2007. Study on the effects of spacer geometry in membrane feed channels using three-dimensional computational flow modeling. *Journal of Membrane Science*, **297**(1), 74-89.
- She, Q., Jin, X., Li, Q., Tang, C.Y. 2012. Relating reverse and forward solute diffusion to membrane fouling in osmotically driven membrane processes. *Water Research*, **46**(7), 2478-2486.
- She, Q., Wang, R., Fane, A.G., Tang, C.Y. 2016. Membrane Fouling in Osmotically Driven Membrane Processes: A Review. *Journal of Membrane Science*, **499**, 201-233.
- Sim, V.S., She, Q., Chong, T.H., Tang, C.Y., Fane, A.G., Krantz, W.B. 2013a. Strategic co-location in a hybrid process involving desalination and pressure retarded osmosis (PRO). *Membranes*, **3**(3), 98-125.

- Sim, V.S.T., She, Q., Chong, T.H., Tang, C.Y., Fane, A.G., Krantz, W.B. 2013b. Strategic Co-Location in a Hybrid Process Involving Desalination and Pressure Retarded Osmosis (PRO). *Membranes*.
- Song, X., Liu, Z., Sun, D.D. 2011. Nano gives the answer: breaking the bottleneck of internal concentration polarization with a nanofiber composite forward osmosis membrane for a high water production rate. *Advanced materials*, **23**(29), 3256-3260.
- Su, J., Chung, T.-S., Helmer, B.J., de Wit, J.S. 2012. Enhanced double-skinned FO membranes with inner dense layer for wastewater treatment and macromolecule recycle using Sucrose as draw solute. *Journal of membrane science*, **396**, 92-100.
- Su, J., Ong, R.C., Wang, P., Chung, T.S., Helmer, B.J., Wit, J.S. 2013. Advanced FO membranes from newly synthesized CAP polymer for wastewater reclamation through an integrated FO-MD hybrid system. *AIChE Journal*, **59**(4), 1245-1254.
- Su, J., Yang, Q., Teo, J.F., Chung, T.-S. 2010. Cellulose acetate nanofiltration hollow fiber membranes for forward osmosis processes. *Journal of membrane science*, **355**(1), 36-44.
- Subramani, A., Badruzzaman, M., Oppenheimer, J., Jacangelo, J.G. 2011. Energy minimization strategies and renewable energy utilization for desalination: A review. *Water Research*, **45**(5), 1907-1920.
- Tan, C.H., Ng, H.Y. 2010. A novel hybrid forward osmosis-nanofiltration (FO-NF) process for seawater desalination: Draw solution selection and system configuration. *Desalination & Water Treatment*, **13**(1-3), 356-361.
- Tang, C.Y., Fu, Q.S., Criddle, C.S., Leckie, J.O. 2007. Effect of flux (transmembrane pressure) and membrane properties on fouling and rejection of reverse osmosis and nanofiltration membranes treating perfluorooctane sulfonate containing wastewater. *Environmental Science & Technology*, **41**(6), 2008-2014.
- Tang, C.Y., She, Q., Lay, W.C.L., Wang, R., Fane, A.G. 2010. Coupled effects of internal concentration polarization and fouling on flux behavior of forward osmosis membranes during humic acid filtration. *Journal of Membrane Science*, **354**(1-2), 123-133.

- Tarnacki, K., Meneses, M., Melin, T., van Medevoort, J., Jansen, A. 2012. Environmental assessment of desalination processes: Reverse osmosis and Memstill®. *Desalination*, **296**(0), 69-80.
- Tirafferri, A., Yip, N.Y., Phillip, W.A., Schiffman, J.D., Elimelech, M. 2011. Relating performance of thin-film composite forward osmosis membranes to support layer formation and structure. *Journal of Membrane Science*, **367**(1–2), 340-352.
- Tirafferri, A., Yip, N.Y., Straub, A.P., Romero-Vargas Castrillon, S., Elimelech, M. 2013. A method for the simultaneous determination of transport and structural parameters of forward osmosis membranes. *Journal of Membrane Science*, **444**(0), 523-538.
- Trenholm, L.E., Schlossberg, M.J., Lee, G., Parks, W., Geer, S.A. 2000. An evaluation of multi-spectral responses on selected turfgrass species. *International Journal of Remote Sensing*, **21**(4), 709-721.
- Valladares Linares, R., Li, Z., Abu-Ghdaib, M., Wei, C.-H., Amy, G., Vrouwenvelder, J.S. 2013a. Water harvesting from municipal wastewater via osmotic gradient: An evaluation of process performance. *Journal of Membrane Science*, **447**, 50-56.
- Valladares Linares, R., Li, Z., Yangali-Quintanilla, V., Ghaffour, N., Amy, G., Leiknes, T., Vrouwenvelder, J.S. 2016. Life cycle cost of a hybrid forward osmosis – low pressure reverse osmosis system for seawater desalination and wastewater recovery. *Water Research*, **88**, 225-234.
- Valladares Linares, R., Li, Z., Yangali-Quintanilla, V., Li, Q., Amy, G. 2013b. Cleaning protocol for a FO membrane fouled in wastewater reuse. *Desalination and Water Treatment*, **51**(25-27), 4821-4824.
- Van der Bruggen, B., Vandecasteele, C. 2002. Distillation vs. membrane filtration: overview of process evolutions in seawater desalination. *Desalination*, **143**(3), 207-218.
- Vrijenhoek, E.M., Hong, S., Elimelech, M. 2001. Influence of membrane surface properties on initial rate of colloidal fouling of reverse osmosis and nanofiltration membranes. *Journal of Membrane Science*, **188**(1), 115-128.
- Wang, K.Y., Chung, T.-S., Qin, J.-J. 2007. Polybenzimidazole (PBI) nanofiltration hollow fiber membranes applied in forward osmosis process. *Journal of Membrane Science*, **300**(1), 6-12.

- Wang, K.Y., Chung, T.S., Amy, G. 2012. Developing thin-film-composite forward osmosis membranes on the PES/SPSf substrate through interfacial polymerization. *AIChE Journal*, **58**(3), 770-781.
- Wang, K.Y., Ong, R.C., Chung, T.-S. 2010a. Double-skinned forward osmosis membranes for reducing internal concentration polarization within the porous sublayer. *Industrial & Engineering Chemistry Research*, **49**(10), 4824-4831.
- Wang, K.Y., Yang, Q., Chung, T.-S., Rajagopalan, R. 2009. Enhanced forward osmosis from chemically modified polybenzimidazole (PBI) nanofiltration hollow fiber membranes with a thin wall. *Chemical Engineering Science*, **64**(7), 1577-1584.
- Wang, R., Shi, L., Tang, C.Y., Chou, S., Qiu, C., Fane, A.G. 2010b. Characterization of novel forward osmosis hollow fiber membranes. *Journal of Membrane Science*, **355**(1-2), 158-167.
- Wang, X., Yuan, B., Chen, Y., Li, X., Ren, Y. 2014. Integration of micro-filtration into osmotic membrane bioreactors to prevent salinity build-up. *Bioresource technology*, **167**, 116-123.
- Wang, Y., Ou, R., Wang, H., Xu, T. 2015a. Graphene oxide modified graphitic carbon nitride as a modifier for thin film composite forward osmosis membrane. *Journal of Membrane Science*, **475**(0), 281-289.
- Wang, Z., Tang, J., Zhu, C., Dong, Y., Wang, Q., Wu, Z. 2015b. Chemical cleaning protocols for thin film composite (TFC) polyamide forward osmosis membranes used for municipal wastewater treatment. *Journal of Membrane Science*, **475**, 184-192.
- Ward, F.A., Pulido-Velazquez, M. 2008. Water conservation in irrigation can increase water use. *Proceedings of the National Academy of Sciences*, **105**(47), 18215-18220.
- Watson, I.C., Morin, O., Henthorne, L. 2003. Desalting handbook for planners. *Desalination Research and Development Program Report*, **72**.
- Wei, J., Qiu, C., Tang, C.Y., Wang, R., Fane, A.G. 2011a. Synthesis and characterization of flat-sheet thin film composite forward osmosis membranes. *Journal of Membrane Science*, **372**(1), 292-302.

- Wei, J., Qiu, C., Tang, C.Y., Wang, R., Fane, A.G. 2011b. Synthesis and characterization of flat-sheet thin film composite forward osmosis membranes. *Journal of Membrane Science*, **372**(1–2), 292-302.
- Wei, J., Qiu, C., Tang, C.Y., Wang, R., Fane, A.G. 2011c. Synthesis and characterization of flat-sheet thin film composite forward osmosis membranes. *Journal of Membrane Science*, **372**(1-2), 292-302.
- Widjojo, N., Chung, T.-S., Weber, M., Maletzko, C., Warzelhan, V. 2011. The role of sulphonated polymer and macrovoid-free structure in the support layer for thin-film composite (TFC) forward osmosis (FO) membranes. *Journal of Membrane Science*, **383**(1), 214-223.
- Wilf, M. 2004. Fundamentals of RO-NF technology. *Paper presented at International Conference on Desalination Costing, Limassol*.
- Wilf, M., Klinko, K. 2001. Optimization of seawater RO systems design. *Desalination*, **138**(1–3), 299-306.
- Wittholz, M.K., O'Neill, B.K., Colby, C.B., Lewis, D. 2008. Estimating the cost of desalination plants using a cost database. *Desalination*, **229**(1–3), 10-20.
- Xie, M., Nghiem, L.D., Price, W.E., Elimelech, M. 2012. Comparison of the removal of hydrophobic trace organic contaminants by forward osmosis and reverse osmosis. *Water Research*, **46**(8), 2683-2692.
- Xie, M., Nghiem, L.D., Price, W.E., Elimelech, M. 2013a. A forward osmosis–membrane distillation hybrid process for direct sewer mining: system performance and limitations. *Environmental science & technology*, **47**(23), 13486-13493.
- Xie, M., Nghiem, L.D., Price, W.E., Elimelech, M. 2013b. Impact of humic acid fouling on membrane performance and transport of pharmaceutically active compounds in forward osmosis. *Water Research*, **47**(13), 4567-4575.
- Xu, T., Huang, C. 2008. Electrodialysis-based separation technologies: A critical review. *AIChE journal*, **54**(12), 3147-3159.
- Yaeli, J. 1992. Method and apparatus for processing liquid solutions of suspensions particularly useful in the desalination of saline water, Google Patents.

- Yang, Q., Wang, K.Y., Chung, T.-S. 2009. Dual-layer hollow fibers with enhanced flux as novel forward osmosis membranes for water production. *Environmental science & technology*, **43**(8), 2800-2805.
- Yangali-Quintanilla, V., Li, Z., Valladares, R., Li, Q., Amy, G. 2011. Indirect desalination of Red Sea water with forward osmosis and low pressure reverse osmosis for water reuse. *Desalination*, **280**(1-3), 160-166.
- Yangali-Quintanilla, V., Olesen, L., Lorenzen, J., Rasmussen, C., Laursen, H., Vestergaard, E., Keiding, K. 2015. Lowering desalination costs by alternative desalination and water reuse scenarios. *Desalination and Water Treatment*, **55**(9), 2437-2445.
- Ye, L., Peng, C.-y., Tang, B., Wang, S.-y., Zhao, K.-f., Peng, Y.-z. 2009. Determination effect of influent salinity and inhibition time on partial nitrification in a sequencing batch reactor treating saline sewage. *Desalination*, **246**(1-3), 556-566.
- Yen, S.K., Mehnas Haja N, F., Su, M., Wang, K.Y., Chung, T.-S. 2010a. Study of draw solutes using 2-methylimidazole-based compounds in forward osmosis. *Journal of Membrane Science*, **364**(1-2), 242-252.
- Yen, S.K., Su, M., Wang, K.Y., Chung, T.-S. 2010b. Study of draw solutes using 2-methylimidazole-based compounds in forward osmosis. *Journal of Membrane Science*, **364**(1), 242-252.
- Yip, N.Y., Tiraferri, A., Phillip, W.A., Schiffman, J.D., Elimelech, M. 2010. High Performance Thin-Film Composite Forward Osmosis Membrane. *Environmental Science & Technology*, **44**(10), 3812-3818.
- You, S., Tang, C., Yu, C., Wang, X., Zhang, J., Han, J., Gan, Y., Ren, N. 2013. Forward osmosis with a novel thin-film inorganic membrane. *Environmental science & technology*, **47**(15), 8733-8742.
- Yu, Y., Seo, S., Kim, I.-C., Lee, S. 2011. Nanoporous polyethersulfone (PES) membrane with enhanced flux applied in forward osmosis process. *Journal of membrane science*, **375**(1), 63-68.
- Zaina, L.A.M., Álvaro, A. 2015. A design methodology for user-centered innovation in the software development area. *Journal of Systems and Software*, **110**, 155-177.

- Zaviska, F., Zou, L. 2014. Using modelling approach to validate a bench scale forward osmosis pre-treatment process for desalination. *Desalination*, **350**(0), 1-13.
- Zeng, Y., Qiu, L., Wang, K., Yao, J., Li, D., Simon, G.P., Wang, R., Wang, H. 2013. Significantly enhanced water flux in forward osmosis desalination with polymer-graphene composite hydrogels as a draw agent. *RSC Advances*, **3**(3), 887-894.
- Zhang, J., Loong, W.L.C., Chou, S., Tang, C., Wang, R., Fane, A.G. 2012. Membrane biofouling and scaling in forward osmosis membrane bioreactor. *Journal of Membrane Science*, **403–404**(0), 8-14.
- Zhang, S., Wang, K.Y., Chung, T.-S., Chen, H., Jean, Y., Amy, G. 2010. Well-constructed cellulose acetate membranes for forward osmosis: minimized internal concentration polarization with an ultra-thin selective layer. *Journal of Membrane Science*, **360**(1), 522-535.
- Zhang, S., Wang, K.Y., Chung, T.-S., Jean, Y., Chen, H. 2011. Molecular design of the cellulose ester-based forward osmosis membranes for desalination. *Chemical engineering science*, **66**(9), 2008-2018.
- Zhang, S., Wang, P., Fu, X., Chung, T.-S. 2014. Sustainable water recovery from oily wastewater via forward osmosis-membrane distillation (FO-MD). *Water Research*, **52**(0), 112-121.
- Zhang, Y., Pinoy, L., Meesschaert, B., Van der Bruggen, B. 2013. A natural driven membrane process for brackish and wastewater treatment: photovoltaic powered ED and FO hybrid system. *Environmental science & technology*, **47**(18), 10548-10555.
- Zhao, D., Wang, P., Zhao, Q., Chen, N., Lu, X. 2014. Thermoresponsive copolymer-based draw solution for seawater desalination in a combined process of forward osmosis and membrane distillation. *Desalination*, **348**, 26-32.
- Zhao, S., Zou, L., Mulcahy, D. 2012a. Brackish water desalination by a hybrid forward osmosis–nanofiltration system using divalent draw solute. *Desalination*, **284**(0), 175-181.
- Zhao, S., Zou, L., Mulcahy, D. 2012b. Brackish water desalination by a hybrid forward osmosis–nanofiltration system using divalent draw solute. *Desalination*, **284**, 175-181.

- Zhao, S., Zou, L., Tang, C.Y., Mulcahy, D. 2012c. Recent developments in forward osmosis: Opportunities and challenges. *Journal of Membrane Science*, **396**, 1-21.
- Zhou, J., Chang, V.W.C., Fane, A.G. 2014. Life Cycle Assessment for desalination: A review on methodology feasibility and reliability. *Water Research*, **61**(0), 210-223.
- Zhu, X., Elimelech, M. 1997. Colloidal fouling of reverse osmosis membranes: measurements and fouling mechanisms. *Environmental Science & Technology*, **31**(12), 3654-3662.